LCH Laboratoire de Constructions Hydrauliques
Laboratory of Hydraulic Constructions

ÉCOLE POLYTECHNIQUE
FÉDÉRALE DE LAUSANNE

Communication 65

Optimization of low-head hydropower recovery in water supply networks

Irene Almeida Samora

Editeur : Prof. Dr A. Schleiss

Lausanne, 2016

Communications du Laboratoire de Constructions Hydrauliques ISSN 1661-1179
Ecole Polytechnique Fédérale de Lausanne
Editeur: Prof. Dr A. Schleiss

PREFACE

Water supply networks in cities with sloping topography may have a considerable potential for the installation of micro hydropower plants. Since these water supply networks are complex systems with many constraints, the identification of the best locations for such micro hydropower installations is a difficult task. With her research project, Dr. Irene Samora made a significant contribution for answering the question how the available low-head hydropower can be recovered in an optimized way in such complex water supply networks.

As a first original contribution the candidate tested experimentally the performance of a novel micro-turbine, consisting of a five blade tubular propeller (5BTP). The latter is suitable for low-head recovery in water supply pipes. In order to find the optimal locations within the water supply networks for installation of micro-hydropower, Dr. Samora developed a powerful optimization algorithm which considers energy production as well as economic objectives. Finally, Dr. Samora suggests a new method for the evaluation of hydropower potential in water supply networks (WSN). All the developments were tested with several case studies in WSN of four cities in Portugal and in Switzerland. With the analysis of synthetic networks, a first attempt was made to develop empirical relationships for the estimation of possible energy production.

We would like to thank the members of the jury, Prof. Petra Amparo López from the Universitat Politècnica de València, Spain and Dr. Jean□Marc Ribi from University of Applied Science Fribourg, Switzerland as well as Dr. Massimiliano Capezzali from Energy Center of EPFL for their helpful suggestions. Furthermore, we want to thank Prof. Cécile Münch-Alligné and Dr. Vlad Hasmatuchi for their support in the testing of the 5BTP in HES-SO Valais and for their insightful comments. Finally, we also thank gratefully the Portuguese Foundation for Science and Technology (FTC) for their financial support under project SFRH/BD/51931/2012 in the frame of joint PhD initiative between IST and EPFL.

Prof. Dr. Anton Schleiss Prof. Dr. Helena Ramos

” We will make electricity so cheap that only the rich will burn candles.”

Thomas Edison

Acknowledgements

This research is supported by LCH and the grant ref. SFRH/BD/51931/2012 issued by FCT under the IST-EPFL Joint PhD initiative. I want to thank both the institutions, IST and EPFL, in which I developed this work.

I want to thank my supervisors, Prof. Helena Ramos and Prof. Anton Schleiss, for their support, their insight and their most valuable advice. I also want to express my deepest gratitude to Dr. Mário Franca and Dr. Pedro Manso for their support in LCH to this research and to my professional development as a researcher.

I thank SFOE, the Swiss Federal Office of Energy, for financing the experimental tests of the turbine. Moreover, I want to thank Prof. Cécile Münch-Alligné and Dr. Vlad Hasmatuchi for their support in the laboratorial experiments in HES-SO Valais and for their insightful comments.

In the course of this work, there has been need for data concerning real networks and I was fortunate to be in contact with the Service de l'eau in Lausanne and Eau de Fribourg. I want to show my appreciation to Mr. Laurent Barras, from Fribourg, and to Mr. Pasquale Giordano, Mrs. Christelle Sanz and Mr. Dominique Zürcher, from Lausanne, for the time and data provided to support this work. I would like to thank Ribi SA, in particular to Mr. Johann Pury, for sharing their data of the Fribourg network.

I want to give my special thanks to Prof. Jean-François Molinari and Prof. Massimiliano Capezzali from EPFL for accepting to be part of the jury that will assess my work.

I extend this gratitude to Prof. Petra Amparo López and Dr. Jean-Marc Ribi for coming from the Universitat Politècnica de València and HES Fribourg, respectively, to be present as an external members of the jury.

From IST, I want to thank Mariana Simão, who performed the CFD simulations of the 5BTP during her Master Project. She was always available not only when I searched for data but also as a friend and a fellow PhD student.

I would like to thank everyone in LCH, EPFL, for all the suggestions and scientific discussions, for motivating me and, specially, for the friendship. In particular, I would like to thank Dr. José Matos for his support.

On a more personal note, I thank my friends, not only in Portugal and Switzerland, but also around the world. We live in a truly connected and international era and I should probably also thank all the communication technology that is helping us stay together. These were four years of great changes in my life and it has been reassuring to know that I can count on so many wonderful people.

My parents were an unconditional support although it was not easy for them to see their daughter move to another country. I thank them for their love, their teaching and their engineering genes.

Finally, I want to thank Matthias Lambert, for his love and patience. He has been the best change in my life.

Lausanne, 5th of September 2016

Abstract

Small scale hydropower is emerging as a decentralized source to satisfy local demand for electricity. The interest in micro-hydropower, which refers to installed power below 100 kW, is increasing since this is a solution with low environmental impact.

Water supply systems are one of the main manmade water systems presenting potential for micro-hydropower. Although some applications already exist in adduction lines, the urban distribution networks remain unexplored. Because these are complex systems in which flows and pressure vary constantly, specific technology and installation schemes for energy recovery are lacking.

This work assesses the potential for hydropower within water supply networks (WSN) and presents an arrangement of micro-turbines specially conceived for this type of installation. The arrangement is based on a novel inline turbine suitable for pressurized systems and its best location within the networks is studied.

The five blade tubular propeller (5BTP), preliminarily designed in the framework of the European Project HYLOW, was further developed and tested in this work. An experimental campaign was conducted with a large range of heads and torque measurements to assess its characteristic curves and to obtain hill charts. The relative positioning of the turbine-generator shaft regarding the pipe bend was modified from a downstream position to an upstream position. Efficiencies of around 60% were found.

The adequate locations in WSN for micro-hydropower plants are identified using an optimization algorithm which considers both the assessment of the energy production and sizing of the main equipment and works. A concept for the implementation of the 5BTP in the field was developed, consisting of an arrangement with up to four turbines inline within a buried chamber created around an existing pipe. Two objective functions, energy production and economic value respectively, are used. A simulated annealing process is developed to optimize the location of a given number of turbines. This procedure takes into account the hourly variation of flows throughout an average year and its effect on the turbine's efficiency. The optimization is achieved by considering the characteristic and efficiency curves of a turbine with different impeller diameters and simulating the annual energy production in a coupled hydraulic model.

After a convergence analysis for different restrictions and numbers of installed turbines, the algorithm was applied to analyze the feasibility of the proposed arrangement in two case studies in Switzerland: a sub-grid of the city of Lausanne and the complete WSN of the city of Fribourg. In both cases, the implementation of the proposed energy recovery solution seems to be feasible. A detailed analysis of the cost breakdown revealed that the cost of additional pipe work, which is required in

each layout to guarantee a by-pass supply in case of maintenance, may have an important role on the investments. Also, the pressure reduction valves locations, if they exist, are likely to be the optimal solutions.

Finally, a methodology to quantify the potential for hydropower based on the excess energy in a WSN is proposed and applied to case studies. It allowed to conclude how much the proposed arrangement can extract from the networks' energy potential. In addition, an attempt was made to produce a conceptual method to estimate the energy produced with one 5BTP based on network parameters and dimensional analysis.

Keywords

Micro-hydropower; Micro propeller turbine; Water supply networks; Optimization algorithms; Energy potential

Resumo

A hidroeletricidade em pequena escala está a surgir como fonte descentralizada para satisfazer a nível local a procura de eletricidade. O interesse na micro-hidroeletricidade, correspondendo esta a potências instaladas inferiores a 100 kW, está a crescer, sendo esta uma solução sem impactes ambientais.

Os sistemas de abastecimento de água são um dos principais tipos de sistemas hidráulicos artificiais que surge com potencial para micro-hidroelectricidade. Apesar de existirem algumas aplicações de mini-hidroeletricidade nas condutas de adução, as redes de distribuição urbanas estão ainda pouco exploradas. Tal é devido à falta de tecnologias e esquemas de instalação específicos para redes distribuição, uma vez que estas são sistemas complexos onde pressões e caudal variam constantemente. São necessárias novas soluções que permitam ter rendimento económico com os caudais e quedas variáveis disponíveis nestas redes.

Este trabalho tem como objetivo avaliar o potencial para hidroeletricidade das redes urbanas de distribuição de água e apresentar um esquema de microturbinas desenvolvido expressamente para esse tipo de instalação. O esquema hidroelétrico é baseado numa nova turbina, propícia a ser instalada em sistemas em pressão, e a sua localização ótima dentro das redes é estudada.

O desenvolvimento da turbina tubular em hélice de cinco pás (5BTP), iniciado no âmbito do projeto europeu HYLOW, foi continuado nesta tese. A turbina foi submetida a uma campanha experimental com uma grande gama de caudais e medição de binário para avaliar as suas curvas características e obter diagramas em colina. A posição relativa do grupo turbina-gerador em relação à curva foi modificada de jusante para montante. Rendimentos da turbina de cerca de 60% foram encontrados.

As localizações adequadas das turbinas dentro das redes urbanas são identificadas utilizando um algoritmo de otimização que considera tanto a produção de energia como as quantidades dos principais equipamentos e construções civis. Um esquema hidroelétrico é proposto com uma até quatro turbinas dentro de uma câmara enterrada, criada em torno de uma conduta existente da rede. Duas funções-objetivo, energia produzida e valor económico respetivamente, são usadas. Um processo de simulated annealing é desenvolvido para otimizar a localização de um dado número de turbinas. Este processo tem em conta as variações horárias de caudal ao longo de um ano médio e o seu impacto no rendimento da turbina. A otimização é conseguida utilizando as curvas característica e de rendimentos da turbina para diferentes diâmetros e o cálculo hidráulico a cada passo no tempo é realizado através de um solver hidráulico associado ao algoritmo.

Após uma análise de convergência para diferentes restrições e número de turbinas a instalar, o algoritmo foi aplicado para avaliar a viabilidade do esquema proposto em dois casos de estudo na

Suíça: uma sub-rede da cidade de Lausanne e a rede completa da rede de Friburgo. Em ambos os casos, a implementação da solução proposta de recuperação de energia é considerada viável. A análise detalhada dos custos revelou que o custo de um by-pass adicional para garantir a continuidade do serviço em caso de manutenção pode ter um papel importante nos investimentos. Concluiu-se também que os locais onde existem válvulas redutoras de pressão, se existirem, são provavelmente as soluções ótimas.

Finalmente, uma metodologia para quantificar o potencial para hidroeletricidade de uma rede é proposta e aplicada a casos de estudo. Esta permitiu concluir quanto do potencial energético das redes é possível extrair com o esquema proposto. Uma tentativa de desenvolvimento de um método conceptual foi ainda realizada com o intuito de estimar a produção de uma turbina com base em parâmetros da rede e análise dimensional.

Palavras-Chave

Micro-hidroeletricidade; Micro turbina em hélice; Sistemas de abastecimento de água; Algoritmos de otimização; Potencial energético.

Résumé

L'hydroélectricité à petite échelle est en train de se développer comme une source décentralisée pour satisfaire des demandes locales d'électricité. L'intérêt pour la micro-hydroélectricité, qui correspond à moins de 100 kW de puissance installée, grandit actuellement en tant que solution sans grands impacts.

Les systèmes d'approvisionnement d'eau sont un des principaux types de systèmes hydrauliques artificiels avec du potentiel pour la micro-hydro. Bien que quelques applications de petite hydroélectricité existent dans des conduites d'adduction, les réseaux de distribution urbains restent encore inexplorés. Cela est dû à l'absence de technologies et de schémas d'installation spécifiques pour les réseaux de distribution, puisque ceux-ci sont des systèmes complexes où la pression et le débit varient constamment. Des nouvelles solutions sont nécessaires, qui soient performantes avec les débits et les chutes variables qui sont disponibles dans ces réseaux.

Ce travail vise à évaluer le potentiel pour l'hydroélectricité des réseaux de distribution en milieu urbain et de présenter un schéma d'installation de micro turbines, développées spécifiquement pour ce type d'application. L'aménagement hydroélectrique est basé sur une nouvelle turbine conçue pour être installée dans des systèmes sous pression et leur localisation optimale au sein du réseau est étudiée.

Le développement de la turbine en hélice à cinq pales (5BTP), initié dans le cadre du projet européen HYLOW, a été continué dans cette thèse. La turbine a été soumise à une campagne expérimentale avec une grande plage de débits et des mesures de couple mécanique afin d'évaluer sa performance ainsi que d'obtenir des diagrammes en colline. La position relative du groupe turbine-générateur par rapport à la courbe a été modifiée de l'aval vers l'amont. Les résultats expérimentaux ont montré des rendements de la turbine d'environ 60%.

Les localisations appropriées des turbines dans les réseaux sont identifiées en utilisant un algorithme d'optimisation qui tient compte non seulement de la production d'énergie mais aussi des quantités des principaux équipements et travaux de génie civil. Un schéma hydroélectrique est proposé avec une à quatre turbines placées dans une chambre souterraine créée autour d'une conduite existante. Deux fonctions objectif, l'énergie produite et la valeur économique respectivement, sont utilisées. Un processus du type « simulated annealing » est développé afin d'optimiser l'emplacement d'un nombre de turbines, compte tenu des changements horaires de débit sur une année moyenne et de son impact dans le rendement de la turbine. Les courbes caractéristiques et de rendements de la turbine pour différents diamètres sont utilisées pour le calcul hydraulique à chaque pas de calcul, réalisé par un solver hydraulique associé à l'algorithme.

Après une analyse de convergence avec différentes restrictions et différents nombres de turbines à installer, l'algorithme a été appliqué pour évaluer la faisabilité du schéma proposé dans deux cas d'étude en Suisse : un sous-réseau de la ville de Lausanne et le réseau complet de la ville de Fribourg. Dans les deux cas, la mise en œuvre de la solution proposée apparaît être faisable. L'analyse détaillée des coûts a montré que le coût du by-pass supplémentaire nécessaire pour garantir la continuité du service en cas de maintenance peut jouer un rôle important dans l'investissement. Il a été également conclu que les endroits où des réducteurs de pression, si existants, sont installés sont probablement les solutions optimales.

Enfin, une méthodologie pour quantifier le potentiel pour l'hydroélectricité d'un réseau est proposée et appliquée dans des cas d'étude. Elle a permis de conclure combien du potentiel énergétique des réseaux il est possible d'extraire avec le schéma proposé. Une tentative de développement d'une méthode conceptuelle a aussi été réalisée, dans le but d'estimer la production avec une turbine sur la base des paramètres du réseau et d'une analyse dimensionnelle.

Mots-clés :

Micro-hydroélectricité ; Micro turbine en hélice ; Systèmes d'approvisionnement d'eau ; Algorithmes d'optimisation ; Potentiel énergétique.

Contents

Abbreviations

5BTP: Five blade tubular propeller

NPV: Net present value

PAT: Pump as turbine

PRV: Pressure reducing valves

WSN: Water supply network

WSS: Water supply system

List of Figures

List of Tables

Chapter 1
Introduction

1.1 Scope and motivation

The present concerns with environment and energy efficiency contribute for a growing new interest in small-scale hydropower. The investment in small scale hydropower is growing all over the world as it is a clean, sustainable and emissions-free source of renewable energy. Small-scale hydropower can be classified in small, mini, micro or pico, depending on the output power and on the type of the adopted scheme (Ramos, 2000; Paish, 2002). There are not yet globally accepted boundaries to define these classes, it depends on the country, but micro-hydro typically refers to schemes below 100 kW (Ramos, et al., 2009a) while pico-hydro usually corresponds to installed power of less than 5 kW (Arriaga, 2010).

A micro-hydropower scheme can generate energy from small rivers, water supply systems, irrigation channels, wastewater treatment plants and pluvial drainage systems. These micro schemes can be used to produce energy to supply a grid or for local consumption. The proximity of the installations to local consumers allow for a decentralized production, minimizing the transmission losses (Ramos, et al., 2010a; Weijermars, et al., 2012). Also, in situations such as remote communities, where it is not economical or even possible to establish a power connection to the national grid, stand-alone small hydro-systems can be used to respond to local energy needs (Joshi, et al., 2005; Jain & Patel, 2014).

Research and investment is currently being undertaken to improve the energy efficiency in existing water infrastructures and in renewable energy technologies. An interesting example is happening in Switzerland where a new federal energy strategy, the Energy Strategy 2050, has motivated the creation of the Swiss Competence Center for Energy Research – Supply of Electricity (SCCER-SoE).

Another example is the European Union which endorsed in 2013 the Energy Roadmap 2050 and has invested between 2007 and 2013 in the 7th Framework Programme for energy research.

A promising opportunity for research in small-scale hydropower production lies within water supply systems (WSS). Although it has been mentioned by several authors that the application of micro-hydropower in WSS is possible, most of the existing applications are in large adduction pipes or reservoirs, outside the urban areas. There is a lack of specific solutions for applications within the networks. Moreover, conventional turbines are often not cost-effective for an installed power under 10 MW (Wiemann, et al., 2008). Other than classical types of turbine, water wheels, hydraulic screws and pumps working in reverse mode are possible alternative technologies for micro and pico-hydropower. Even so, to adapt to the variable discharge conditions and low heads which can be involved in micro and pico-hydro schemes, research is being carried out for the development of new conversion technologies.

1.2 Research questions

Globally, the present study aims at the development of optimization tools and discussion of solutions for micro-hydropower energy production in urban water supply networks (WSN). A possible technology to exploit the existing potential in the urban network, the five blade tubular propeller (5BTP) micro-turbine, is fully tested. Its performance is simulated and an optimization tool for its placement within WSN is developed. Finally, the methods are applied to case studies adapted from real networks. The following questions are aimed by this research:

Q1 – Is the 5BTP turbine an appropriate equipment to apply in urban water supply networks?

Q2 – Which are the optimal locations within the networks for micro-hydropower?

Q3 – How much potential is there in water supply networks for micro-hydropower?

1.3 Report structure

This report is organized in seven chapters and three appendices. Even if the main chapters are based on submitted reviewed papers, the document was organized to avoid repetitions of content between sections of different chapters.

In this Chapter 1, a short introduction and the main motivation and objectives of this research have been presented.

Chapter 2 is dedicated to the state-of-the art, in which the main contributions to date on the topic of micro-hydro are presented, as well as some theoretical background on hydraulic machines and economic analysis. The gaps of knowledge in this topic, as well as some concepts required for the report comprehension, are herein presented.

In Chapter 3 the case studies used for testing the developed algorithms and methodologies are presented.

Chapter 4 is devoted to the experimental characterization of the 5BTP turbine, where the studied turbine is described and the laboratory setup, measuring equipment and experimental procedure are presented, as well as the results obtained.

In Chapter 5 the location of micro-hydropower turbines within urban WSNs is discussed based on a developed optimization algorithm and its application to case studies. The optimization was carried considering energy production objectives, as well as economical retribution.

Chapter 6 presents a method for the evaluation of the potential for micro-hydropower exploitation in WSNs.

Finally, in Chapter 7, the main conclusions are drawn with suggestions and recommendations for future works.

Three appendices are included at the end of the report. The first, Appendix A, presents the raw results from the experimental procedure, described in Chapter 4. The second, Appendix B, presents a visual appreciation of the convergence tests of the optimization algorithm presented in Chapter 5. The third, Appendix C, presents the results from an exploratory analysis of synthetic networks described in Chapter 6.

Chapter 2
State-of-the-art

Excerpts of Chapter 2 have been used in the author's scientific articles, presented in the list of References.

2.1 The role of hydropower

Water and energy are closely connected. Electricity production depends highly on water, not only for hydropower but also for cooling systems of thermal power plants (Lior, 2012). On another hand, about 2-3% of the world energy is consumed in water and wastewater operations for extraction, treatment, transmission, distribution, use and disposal (Olsson, 2012). According to the typical load demand curves of water and energy consumption, the periods of highest consumption occur at the same time for both resources (Ramos, et al., 2010b; Ramos, et al., 2011a). This link between water and energy, recently described as the water-energy nexus, implies the need for a more integrated management of both resources. It is no surprise that with the growth of water consumption, energy needs will also grow (Keeling & Sullivan, 2012). Considering this interdependency during planning and policy making can lead to significant energy savings (Shrestha, et al., 2012; Vilanova & Balestieri, 2014).

Hydropower is the biggest renewable electrical power source to date, providing 13% of the electricity in Europe (ESHA, 2005) and around 15% of worldwide electricity (Deng, et al., 2012). Hydropower is the oldest renewable electricity source and its share is considerable since the 1970's (Figure 2.1). In 2012, 19 countries in the world depended on hydropower for more than 90% of their electricity supply (Paraguay, Bhutan, Laos, Kyrgyzstan, Zambia, Mozambique, Ethiopia, Norway, Tajikistan, Congo-Brazzaville, Nepal, Congo-Kinshasa, Albania, Myanmar, Colombia, Ghana, Malawi, Central African Republic and French Guiana) (IRENA, 2012; EIA, 2013). In 2012 and worldwide, the renewable energy production represented 4 699 TWh, from which 78% came from hydropower (Liébard, et al., 2013).

In the past 200 years, there has been a worldwide increase in energy demand. The world population is growing and more energy is required to enhance the living conditions and comfort of the population (Omer, 2008). At the same time, over 80% of global energy supply relies on fossil fuels

and on nuclear power, the first with heavy impact on the environment, and the latter with potentially high security risk of which the world is now more aware after the accident of Fukushima (Wüstenhagen & Menichetti, 2012). To ensure safe energy supply and at the same time tackle the problem of carbon emissions, any contribution of renewable energy generation is welcome. Energy supply and renewable sources are hence a major topic of political discussion and scientific research (Gan, et al., 2007; Burdis, 2009). Wind and solar power are getting most of the attention nowadays, but hydropower is getting another look in less conventional areas, such as small scale production and hybrid solutions (Jain & Patel, 2014).

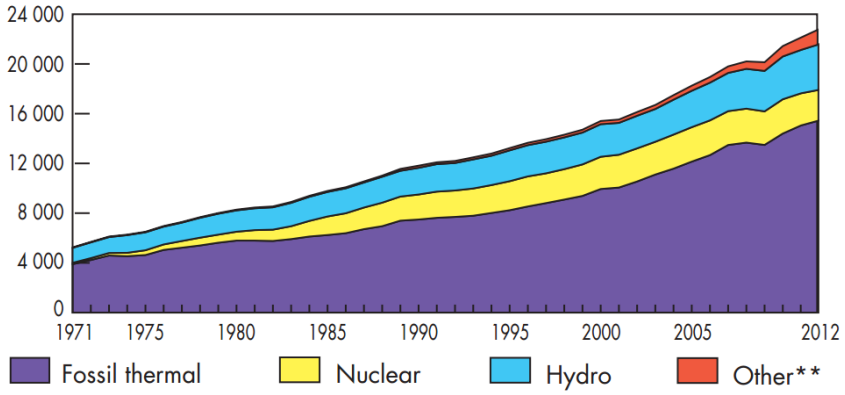

Figure 2.1 World electricity generation from 1971 to 2012 by source in TWh (** includes geothermal, solar, wind, biomass) (IEA, 2014).

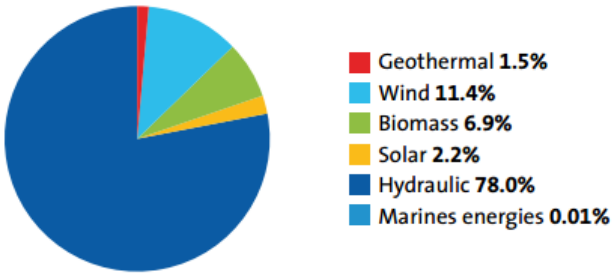

Figure 2.2 Distribution of electricity generation from renewable sources in 2012 (Liébard, et al., 2013).

Small scale hydropower had a major role on the onset of the industrial era in many regions (first for mechanical power, later for electricity production) through the development and refinement of water wheels, which is a technology known ever since antiquity (Paish, 2002). The invention of the water turbine and electrical generators led to the development of an increasing number of hydroelectric units (Abbasi & A., 2011), which, along with the widespread construction of power lines, became more prominent after WWI for run-of-the-river plants and after WWII for large hydro. However, the present concerns with global warming, greenhouse gases and residual risks linked with certain technologies provide a renewed opportunity for small and even micro-hydro, which allows for decentralized power generation for local demand. A decentralized production has the advantage of reducing transmission losses (Weijermars, et al., 2012). This type of production is

expected to increase in Europe, as a consequence of the increase of the share of energy supply technologies coming from renewables (EU, 2011).

In Europe, hydropower stations with an installed power lower than 10 MW are considered as small power plants whereas the limit reaches 50 MW in China. In Portugal, 357 MW with hydropower stations below 10 MW were already installed in 2012 (DGEG, 2013). In Switzerland, small-hydropower represents 10% of the hydroelectricity, 77% of this production is performed by plants with 1 to 10 MW of installed power. Nevertheless, the production of micro power stations lower than 300 kW is not negligible, reaching 9 % of small hydroelectricity (SFOE, 2013).

A micro-hydropower scheme, also referred to as unconventional hydropower, uses small heads or small flow discharges to generate electricity. Although it can be set in small rivers, the application of micro-hydropower in human built environments has the advantage of having small environmental impacts, which contributes to a bigger public acceptance of the technology, and reduced costs, since most infrastructures are already in place. Considering only the later type of installation, the main applications of micro-hydro are water supply systems, sewage treatment, pluvial drainage systems and irrigation systems.

2.2 Hydropower schemes in water supply systems (WSS)

A WSS is a set of civil infrastructures (reservoirs, pipes and others), hydro-mechanical facilities, electrical equipment and services that extracts, conveys and distributes water to consumers. This distribution must be compatible with the demand in both quantity and quality (Vilanova & Balestieri, 2014). In any WSS, the movement of water requires a hydraulic head which is provided either by gravity or through the conversion of electrical energy for pumping. The energy required to pump and treat water constitutes one of the largest operational costs for water suppliers (Ramos, et al., 2011a; Fayzul, et al., 2014).

A sub-grid of a WSS, also called “district metered area”, is a part of the network between nodes where the pressure is controlled. This pressure is maintained constant or follows a certain schedule (Ulanicki, et al., 2000) to ensure that there is an optimal pressure distribution in all the downstream branches. This is normally ensured by Pressure Reducing Valves (PRVs) but recent studies by Carravetta, et al. (2012) have proposed their replacement by pumps as turbines (PATs).

The use of PRVs or even micro-turbines in a WSS may seem illogical, since most systems need pumping at certain points. However, in certain cases, energy dissipation is imperative to control pressure to the consumer (Andolfatto, et al., 2016) or to minimize leakage and to achieve important monetary savings due to the reduction of water losses (Carravetta, et al., 2012; Carravetta, et al., 2013; Xu, et al., 2014; Fecarotta, et al., 2015). The use of operational pressure control has been proven to be cost-effective for reducing leakage problems (Ulanicki, et al., 2000; Ramos & Ramos, 2009; Jain & Patel, 2014; Vicente, et al., 2016). Water loss occurs due to the structural deterioration of the pipes (Xu, et al., 2014) and connections between pipes. Local energy dissipation is seen to

reduce the frequency of pipe bursts (Fantozzi, et al., 2009), ensure the quality standards of water supply (Carravetta & Giugni, 2006) and protect roads and buildings foundations from underground cavities originated by water losses (Fecarotta, et al., 2014). The use of turbines instead of PRVs for the excess pressure dissipation allows recovering part of this energy which is converted to electricity (Ramos, et al., 2010b; McNabola, et al., 2014a; Su & Karney, 2015). The hydraulic grade line principle associated with the effect of a turbine operation is quite similar to a PRV, as the pressure drop across the turbine also allows some downstream pressure control (Ramos, et al., 2010a). These solutions would take advantage of power production based on the available hydraulic energy of the WSS.

Such energy recovery would contribute to an improvement of the system's efficiency. Not only in terms of energy balance, but also of operational efficiency, due to the reduction of water leakage, and of maintenance, contributing to a longer life of the equipment.

The study presented in Gallagher (2015) has shown that there is an economical interest in micro-hydropower in WSS. This study was performed at a regional scale, identifying PRVs and reservoirs where there is potential for energy recovery. Moreover, there is potential for energy production within the urban network itself. Besides the locations where PRVs are installed, there are also areas within the grid that have more pressure than necessary, even if not excessive, because of their connection to other higher areas. The energy produced in these locations may be enough to justify the installation of a grid-connected generator or to be consumed locally (Ramos, et al., 2011a), the latter having the advantage of providing financial savings from avoiding external consumption and expensive electrical connections (Williams, et al., 1998).

Finally, the evaluation of the potential and feasibility of energy recovery in WSS can be found in the literature (McNabola, et al., 2011; Gallagher, et al., 2015) but there is a lack of guidelines for the case of urban networks.

2.3 Optimal locations of hydropower in water supply systems

The adaptation of WSSs to produce energy has the advantage of leveraging components that already exist (i.e., tanks, pipe lines and valves). Furthermore, continuous supply is guaranteed by consumption throughout the day (Vieira & Ramos, 2008; Ramos, et al., 2010a; Kougias, et al., 2014). However, the choice of locations for the installation of micro-hydropower is not straightforward if one considers closed WSNs. The ideal location depends on numerous factors: the flow rate, which in a urban system is highly variable along the day and with the position and directly impacts the efficiency of the turbine; the available head, since the micro-hydro operation should not affect the quality of the service to the population and thus service pressures ought to be guaranteed; and the geometry of the network, due to the distribution of the flow within closed meshes of a network. Limitations on pressure imposed by regulators must also be respected.

Many studies can be found in the literature on optimization of the positioning of PRVs within networks, such as Vairavamoorthy & Lumbers (1998) and Araújo, et al. (2006), among others.

Nevertheless, the optimal location of PRVs cannot be directly applied for the case of optimal location of turbines. When optimizing the positioning of PRVs, the main goal is to reduce water losses due to leakage and not to maximize energy production. Since the first only depends on the head drop across the valves whereas the second depends also on the flow rate, the results are not necessarily the same (Fontana, et al., 2012). The quantification and the positioning of turbines in WSNs that maximizes the energy potential while keeping pressure limits at adequate levels is a promising subject of research (Corcoran, et al., 2015).

A few strategies can be found in the literature for locations to install turbines in WSSs. Carravetta, et al. (2012) proposed the placement in the inlet nodes of network districts. Araújo, et al. (2006) suggested the identification of a number of nodes with energy potential within the entire network. Sitzenfrei & Leon (2014) developed a complex methodology with different phases that combines GIS techniques and sensitivity analyses. The first study limits the placement of a turbine to a particular node, whereas the other two imply long and time-consuming analyses.

The approach of using stochastic optimization algorithms has been investigated in network design and location of control valves (Cunha & Sousa, 2001; Farmani, et al., 2005; Araújo, et al., 2006; Ramos, et al., 2010a; Sousa, et al., 2015). Nevertheless, the use of these techniques for the current problem has not yet been thoroughly studied. Stochastic methods in which the generation of solutions is based on random procedures are particularly suited for problems that do not have an exploitable structure (Pardalos, et al., 2000). At each moment, these algorithms use the previously gathered information to decide which candidate solution should be tested in the next iteration. As a result, these approaches offer simple application and can be applied in many different types of discrete and continuous problems. Nevertheless, these approaches do not guarantee optimal solutions and it is not determined when the generation of solutions should be halted (Youssef, et al., 2001).

2.4 Hydropower schemes in sewage treatment

In wastewater treatment plants there is also a large consumption of energy. In Switzerland a total of 0.6 TWh/year is used in wastewater treatment, of which 0.5 TWh/year is electricity (Bryner, 2011). Considering the population of Switzerland, the energy consumption is of approximately 60 kWh/year/inhabitant. In the USA, approximately 34 billion gallons of wastewater are produced every day (NYSERDA, 2008) giving a total of 15 TWh/year. This accounts for 25–40% of the operating budgets for wastewater utilities (EPA, 2013). Only in the New York State, 1.75 to 2.0 billion kWh/year of electricity are consumed for the wastewater sector (NYSERDA, 2010). Considering the population of the USA, the total energy consumption is of approximately 48 kWh/year/inhabitant. In general, it has been estimated that the transport and treatment of wastewater represents 3 to 5% of the energy consumption of a country (Chen & Chen, 2013).

Recent developments have shown that it is possible to attenuate this consumption with energy recovery in the wastewater systems. The generation of energy in a wastewater treatment plant

(WWTP) can be consumed locally or be exported to the grid (Pakenas, 1995). Nowadays, this recovery can be achieved with methane recovery from sludge digesters, sludge incineration and hydropower (Zakkour, et al., 2002). However, it is important that the performance of the system remains unaffected.

One advantage of hydropower generation is the possibility to match the capacity factor of a turbine with the flow profile and energy consumption. High and low flows correspond to high and low energy usage in the treatment works and thus the turbine will produce power to match the needs (Gaius-obaseki, 2010).

Furthermore, there can be a positive effect on water quality with the increase of dissolved oxygen concentrations in the effluent stream after hydropower production (Zakkour, et al., 2002). Also, it is environmentally friendly, since it is a renewable energy source, there are no emissions of gases and there is no need for large civil works. It does not require a large dam and there is no flooding of land (Saket, 2008).

The hydropower plant can be placed upstream or downstream from the WWTP. In the first case, the raw wastewater is collected in a water tank and needs a preliminary filtering before entering a penstock that will lead it to the turbine immediately upstream the WWTP. In spite of the existence of a preliminary treatment, frequent maintenance works are predictable in these cases and all mechanical parts should be easily accessible. In the second case, the treated effluent from the WWTP is directed to a penstock or an open channel and goes through an energy converter before being discharged into the receiving water body (Bousquet, et al., 2015).

Some cases already exist around to world of hydropower plants installed in wastewater systems. Switzerland is the country with most installations of this type and the Pelton turbine is the technology most commonly used. Nevertheless, there is a considerable variety of equipment that can be applied, such as hydraulic screws, Francis turbines, Kaplan turbines and pumps as turbines.

2.5 Hydropower schemes in pluvial drainage systems

The sprawl of European cities has been happening since the mid 1950', having become bigger but less compact. In fact the space occupied by urban areas is increasing faster than the population itself, according to the European Environment Agency (EEA), and even in regions where the population is decreasing, urban areas are still growing. The same trend can also be seen in the United States and China (EEA, 2006; EEA, 2011; PLUREL, 2011).

The growth of urban areas implies an increase of impermeable areas, which has a direct impact on rainwater drainage costs and in the complexity of these systems (Neves, 2005; Tingsanchali, 2011). A less adequate management of urban drainage systems can have serious consequences, such as floods or pollution problems. In fact, the intermittent discharges from combined sewer overflows are a major source of water pollution in urban areas (David, et al., 2010).

Hence, the concept of SUDS – Sustainable Urban Drainage System – has emerged to include in the planning of drainage systems other factors such as water quality, social impacts and environmental issues (Santos, 2011). For each particular location, decision makers must study and select the best combination of practices that result in the most cost-effective and achievable management strategy possible (Lee, et al., 2012).

The use of storage ponds is an already frequent solution in SUDS (Santos, 2011). These reservoirs can be built underground or as a lake (Figure 2.3) and allow a controlled discharge of the inflowing volumes of water, reducing the downstream peak flow. The outflow is usually discharged into the environment or lead to treatment plants. However, these water volumes have potential to be used for electricity production before being returned to the water bodies. New solutions for improving the elasticity of water systems, i.e. that maximize the exploitation of the available resources inside the system, are currently emerging, such as micro-hydropower.

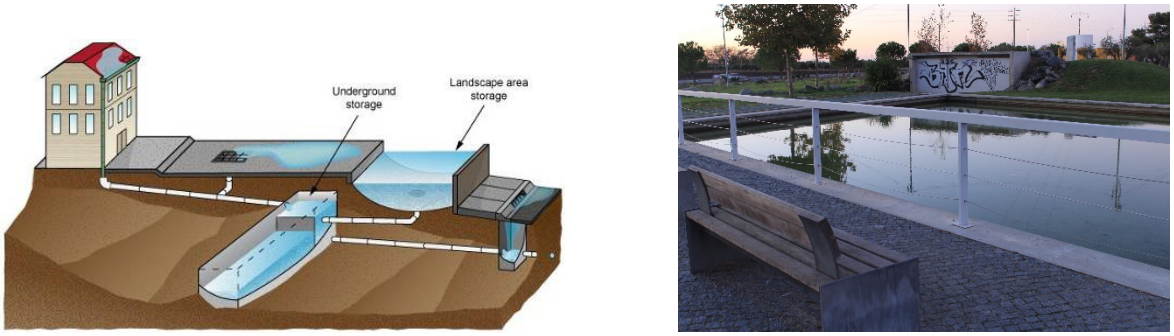

a) b)

Figure 2.3 Types of retention ponds. a) Underground (License to Plumb, 2009); b) Lake.

By installing turbines downstream one or more retention ponds, advantage can be taken from the head created in retention ponds to produce energy (Ramos, et al., 2012). In addition to hydropower production, there are other potential uses for these ponds, such as the storage of water for irrigation or reserve for fire and, in lake type reservoirs, recreational uses and leisure or ecological purposes.

Ramos, et al., 2013a (2013a) have proposed a methodology for the design of storage ponds, in terms of volume and operational water height, in order to maximize the energy production.

2.6 Hydropower schemes in irrigation systems

The agricultural sector is the leader in what concerns water use, representing over 80% of the global water consumption (Valadas, 2002). According to Valadas & Ramos (2003), the application of micro-hydro in irrigation systems can be applied in three conditions: systems that need to transfer volumes of water from a higher point to a lower point; main irrigation channels where there is excess of energy; and systems in which, due to their seasonality, it may be possible to transfer water for other uses such as hydropower production. These systems are usually not pumped and have guaranteed flow in some parts of the year.

There are already a few examples of installations and of small-hydropower schemes in irrigation systems. Wang, et al. (2008) studied the profitability of installing micro-hydropower plants in some selected canals of the Chia-Nan Irrigation Association in Taiwan, Adhau, et al. (2010) studied the installation of micro-hydropower in irrigation sites in India and Suwa (2009) estimated that there is a potential of more than 1.2 TW of electricity a year in irrigation water in Japan. In Portugal, a recent example of implemented small power is the Roxo Dam in the Alqueva region, with 22 MW of installed power, belonging to a scheme of seven small-hydropower schemes (Dias, 2016).

In irrigation channels, there are two types of configuration where a turbine can be installed. If the turbine is installed in line with the channel, the channel needs to be large enough to allow a lateral by-pass. If the channel cannot be enlarged, an intake can be installed. The intake is connected to the powerhouse though a pipeline and the flow returns to the channel downstream. Since, normally, there are no fish in these irrigation channels, there is no need for fish-ways (ESHA, 2005).

The potential for hydropower in irrigation schemes is a current subject of research and recently Pérez-Sánchez, et al. (2016) has presented a methodology to estimate it based on the determination of the demand and EPANET for network modelling.

2.7 Hydraulic machines for small heads

The turbine technology for micro-hydropower is still largely unexplored. Conventional turbines are often not cost-effective for micro-hydro, mostly due to their large diameters and expensive civil engineering works (Wiemann, et al., 2008; HYLOW, 2010). Many investigators have attempted to use different turbines in the micro production range. However their experience was not much encouraging as it resulted in complicated arrangements and high costs of installation (Jain & Patel, 2014). Consequently, special converters are needed for the exploitation of this source of renewable energy (HYLOW, 2010).

There are several hydropower technologies currently being employed in low-headed schemes. The most frequently used are the water wheels, the Archimedes screw working in reverse, the cross-flow turbine and PAT.

Water wheels have been used since antiquity for conversion of hydraulic energy to mechanical energy. They were originally built of wood, but with the industrial revolution new materials such as iron allowed to improve their efficiency. This technology almost disappeared in the 1950's and 60's, but it is currently gaining a renewed importance for electricity production. There are three basic types of water wheels, depending on the used head differences: overshot water wheels, breastshot wheels and undershot or Zuppinger wheels. Nevertheless, between these basic types, there have been a large number of intermediate forms. Nowadays, all modern wheels employ the potential energy of the water and are built in steel. (Müller, 2004).

In overshot water wheels (Figure 2.4), the water is caught in 'buckets' or cells which are formed in a way so that the water jet from the inflow can enter each cell at its natural angle of fall. The outflow is located at a very low level. The cells are designed as narrow as possible, so that the weight of the water can become effective almost immediately, and should only be filled with up to 30 - 50% of its volume, to avoid losses. The opening of each cell is slightly wider than the jet, so that the air can escape. This shape of the cells retains the water inside until the lowermost position. For the design of this type of wheel, the diameter is determined by the head difference, although it has to be decided whether the wheel will be operated with free or regulated inflow since this affects the available head. The wheel speed and the number, depth and shape of the cells then has to be determined as well as the width of the wheel for a given design flow volume and wheel speed. The inflow detail with or without a sluice gate has to be designed so that the design flow volume can be guided into the wheel (Müller, 2004).

The Zuppinger or undershot wheel (Figure 2.5) was developed in the 1850's and can be used for very small head differences (0.5 – 2.5 m) and large flow volumes (0.5 to 0.95 $m^3/s/m$). This wheel employs only the potential energy of the flow as the principal driving force and the water enters over a weir, so that the cells can be filled rapidly. The geometry of the blades was designed to avoid losses at the water entry, to gradually reduce the water head in each cell and finally to discharge the water, again, with a minimum of losses (Müller, 2004). Its peak efficiency is 70 to 74%, and power ratings range from 3 to 100 kW. With diameters from 4 to 7.5 m and rotation speed from 3 to 6 rpm, the wheels have a slow speed, which means that expensive gearing is obligatory (HYLOW, 2012).

The breastshot wheels (Figure 2.6) are similar to the undershot wheels, but the inflow enters at a slight depth below the axle (Bresse, 1987). These wheels were developed for head differences of usually 1.5 to 4 m (Müller, 2004). The water enters the wheel with a steep angle to ensure a rapid filling of each cell and the buckets are shaped so that the resultant force acts in the direction of the wheel's motion, and so that the cell walls exit the water downstream at a right angle, to avoid losses. The cells are ventilated in order to let the air escape during inflow, and to let air into the cell when the cell starts to rise again above the lowermost point (Müller, 2004).

The Archimedes screw is a technology for pumping that exists since antiquity. Its application in reverse operation has led to more research on its efficiency and optimal configurations. It consists of a helical screw that can be applied on rivers with low heads (Müller & Senior, 2009; Lyons, 2014). Schleicher, et al. (2014) proposed a geometry of the blades optimized by CFD analysis in which a peak efficiency of 72% was reached.

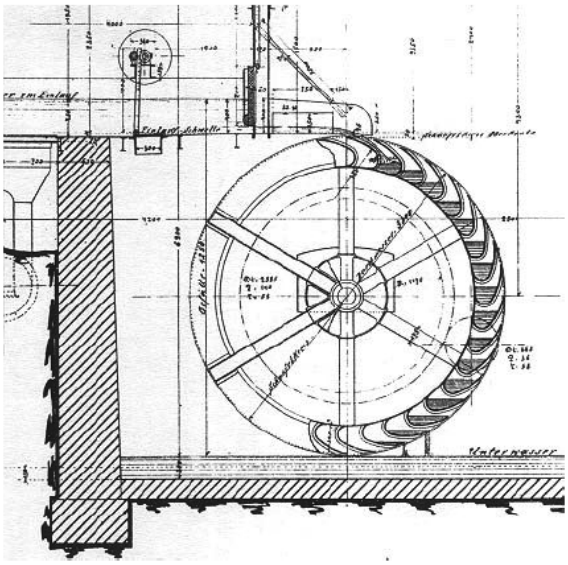

Figure 2.4 Overshot water wheel (adapted from Müller (1899)).

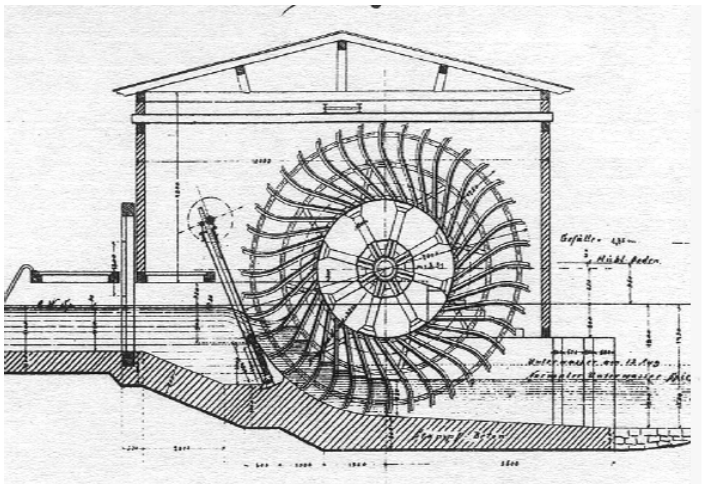

Figure 2.5 Zuppinger (or undershot) water wheel (adapted from Müller (1899)).

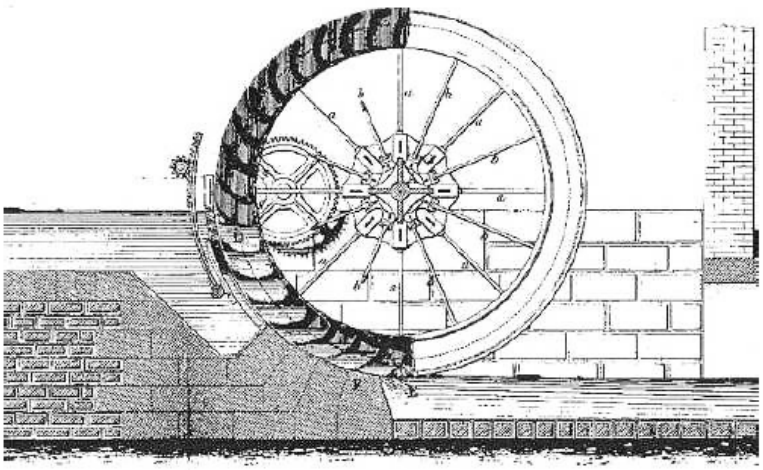

Figure 2.6 Breastshot wheel (adapted from (Fairbairn, 1874)).

A PAT is a hydraulic pump running in reverse mode so that, in conjunction with an induction generator, it recovers energy. The mass production of pumps and its smaller complexity makes them a low cost solution (Ramos & Borga, 1999; Ramos, 2000; Carravetta, et al., 2012; Carravetta, et al., 2013; Jain & Patel, 2014). In fact, almost all centrifugal pumps, both radial and axial flow, can be operated in reverse (Thode & Azbill, 1984). Figure 2.7 shows the range of application of different PATs. There are, however, a few exceptions. Self-priming pumps cannot be used in turbine mode due to the presence of non-return valve. Dry-motor submersible pumps containing fin cooling arrangement for the motor are also not suitable for turbine mode operation due to overheating. Wet-motor submersible borehole pumps usually contain a non-return valve (Jain & Patel, 2014).

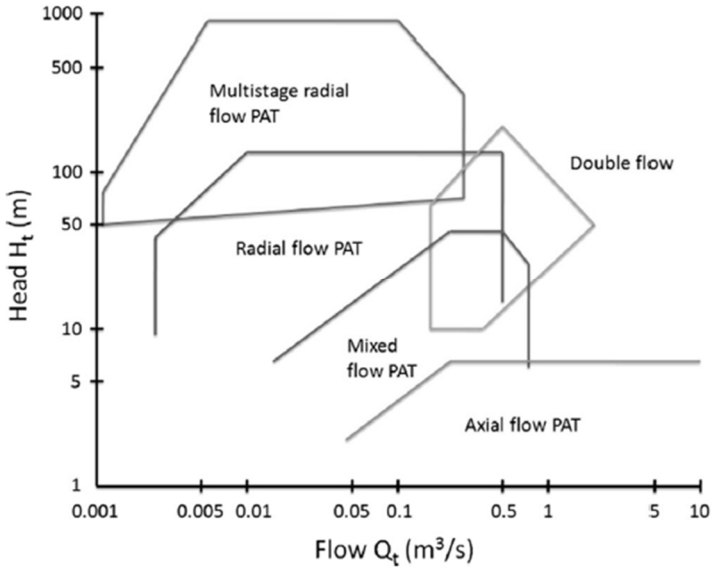

Figure 2.7 Operating heads and flows of PATs (adapted from Jain & Patel (2014)).

An advantage in the use of a PAT is the fact that its technology has been explored with positive results. According to the manufacturers, it is possible to use PATs with relatively high efficiency, up to 85% (Ramos, et al., 2010a). Other advantages are the availability for a wide range of heads and flows, short delivery time, availability in a large number of standard sizes, ease of availability of spare parts, easy installation (Jain & Patel, 2014). Nevertheless, the main disadvantage of using a PAT is the difficulty of finding the characteristics needed to select the correct pump for a particular site. Fixed flow rate PATs are only suitable for sites where there is a sufficient supply of water throughout the year (Williams, 1996) and there is still no standard design criteria available for highly variable flow-rates and pressure heads (Carravetta, et al., 2012). The efficiency of a PAT is very sensitive to changes of flow, which means that an inappropriate pump selection will result in an undesired output, and ultimately in the failure of the project (Ramos, et al., 2009a). In situations where multiple discharge values are plausible, it is also possible to consider the use of two or more PATs (Caxaria, et al., 2011; Fecarotta, et al., 2015).

The geometric parameters of a pump are designed to rotate in a certain direction. When the operation is reversed, head losses are meant to appear in the passage through the blades that cause

a loss of efficiency (Viana, 2012). The relationship between the machine's efficiency working as a pump and as a turbine is, therefore, not direct. Also, rarely do pump manufacturers offer performance curves of their pumps in turbine mode, making it difficult to select a suitable pump to run as a turbine for a particular operating condition.

In a cross-flow turbine, the jet of water of rectangular section enters the top of the rotor through the curved blades, emerging on the far side of the rotor by passing through the blades a second time. The shape of the blades is such that on each passage through the periphery of the rotor the water transfers some of its momentum, before falling away with little residual energy (Paish, 2002). It is usually classified as an impulse or jet-free turbine due to its original design, similar to the Zuppinger wheel. However, with the current design there is a slight positive pressure in the gap between blades in the first water passage (Haimerl, 1960). The efficiencies of this turbine lie between 61 and 91%, and throughout a large range of flow discharge (Walseth, 2009). The cross-flow turbine has outputs between a few kW and 5 MW and net heads from just 2.5 m to 200 m (OSSBERGER, 2016). As it is typical from impulse turbines, the efficiency of the cross-flow does not change greatly with the flow. This attribute can be decisive in sites with strong seasonal changes in the flow (Simão & Ramos, 2010).

Other than these well-known technologies, research has recently been carried for the development of new turbines for low heads. Some examples are herein presented.

The hydroelectricity group in University of Applied Sciences and Arts Western Switzerland in Sion (HES-SO VS) and the Laboratory of Hydraulic Machines (LMH) at the École Polytechnique Fédérale de Lausanne (EPFL), Switzerland, have designed and developed an axial counter-rotating turbine to be installed inline pipes. Numerical simulations were performed with ANSYS CFX and three prototypes were built for laboratory testing. The first turbine prototype with a 50 mm radius was designed to recover 10 m on each runner for 8.7 l/s at the best efficiency point (Münch-Alligné, et al., 2014) and tested in an elbow configuration at EPFL-LMH. A second prototype in a bulb configuration has been developed and tested by the Hydroelectricity group of the HES-SO VS. The bulb configuration is particularly interesting as it allows encapsulating the two generators, one for each runner, internally (Melly, et al., 2014; Biner, et al., 2015). Now a multi-stage "straflo" design is under development to provide a family range of turbines from 5 to 25 kW.

The free vortex propeller was designed by Sing & Nestmann (2009) to recover gross heads from 1.5 to 2 m for open channel flows. The blades of the propeller were optimized using the free vortex theory considering flows from 60 to 75 l/s. An experimental test-rig was assembled and tests were satisfactory, resulting in 810 W of maximum power with 73.9% of efficiency.

A flexible foil vertical axis turbine has been studied by Zeiner-Gundersen (2015) for river, ocean, and tidal applications. Its flexible behavior was inspired on the dynamic characteristics of aquatic animals. A model with 9 m of diameter was tested, with five wings connected to a 7 m tall central

main shaft holding the blades. Its best efficiency of 0.37 was achieved for a velocity of 0.79 m/s and up to 17 kW were generated.

Within the scope of the EU-Project HYLOW (HYdropower converters with very LOW head differences, 2008 to 2012), which was aimed at studying new hydropower converters for very low head differences, a few designs were proposed:

- The Rotary Hydraulic Pressure Machine (RHPM), developed in the University of Southampton, in the UK. This machine has a wheel with a diameter between 1.5 m and 7.5 m which rotates about a horizontal axis. It was envisaged that the RHPM could be employed with fall heights under 5 m in any conventional diversion or run-of-river installation and would also be particularly suited for installation into bays of existing weir structures (Senior, et al., 2008).

- The Hydrostatic Pressure Machine (HPM), also developed in the University of Southampton, for river applications with head differences between 1 and 3 m. Prototypes of this converter were investigated, including a full-scale one installed in a river (Andreev, et al., 2012).

- The Free Stream Energy Converter (FSEC), inspired by boat mills, was tested at various scales at the University of Rostock, in Germany. Its application is also envisaged for small rivers (Batten & Müller, 2011).

- And a Five Blade Tubular Propeller (5BTP), developed in Instituto Superior Técnico (IST), in Portugal (HYLOW, 2010) and which will be further developed in this research (see Chapter 4).

2.8 Basic equations for turbo machines

Hydraulic machines are devices that allow transmissions between hydraulic and mechanical energies. Depending on the direction of that transformation, the machine is either a turbine or a pump. According to their mechanical characteristics, the hydraulic machines can also be divided in turbo, volumetric engines and water wheels.

In turbo machines, the movement is circular and there is an interaction between the blades of the runner and the fluid. The turbo turbines are divided in two types: impulse and reaction. In impulse turbines, the runner is set into motion by the fluid at atmospheric pressure both before and after contact with the blades. On the contrary, in reaction turbines, there is a change of the fluid's pressure as it passes through the runner (Quintela, 1981). In this way, the reaction turbines use the oncoming flow of water to generate hydrodynamic lift forces to propel the runner blades. Their runner always functions within a completely water-filled casing (Khan & H., 2009). The reaction turbines and the pumps can also be classified according with the relation between the movement direction and the runner: radial, axial or mixed.

For a given available head H_u (m) given by the difference of energy between the upstream and downstream sections of the turbine, the power provided by the flow Q (m^3/s) to the machine is

$$P_h = \rho g Q H_u \tag{2.1}$$

where ρ is the water's density (kg/m^3). The power in the turbine's wheel is given by its angular velocity ω and its torque Γ:

$$P_{mec} = \omega\Gamma = \frac{2\pi N}{60} \cdot T_{mec} \tag{2.2}$$

where N is the rotation speed (rpm) and T_{mec} is the mechanical torque (Nm). P_h is bigger than P_{mec}, since there are energy losses inside the turbine. Thus, the hydraulic efficiency can be obtained by:

$$\eta_h = \frac{P_{mec}}{P_h} \tag{2.3}$$

Considering the movement of a water particle inside the turbine's runner, one can define for each instant a velocity triangle composed by the absolute velocity V, the relative velocity W and the peripheral velocity C (Figure 2.8).

$$\vec{V} = \vec{W} + \vec{C} \tag{2.4}$$

Considering that index 1 corresponds to the upstream section and index 2 corresponds to the downstream section of the runner, the torque is given by:

$$\Gamma = \rho Q (V_1 r_1 \cos\alpha_1 - V_2 r_2 \cos\alpha_2) \tag{2.5}$$

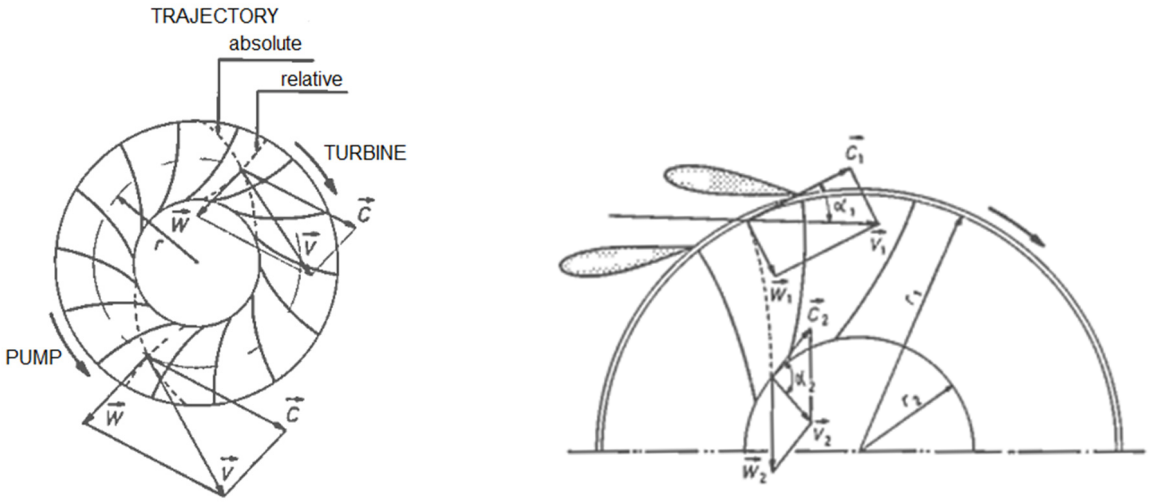

a) b)

Figure 2.8 Velocity triangles. a) Radial turbine/pump; b) Axial turbine (adapted from (Quintela, 1981)).

Replacing in Equation (2.3), the efficiency can be defined as

$$\eta_h = \frac{\rho Q(V_1 \omega r_1 \cos\alpha_1 - V_2 \omega r_2 \cos\alpha_2)}{\gamma Q H_u} =$$
$$= \frac{V_1 C_1 \cos\alpha_1 - V_2 C_2 \cos\alpha_2}{g H_u} = \quad (2.6)$$
$$= 2(v_1 c_1 \cos\alpha_1 - v_2 c_2 \cos\alpha_2)$$

where v_i and c_i are specific velocities that relate the real speeds with a Torricelli-bared velocity.

$$v = \frac{V}{\sqrt{2gH}}$$
$$c = \frac{C}{\sqrt{2gH}} \quad (2.7)$$
$$w = \frac{W}{\sqrt{2gH}}$$

The condition of equal efficiency for two geometrically similar turbo machines can be expressed by the equality of specific velocities.

$$v = v'$$
$$c = c' \quad (2.8)$$
$$w = w'$$

From these equalities, we can deduce that

$$V/V' = C/C' = W/W' = (H/H')^{1/2} \quad (2.9)$$

The relation between C throughout a circumference with diameter D and the number of rotations per minute n allows concluding that

$$\frac{n}{n'} = \left(\frac{H}{H'}\right)^{1/2} \frac{D'}{D} = \left(\frac{H}{H'}\right)^{3/4} \left(\frac{Q'}{Q}\right)^{1/2} = \left(\frac{P'}{P}\right)^{1/2} \left(\frac{H}{H'}\right)^{5/4} \quad (2.10)$$

The same logic can be applied to the same machine ($D = D'$),

$$\frac{n}{n'} = \left(\frac{H}{H'}\right)^{1/2}$$
$$\frac{Q}{Q'} = \left(\frac{H}{H'}\right)^{1/2} \quad (2.11)$$
$$\frac{P}{P'} = \left(\frac{H}{H'}\right)^{3/2}$$

When choosing a turbo-machine, the most important parameters are the flow Q, the head H, the installed power P, the efficiency η, and the rotational speed, n. These parameters can be linked through performance or characteristic curves. As can be demonstrated by Equation (2.11), if there is a change in the rotation speed, the head and flow must also be modified in order to obtain the same efficiency. Efficiency is dependent on the rotation speed and performance curves at different speed are known as hill charts, where points of constant efficiencies are extended into contour lines around the best efficiency point (BEP), which represents the operating conditions (N, Q, n) with maximum efficiency – Figure 2.9. There are two operating points that are also important to mention: the no-load and overspeed. When in a no-load condition, the flow rate is too low for producing any power. In an overspeed situation, the turbine is fully open and disconnected from the generator, which leads to the runner rotating without any constrain. No power is produced, and the rotation speed usually rises with the head.

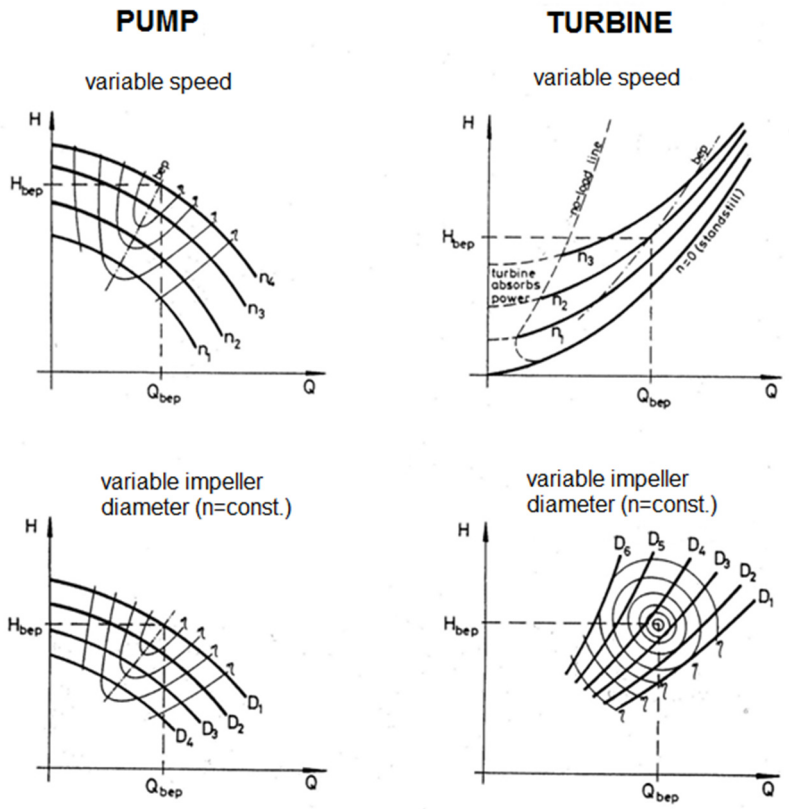

Figure 2.9 Hill charts considering radial machines (adapted from (Chapallaz, et al., 1992)).

2.9 Economic analysis

To infer the feasibility of any small-hydropower project an economic analysis is needed. This analysis is usually based on the estimation of costs and revenues over an expected period of operation. The profitability is then evaluated considering economic indexes that allow comparing between different solutions. Among these, the net present value (NPV), the payback period (PP) and the average cost price of the kWh (CP) are considered in this study.

The economic analysis of a small-hydropower scheme foresees investment costs and revenues over a certain period of time, nevertheless their respective estimates are based on market prices referred to the year in which the study is carried (Portela, 2000). To take into account the inflation, which is the increase in the general price of goods and services over time, and other effects such as interest rates, the state of economy, risk of investment, the future value of monetary fluxes can be transposed to the present time by means of a discount rate. This way, constant market prices are considered and the comparison of costs and benefits is done at present time.

If T_a is the number of years of operation and r the discount rate, one monetary unit of today will be $(1+r)^{T_a}$ monetary units by year T_a and, reversely, one monetary unit in year n will be worth $1/(1+r)^{T_a}$ monetary units today. Hence, the present value of a single monetary flux occurring in year i, C_i, is given by Equation (2.12) and the present value of a sequence of annual monetary fluxes is given by Equation (2.13).

$$PV = \frac{1}{(1+r)^i} C_i \tag{2.12}$$

$$PV = \sum_{i=1}^{T_a} \frac{1}{(1+r)^i} C_i \tag{2.13}$$

If the monetary annual fluxes are constant, the present value of the sequence can be reduced to

$$PV = C \frac{(1+r)^{T_a} - 1}{r(1+r)^{T_a}} \tag{2.14}$$

The NPV of a certain year is an economic index given by Equation (2.15), where all elements are transposed to the year 0 of operation. The bigger the NPV the more profitable is the project. By the end of the expected operation period, n years, the NPV_{T_a} should be positive.

$$NPV = Revenues - Capital\ Costs - Operational\ Costs - Maintenance\ Costs \tag{2.15}$$

The cash flow is the movement of money into or out of the project during a period of time, usually a year. Hence, the NPV is the cumulative cash flow, transposed through the discount rate to the year 0.

The payback period, PP, represents the number of years it takes before cumulative forecasted cash flows equal the initial investment (Portela, 2000). The cost price of the kWh, CP, represents the ratio between the present value of all costs and average annual energy produced (E_{annual} in kWh). If this indicator is lower than the nominal unitary energy-selling price, the project is considered profitable (Portela, 2000).

$$NCP = \frac{(Capital\ Costs + Operational\ Costs + Maintenance\ Costs)}{\frac{(1+r)^{T_a} - 1}{r(1+r)^{T_a}} E_{annual}} \tag{2.16}$$

2.10 Incentive policies for small-hydropower

2.10.1 Types of incentive policies

From an economical point of view, small-hydropower schemes also have the advantage of benefiting in many countries from policies favorable to renewable energies. There is a generalized acceptance of the importance of promoting renewable energy sources to ensure environmental protection and sustainable development (Romero, et al., 2012). In fact, incentive policies exist in virtually all high energy-consuming countries and support for renewables is likely to reach also the developing countries (Donovan & Nuñez, 2012).

There are several ways for a government to promote renewable energies. The objectives may be seen from a perspective of decreasing greenhouse gas emissions or of ensuring energy security (IEA, 2004). In practice, the main policy instruments may be divided into five groups: subsidies or tax incentives, where fiscal reductions of costs exist for consumers or producers; renewable energy funds, which finance producers through fund transfers, market applications or research; voluntary green schemes, where the consumers are mobilized to prefer renewable energies; green certificate schemes where there is an obligation for the consumers to use certified renewable energies; and price-based instruments, which are financial schemes that ensure a premium payment to renewables (Gan, et al., 2007).

Concerning price-based instruments, the feed–in tariffs guarantee the exploiter of renewable electricity a certain price to sell each kWh over a long period of time, commonly 20 years. Another modality is the feed-in premiums, in which a premium above the average spot electricity market price is offered (ESHA, 2012).

In 2012, 21 countries of the UE had either one of the modalities or a combination of the two (ESHA, 2012). Switzerland, Turkey, Serbia, Bosnia and Herzegovina and Montenegro also have feed–in tariff schemes. In the USA, 15 states have a green certificate scheme, in which the percentage of sales of electricity coming from renewable sources is required to gradually increase (Gan, et al., 2007). In Canada there are funds for research and development, but also a feed–in tariff in Ontario, green certificate schemes in Prince Edward Island and Nova Scotia and tax reliefs nationwide to renewables. In Asia, most countries, such as China, Japan, Indonesia and Thailand, have feed–in tariff schemes. The same happens in Africa, in Egypt, Algeria, Nigeria and Ghana. In South America the policies are more dispersed; Uruguay, Ecuador have feed–in tariff schemes, Argentina has a Fiduciary Fund and tax reliefs and Brazil has energy auctions. Both Australia and New Zealand have market-based instruments (IEA, 2015).

It is worth however to mention that the feed-in-tariffs regulations vary considerable between countries and, for example, in UK a micro-hydropower plant downstream from any pumping station is not eligible for the subvention.

These policies should be considered when analyzing unconventional renewable sources, as they can have a significant impact on their feasibility.

2.10.2 The Swiss feed–in tariff scheme

In Switzerland and for the particular case of hydropower plants, the feed–in tariff scheme is based on three parameters: the installed power, the head and the investment on hydraulic works. The tariff (t in CHF/kWh) is hence composed by three elements:

$$t = Base + Bonus_{head} + Bonus_{hydraulic\ works} \quad (2.17)$$

The $Base$ tariff is dependent on the installed power according to Table 2.1. This $Base$ tariff is only applicable on installations where the water course is already in use or on installations where the energy production is not the main goal of the system. For new fluvial installations, the base tariff has other values and classes. All presented values were approved in January 1st 2014.

The $Bonus_{head}$ is based on the total head of the installation, not comprising head losses. It is also divided in sub-classes, as presented in Table 2.2

Finally, the $Bonus_{hydraulic\ works}$ is given if there has been a rehabilitation of the hydraulic works, according to Table 2.3. Nevertheless, if these works represent less than 20% of the project costs, then the bonus is not given. Also, if they represent more than 20% but less than 50%, the bonus is not entirely applied and is given by a linear interpolation as shown in Figure 2.10.

Table 2.1 Base tariff for hydropower plants in man-built systems in Switzerland (SFC, 1996; SFC, 2014).

Installed power	Base (ctsCHF/kWh)
≤ 10 kW	31.3
≤ 50 kW	23.1
≤ 300 kW	15.6
≤ 1 MW	10.8
≤ 10 MW	6.0

Table 2.2 Bonus for head class in hydropower plants in Switzerland (SFC, 1996; SFC, 2014).

Head (m)	$Bonus_{head}$ (ctsCHF/kWh)
≤ 5	6.1
≤ 10	3.7
≤ 20	2.7
≤ 50	2.0
> 50	1.3

Table 2.3 Bonus for hydraulic works in hydropower plants in man-built systems Switzerland (SFC, 1996; SFC, 2014).

Installed power	$Bonus_{hydraulic\ works}$ (ctsCHF/kWh)
≤ 10 kW	7.5
≤ 50 kW	5.4
≤ 300 kW	4.1
> 300 kW	3.4

The total time of the feed–in tariff is 15 years and there is a maximum tariff value of 0.4 CHF/kWh independently of the bonuses.

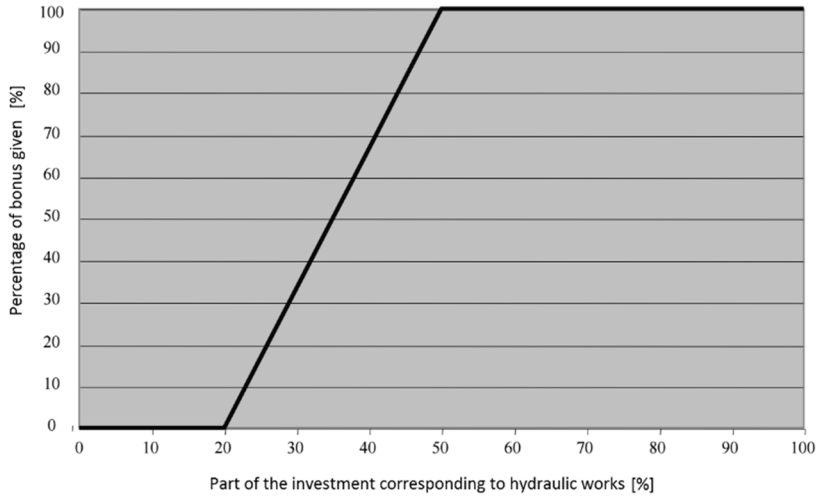

Figure 2.10 Interpolation for bonus for hydraulic works in hydropower plants in man-built systems Switzerland (SFC, 1996; SFC, 2014).

2.11 Summary of the state-of-the-art and assessment needs

There are clear advantages in the exploitation of micro-hydropower in man-built environment. Firstly, there are small or non-existing environmental impacts; secondly, money saving from the use of already existing equipment, construction and electric connections is possible. Within the identified man-made systems in which it is possible to install a micro-hydropower scheme, the WSS present some advantages. These are pressurized systems, where the turbine operation can be done within the existing pipes with some modifications. Also, the flow discharges are guaranteed during most hours of the day, although low consumptions may be verified during the nights, which are not dependent on the weather. Moreover, the proximity of the installations to local consumers allow for a decentralized production, minimizing the transmission losses.

Hence, the development of a turbine for inline installation in a pressurized pipe adapted to low head operations and relatively small flow discharges is particularly interesting for drinking WSNs. However, since the ideal location of an arrangement of turbines in a meshed urban network is not straightforward, there is need for simulation and optimization in the identification of the best solutions. Also, conceptual construction solutions are needed to guide practitioners in the detailed design for implementation of micro-hydropower plants. Finally, the potential assessment of the existing systems for micro-hydropower is nonexistent and hence there is a lack of knowledge on how much energy could be recovered from urban WSNs. The main body of the report covers these needs with conceptual proposals.

Chapter 3
Description of case studies

3.1 Introduction

In this Chapter, six case studies are presented which will support and be used to test the methods and algorithms developed in this research. In sub-chapter 3.2 is described the Portuguese Beiriz Power Plant, which will be used for testing the algorithms concerning turbine operation upstream from a storage tank developed in sub-chapter 5.2. In sub-chapters 3.3, 3.4 and 3.5 are presented three water supply networks, the first two sub-grids of the water supply system of the Swiss city Lausanne and the last one the complete water supply network of the Swiss city Fribourg. These case studies will be used both in chapter 5 and chapter 6 to test the developed algorithms and validate the interest of micro-hydropower. Finally, sub-chapter 3.6 presents the Portuguese Beliche Power Plant, in which is installed a PAT. This machine will be compared in sub-chapter 5.4 to the 5BTP turbine studied in this work.

3.2 Beiriz Power Plant

The Beiriz Power Plant is being installed upstream from the Beiriz storage tank, in North of Portugal (Figure 3.1), and belongs to a WSS of Águas de Portugal (AdP) in the Póvoa do Varzim municipality.

A storage tank (Figure 3.2) is divided in three cells. One of them inactive (C1) and the other two, C2 and C3, are connected and have together a total capacity of 10000 m^3 (Figure 3.2). The total water height of each cell is 3 m. A cross-flow turbine will be installed by-passing a DN600 valve that controls the intake of the tank. The maximum operating flow of the cross-flow turbine was fixed in 136 l/s and the minimum in 24 l/s. A generation of about 52 MWh/year is estimated in the original project (Cenor, 2011). The turbine is installed upstream from one of the cells (C3) and is set to operate with a constant discharge rate, corresponding either to the average monthly flow or to the maximum operating flow, whichever is the smallest. The average monthly flow should be actualized every year according to the previous records. When the incoming flow is higher than the maximum allowed by the turbine, it is discharged into the other cell (C2).

Figure 3.3 presents the duration curve of average hourly flows, as well as the maximum discharge rate allowed by the turbine.

Figure 3.1 Location of Beiriz (adapted from Ezilion Maps (2015)).

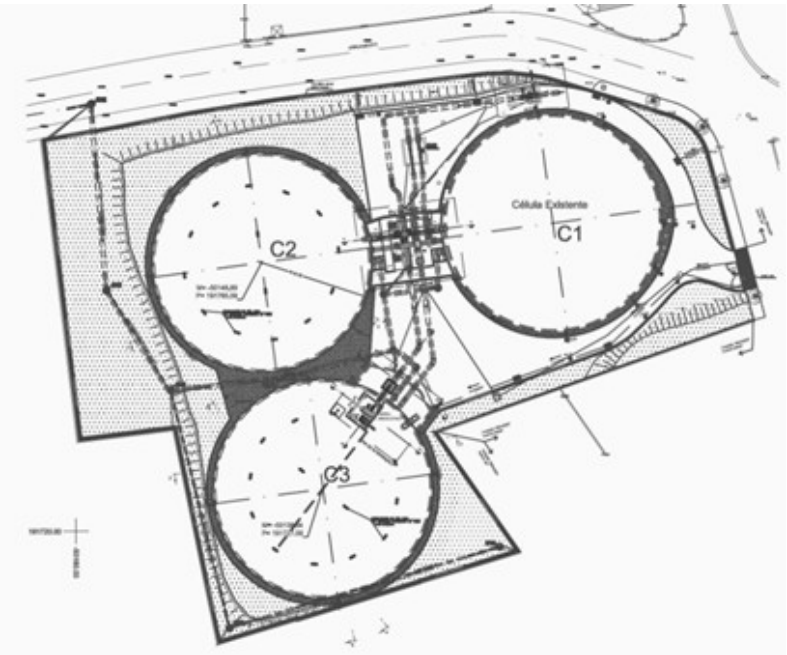

Figure 3.2 Beiriz tank (Cenor, 2011).

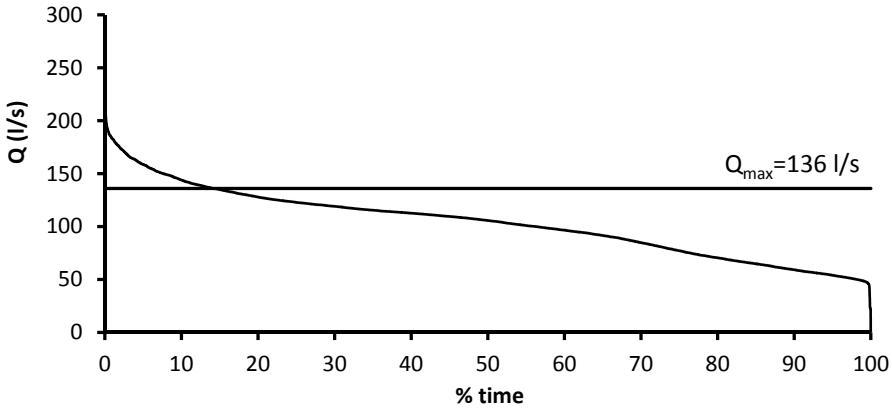

Figure 3.3 Average hourly flow duration curve (Cenor, 2011).

3.3 Lausanne: water supply network 1

A sub-grid of the WSN of the city of Lausanne (Figure 3.4), will be used as case study with a real topography and flow values. The network model was provided by *eauservice*, the water management company of the city, together with hourly flow data from five years of measurements (2009-2013). Some hypothesis were assumed to adapt it to a purely gravity operation.

Figure 3.4 Location of Lausanne, Switzerland (adapted from Ezilion Maps (2015)).

The closed sub-grid considered (Figure 3.5) has 335 branches and 312 nodes, with two boundary nodes represented is the model as a head reservoir and an upstream tank. The tank is a representation of a real infrastructure. The network contains a total of 17 km of pipes and a maximum difference of elevation of 128 m (Figure 3.6). The average hourly inflow is 124 l/s (aprox. 4 hm^3/year). All pipes in the model have a roughness coefficient of Darcy-Weisbach of 1 mm. The diameters range between 61.4 and 1000 mm (Figure 3.7), being 150 mm the most frequent.

3.4 Lausanne: water supply network 2

This second network case study is another sub-grid of Lausanne's WSN, with 126 branches, 117 nodes and a total of 10.5 km (Figure 3.8). This model was also provided by eauservice, the water management company of the city, together with hourly flow data from three years of measurements (2009-2011). A few hypothesis were assumed to adapt it to a closed network, having a downstream node been replace by a node with equivalent consumption.

The maximum difference of elevation is of 120 m (Figure 3.9) and the average hourly inflow to the network is 0.2 l/s (aprox. 6 dam^3/year). All pipes in the model have a roughness coefficient of Darcy-Weisbach of 1 mm. The diameters range between 80 and 204 mm (Figure 3.10), being 150 mm the most frequent.

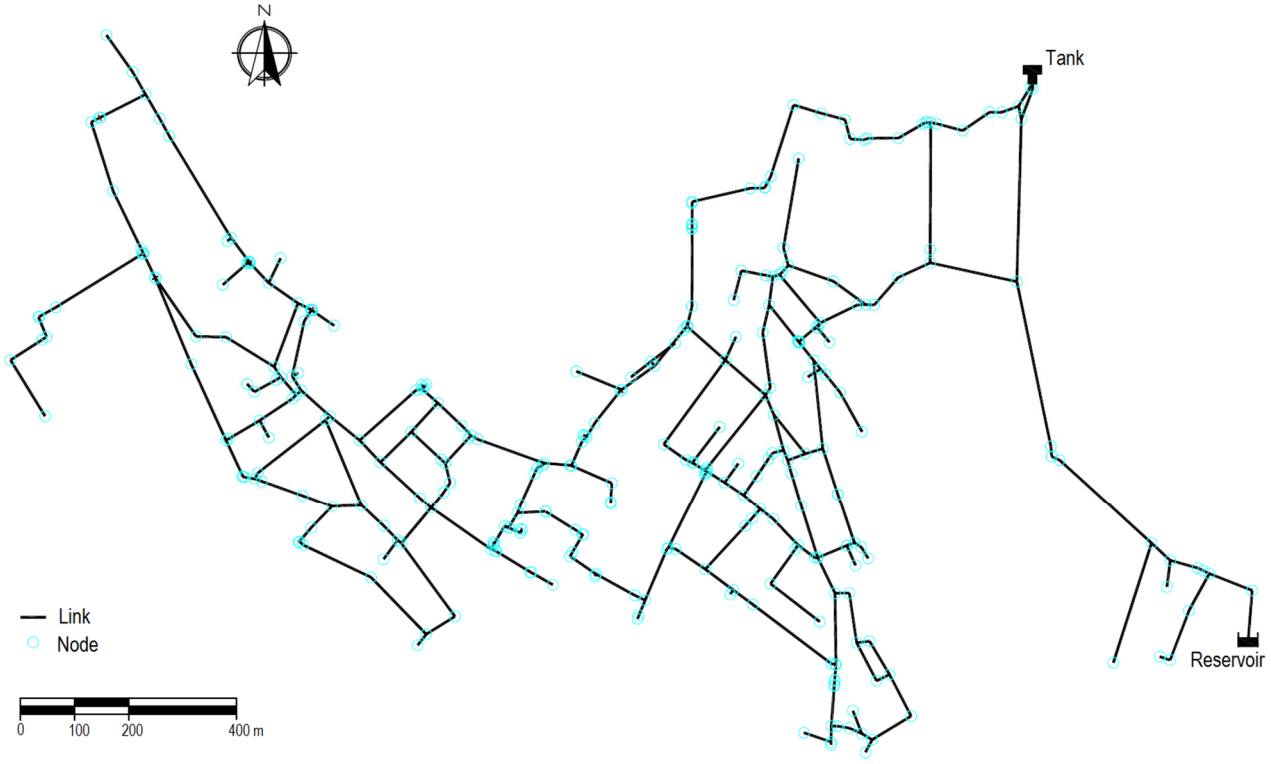

Figure 3.5 Sub-grid 1 of Lausanne WSN.

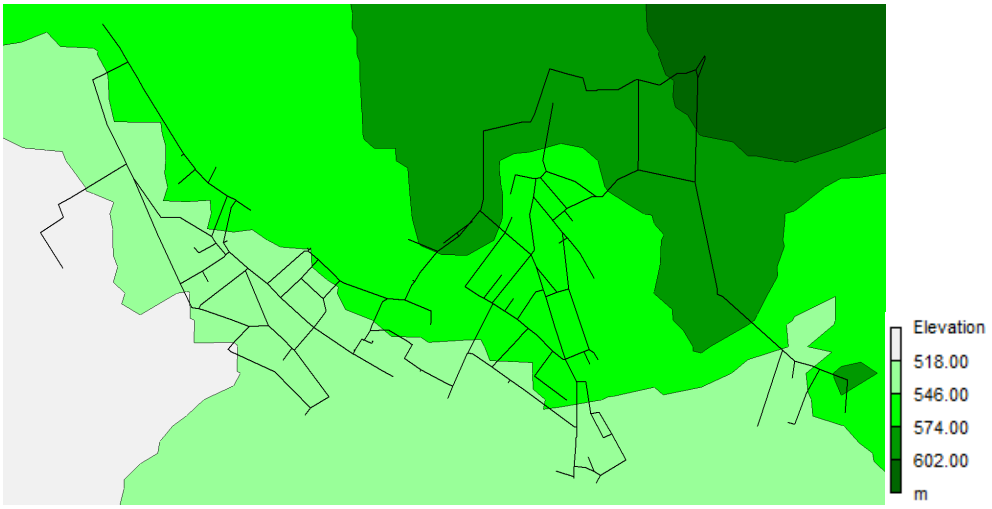

Figure 3.6 Sub-grid and corresponding elevations of sub-grid 1 of Lausanne WSN.

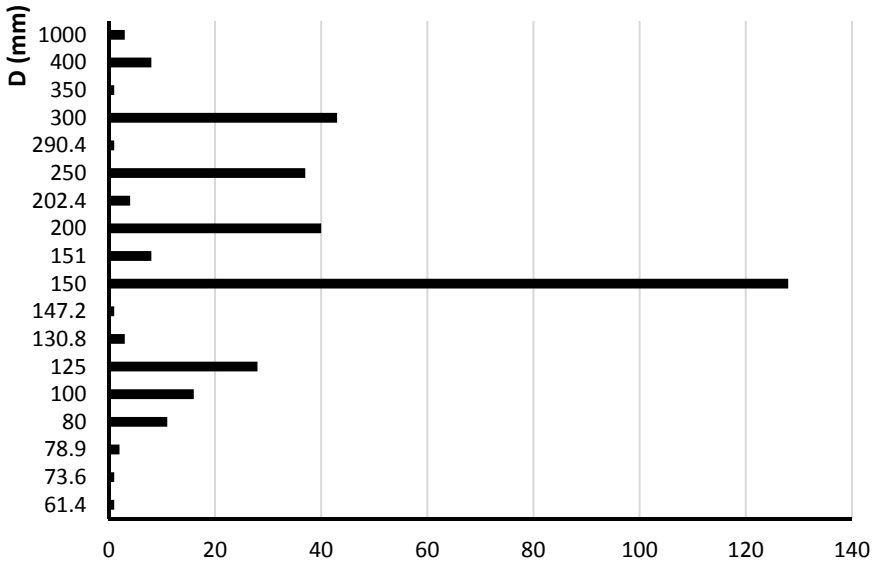

Figure 3.7 Diameters distribution of sub-grid 1 of Lausanne WSN.

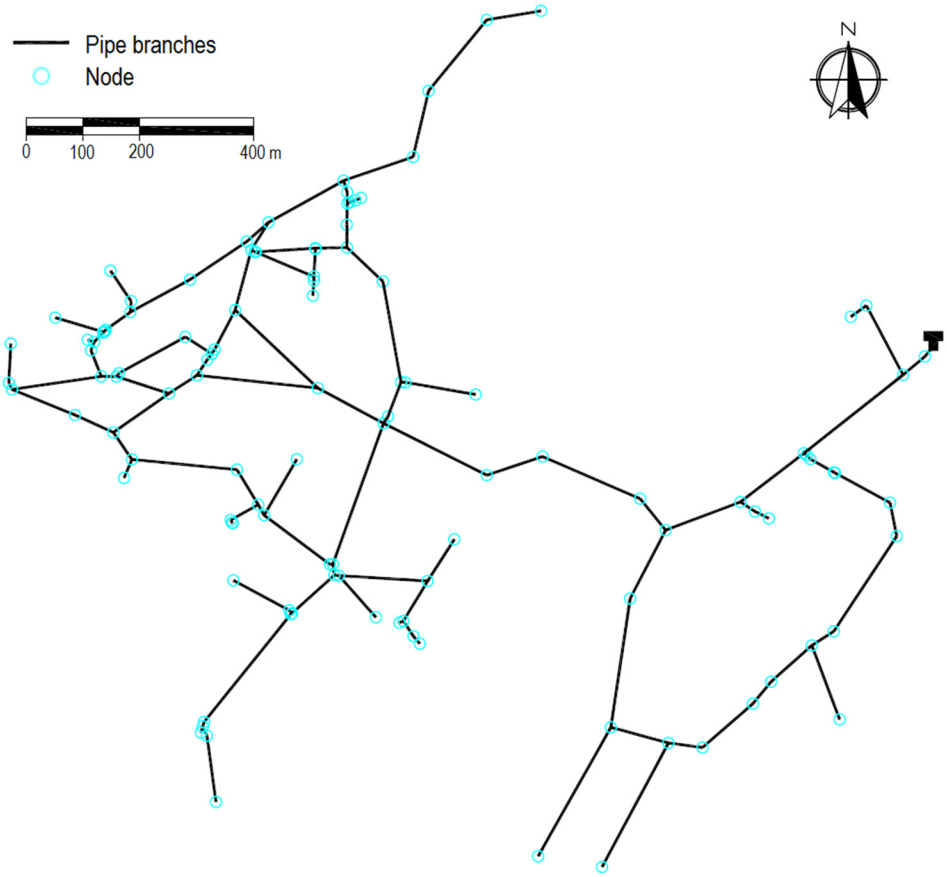

Figure 3.8 Sub-grid 2 Lausanne WSN.

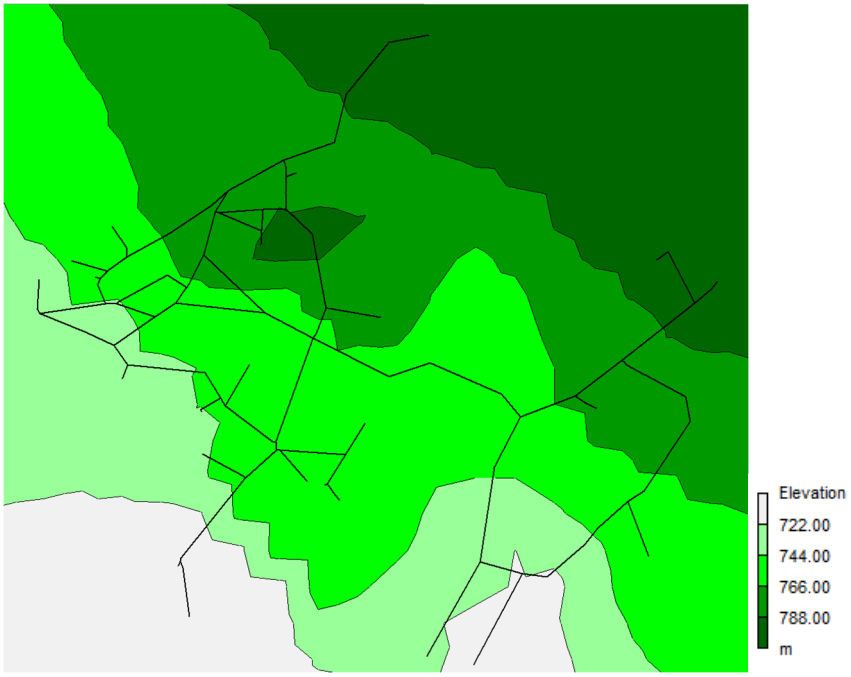

Figure 3.9 Sub-grid and corresponding elevations of the sub-grid 2 of Lausanne WSN.

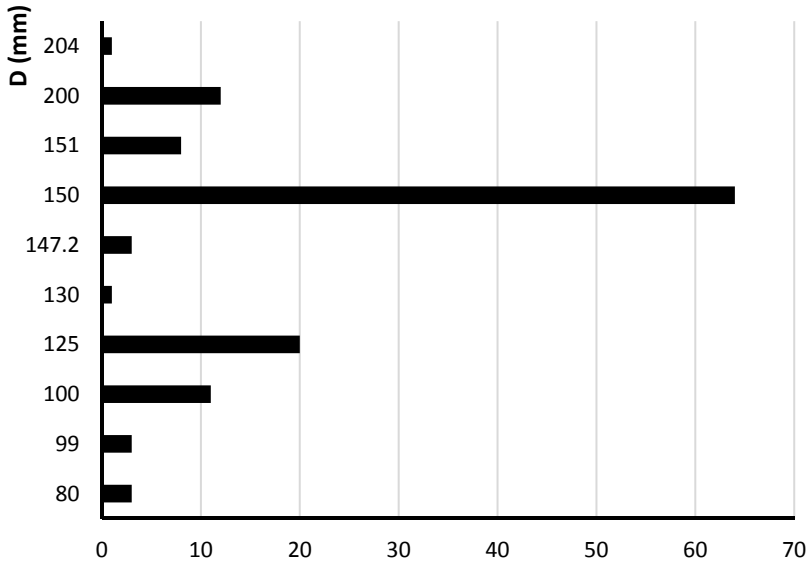

Figure 3.10 Diameters distribution of sub-grid 2 of Lausanne WSN.

3.5 Fribourg

The urban WSN model of Fribourg (Figure 3.11), which can be seen in Figure 3.12, has 2972 links and 2805 nodes covering 135 km and a total elevation difference of 216 m. The population served by the WSN is of about 38 000 persons, making this a small sized European city. The network model, provided by the Industrial Services of Fribourg, possesses nine PRV, seven water tanks/"reservoirs" and four pumping stations. The reservoirs are considered as fixed level sources.

Figure 3.11 Location of Fribourg, Switzerland (adapted from Ezilion Maps (2015)).

All pipes in the model have a roughness coefficient of Darcy-Weisbach of 0.4 mm. The diameters range between 61.4 and 508 mm (Figure 3.13), being 150 mm the most frequent.

The network serves around 39 Mhab. According to the gathered data, an average daily consumption of $Q_{h,average}$ = 0.108 l/s was associated to each node and the daily pattern of consumption presented in Figure 3.14 was applied to obtain an hourly variation.

In its current status, the pumping operations within the model consume 128 MWh/year, according to Table 3.1, considering a total efficiency of 60%.

Table 3.1 Pump operating conditions and energy consumption in the network of Fribourg.

Pump station	H_{med} (m)	Q_{med} (l/s)	P_{med} (kW)	E (MWh/year)
1	80	5.4	7	60
2	45	18.8	13	111
3	60	5.8	6	48
4	58	3.7	3	31
Total	244	33.7	29	250

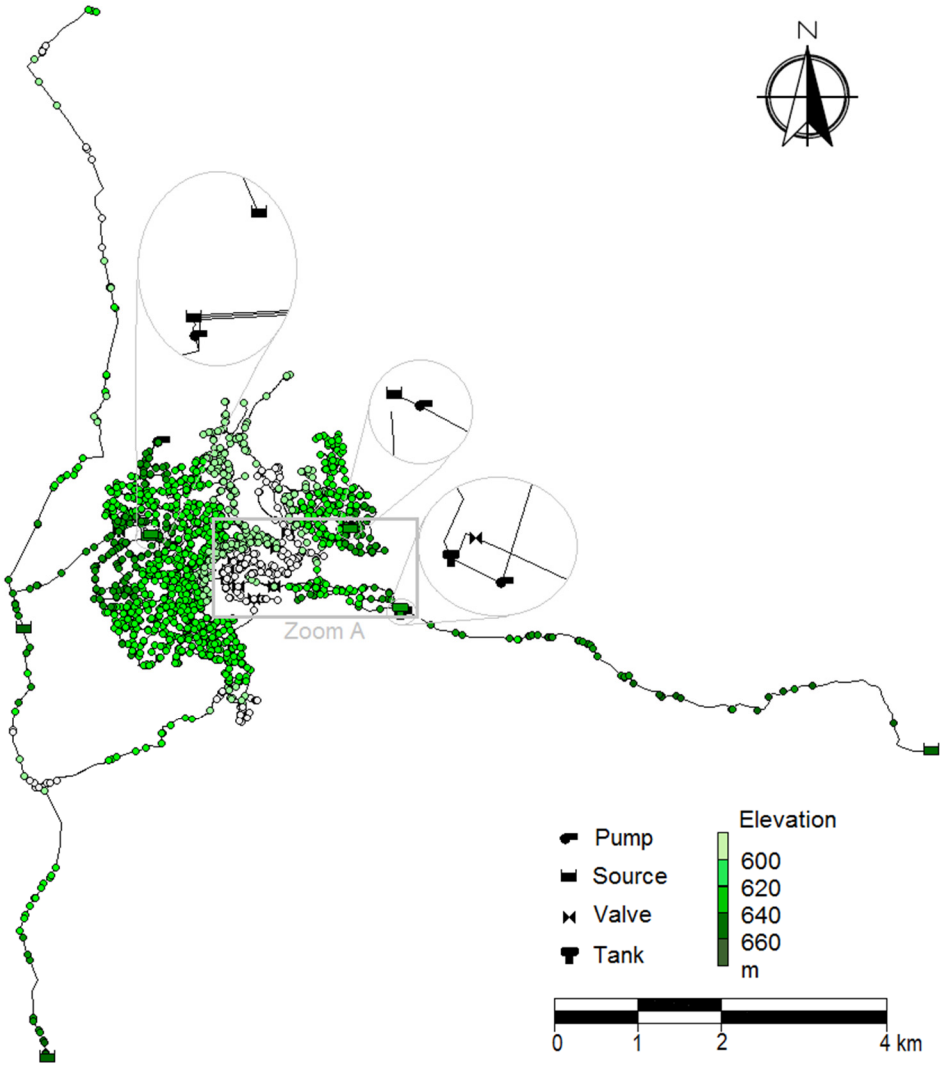

Figure 3.12 Fribourg WSN.

3.6 Beliche

The Beliche dam (Figure 3.15) was built within the Águas do Algarve S.A. Multi-Municipal Water Supply System for irrigation and water supply purposes. Downstream from this dam is the Beliche water treatment plant in which a micro-hydropower station was installed in 2008 and connected to the grid in 2011 (Ramos, et al., 2014).

The micro-hydropower plant has two PAT installed in parallel within an existing valve's chamber, although there's space for a future third PAT to be installed (Figure 3.16). This system is in by-pass to the main pipeline that supplies the water treatment plant.

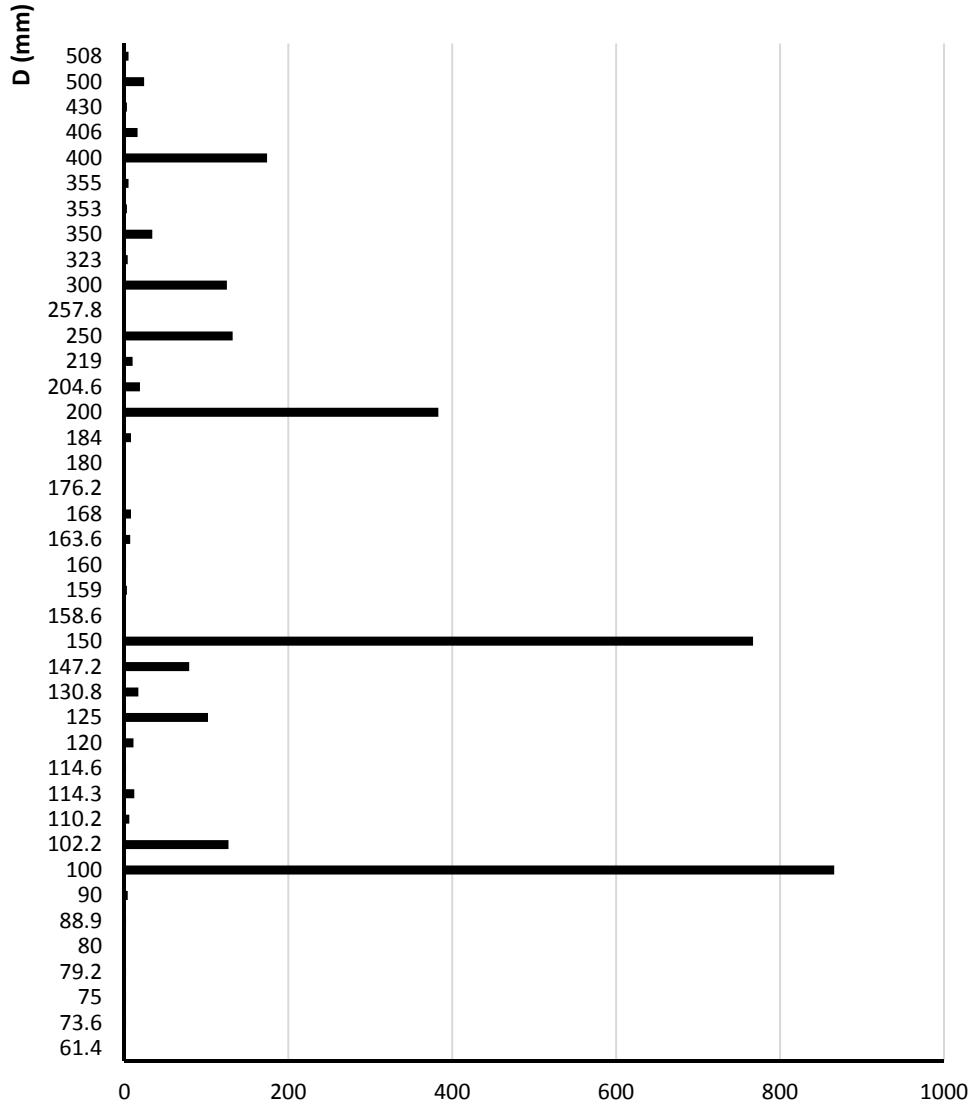

Figure 3.13 Diameters distribution of the Fribourg WSN.

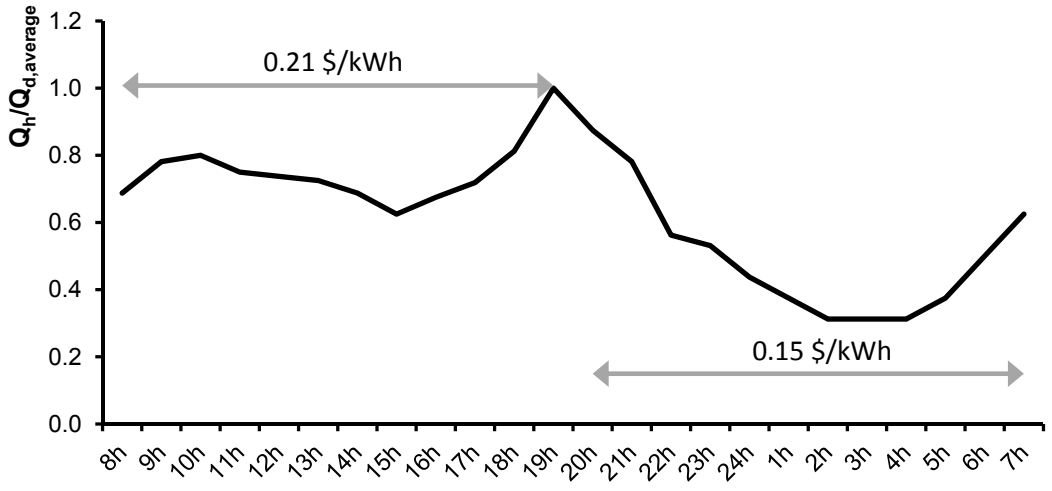

Figure 3.14 Pattern of hourly variation of consumption along the day, adapted from Hickey (2008), with the indication of the energy buy-prices which vary within the day.

Figure 3.15 Location of Beliche (adapted from Ezilion Maps (2015)).

The design head in Beliche hydropower station is 16.3 m and the corresponding flow rate is 96.2 l/s, which is approximately the average inflow discharge. The installed machines are the KSB model ETANORM SYT, with a runner of 160 mm (Ramos, et al., 2014). To obtain the characteristic curves of this model working in reverse operation, a set of experimental tests were carried out in another water treatment plant in the region, in the course of a Master Project in 2013 (Livramento, 2013). These tests were performed under physical and hydraulic conditions similar to those verified in Beliche, using a submersible pump.

The first tests were performed with atmospheric downstream pressure and considering different rotation frequencies. The electric power and the efficiency obtained in this situation are presented in Figure 3.17. Since the frequency that led to the best results (50 Hz) is also the frequency of the national grid, new tests were carried out with 3 m of downstream pressure in order to simulate the height difference between the turbine and the outlet connected to the treatment plant. The obtained results are presented in Figure 3.18.

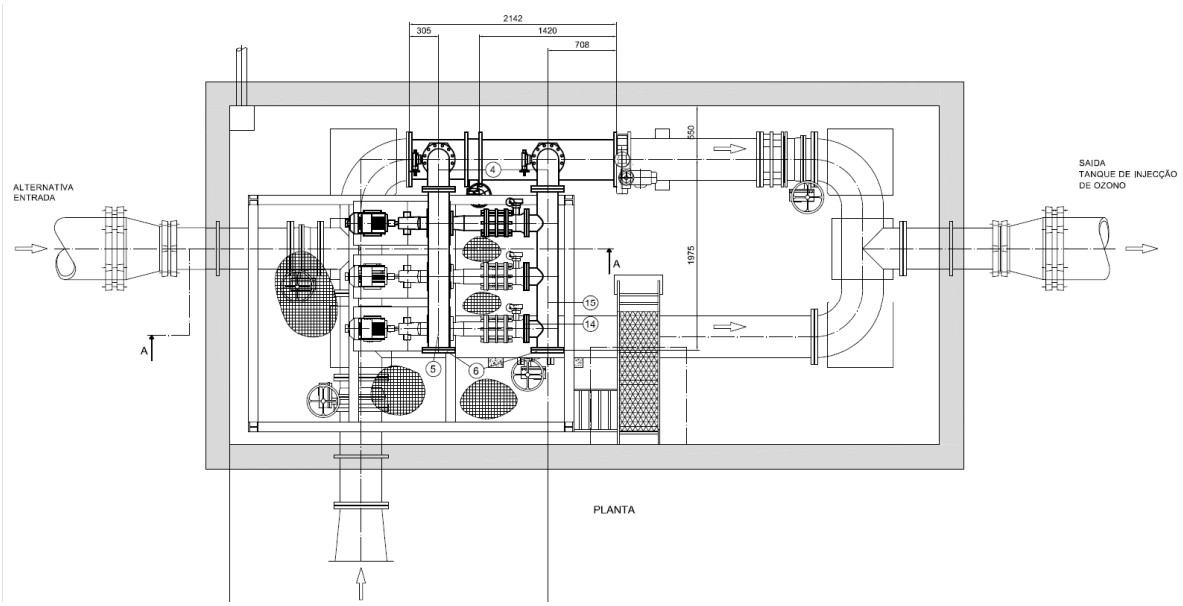

Figure 3.16 Plan view of the Beliche micro-hydropower plant (adapted from Ramos, et al. (2014)).

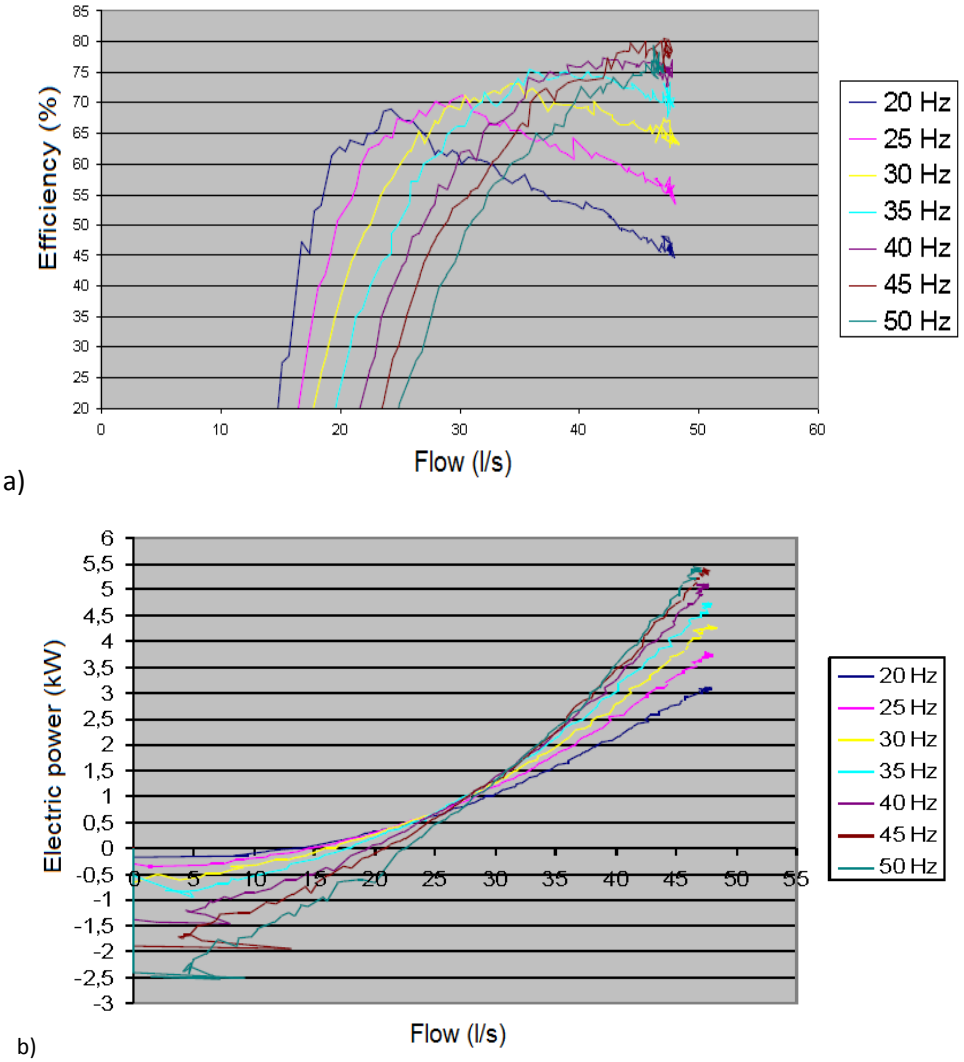

Figure 3.17 Efficiency (a) and electric power (b) curves for atmospheric downstream pressure conditions (adapted from Ramos, et al. (2014) and Livramento (2013)).

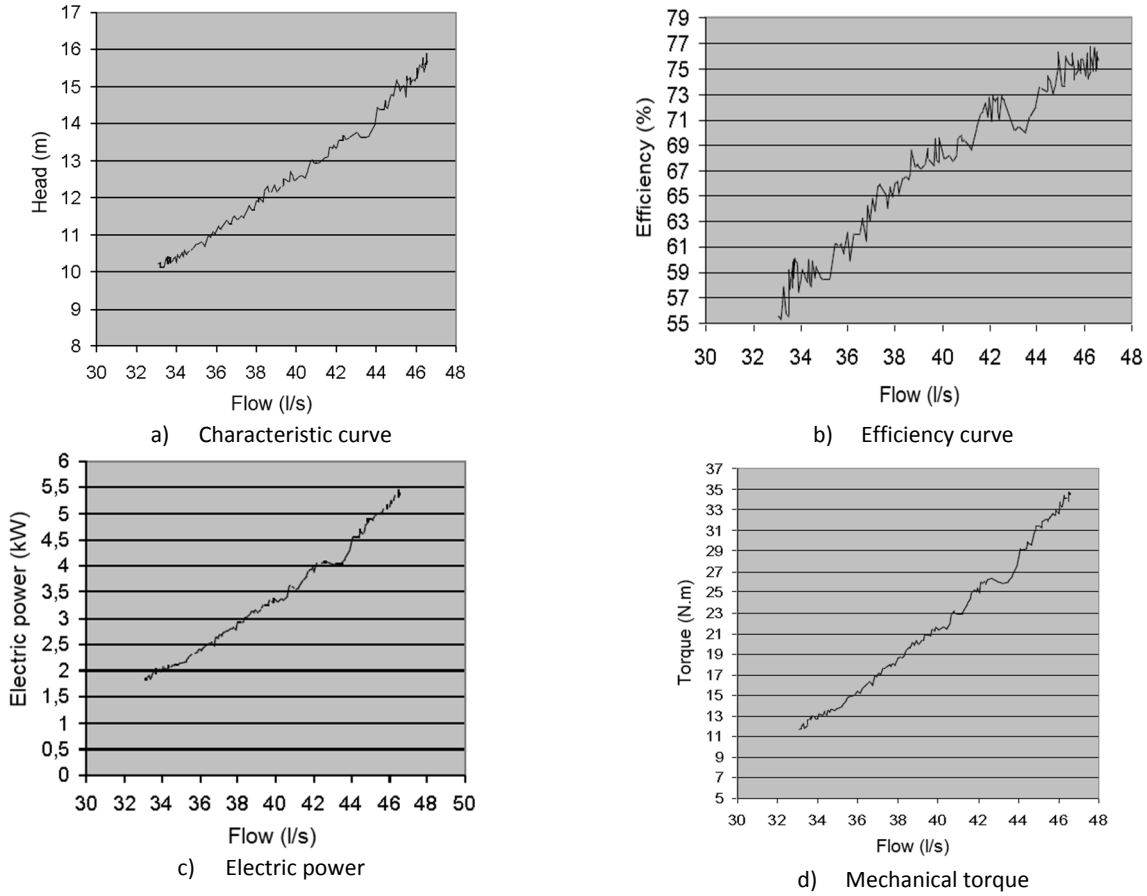

Figure 3.18 Results of the experimental tests for 1500 rpm (50 Hz) and 3 m of downstream pressure (adapted from Ramos, et al. (2014) and Livramento (2013)).

Chapter 4

Experimental characterization of the five blade tubular propeller

Chapter 4 is based on the scientific article "Experimental characterization of a five blade tubular propeller for inline installation" by I. Samora, V. Hasmatuchi, C. Münch-Alligné, M. J. Franca, A. J. Schleiss and H. M. Ramos published in 2016 in Renewable Energy and on the conference article "Energy production with a tubular propeller turbine" by the same authors presented in the 28th IAHR Symposium on Hydraulic Machinery and Systems. The experimental work presented hereafter is original and was performed by the author in collaboration with Dr. Hasmatuchi.

4.1 Introduction

The presented state of the art (sub-chapter 2.7) reveals that research is being carried to design new technologies for micro-hydro since the traditional large-scale turbines are not easily applicable for such low heads and flows. The presented ongoing research can be divided in two main fields of application, for small rivers and for pressurized systems. In the case of pressurized systems, cross-flow turbines, although considered expensive, can work on a wide range of net heads, from 1.75 to 200 m. PAT are less costly but they are sensitive to flow variations. The development of a tubular turbine that can be installed inline in pressurized pipe is thus considered interesting.

The installation of turbines inline a pipe is particularly attractive for applications in WSSs. The present chapter focuses on the presentation of the results of laboratorial experiments from the testing of the 5BTP. The development of this turbine started during the HYLOW Project with numerical simulations and a few primary experimental tests, but laboratorial optimization and validation with wide ranges of discharge and rotational speed were still needed. In sub-chapter 4.2 the background development of the turbine is summarized. The experimental methodology is presented in sub-chapter 4.3, followed by the results in sub-chapter 4.4. In sub-chapter 4.5 the results are discussed and the main conclusions are presented in sub-chapter 4.6.

4.2 Background and optimization of the 5BTP

The HYLOW Project (2008-2012) was a research project funded by the European Commission's 7th Framework Program with the aim of developing novel hydropower converters for very low heads. IST, one of the partners, was involved with the study of small converters for pressurized flows. Initially, turbines and positive displacement concepts were investigated but it was found that positive displacement converters are only suitable for vary small discharges and high heads, leading to unfavorable pressure surges. Therefore, the research on turbines was deepened further for turbines, based on CFD modeling and laboratorial tests.

Propeller turbines are axial turbines that are usually adequate for operation under low head and high flow rates (Caxaria, et al., 2011; Elbatran, et al., 2015). They have been mainly used in small and mini-hydro schemes, but their application for micro-hydro is still at the beginning. Nevertheless, scaling-down from a large turbine cannot be directly applied on this case due to associated scale effects, as it has been verified by Ramos, et al. (2009b), but also because the economic and manufacturing constraints are not the same (Sing & Nestmann, 2009). To overcome this limitation, numerical simulations were done in the FLUENT model, a Navier-Stokes solver, considering different turbine configurations (Ramos, et al., 2009a). A k-ε turbulence model was used and the meshes were generated with a TGrid unstructured mesh technique with refinement in areas of difficult modelling. *TGrid* requires a discretized boundary mesh consisting of triangular and quadrilateral faces in 3D. Four types of boundary conditions were defined: inlet and outlet pressure, impeller, defined as moveable walls with rotational speed around the rotation shaft, and the tubular wall, with the imposition of the condition of impermeability (Simão, 2009; Ramos, et al., 2013b).

The initial geometry of the 5BTP is presented in Figure 4.1 for the case of a 200 mm impeller. It consisted of a runner with five curved blades and two bulbs. It was conceived to be installed in a 90° curved pipe, to allow the connection of a rotating axis with an external generator. The geometry of the axial turbine, including the blade slopes, was numerically investigated and optimized for prototypes with impeller diameters of 100 mm and 200 mm and with a maximum thickness of 1 mm (Ramos, et al., 2009a; Ramos, et al., 2011b).

The CFD analysis was performed for discharges between 5 and 20 l/s for the 100 mm impeller and for discharges between 70 and 155 l/s for the 200 mm impeller. Flow velocities and total pressures were analyzed, as well as turbulence, including Reynolds shear stress distribution (Simão, 2009). Finally, theoretical characteristic and efficiency curves were obtained, as presented in Figure 4.2. It was concluded that this turbine could be the most attractive among the studied machines in IST during the program, since it showed to have efficiencies of 20 to 80% in CFD modeling.

To compare and validate the results obtained numerically, a few laboratorial tests were performed in IST (Ramos, et al., 2013a) using a prototype with a diameter of the impeller of 100 mm developed in PVC (the bulbs) and brass (the impeller) – Figure 4.3. A 500 W DC permanent-magnet machine,

derived from an electrical scooter, was used to simulate a generator and a 6 Ω rheostat was connected to force an electrical load in the system (Caxaria, et al., 2011).

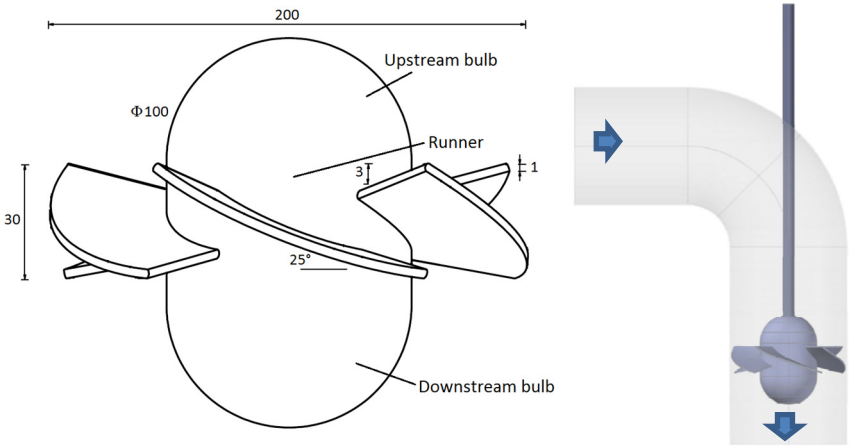

Figure 4.1 Geometry of the 5BTP for 200 mm of diameter and its disposition inline the pipe.

To have full hill diagrams and reliable empirical data of the turbine performance, a new experimental installation was prepared at the HES-SO Valais Laboratory, which is specialized in small turbine testing. A new configuration of the hydraulic circuit was adopted. The turbine has been placed upstream a curved (45°) pipe to minimize flow head losses.

4.3 Methods

4.3.1 Experimental setup and instrumentation

A new model of the 5BTP was tested in the facilities of HES-SO Valais, in a universal test rig designed to assess the hydraulic performance of different types of small-power turbomachines (up to 10 kW) and other hydraulic components (Hasmatuchi, et al., 2015a; Hasmatuchi, et al., 2015b). With the new installation, a number of changes in the configuration of the machine were introduced for optimization of the turbine performance and for adaptation to the existing setup, making it distinct from the previous one in IST.

Firstly, the nominal diameter of the turbine model, previously planned for 100 mm as at IST, was reduced since the maximum available flow-rate in the installation (50 m^3/h), not enough to cover the whole range of application that was verified numerically to be interesting. The new model was hence designed for 85 mm of diameter.

The distance between the blades and the pipe walls was reduced to 0.1 mm in order to minimize the leak losses and to allow a better comparison with the CFD model. Indeed, the latest did not consider any tip clearance thus the totality of the flow participating to the energy conversion in the system.

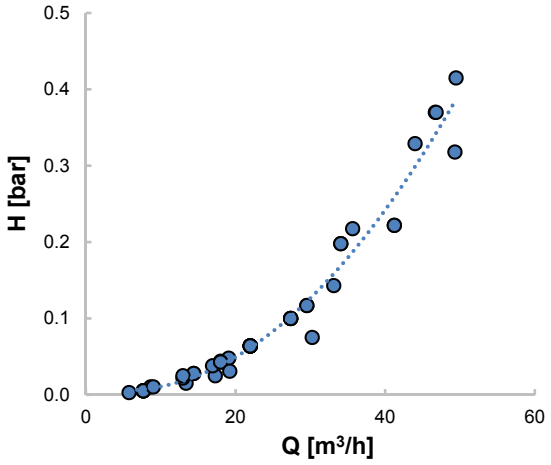

a) Relationship between discharge (Q) and head (H)

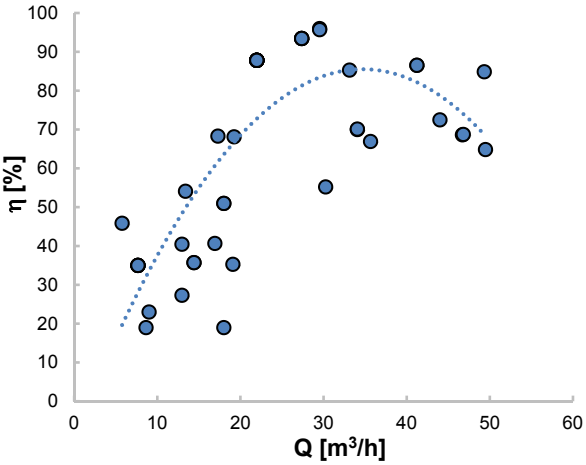

b) Relationship between discharge (Q) and efficiency (η)

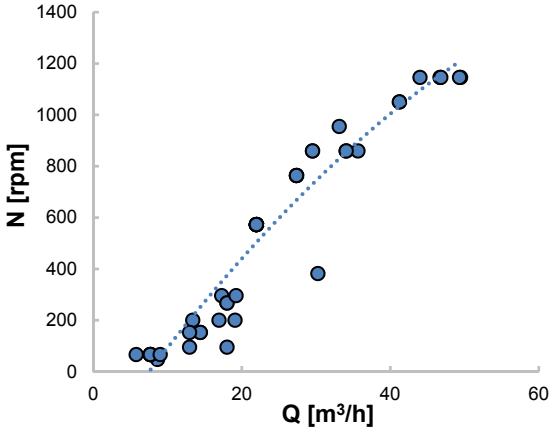

c) Relationship between discharge (Q) and rotation speed (N)

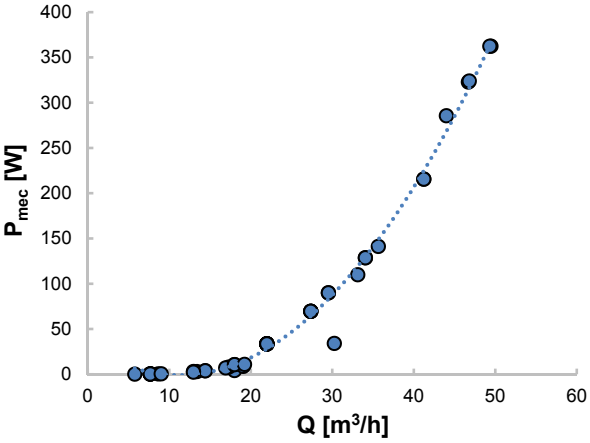

d) Relationship between discharge (Q) and mechanical power (P_{mec})

Figure 4.2 Characteristic and efficiency curves obtained from CFD numerical analysis of a 5BTP with a 100 mm impeller diameter.

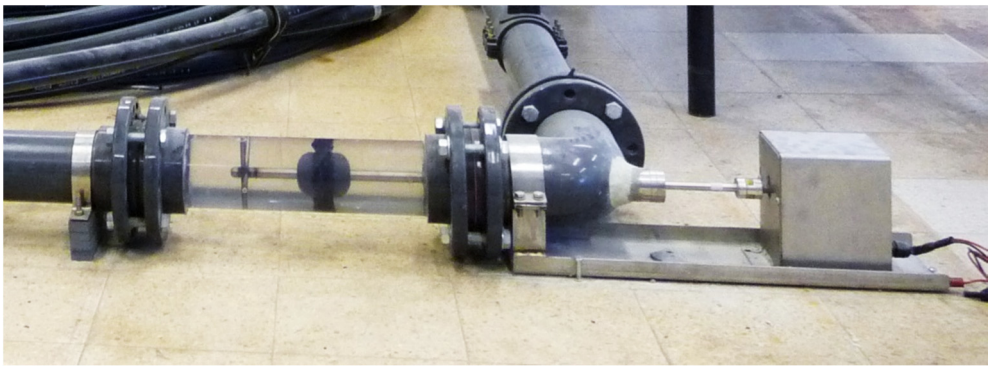

Figure 4.3 Laboratorial apparatus at IST.

Changes were also applied to the shape of the turbine (Figures 4.4 and 4.5). The downstream bulb disappeared, the diameter of the hub being maintained up to the exit from the elbow. The hub houses the ceramic bearings and the main shaft of the turbine. The upstream bulb was elongated to obtain straighter velocity streamlines approaching the runner, which has the second advantage of providing a better reading in the pressure transducer. The runner and the bulb were produced separately in different materials, the runner in bronze, while the bulb in black POM (polyoxymethylene). The thickness of the blade of 1.7 mm was chosen after an analysis of the structural resistance, corresponding to a safety factor of 3 considering a pressure of 30 m and the momentum for 1600 rpm.

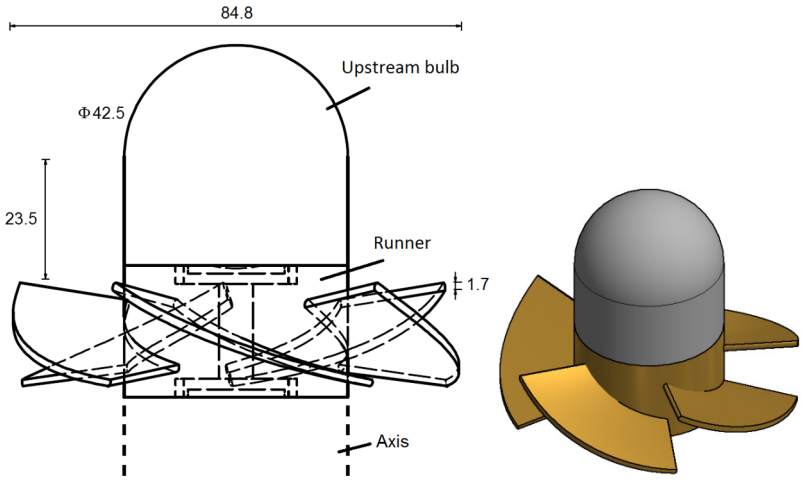

Figure 4.4 Final design of the 5BTP. Left: design scheme. Right: 3D visualization.

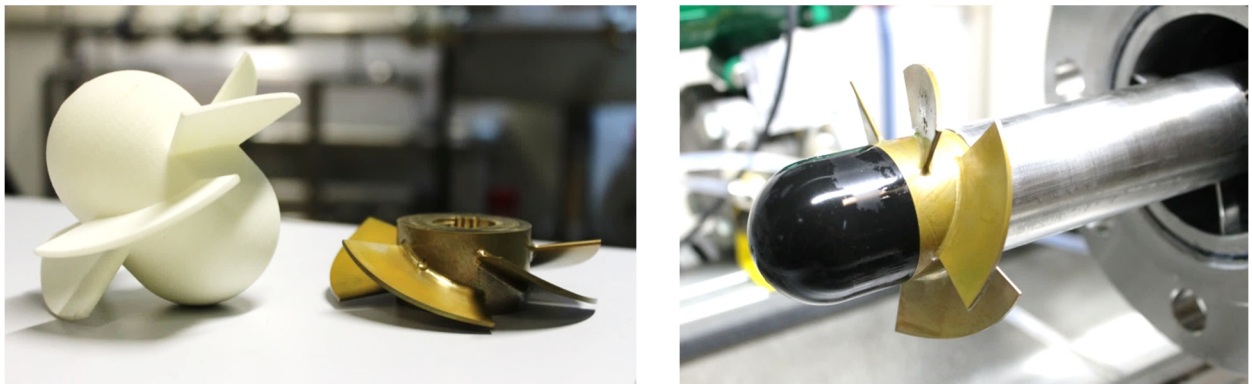

a) b)

Figure 4.5 Pictures of the 5BTP. a) Comparison of the initial design, on the left, and the final design, on the right. b) Runner, bulb and shaft of the final design.

The angle of the curve, necessary to allow the communication between the runner and an external generator, was changed from 90° to 45° to reduce flow head losses. Additionally, the turbine was placed upstream from the curve to ensure a uniform distribution of the upstream flow velocity, and also with the goal of reducing fictions losses. In Figure 4.6 the final experimental setup is presented.

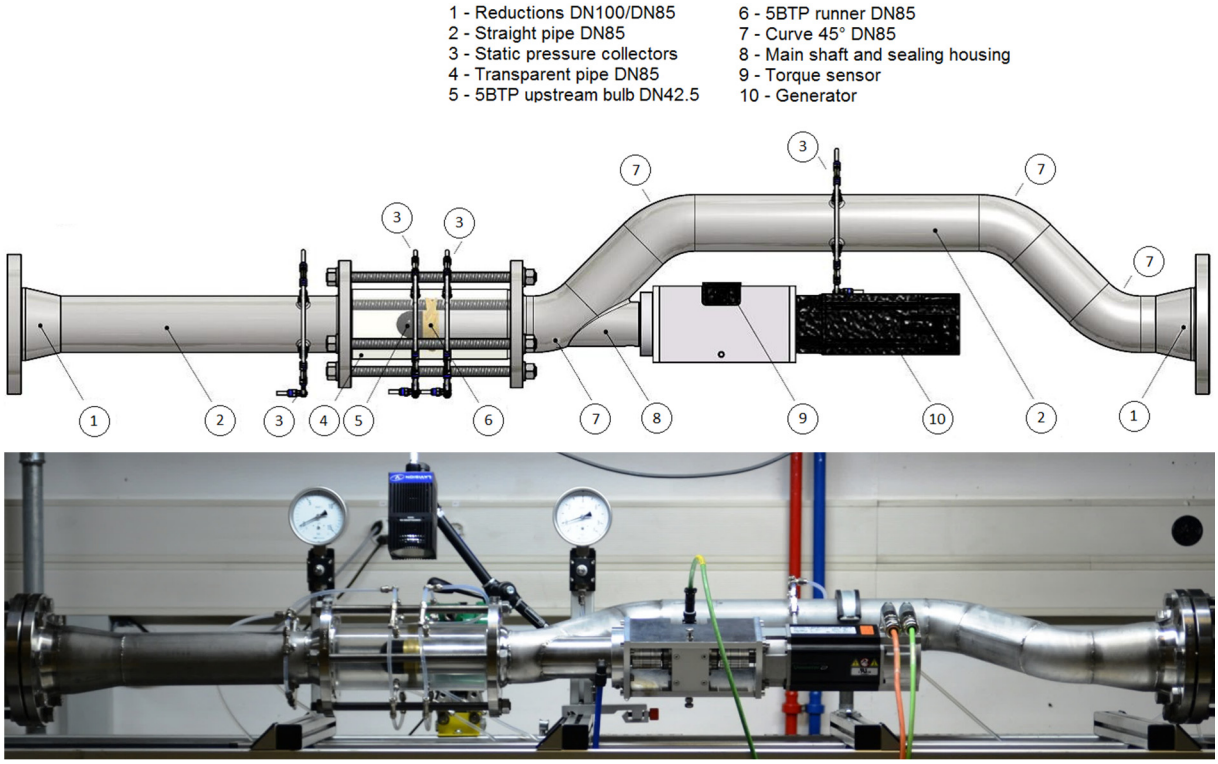

Figure 4.6 Experimental setup. Top: scheme of components. Below: photo of the installation.

As showed in Figure 4.6, four pressure transducers are installed, one upstream from the runner, two immediately upstream and downstream the runner and a fourth downstream the curve. These transducers were connected to three absolute and two differential pressure sensors, with accuracies between ±0.05%, and ±0.5%.

The flow was measured with an electromagnetic flowmeter with ±0.5% of accuracy, the temperature of the water being controlled with a probe. A permanent magnet generator with 1.23 kW and a maximum speed of 4880 rpm was used to impose the rotation speed. The torque was measured with a sensor working from a range of -4 to 4 Nm and a measurement accuracy of ±1%. All instrumentation was calibrated before the experiments.

4.3.2 Similarity analysis

During the experimental procedure, only the turbine with diameter of 85 mm was tested. Nevertheless, the results obtained can be extrapolated to other geometrically similar turbines with different diameters. In fact, for two machines geometrically similar, if it is considered that there is a kinematic and dynamic similarity between them, then the relation presented in Equation (2.10) is valid if the efficiency is also the same. Hence, from the performance of the measured machine, i.e. the characteristic and efficiency curves, the performance for other diameters can be obtained.

Since cavitation can affect the performance of turbomachinery, the influence of this phenomena on the hydraulic characteristics of the turbine was also investigated. In this sense, the pressure level of the test rig should be imposed so that cavitation occurs in similar conditions as in a typical pressure

system for drinking water distribution. For the similarity between cavitation in the model and cavitation in a prototype, the Thoma's cavitation factor was considered. The Thoma's cavitation factor is a dimensionless number given by

$$\sigma = \frac{NPSE}{E} \tag{4.1}$$

where NPSE is the net positive suction energy (J/kg) and E the specific hydraulic energy downstream from the runner (J/kg). The NPSE is given by

$$NPSE = (\rho g H_s + p_{atm} - t_{va})/\rho + (C_m^2)/2 \tag{4.2}$$

where ρ is the water density (kg/m^3), g is the acceleration due to gravity (m/s^2), H_s is the setting level of the machine (m), p_{atm} is the atmospheric pressure (Pa), t_{va} the vapor pressure of water (Pa) and C_m is the mean velocity downstream from the runner (m/s). If this value is bellow a critical value, cavitation is likely to occur (Balachandran, 2011).

To compare the behavior of the model towards the cavitation, it was considered that the number of Thoma should be the same between the model and the prototype. Considering an average pressure level was of 35 m, which is a reasonable value for pressure in a WSN, the test rig should then have an imposed pressure of 22.62 m.

Nevertheless, after a few tests, it was verified that for an imposed pressure equal to the atmospheric one, there was no cavitation occurrence for the range of flows planned to be tested. In conclusion, there is no effect of cavitation in the efficiency of the turbine. Hence, the pressure level was left at an imposed value of 10 m.

4.3.3 Experimental procedure

To assess the performance of the turbine, measurements were performed in the installation covering a range of flows between 5 and 50 m^3/h and keeping the rotating speed constant. For each value of rotational speed imposed by the generator, between 50 and 2750 rpm, the flow was progressively varied to generate measurement points of flow, pressure (Figure 4.7) and torque. All collected data is presented in Table.A 1 of Appendix A.

From the pressure measurements, the characteristic curves, i.e. the relationship between flow and head, were obtained for each fixed rotational speed. To define the efficiency curves, i.e. the relationship between flow and efficiency, the hydraulic power P_h (W), the mechanical power P_{mec} (W) and the efficiency η_h were calculated according to the following Equations (2.1) to (2.3), where Q is the flow (m^3/s), H_u is the head (m) obtained by the difference of pressures measured with the transducers at the downstream and upstream edges of the circuit, ρ is the water's density (kg/m^3), N is the rotation speed (rpm) and T_{mec} is the mechanical torque (Nm), measured with the torque sensor. All the tests were performed with water temperatures between 15° and 25°C.

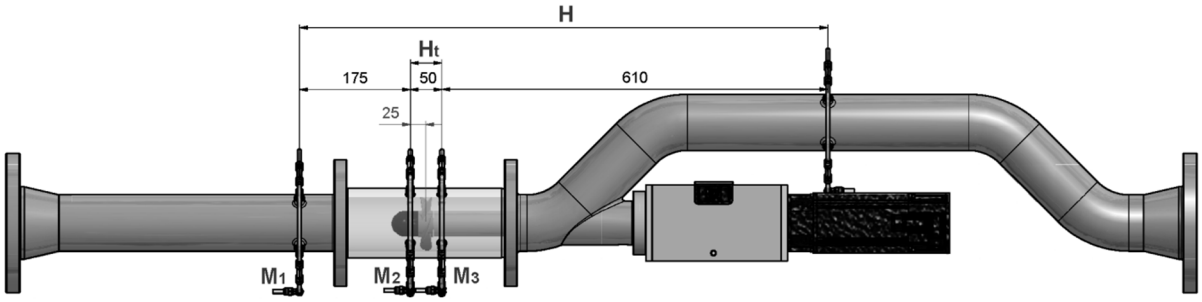

Figure 4.7 Location of measurements of pressure.

4.4 Results

4.4.1 Performance

The results of the performance assessment are presented in Figure 4.8, where we can analyze the total head between the pressure transducers further upstream and downstream, the efficiency, the rotation speed and the mechanical power as function of the discharge for the model with 85 mm of impeller diameter. For twelve fixed values of rotation speed, a total of 203 operation points were measured. The efficiency was calculated according to Equation (2.3).

For a fixed rotation speed, the efficiency increases rapidly with the increase of the discharge until a maximum is reached and then it slowly starts to decrease. Nevertheless, the mechanical power always increases with the increase of the discharge, showing that the augmentation of the head compensates the decreasing of efficiency. For the same discharge rate, the higher the rotation speed the higher the smaller head drop is, as typically verified in axial turbines. In radial turbines, the effect is the opposite, as shown in the example of Figure 2.9.

The hill charts of the turbine can be obtained by interpolation between the measured data. In Figure 4.9a) the hill chart relating flow, rotation speed and efficiency is represented, showing the peak of efficiency between 750 and 1000 rpm, for flows between 15 and 25 m^3/h. In Figure 4.9b) the hill charts relating flow, head and efficiency is presented, showing that the peak for discharges between 15 and 25 m^3/h occurs for a head bellow 0.2 bar.

The obtained BEP corresponds to an efficiency of around 64%, held at a rotation speed of 750 rpm, a flow of 16 m^3/h and 0.34 m of head. The maximum mechanical power measured was of around 330 W, for a maximum flow of 48 m^3/h, 0.48 bar of head and 1500 rpm of rotation speed.

The turbine specific speed N_S is defined as the speed of a geometrically similar turbine that, according to the affinity law (Equation (2.10)) produces a unit power (here considered in horse power) under a unit head (1 m). It is given by the turbine's BEP according to the expression:

$$NN_S = N_{BEP}\frac{P_{BEP}^{1/2}}{H_{BEP}^{5/4}} = 283\ [m, kW] = \ 330\ rpm\ [m, h.p.] \tag{4.3}$$

where P_{BEP} is the power, N_{BEP} the rotation speed and H_{BEP} the head, all corresponding to the BEP. The turbine presents a high specific rotation speed, as it would be expected from a propeller. Axial turbines have the highest specific rotation speeds, usually over 310 rpm ["m,h.p."] (Desphande, 2010).

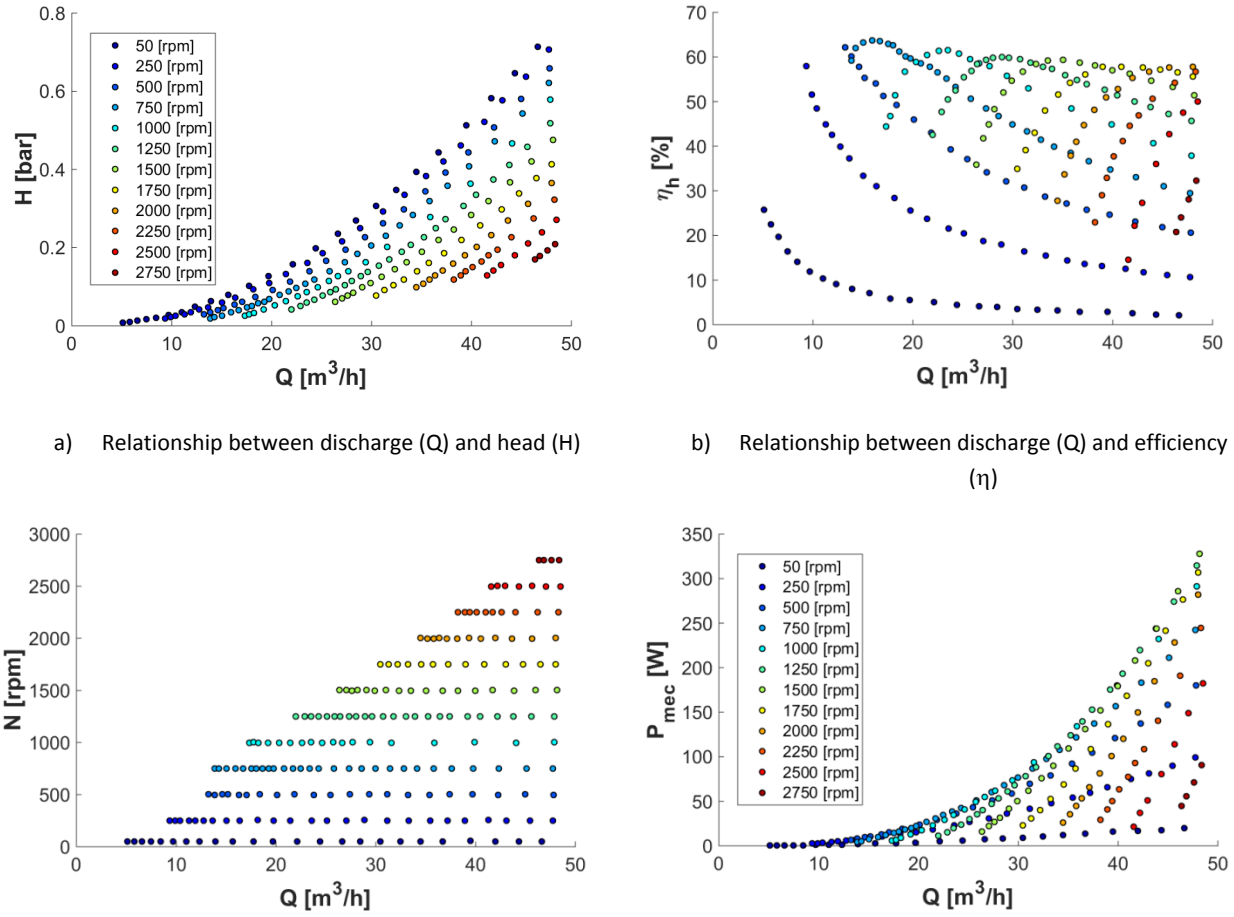

a) Relationship between discharge (Q) and head (H)

b) Relationship between discharge (Q) and efficiency (η)

c) Relationship between discharge (Q) and rotation speed (N)

d) Relationship between discharge (Q) and mechanical power (P_{mec})

Figure 4.8 Characteristic and efficiency curves obtained from the experimental results.

4.4.2 Runaway conditions

Additional measurements were performed in runaway conditions, where the generator was physically detached to eliminate any supplementary friction. In this conditions, no power is produced and the rotation speed increases with the discharge. It is imperative to know the rotation speed of the turbine in runaway conditions when selecting the generator. In case of a sudden electrical load rejection, both turbine and generator will rotate without control until the problem is

solved and this rotation should not overheat the generator. All collected data under runaway conditions is presented in Table.A 2 of Appendix A.

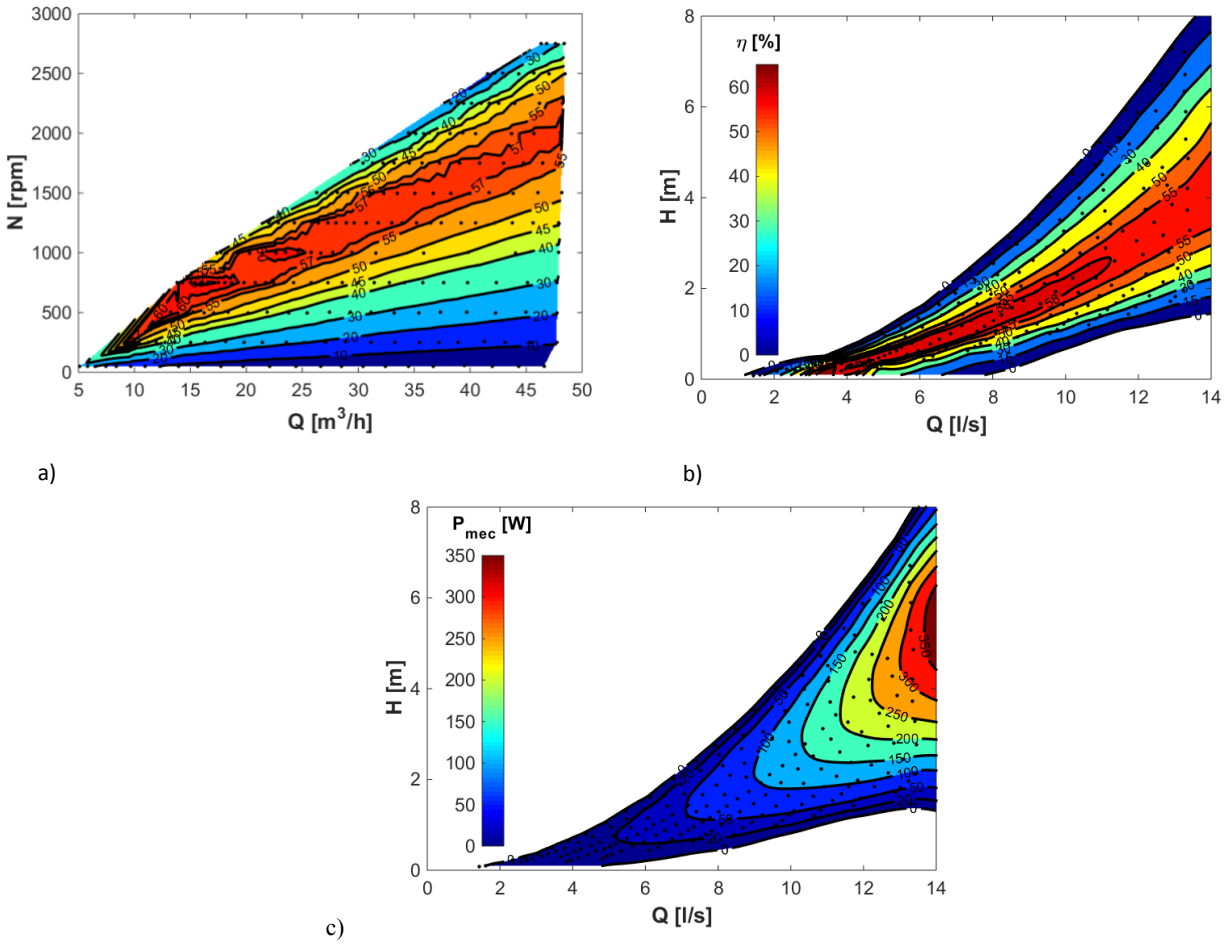

Figure 4.9 Hill charts: a) Efficiency as a function of the discharge and rotation speed; b) Efficiency as a function of the discharge and head; c) Mechanical power as a function of the discharge and head.

Additionally, it has been shown that reaction turbines, in particular when the specific speed is low, runaway conditions can induce dangerous overpressures during load rejection (Taulan, 1983; Ramos & Almeida, 2002). As can be seen on Figure 4.10, for turbines with specific speeds over 250 rpm, which is the case of Kaplan turbines and high specific speed Francis, the transient discharge tends to increase, while for lower specific speeds, the flow drops with the transient overspeed (Ramos, 2000). To test if transients are formed within the considered range of discharges, pressure measurements were also performed with no control over the rotation speed.

The results of both pressure and rotation speed measurements are presented in Figure 4.11 by the red lines. The pairs of measurements of discharge, head and rotation speed presented before are herein presented for comparison.

For the same discharge, the available head is lower, resulting in a higher downstream pressure along with a higher rotation speed. Nevertheless, it was not registered any pressure surge and discharge

tends to increase, as expected from Figure 4.10. The 5BTP is an axial turbine, hence there is no flow drops in overspeed conditions, and therefore no instabilities were noticed. Thus, within this range of flow rates, there is no danger of pressure surges due to load rejection.

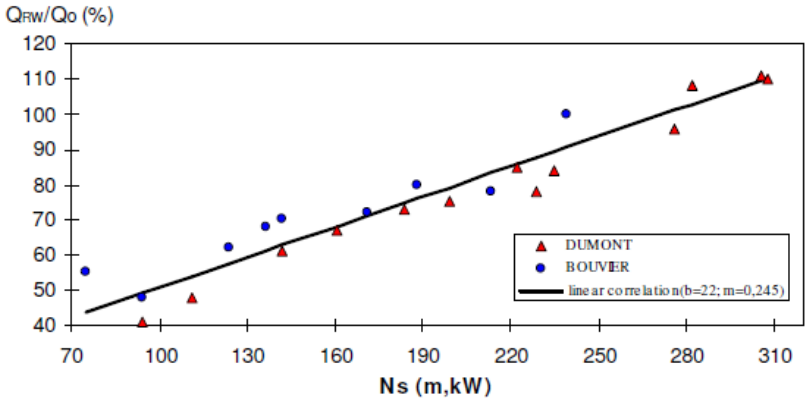

Figure 4.10 Overspeed effect on discharge variation of reaction turbines (Ramos, 2000).

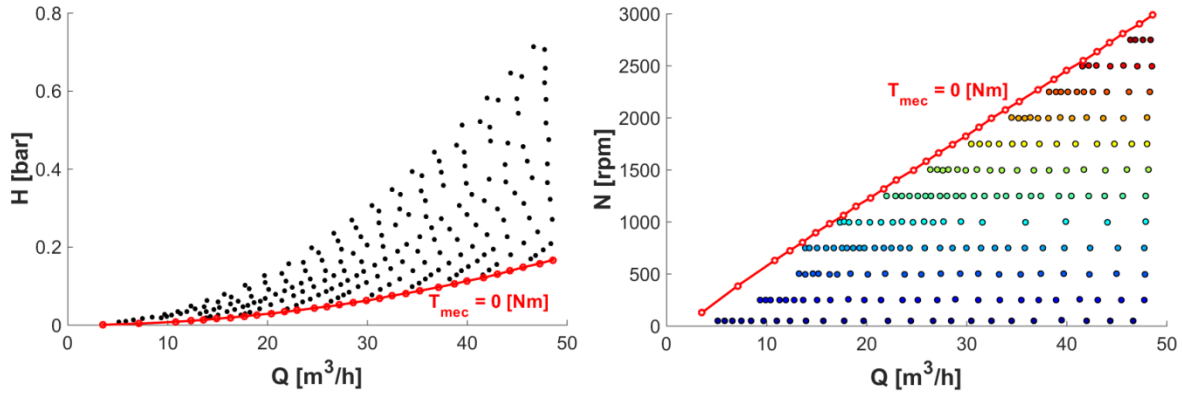

Figure 4.11 Characteristic curve and rotation speed in runaway conditions.

4.4.3 Uncertainty

To conclude the experimental campaign, the measurements were repeated for one fixed rotation speed to estimate an average variability of the results and obtain an estimation of the error associated with the experimental procedure. The rotation speed was fixed at 1000 rpm, as it is a value for which it was possible to cover a wide range of flows with adequate precision, giving a better outlined efficiency curve (Figure 4.8b)). The results of this repetition are given in Figure 4.12, where it is visible a good superposition in all characteristic and efficiency curves.

4.5 Discussion

Considering the performance of the turbine, it is noticeable in Figure 4.8b) that the maximum efficiency reached for each constant rotation speed test is not the same. Since the turbine running with different rotation speeds can be considered as two similar machines, it is noticeable that this means the affinity law, Equation (2.11), is not verified. The reason for this is the fact that the affinity law does not take into account factors, such as viscosity, that do not scale with velocity and whose

magnitude depend on the machine size (Simpson & Marchi, 2013). Nevertheless, the dimensions of the model are quite small. For prototypes with larger diameters, the scale effects will be reduced, possibly resulting in improvements on the hydraulic efficiency.

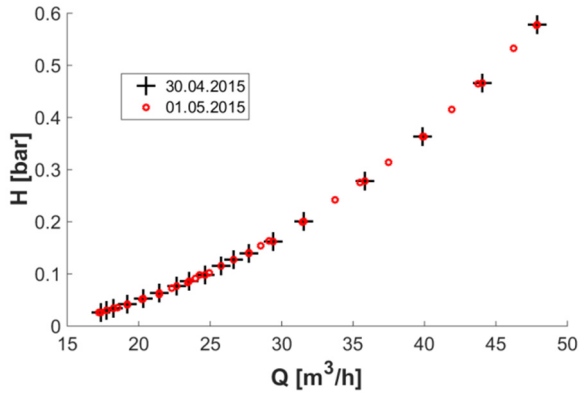

a) Relationship between discharge (Q) and head (H)

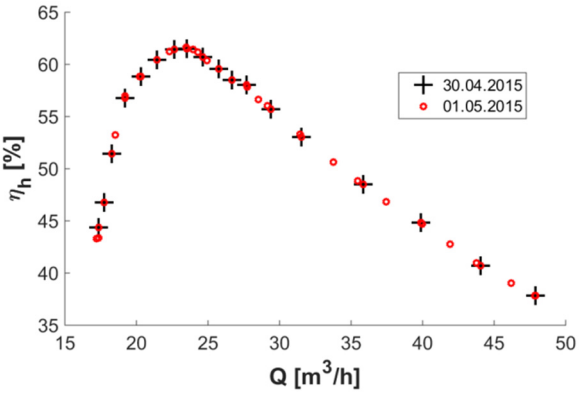

b) Relationship between discharge (Q) and efficiency (η)

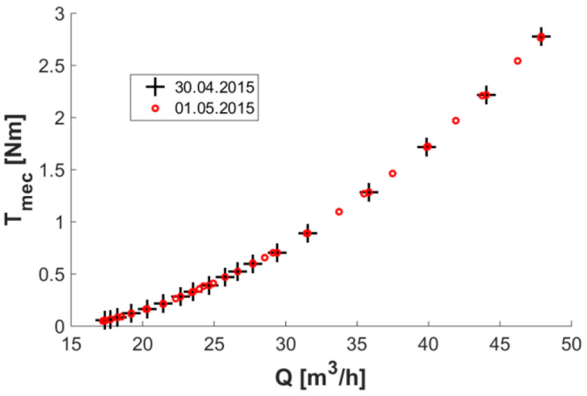

c) Relationship between discharge (Q) and mechanical torque (T_{mec})

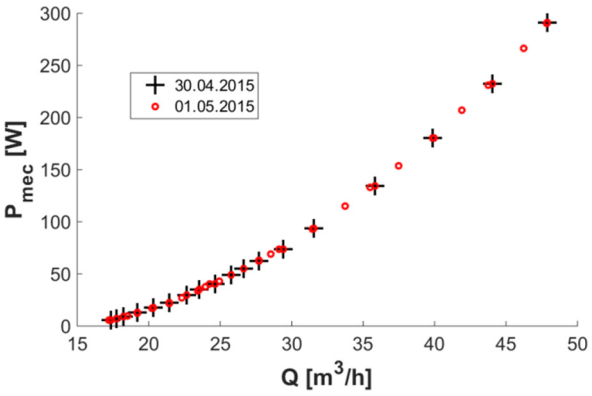

d) Relationship between discharge (Q) and mechanical power (P_{mec})

Figure 4.12 Characteristic and efficiency curves repetition for 1000 rpm.

If the performance results are made dimensionless, considering the rotation speed factor N_{ED}, the flow factor Q_{ED} and the torque factor T_{ED} (IEC, 1999), we obtain the curves of **Error! Reference source not found.**. The advantage of this is to visualize all operating conditions of a turbine model, regardless of the diameter (IEC, 1999). These parameters are given by the following equations:

$$N_{ED} = \frac{ND_e}{60\sqrt{E}} \tag{4.4}$$

$$Q_{ED} = \frac{Q}{D_e^2\sqrt{E}} \tag{4.5}$$

$$T_{ED} = \frac{T_{mec}}{\rho D_e^3 E} \tag{4.6}$$

where D_e is the external diameter of the runner (mm) and E the specific energy (J/kg).

The dimensionless characteristic curves allow us to visualize that the operating points of the turbine are approximately aligned over a single curve although the rotation speed varies. This can be justified by the fact that the blades of the turbine are fixed, unlike the Kaplan turbines. On the contrary, we can verify different curves for the efficiency depending on the rotation speed of the runner.

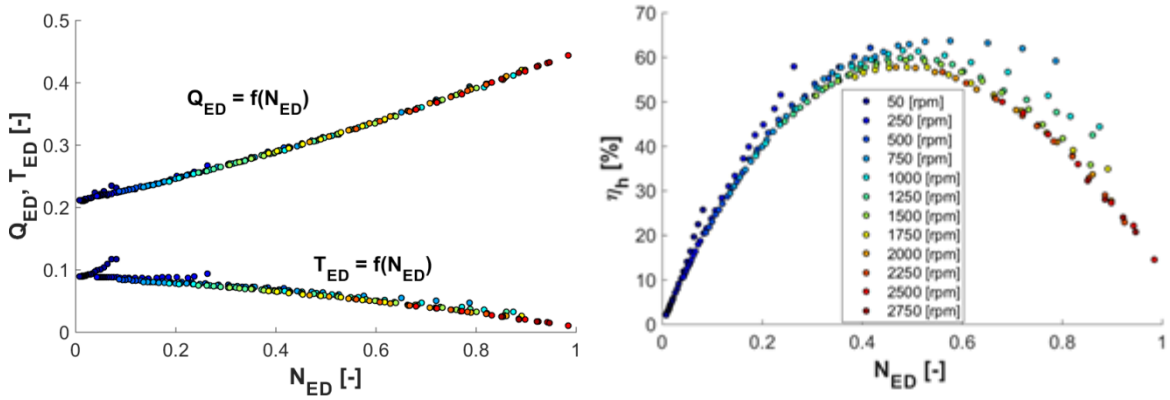

Figure 4.13 Dimensionless characteristic and efficiency curves.

Another dimensionless characteristic curve can be obtained if presents the discharge ϕ and the energy Ψ coefficients are considered (Figure 4.14). These coefficients depend on the head H (m), on the angular speed ω (rad/s), on the runner diameter D_t (m), on the discharge rate Q (m^3/s) and on the surface occupied by the fluid A (m^2). Once again, the operating points are aligned over a curve.

$$\Psi = \frac{8E}{2\omega D_e^2} \tag{4.7}$$

$$\phi = \frac{2Q}{A\omega D_e} \tag{4.8}$$

To compare the measurements with the characteristic and efficiency curves obtained in CFD (Figure 4.2), these had first to be transformed from a 100 mm runner to 85 mm. This was accomplished with the affinity law for turbomachines (Equation (2.10)). As we can see from Figure 4.15, the model was able to predict approximately well the characteristic curves, but it largely overestimates the efficiency. However, the design in CFD is fairly different from the tested model, hence the direct comparison must be done with reservations.

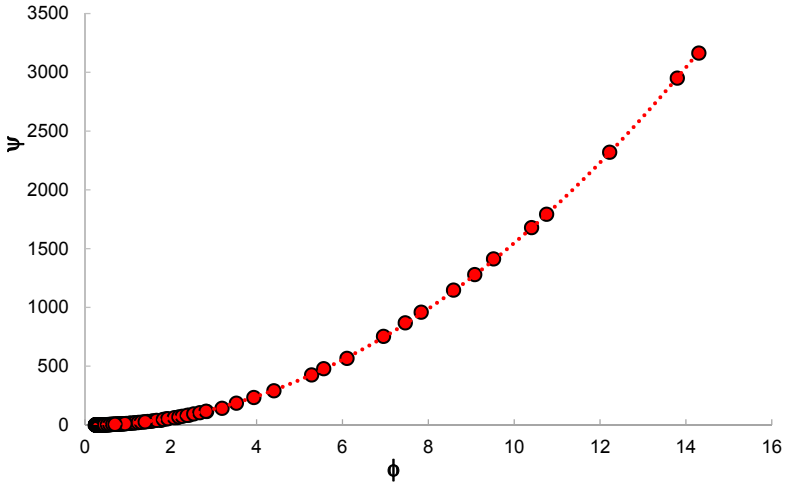

Figure 4.14 Dimensionless characteristic based on discharge and energy coefficients.

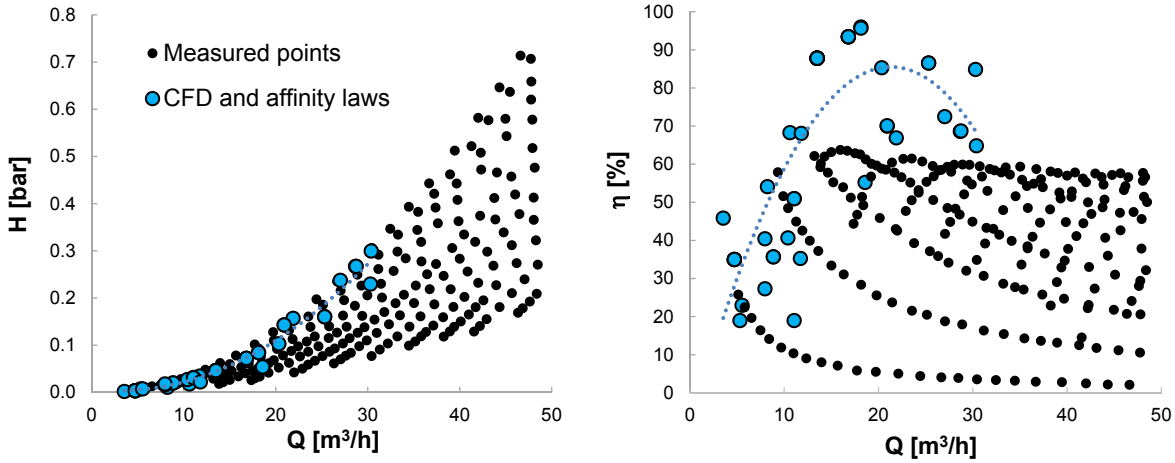

Figure 4.15 Comparison between measured performance points and CFD results.

Finally, in order to maximize the mechanical power generated for each flow-rate, the rotation speed of the turbine can be adjusted according to Figure 4.16. In all the operation points where the energy production for the discharge was the maximum, the efficiencies were below the maximum efficiency that could be achieved with that rotation speed (overload operating regime). The efficiencies are compensated by the higher head turbinated, according to the characteristic curve of Figure 4.17.

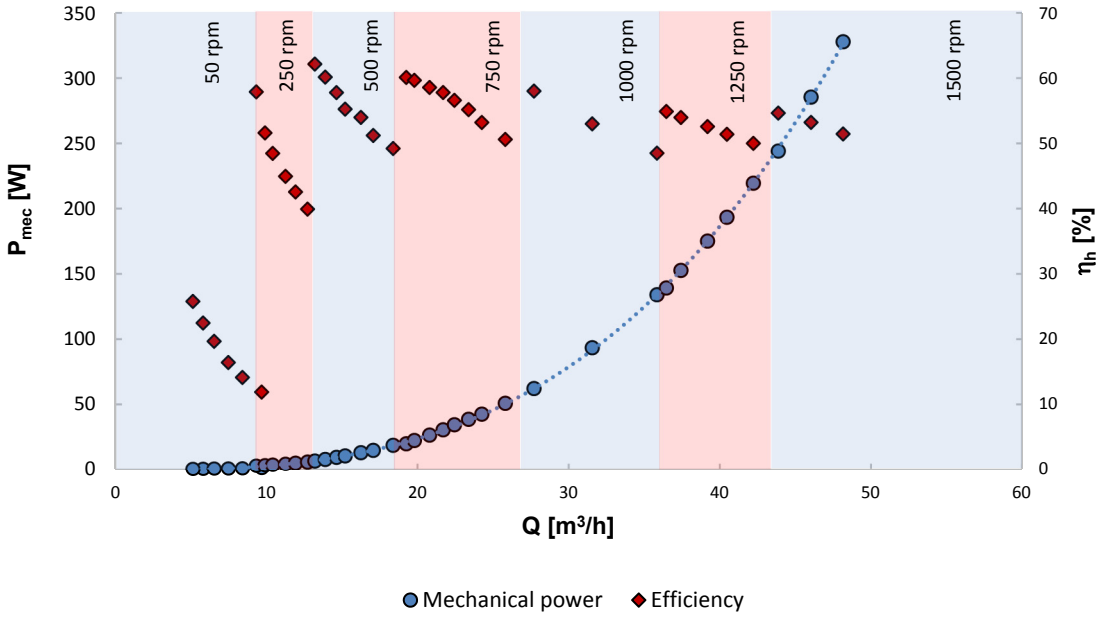

Figure 4.16 Curve for maximum mechanical power production and respective efficiencies and rotation speeds.

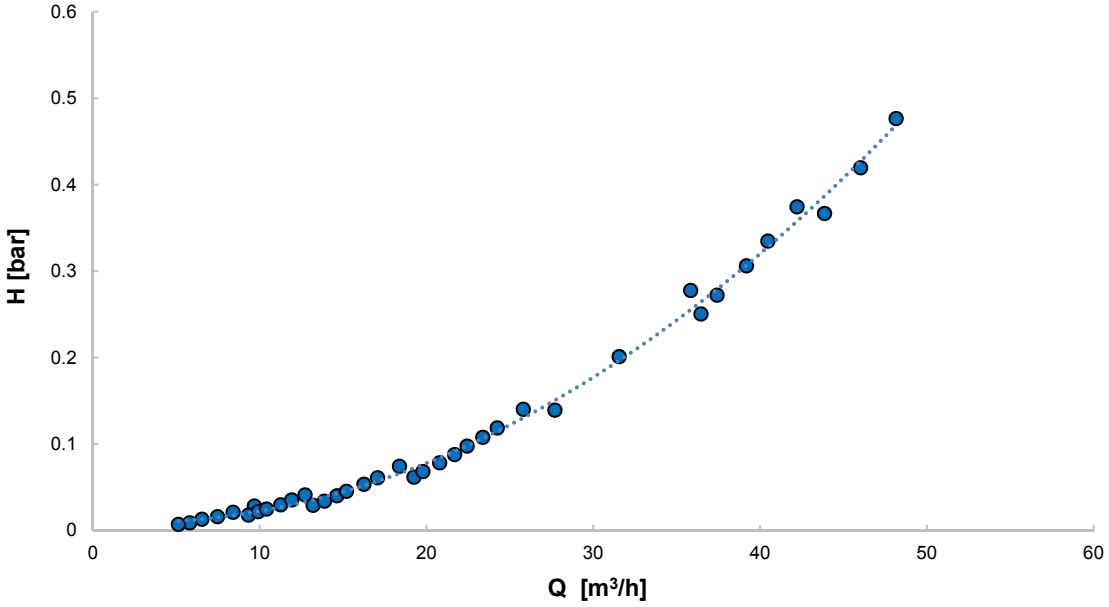

Figure 4.17 Characteristic curve considering the maximum mechanical power production.

4.6 Conclusion

In conclusion, an experimental campaign was conducted on a turbine for micro-hydropower applications that has been in development since 2008. A new model with a diameter of 85 mm was optimized and tested, allowing recovering energy from flows between 5 and 50 m^3/h by extracting heads under 7.5 m. The best efficiency point was identified for a 750 rpm rotation speed, with an operation point of 15.95 m^3/h and 0.34 bar of head, resulting in a 63.75% of efficiency. The

maximum power obtained was of 328 W, for 1500 rpm of rotation speed, 48.15 m^3/h of flow, 4.76 m of head and an efficiency of 51.45%. These results can be extrapolated for higher diameters through the affinity laws of turbomachines. For example, the point of maximum power measured would correspond to 71 kW for a diameter of 250 mm (Q, H)=(1225 m^3/h, 4.1 bar) and to 2.3 MW for a diameter of 500 mm (Q, H)=(9801 m^3/h, 16.5 bar).

The turbine has proved to have potential for further development since the results of the experimental tests were satisfying, with efficiencies around 60%, which are considered good for such small machine.

Chapter 5
Optimization of the locations for micro-hydropower in water supply systems

Sub-chapter 5.3 is based on the scientific article "Simulated annealing in optimization of energy production in a water supply network" by I. Samora, M. J. Franca, A. J. Schleiss and H. M. Ramos published in 2016 in Water Resources Management. Sub-chapters 5.4 and 5.5 is based on the scientific articles "Opportunity and economic feasibility of inline micro-hydropower units in water supply networks" by I. Samora, P. Manso, M. J. Franca, A. J. Schleiss and H. M. Ramos published in the Journal of Water Resources Planning and Management and "Energy recovery with micro-hydropower plants in the water supply networks: the case study of the city of Fribourg" published in Water, respectively. The simulations and algorithms hereafter are original and were developed and performed by the author.

5.1 Introduction

As highlighted in the state of the art (sub-chapter 2.2), WSSs present promising conditions for the installation of micro-hydropower. However, since the concept is relatively recent, there is still a lack of knowledge and experience in identifying the potential locations of turbines is these systems. The varying conditions in these systems, caused by the consumption schedules of the population, hinder this task and small step simulations are needed.

To fill in this gap and provide guidelines to tackle the difficulties that can arise from the installation of turbines in WSS, three models are developed in this chapter: the first model, in sub-chapter 5.2, simulates the installation of a turbine upstream from a storage tank; the second and third models, presented in sub-chapters 5.3 and 5.4, are applied to WSNs and optimize the placement of turbines through respectively energetic and economic points of view. Finally, in sub-chapter 5.5, a few practical advices are summarized based on the drawn conclusions.

5.2 Micro-hydropower installation upstream from a storage tank

5.2.1 Methodology

An interesting location for micro-hydro production in WSS is upstream from storage tanks since a tank offers conditions for turbine regulation and attenuates the effect of daily variations in the turbine operation. In this sub-chapter 5.2, a model was developed to optimize the operation of a hydropower plant installed upstream from a storage tank. For this purpose, a methodology was developed resorting to a genetic algorithm to maximize the energy production while ensuring the main functionality of the tank.

The genetic algorithm is an evolutionary algorithm which has already been applied to a great variety of problems. It is based on the Darwin's evolution laws and treats a data population that is object to random actions similar to those that occur in biological evolution, such as reproduction and mutation. The treatment selects the surviving individuals, depending on their "fitness" (Araújo, et al., 2006; Mora, 2012). In each cycle, the algorithm analyses the fitness of a group of solutions, called generation. The best solutions are then recombined and mutated to originate a new generation. This cycle repeats itself until a stopping criteria is met (Mora, 2012).

With this algorithm, an operational methodology was implemented to a particular case study of a regulation tank in north Portugal to assess its benefits. The model is defined in section 5.2.2 and its application to the case study is described in section 5.2.3. In section 5.2.4 the results are presented and in section 5.2.5 the main conclusions are drawn.

5.2.2 Model

Working principles

The model developed to optimize the energy production in a storage tank of a WSS considered the installation of one or more micro-turbines immediately upstream from a tank – Figure 5.1. This tank may be a regulation tank, a distribution tank or even a water treatment plant.

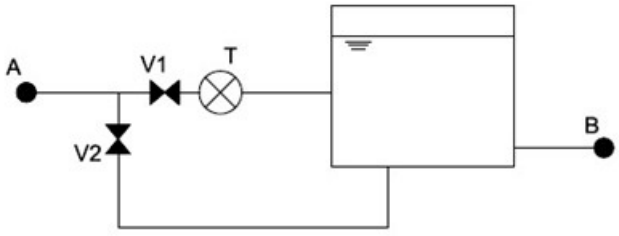

Figure 5.1 Model 1: scheme.

In this scheme, point A represents an upstream node, where the head pressure is known or can be estimated. The turbine (or group of turbines), represented by point T, is considered to have the ability of controlling the flow and valve V2 controls the opening and closure of a by-pass circuit. The

valve V1 controls the admission to the turbine and Point B represents a downstream node, where the demanded flow is imposed. Generally, this demand is not constant, but follows a daily pattern.

The operational rules in this type of configuration depend on a large variety of factors, such as the limitations of the machinery, the size of the tank and the characteristics of the demand. The restrictions related with the machinery are the flow discharged by the valve V2 and the maximum and minimum flows through the turbine. Regarding the tank, the shape and volume are usually defined by the necessities of the downstream network and the topographic conditions. As this model is meant for a WSN, restrictions related with water quality in the tank may also be necessary, thus minimal daily and monthly variations may also be imposed.

An algorithm was developed to estimate, for each month, the level variation in the tank that maximizes the energy production with the defined restrictions. The genetic algorithm was used to minimize the following objective function:

$$OF = {}^{1}/_{\sum E_n} \tag{5.1}$$

where E_n (kWh) is the energy produced during the nth hour,

$$E_n = \rho g \sum_{n=1}^{N} \eta_{tgn} \eta_{fn} Q_n H_n \Delta t \tag{5.2}$$

and Q_n (m^3/s) is the turbinated flow, H_n (m) is the available head, both during the nth hour, γ is the water specific weight, Δt corresponds to one hour and η_{tg} and η_f are the group and the current-transformer efficiencies.

The optimization algorithm searches for the series of inflows that leads to the highest energy production, calculated through Equation (5.2), respecting the limits of volume and the daily and monthly level variation. The output is the corresponding volume variation inside the tank. This output is not a real result, but only a prediction, as the future real demand is unknown.

The definition of the average hourly series is based on applying a difference of squares method to a real or generated hourly series. The user can insert an hourly series or a daily series, but in the case of a daily series, an hourly series is generated by applying a pattern of daily variation.

As the initial iteration strongly influences the genetic algorithm, the user has the possibility to define it. If the user does not choose to do so, the initial iteration will be considered as equal to the average hourly series or to the minimum operational point, whichever is the lowest.

To operate in continuum with the best efficiency, the valves and the turbine should be able to react to changes in the demand. Hence, an operational methodology was developed to perform instantaneous decisions in the operation. Using the optimized series of variation of volume inside the tank as a preview, the operation tries to follow it as a schedule, adjusting itself according to the

real demand. As long as the real-time volume inside the tank is within a fixed ΔV from the forecast, the turbinated flow is set as previewed. If not, corrections are applied to force the level to reach the prevision. This procedure is further explained bellow.

Operational methodology

The goal of the operational methodology is to allow the system to be independent, auto-regulating and also updating every year. The regulation of the valves and hence of the turbine operation is function of the level inside the water tank and the reading of flow discharge in the entrance of the system. Considering that Q_{disch} is the by-pass flow through valve V2, Q_{max}^{T} and Q_{min}^{T} are the maximum and minimum turbine flows and V_{max}^{res} and V_{min}^{res} are the maximum and minimum volumes of the reservoir, the methodology considers the following steps:

1. Estimation in the beginning of each month of the average hourly flow series for that month ($Qout_p$), based on the records of the same month in the past year.
2. Reading of the initial level in the reservoir and hence obtain the initial volume V_{real}.
3. The optimization algorithm is run three times, to reduce the probability of reaching a local maximum, considering the average hourly flow series and the measured initial level.
4. Adoption of the result with best output of the objective function. With these results, the series of variation of volume inside the reservoir (V_p) is assumed as a preview.
5. Application of the operational algorithm, presented in Figure 5.2, in each hour (t) during that month. Assume a ΔV_{max}.

The regulating valves are controlled according to the following rules:

- If $Qi_{(t)} = 0$, all valves are closed.
- if $Qi_{(t)} = Q_{disch}$, V1 is closed and V2 is opened.
- else, V1 is opened, and V2 is closed.

If the optimization algorithm does not provide any possible solution, it may occur that the given restrictions could not be respected during that particular month. This can be the case of high demand months, when there is almost no storage inside the reservoir. Thus, as the restrictions with level variation are linked to water quality problems, it was considered that the condition of water quality is verified without a need for regulation.

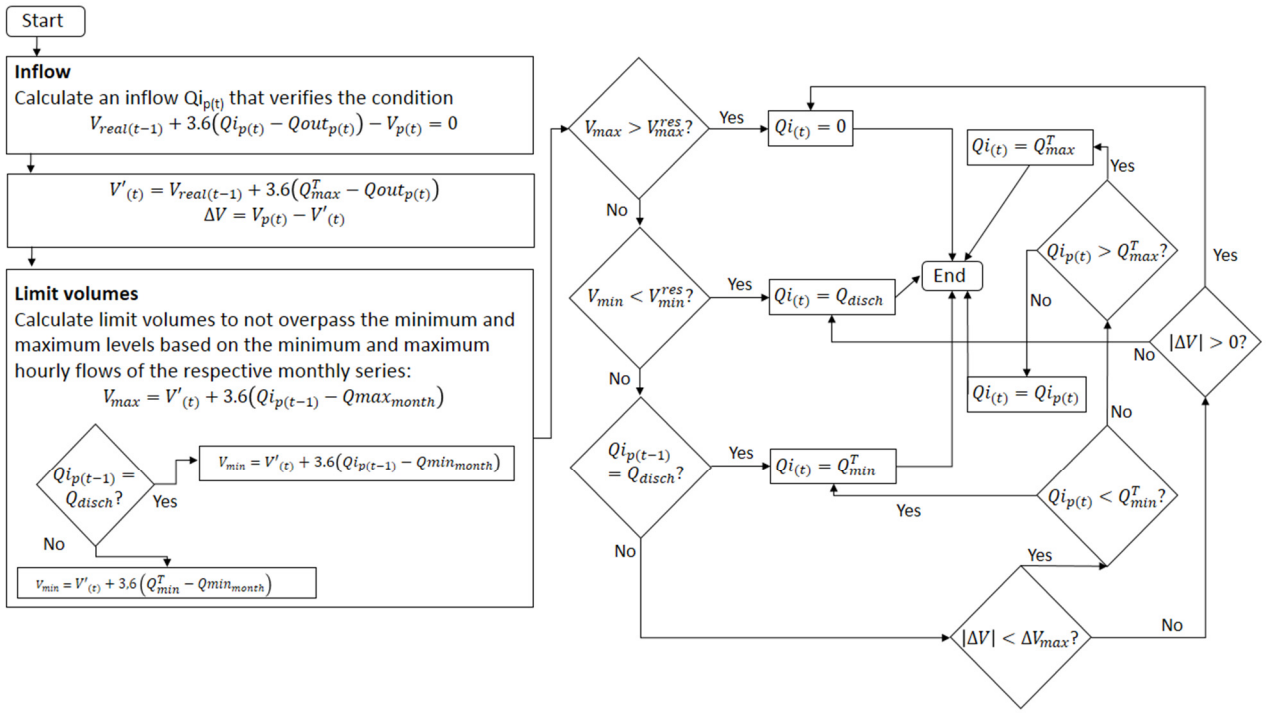

Figure 5.2 Model 1: Algorithm for defining operational flow.

5.2.3 Case study description

To exemplify the usefulness of the developed methodology, the optimization algorithm was applied to the Beiriz Power Plant (sub-chapter 3.1). Since the tank downstream the Beiriz Power Plant is overly dimensioned for the actual demand, a simple approach using the demanded flow would keep the level inside the tank stable. This solution cannot be applied due to problems of water quality.

In this case study, valve 2 corresponds to the all-or-nothing type of valve, with a discharge of 400 l/s. For this reason, it was considered that valve 2 has no impact on the optimization algorithm and would only be used for the real-time regulations (representing the Q_{disch} in Figure 5.2). Consequently, the maximum and minimum allowable values for incoming flow were set as the maximum and minimum turbine operating points.

To ensure the water renovation inside the tank, it was established that the level should go from the maximum to the minimum (variation of 3 m) at least once in a month and that there should be a variation of 0.007 m per day. Also, it was considered that 1/3 of the total volume should always be guaranteed as reserve in case of fire or malfunction. The original project (Cenor, 2011) predicts a generation of about 52 MWh/year, but it did not respect the daily variation.

The pressure in point A was considered constant (8.8 bar) and the available heads were calculated from the head losses between point A and the turbine.

For the calculation of energy production, average hourly flows and the hourly pressure data of February to December 2010 were used. Based on the available hourly flow series, an average daily

variation was established for each month. For this pattern generation, the average flow of each hour of the day during a given month is calculated, ignoring values that are considered too extreme by means of applying a difference of squares method. Figure 5.3 presents the average hourly flows from February to December 2010.

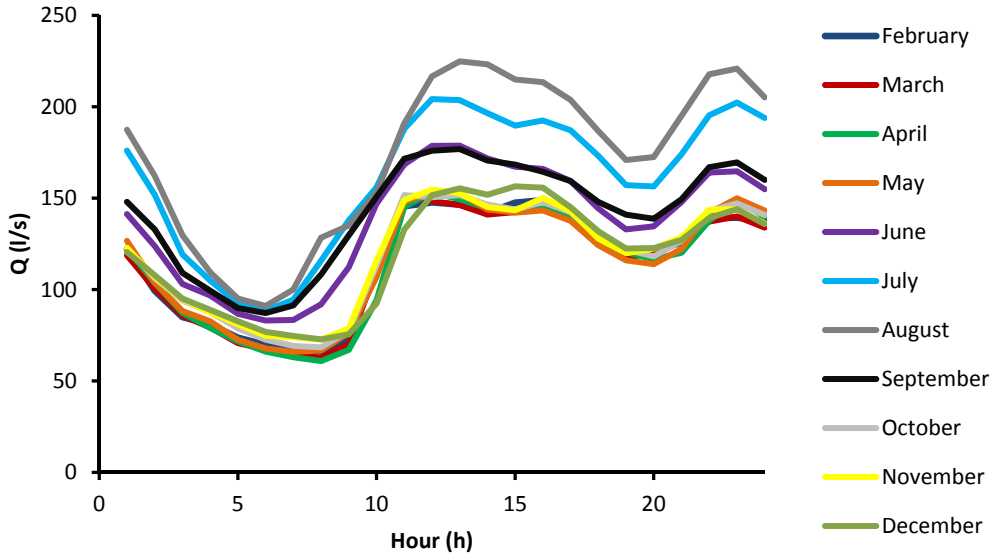

Figure 5.3 Average hourly flows for each month.

The daily pattern is similar throughout the year and it is even almost the same for the months between October and May. The summer months, June to September, have higher flow values.

5.2.4 Results

The described optimization algorithm and operational methodology were applied to the case study considering the months of February to December. The months from the summer period (June, July, August and September) were not feasible to optimize, since it is the period with the highest demand and the restriction for varying the level inside the tank 3 m in the duration of one month proved to be unfeasible. The reservoir operates continuously with constant low levels in this period.

As the data available was from 2010, the operational methodology considered demands in 2010 as the real scenario (1st scenario), but also two other flow series: one of these series considered the occurrence of a daily pattern obtained from the minimum registered flows in each hour for the considered month (2nd scenario), and another for a daily pattern obtained from the maximum registered flows in each hour for the considered month (3rd scenario). A ΔV of 740 m^3, corresponding to 0.34 m, was fixed to evaluate the need for corrections in the operation. For the summer period, it was considered that the condition of water quality is verified without a need for regulation. Hence, the simulation was done with a simple on-off operation.

In Table 5.1 are presented the results obtained with the optimization algorithm and with the application of the methodology for the three considered scenarios. The initial level in February was

considered the same for the three scenarios, hence the same algorithm prediction for this month. The semi-total refers to the optimized months.

Table 5.1 Energy produced (kWh) from the application of the optimization algorithm and operational methodology.

Month	1st scenario: Real flow values		2nd scenario: Minimum flows		3rd scenario: Maximum flows	
	Algorithm prediction	Methodology application	Algorithm prediction	Methodology application	Algorithm prediction	Methodology application
February	44192	42801	44192	27321	44192	37661
March	48789	46670	48730	32295	48948	45701
April	46877	46972	46877	37448	47025	49049
May	49623	49227	49623	40319	49702	50369
June	-	47862	-	47198	-	46831
July	-	47067	-	48707	-	42973
August	-	45471	-	48310	-	42456
September	-	48265	-	45219	-	48389
October	50593	50942	49663	42631	51354	52099
November	49159	48481	49893	40731	49011	44969
December	50225	45423	50329	35422	50910	49111
Semi-total	339458	330516	339306	256167	341143	328960
Total	-	519181	-	445602	-	509609

It is important to note that the values of energy produced with the application of the methodology are close to the optimal obtained with the algorithm. Also, the 1st scenario reached a higher energy production, which is only natural as it is the case where the flow is the closest to the prediction.

The result is close to the generated power obtained in the original project, without the optimization. This indicates that the introduction of an obligatory daily variation does not affect the viability of the project if the regulation of flow is optimized.

In Figure 5.4 are presented the results obtained with the optimization algorithm during the process for the 1st scenario. It is interesting to observe that, in all months, the optimized solution follows a pattern, starting at a high point, decreasing the level until reaching the minimum and afterwards increasing again to a high volume.

In Figure 5.5 is presented the variation of volume inside the reservoir for the complete simulation time for the 1st scenario. It is visible that there is almost no variation of the level during the summer period, confirming the hypothesis of no-need to control the water quality in this period.

5.2.5 Conclusions

The developed methodology allows estimating a monthly operation that optimizes the energy production, while forcing the volume inside the storage tank to change. This restriction is linked with the need for water renovation to ensure the quality for water supply.

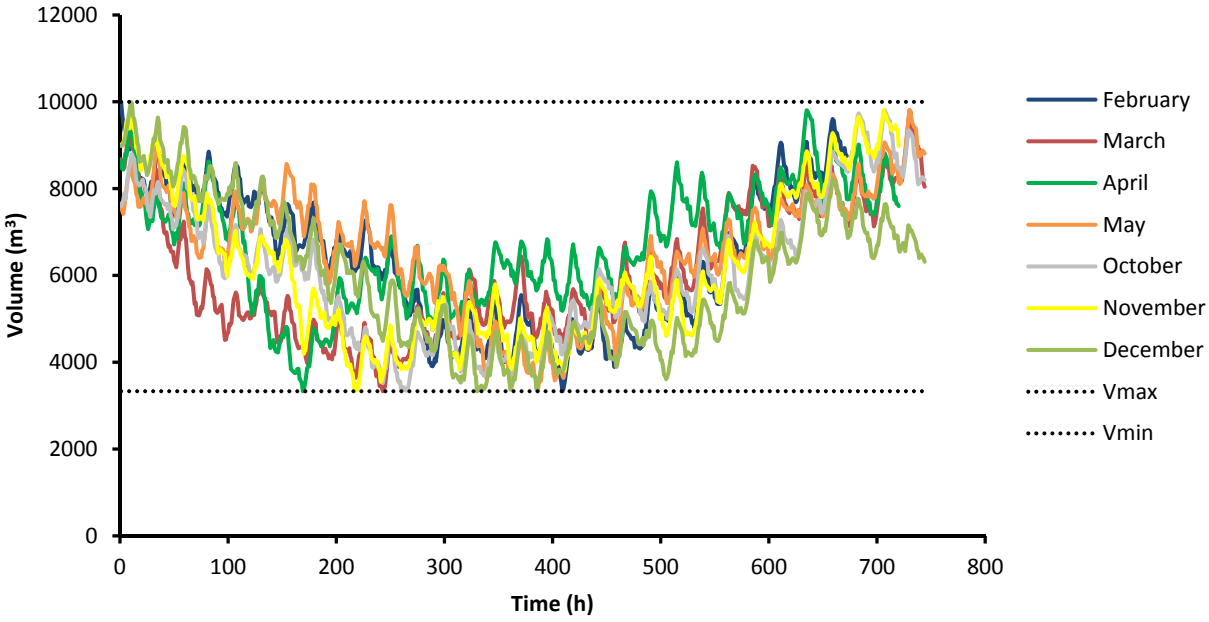

Figure 5.4 Results of the optimization algorithm simulations for every considered month in the 1st scenario.

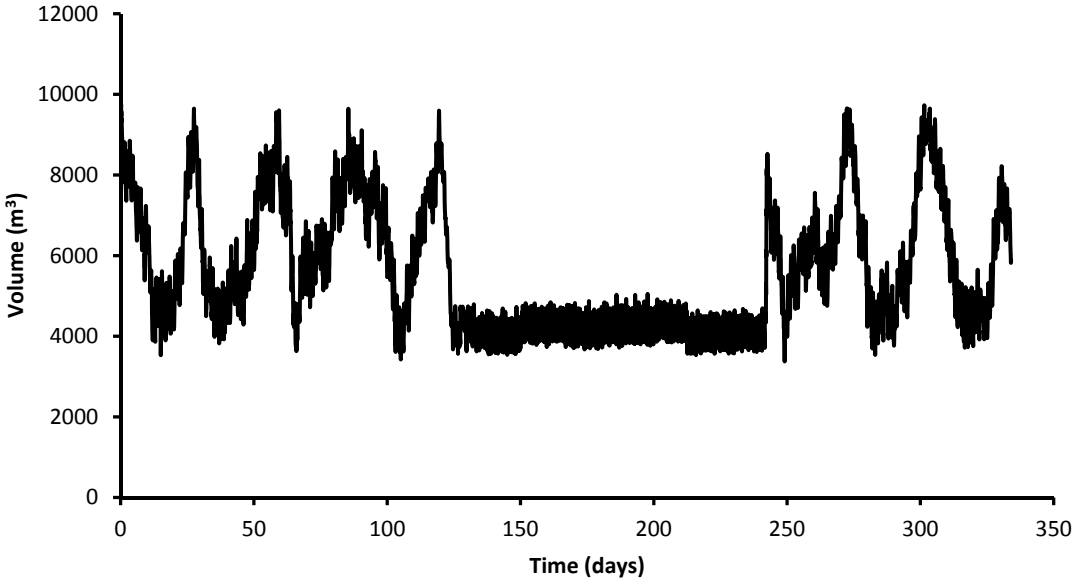

Figure 5.5 Volume variation in the reservoir throughout the simulation time in the 1st scenario.

Based on a prediction of the demand, an optimization process based on a genetic algorithm searches for a solution that maximizes the energy produced in each month. That change of volume is then applied to the system, which makes use of valves to control the real water volume inside the tank. This system implies an hourly monitoring of the volume in the tank and the demanded flow.

Hence, the methodology permits to establish operational rules to maximize the energy production. In the following years the demand variation is estimated based on new records of demand. This

way, even if the conditions of consumption change, the system adapts itself to new demand patterns.

5.3 Optimization of energy production in a water supply network

5.3.1 Methodology

This sub-chapter 5.3 proposes a solution for improving the energy efficiency in WSNs that considers the use of micro-turbines for electricity generation in WSNs. In WSNs, particularly in cities with considerable geodesic differences, areas exist where the pressure is greater than necessary. However, as referred in the state of the art, the choice of placement within a network is not a straightforward problem due to the variability of discharges and redundancy of branches. Moreover, minimum pressure levels have to be ensured in order to guarantee the quality of water supply to the population.

Herein, the development of a novel technique to find the location of micro-turbines within a WSN which maximizes the annual energy production is presented. The technique consists on an algorithm created which is based on the simulated annealing strategy. A strategy for the application of micro-hydropower plants in WSNs is thus proposed, addressing pressure constraints, flow variability and the complexity of the networks with closed loops.

The simulated annealing approach is a heuristic strategy that has proven to be robust and versatile (Rutenbar, 1989; Youssef, et al., 2001). A brief review of this technique together with its implementation on the particular model of WSNs is presented in section 5.3.2. To test the performance of the algorithm, a study was developed in a sub-grid of the Lausanne WSN. Section 5.3.3 presents the case study used for the testing of the algorithm. Section 5.3.4 defines the main function of the model based on testing with one, two and three. Finally, the main conclusions are drawn in section 0.

5.3.2 Model

Working principles

The goal of the model herein developed is to optimize the location of a chosen number of turbines in a network. This goal is achieved by applying a simulated annealing process coupled with a hydraulic solver to maximize the energy production through the minimization of a cost function defined as

$$f(X) = {}^{1}/_{\sum_{t=1}^{T} E_t(X)} \tag{5.3}$$

where $X(x_1, \dots, x_n)$ is a vector with the position of n turbines in the network, and E_t (kWh) is the energy produced during the t^{th} hour for a total simulation time of T:

$$E_t(X)=\rho g \sum_{n=1}^{N} \eta_{tgn}\eta_{fn} Q_n H_n \Delta t \quad (5.4)$$

where g is the gravitational acceleration (m/s^2), ρ is the water density (kg/m^3), Δt is the time step (h), N is the number of turbines and, for each turbine, Q_n (m^3/s) is the nominal turbinated flow, H_n (m) is the available head, and η_{tgn} and η_{fn} are the turbine and the generator efficiencies, respectively.

The cost function of each tested solution is obtained by the flow and head drop at each turbine calculated from the hydraulic state of the network in each tth hour. The hydraulic state of the WSN is calculated using the commercial software EPANET 2.0. This software was developed by the United States Environmental Protection Agency and models the hydraulic state and water quality in water networks using the gradient method (Rossman, 2000). Each turbine was simulated in the program as a singular energy drop whose head-loss coefficient is calculated as a function of the turbine characteristic curve.

Simulated annealing is a probabilistic method based on the process of heating of steel and ceramics and consists of a discrete-time inhomogeneous Markov chain (Bertsimas & Tsitsikis, 1993). A Markov chain is a sequence of random variables in which each variable depends only on the state of the system of the previous iteration. Moreover, simulated annealing is not a pre-defined mechanical sequence of computations but a strategy for solving combinatorial optimization problems (Rutenbar, 1989).

The method begins with an initial feasible solution (Figure 5.6), in this case it is a particular position vector of a number of turbines in the network, to which a cost value is associated as given by Equation (5.3). In each iteration, a small random change is applied to the previous solution to generate a new solution, referred to as a neighbor solution, with a different cost value (Azizi & Zolfaghari, 2004). The neighborhood $Y(x)$ of a solution x is a set of solutions, known as neighbors, that can be reached from x by a simple change. This change, referred to as the neighborhood function, is user defined.

The neighborhood function strongly influences the convergence of the model, and no theoretical rules are available. For example, the size of the neighborhood should not be too small compared with the total solution space cardinality because the process might not occur sufficiently fast. Nevertheless, if the size of the neighborhood is too large, the algorithm might not be able to focus on specific areas (Henderson, et al., 2003). Adaptive neighborhoods have been proposed by several authors, particularly for problems with continuous variables (Chapallaz, et al., 1992; Yao, 1993; Martins, et al., 2012) in which the size of the neighborhood changes according to the previously visited solutions. Finally, it was concluded that the neighborhood is heavily problem-specific (Henderson, et al., 2003).

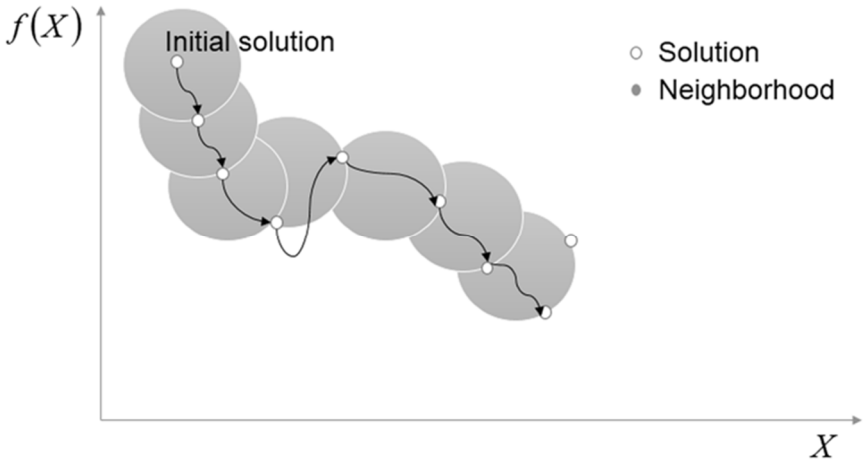

Figure 5.6 Scheme of the optimization process of the simulated annealing.

The neighborhood gives the ability to control the generation of new solutions and adapt it to the specific problem. Given these characteristics, the neighborhood function was thoroughly analyzed in this sub-chapter 5.3. Different types of neighboring properties were analyzed for the installation of one, two and three turbines in a network to assess the fastest convergence for this problem. This process, carried out in two separate stages, is presented in section 5.3.4.

Once a new solution is generated, it is subjected to an acceptance criterion: If the candidate solution Y is better than the previous solution X, it is immediately accepted; if not, then it is accepted with a probability given by

$$\alpha_{XY} = min\left(\frac{e^{-\frac{f(Y)}{\theta}}}{e^{\frac{f(X)}{\theta}}}, 1\right) \tag{5.5}$$

where θ is a control parameter known as temperature. If θ is high, this probability is also high, and it is easier for the algorithm to escape from local optima.

The temperature is not constant; it is classically high at the beginning and progressively decreases to speed the convergence of the method. Most theoretical papers on simulated annealing focus on the function for the temperature update, known as cooling schedule (Walid, 2004). For this case, the cooling schedule presented in (Laarhoven, et al., 1992) was considered in which the temperature depends on the standard deviation of the cost values of the solutions already obtained and an empirical parameter δ:

$$\theta_{k+1} = \frac{\theta_k}{1 + \left[\theta_k \ln(1+\delta)/3\sigma_k\right]} \tag{5.6}$$

In addition, many methods for the initial temperature θ_0 are proposed in the literature. Most of these methods are based on obtaining randomly initial solutions and extracting the statistics of the

cost function, i.e., mean and variance (Varanelli & Cohoon, 1999; Walid, 2004). However, the method proposed by (Kirkpatrick, et al., 1983) was applied because it is one of the simplest approaches. According to (Kirkpatrick, et al., 1983), the initial temperature can be estimated as

$$\theta_0 = \Delta f_{max} \tag{5.7}$$

where Δf_{max} is the maximal cost difference between any two neighboring solutions.

Input data

The physical characteristics of the network are modeled in the EPANET 2 software and the system is simulated by means of branches and elements connected by nodes. The user provides information on the demand at each node, the restrictions, and the turbine characteristics.

The demand at each node of the network must be fulfilled. Simulation of a full year was considered by assuming a single average water demand for each month, which is defined at each node by an hourly curve, one for weekdays and another for weekends/holidays. The number of days considered as weekends or holidays for each month is required and depends on the year and region.

In any WSN, restrictions exist on the maximum and minimum pressures at any point and are typically imposed by regulatory organizations for design and safety reasons. These restrictions can be introduced as constraints on the algorithm. The user might also indicate particular branches at which the minimum pressure is distinct, higher or lower than the rest of the network. In addition, branches in which it is known that the installation of turbines is not possible can be excluded from the optimization process.

Finally, the turbine model consists of characteristic curves for head, discharge and efficiency, and the respective impeller diameter. These curves can be defined by a second-degree approximation.

Simulation process

Based on an initial scenario with no turbines installed, the model begins by associating an appropriate impeller diameter with each branch of the network. The definition of a diameter is accomplished by stating that the flow for which a turbine should have the best efficiency is the 70th percentile of the annual series of flows in that branch. With this information, the corresponding characteristic ($H(Q)$) and efficiency ($\eta(Q)$) curves are obtained by applying the similarity laws. If the diameter resulting from this process is smaller than 100 mm, then the installation of a turbine in that branch is considered impossible.

The branches are ordered by potential for energy production, corresponding to an average production calculated with the maximum and minimum flows of the initial scenario (Qi) and the head drop that would be obtained in the turbine with these flows, as shown in Equation (5.8):

$$P(x) = \frac{Qi(x)_{\max H(Qi(x)_{\max})} + Qi(x)_{\min H(Qi(x)_{\min})}}{2} \tag{5.8}$$

Based on the potential chain, the neighborhood function is defined as follows:

- From an initial solution $X = (x_1, x_2, \dots, x_n)$, where n is the number of turbines and x_i is the location of each turbine, a new solution $Y = (y_1, y_2, \dots, y_n)$ is generated by applying the neighborhood function to each x_i.
- The neighborhood function is given by

$$I(y_i) = I(x_i) \pm D \tag{5.9}$$

where $I(x_i)$ is the index of the solution x_i in the potential chain previously obtained.

- D is obtained by generating a random number between D_{min} and D_{max}. The D_{max} is set as 5% of the number of branches in the network, and D_{min} is 0 or 1, depending on whether the function allows the variable x_i to remain the same or not.

For each iteration, a position vector of turbines is chosen. In these conditions, a full year is simulated to calculate the turbinated flow, the head drop, the efficiency at each hour, and finally, the produced energy.

For the case study, other aspects were added to the neighborhood function, i.e., the direction in the potential chain, the memory of previously visited solutions and previously rejected solutions, and whether the changes are applied in all locations or only one (Figure 5.7). First, different types of neighborhoods were tested to select the one with the best convergence to the optimal result. Second, using the best neighborhood function, simulations were performed with consideration of restrictions in the network.

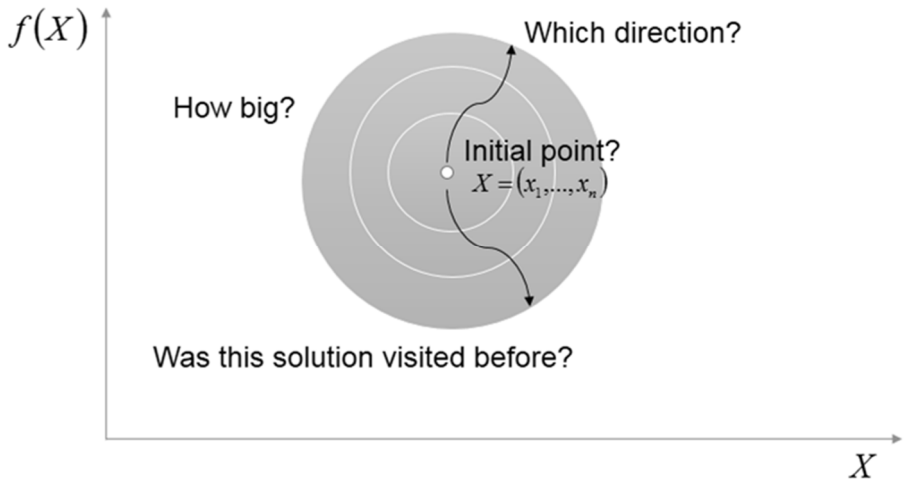

Figure 5.7 Definition of the neighborhood.

Figure 5.8 presents the general flowchart of the developed algorithm.

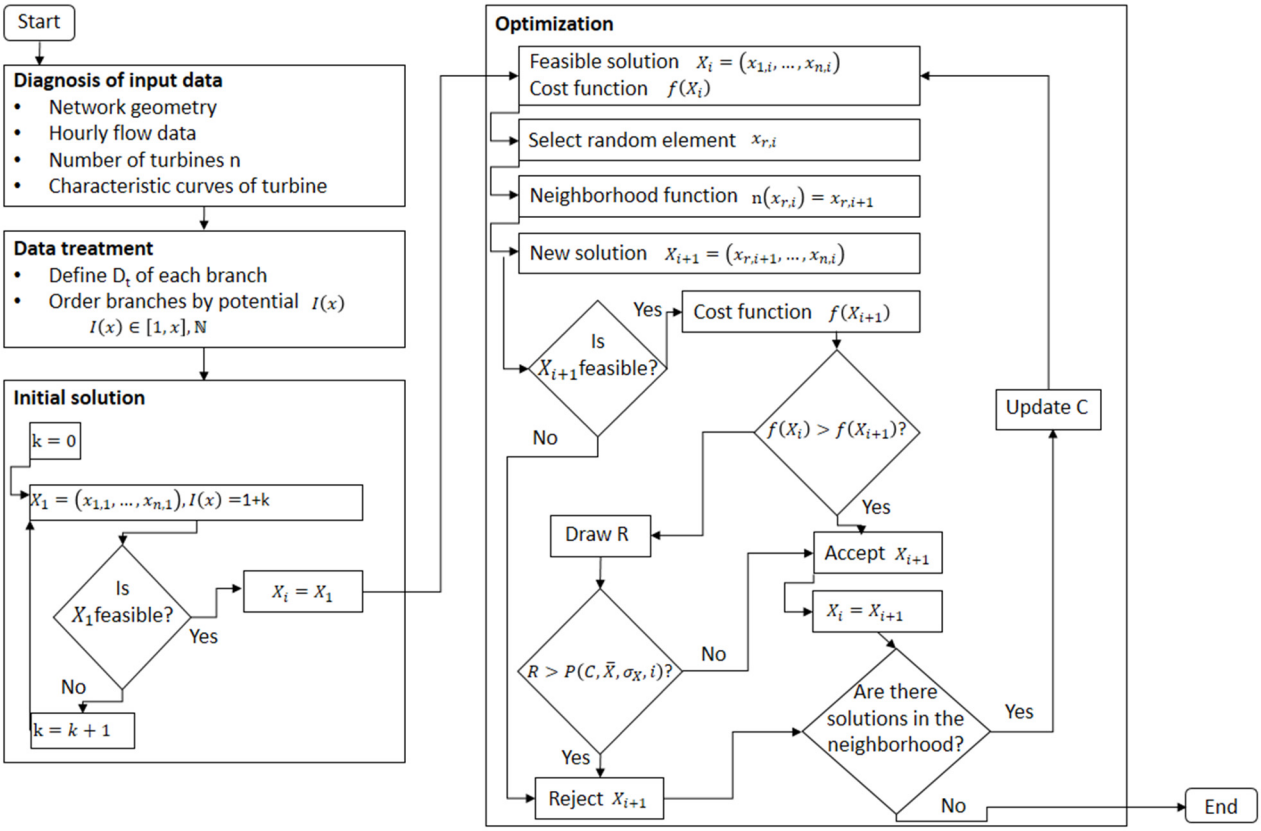

Figure 5.8 Model 2: Algorithm for identification of optimal locations in a WSN.

5.3.3 Case study description

The current model was applied to the case study of a sub-grid 1 of the WSN of the city of Lausanne presented in sub-chapter 3.3, thus testing the convergence of the developed algorithm on a real network and with real flow values. The proposed solution is appropriate for urban areas with topographic differences and slopes, as is the case in Lausanne. A few hypothesis were assumed to consider a fully gravity operation in the network.

The so-called node “tank” (Figure 5.9) was assumed as a regulation tank located upstream of the network, and the so-called node “reservoir” was defined to represent the network downstream of the considered sub-grid. Because the tank represents a real infrastructure, its physical characteristics are incorporated into EPANET and, for the simulations, the tank was considered half full. In contrast, the reservoir is defined as fictional and obliges a constant pressure downstream.

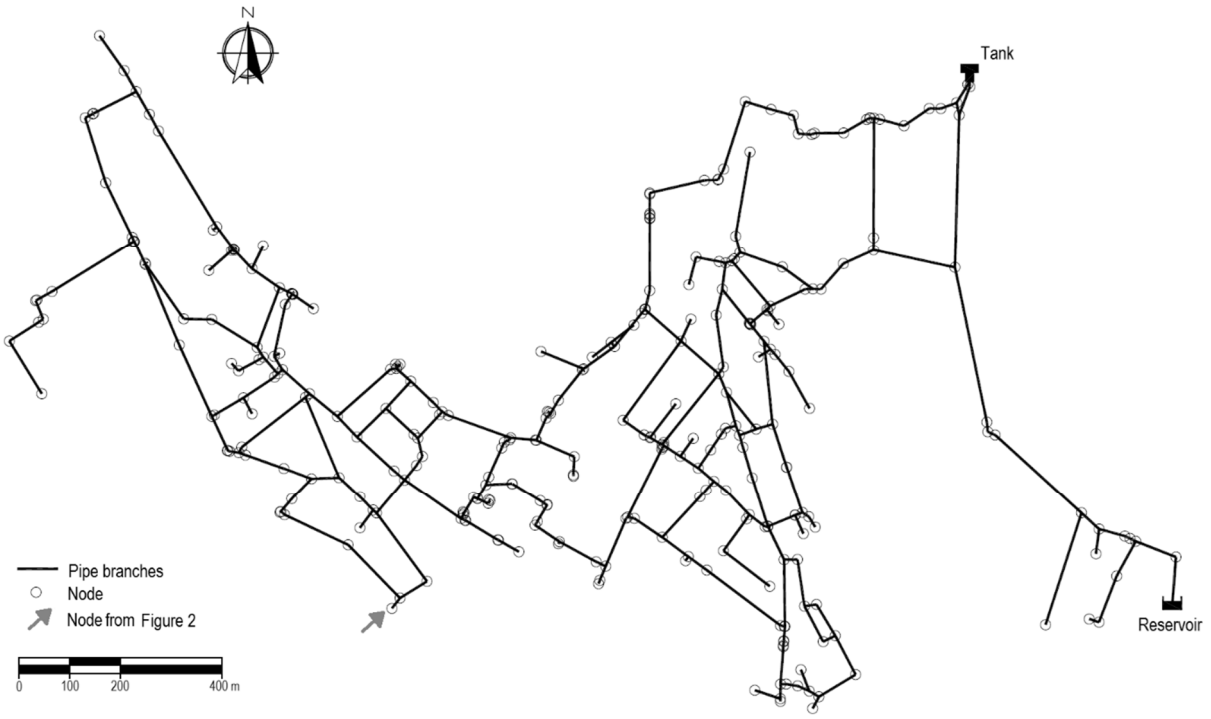

Figure 5.9 Closed sub-grid of the WSN used as a case study.

The hourly flows at the outlet of the tank for the period between 2009 and 2013 were distributed through the nodes of the network according to the average spatial flow distribution. In Figure 5.10 are presented the demand data and the average values for the outflow of the upstream tank.

For each node, the series were separated into weekdays and weekends/holidays, and an average series was obtained for each month. Figure 5.11 presents the average variation of flows in one randomly selected node identified in Figure 5.9. The shape of the curves is similar from month to month but slightly changes between weekdays and weekends/holidays.

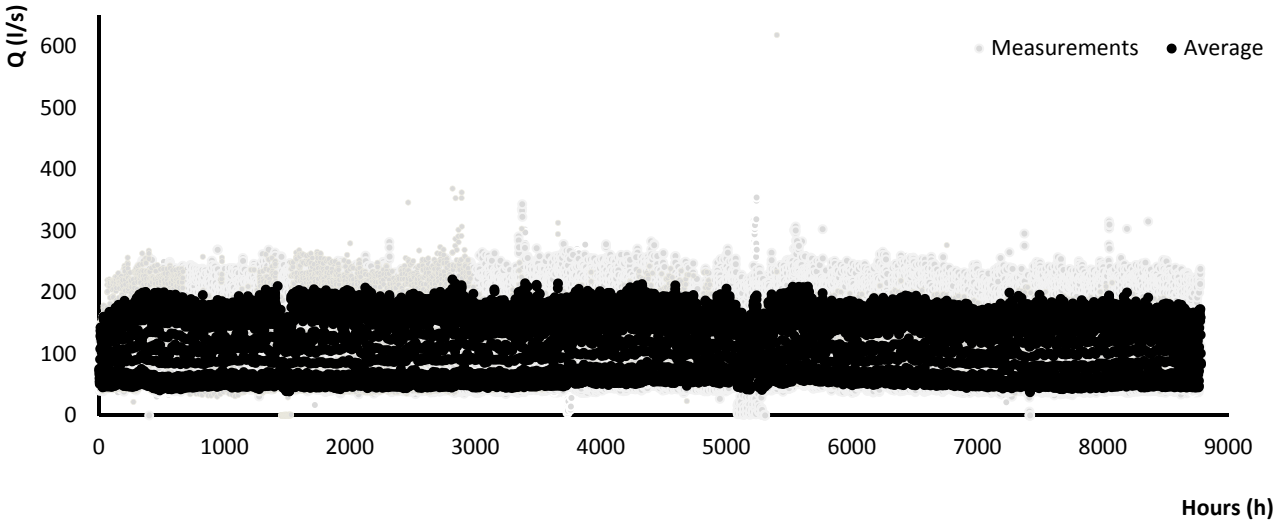

Figure 5.10 Measurements at the outlet of the tank and average value per hour.

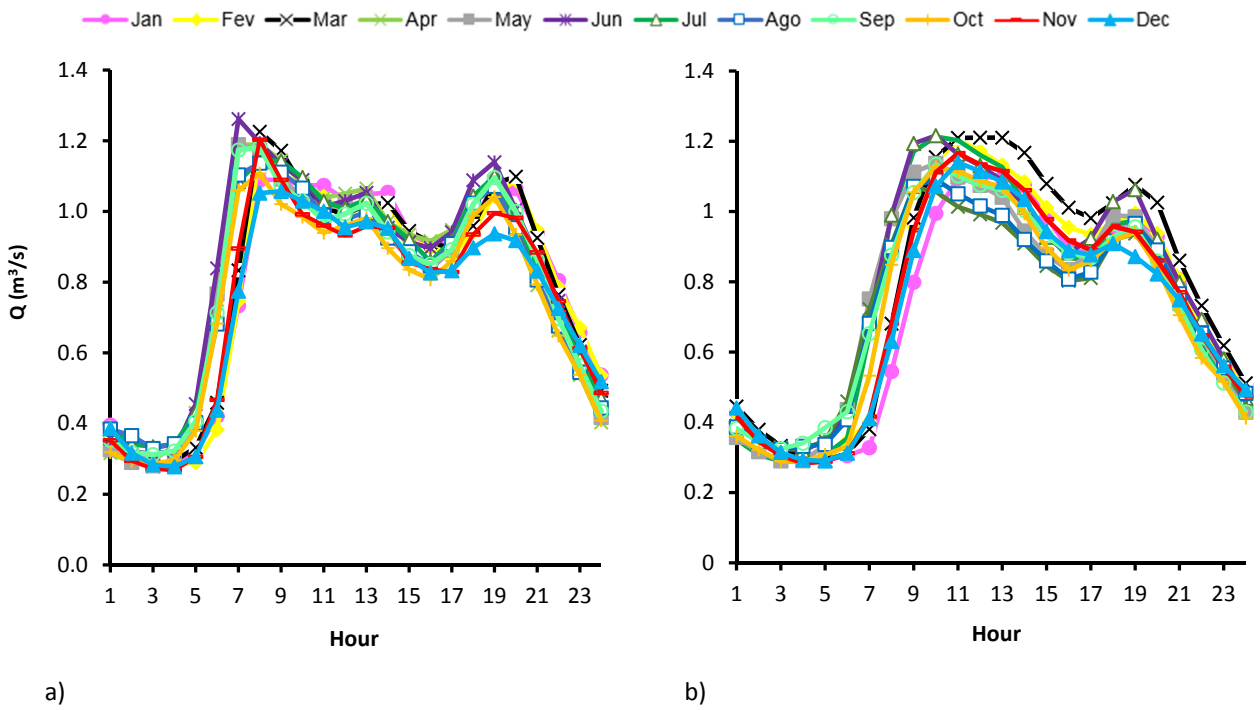

Figure 5.11 Average variation of flows in one randomly selected node. a) Weedday; b) Weekend/holiday.

A limit of 10 m of pressure was imposed on every node, with the exceptions of the two boundary nodes and six others for which the pressures were already less than 3 m in the original EPANET files because they are nodes without consumption in particular topographic areas of the network. These exceptions to the restrictions were a consequence of the manner in which the network is explored in reality.

The model was tested by considering the installation of one, two and three turbines under different restriction scenarios. Without considering any restrictions, there are 335 possible combinations for the installation of one turbine, which corresponds to the number of branches, 55 945 possible combinations for two turbines and more than six million for three turbines.

5.3.4 Results

Chain of potential

For the defined neighborhood function, it is necessary to order the branches by energy potential in what is referred to as the chain of potential. For a clearer reading of the results in the following sections, the branches were numbered between 1 and 335, and in Table 5.2, the 20 first positions of the chain of potential are presented, i.e., the 20 branches of the network with the highest potential. Based on Figure 5.12, it becomes obvious that the highest flows occur in the connection path between the water tank and the reservoir. This order of the chain of potential, as explained in section 5.3.2, is important for the generation of new solutions.

Table 5.2 Branches in the network ordered by decreasing potential (only 20 branches).

Order	Position	Order	Position
1	335	11	123
2	127	12	333
3	139	13	14
4	142	14	67
5	206	15	121
6	156	16	164
7	57	17	293
8	128	18	107
9	163	19	102
10	116	20	37

First stage of neighborhood definition

In an initial stage, the installation of one and two turbines without any restrictions apart from the nodal minimum pressure was considered as a reference for the definition of the neighborhood function.

The algorithm was tested for the neighborhood functions defined in Table 5.3. Because all variables x_i may change, Dmin is allowed to be zero such that repetition of positions is allowed. The initial point was considered starting from a low position and from the highest position of the potential chain, and the direction refers to the signal $\pm$ in Equation (5.9). The memory property refers to the recording of previous visited solutions such that they are not repeated. Allowing repetition of solutions means that the algorithm will waste iterations analyzing position vectors that have already been tested, whereas not allowing this repetition will force the algorithm to always try new solutions. Allowing repetition will have consequences on the cooling schedule, but the contrary may lead to a position vector in which all neighboring solutions have already been tried. An intermediate possibility was also considered with recording of previous solutions for only every 50 iterations.

For the installation of one and two turbines, a series of ten runs of the model up to a maximum of 100 and 200 iterations, respectively, were conducted. It was assumed that the turbines could be placed in any branch in the network, except for the installation of one turbine. Because it was verified that the optimal point for one turbine is the location with the highest potential, it was not allowed to use that particular when installing only one unit. Allowing the turbine to be installed in that branch would mean that the neighborhood solutions that start at the highest potential would find the optimum in the first iteration.

Tables 5:4 and 5:5 present the maximum energy productions achieved, and hence, the inversion of the minimum values of the cost function $f(X)$ (Equation (5.3)) for the installation of one and two turbines, respectively. The fact that the input flows were averaged over the month (conf. Figure 5.3) introduces an error of less than 1% but with clear advantages on the computational effort.

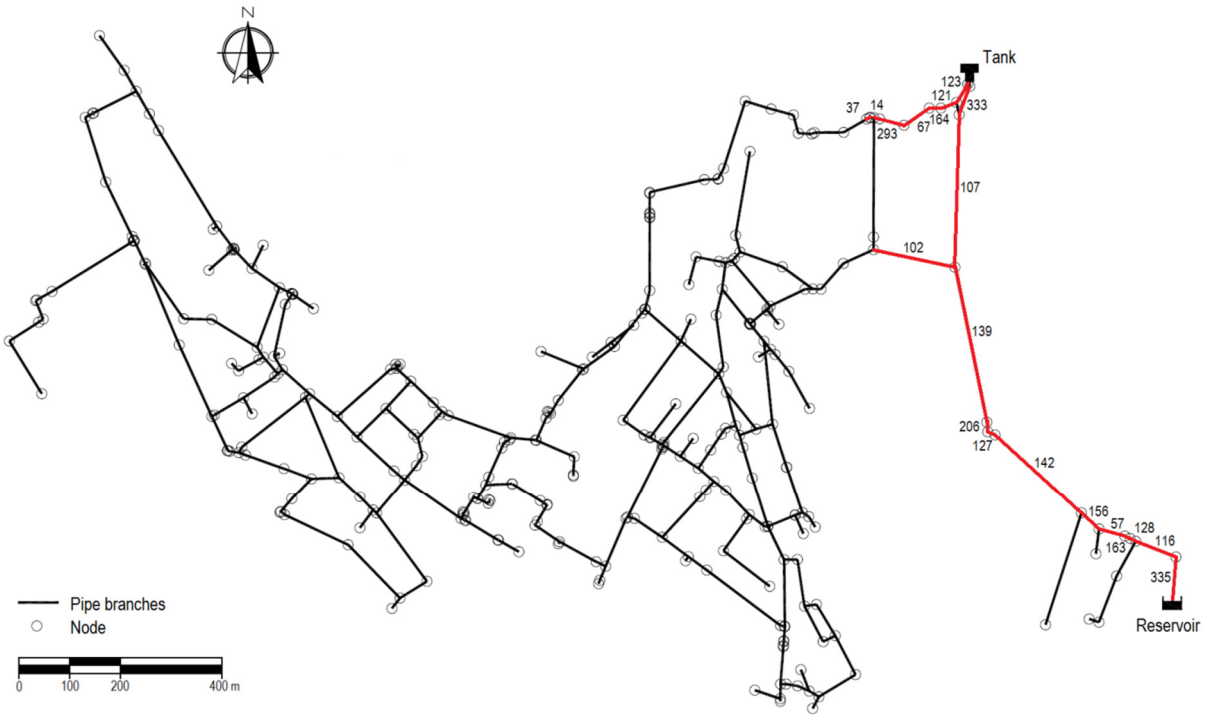

Figure 5.12 Identification of the highest potential locations in the network.

Tables 5:4 and 5:5 also present the branches X corresponding to the best solutions as well as the index of the chain of potential $I(X_n)$), the number of runs in which they were reached, and the iteration of occurrence. For analysis of the speed of convergence, the average iteration of occurrence of the best solution is also presented. The more often the maximum value is reached, the more robust the model will be. The sooner the solution is reached, the faster will be the convergence.

Table 5.3 Definition of the neighborhood functions of the first stage.

Name	1	2	3	4	5	6
Number of changing variables	N	N	N	N	N	N
D_{min}	0	0	0	0	0	0
Initial position vector	Low potential	Low potential	Low potential	Highest potential	Highest potential	Highest potential
Direction of random changes in the chain of potential	Probability of 70% of rising in the chain of potential unless it is impossible	The order of potential always increases unless it is impossible	The order of potential always increases unless it is impossible	The order of potential always increases unless it is impossible	The order of potential always increases unless it is impossible	The order of potential always increases unless it's it is impossible
Memory of accepted solutions	The algorithm does not allow repetition of accepted solutions	In every 50 iterations, the algorithm does not allow repetition of accepted solutions	The algorithm does not allow repetition of accepted solutions	In every 50 iterations, the algorithm does not allow repetition of accepted solutions	The algorithm does not allow repetition of accepted solutions	No memory

Table 5.4 Simulations results with one turbine for neighborhood function definition.

Neighborhood function	1	2	3	4	5	6
$f(X)^{-1}$ (MWh)	60	60	60	60	60	60
$X = x_1$	333	333	333	333	333	333
$I(X)$	12	12	12	12	12	12
Reached in n° of runs	10	10	10	10	10	10
Iterations when reached	[30, 16, 16, 59, 30, 73, 73, 58, 28, 55]	[3, 58, 22, 59, 34, 32, 83, 61, 37, 50]	[28, 50, 27, 47, 48, 47, 30, 40, 37, 8]	[13, 2, 6, 54, 41, 21, 54, 50, 2, 36]	[16, 6, 19, 10, 16, 2, 2, 2, 2, 16]	[6, 3, 2, 38, 36, 7, 2, 9, 25, 33]
Average iteration of occurrence	44	44	36	28	9	16

Table 5.5 Simulations results with two turbines for neighborhood function definition.

Neighborhood function	1	2	3	4	5	6
$f(X)^{-1}$ (MWh)	128	128	128	128	128	128
$X = (x_1, x_2)$	(333, 335)	(333, 335)	(333, 335)	(333, 335)	(333, 335)	(333, 335)
$I(X)$	(12, 1)	(12, 1)	(12, 1)	(12, 1)	(12, 1)	(12, 1)
Reached in n° of runs	1	5	6	7	4	3
Iterations when reached	164	[85, 167, 67, 106, 41]	[62, 177, 105, 104, 70, 127]	[60, 40, 122, 96, 59, 149, 101]	[5, 37, 154, 185]	[114, 71, 180]
Average iteration of occurrence	164	93	108	90	95	122

In the graphics of Appendix A are presented the 10 runs of all simulations performed.

For the installation of one turbine, the optimal result was found in every run. Among neighborhood functions 1, 2 and 3, the difference of speed of convergence is not overly large because the average iteration of occurrence is similar, but the neighborhood functions that begin at a high potential point are clearly faster. The frequency of recording of the previous solutions does not strongly influence the results because the solution is reached mostly before the 50th simulation.

When two turbines are considered (Table 5.5) starting at a high potential point proves to have the advantage of guaranteeing a good solution but does not guarantee finding the optimal one. Moreover, it is clearly better to define the neighborhood as an increase of potential whenever possible. Function 5 is faster, but is successful less frequently than functions 3 and 4. Function 3 starts with a too low potential solution, whereas function 5 is never allowed to go backwards because repetition is not permitted. Nevertheless, function 6 rarely reached the maximum, proving that it is important to record the previous solutions.

Because the neighborhood function 4 gives the more frequent results, it was adopted for further testing.

Installation of one and two turbines for different restriction scenarios

For the chosen neighborhood function, the installation of one and two turbines was simulated considering that it is not possible to install these units in certain branches of the network. The purpose of this test is to evaluate the convergence to solutions other than the unrestricted optimal

point already found. In this way, the algorithm will begin at a different initial point and might find a different optimal solution. Hence, the following cases types were considered:

1. No restrictions;
2. Restrict the installation in the branch with the highest potential (ID=335 in Figure 5.12 and Table 5.2);
3. Restrict the installation in the branch with the second highest potential (ID=127 in Figure 5.12and Table 5.2);
4. Restrict the installation in ID=335 and ID=127;

For each case, ten runs were conducted with a maximum of 100 and 200 iterations for the installation of one and two turbines, respectively. The results are presented in Tables 5.6 and 5.7.

Table 5.6 Results from the installation of one turbine with neighborhood function 4.

Case type	1	2
$f(X)^{-1}$ (MWh)	68	60
$X = (x)$	335	333
$I(X)$	1	12
Reached in n° of runs	10	10
Iterations when reached	[1, 1, 1, 1, 1, 1, 1, 1, 1, 1]	[52, 2, 66, 2, 27, 13, 3, 11, 21, 2]
Average iteration of occurrence	1	20

For the installation of one turbine only, the cases of type 1 and 2 were considered because type 3 will always start at the highest potential point, yielding the same result as case type 1, and type 4 will give the same result as case type 2.

Table 5.7 Results from the installation of two turbines with neighborhood function 4.

Case type	1	2	3	4
$f(X)^{-1}$ (MWh)	128	111	128	102
$X = (x_1, x_2)$	(333, 335)	(127, 333)	(333, 335)	(14, 333)
$I(X)$	(12, 1)	(2, 12)	(12, 1)	(13, 12)
Reached in n° of runs	7	9	7	7
Iterations when reached	[60, 40, 122, 96, 59, 149, 101]	[38, 88, 41, 19, 36, 49, 3, 41, 181]	[13, 15, 199, 47, 10, 60, 84]	[194, 91, 99, 111, 60, 44, 193]
Average iteration of occurrence	90	55	61	113

The best solution was found in all runs for the installation of one turbine. For case type 1, the best solution is also the solution with the highest order of potential, and thus, it is the initial solution.

For the installation of two turbines, all cases were considered to verify the convergence under different initial points because disallowing the highest potential points influences the starting solution.

For all cases of two turbines, the convergence of the algorithm is rapid and has a high probability of occurrence but was not reached in every run. Given these results, it was decided that the neighborhood function could still be improved, and thus, a second stage of neighborhood definition was performed.

Second stage of neighborhood function definition

The larger the number of turbines, the more difficult it is to find the global optimum because the degrees of freedom of the neighborhood are increased.

The installation of three turbines with the algorithm previously defined (even for a maximum of 300 iterations) did not give confident results (neighborhood function 4 of Table 5.8). Thus, a new neighborhood definition is needed to improve the convergence. New neighborhood functions for testing were thus defined, as presented in Table 5.8. Because functions 9 and 10 only allow one position to change per iteration, the minimum draw D_{min} is no longer allowed to be zero to force the generation of a new solution.

The results of the second stage of neighborhood definition are presented in Table 5.8.

For functions 4 and 8, the optimal point is only reached three times, and for function 7, only the second best point is reached. However, for functions 9 and 10, the maximum was always reached. These functions are slower than function 4 but always found the best solution, thus proving that only changing one branch at a time is better than changing all three.

Table 5.8 Definition of the neighborhood functions of the second stage.

Name	4	7	8	9	10
Number of changing variables	N	N	N	1	1
D_{min}	0	0	0	1	1
Initial position vector	Highest potential	Highest potential	Highest potential	Highest potential	Highest potential
Direction of random changes in the chain of potential	The order of potential always increases unless it is impossible	The order of potential always increases unless it is impossible	The order of potential always increases unless it is impossible	The order of potential always increases unless it is impossible	The order of potential always increases unless it is impossible
Memory of accepted solutions	In every 50 iterations, the algorithm does not allow repetition of accepted solutions	In every 50 iterations, the algorithm does not allow repetition of accepted solutions	In every 50 iterations, the algorithm does not allow repetition of accepted solutions	In every 50 iterations, the algorithm does not allow repetition of accepted solutions	No memory
Memory of rejected solutions	No memory	In every 50 iterations, the algorithm does not allow repetition of rejected solutions	The algorithm does not allow repetition of rejected solutions	The algorithm does not allow repetition of rejected solutions	The algorithm does not allow repetition of rejected solutions

Table 5.9 Simulations results with three turbines for neighborhood function definition.

Neighborhood function	4	7	8	9	10
$f(X)^{-1}$ (MWh)	262	167	262	262	262
$X = (x_1, x_2, x_3)$	(127, 333, 335)	(14, 333, 335)	(127, 333, 335)	(127, 333, 335)	(127, 333, 335)
$I(X)$	(2, 12, 1)	(13, 12, 1)	(2, 12, 1)	(2, 12, 1)	(2, 12, 1)
Reached in n° of runs	3	3	3	10	10
Iterations when reached	[90, 22, 69]	[133, 57, 65]	[53, 277, 215]	[224, 181, 141, 6, 172, 145, 93, 120, 63, 11]	[85, 202, 96, 182, 210, 49, 145, 138, 150, 163]
Average iteration of occurrence	60	85	182	116	142

It is important to note that the definition of functions 9 and 10 only differs beyond the 50th iteration (Table 5.8). The average iteration of occurrence for function 9 is 116, whereas for type 10, it is 142. The periodic record of previously visited solutions makes the algorithm faster, and hence, the neighborhood function 9 was adopted for further testing.

Final results

After the second stage of definition of the neighborhood function, the restriction case types from before were repeated for the installation of two and three turbines. The results presented in Table 5.10 show the best solutions found for all considered case types and for the installation of two and three turbines. The respective positions in the network, the indices in the potential chain, the number of runs in which the results were reached, and the iterations at which they occurred are also given.

Table 5.10 Results from the installation of two and three turbines with neighborhood function 9.

Case type		1	2	3	4
Installation of two turbines	$f(X)^{-1}$ (MWh)	128	111	128	102
	$X = (x_1, x_2)$	(333, 335)	(127, 333)	(333, 335)	(14, 333)
	$I(X)$	(12, 1)	(2, 12)	(12, 1)	(13, 12)
	Reached in n° of runs	9	9	10	10
	Iterations when reached	[75, 100, 57, 65, 42, 92, 12, 130, 135]	[88, 85, 4, 2, 70, 69, 28, 40, 35]	[61, 34, 100, 11, 134, 39, 78, 73, 77, 2]	[74, 109, 60, 63, 64, 20, 137, 13, 59, 111]
	Average iteration of occurrence	79	47	61	71
Installation of three turbines	$f(X)^{-1}$ (MWh)	262	147	167	132
	$X = (x_1, x_2)$	(127, 333, 335)	(14, 127, 333)	(14, 333, 335)	(14, 142, 333)
	$I(X)$	(2, 12, 1)	(13, 2, 12)	(13, 12, 1)	(13, 4, 12)
	Reached in n° of runs	10	9	10	8
	Iterations when reached	[224, 181, 141, 6, 172, 145, 93, 120, 63, 11]	[217, 237, 104, 145, 106, 81, 234, 282, 174]	[20, 23, 160, 210, 148, 126, 269, 234, 166, 127]	[117, 198, 169, 202, 267, 6, 206, 186]
	Average iteration of occurrence	116	176	148	169

For all cases of two turbines, the convergence of the algorithm was improved compared with that of Table 5.7. Still, the convergence was not perfect because, in certain cases, the algorithm became trapped in a position vector in which all neighboring solutions had already been visited. This situation illustrates the disadvantage of not allowing the repetition of solutions. In addition, for the installation of three turbines, all cases showed good convergence, therefore validating the application of this neighborhood.

The installation of one, two and three turbines correspond to a recovery around 1%, 2% and 5%, respectively, of the energy needed to pump the average hourly flow incoming into the sub-grid, considering the elevation of the upstream water tank, the elevation of Lake Geneva and a pump with 0.6 of efficiency.

5.3.5 Conclusions

This sub-chapter presents an algorithm for selecting the optimal locations to install micro-turbines in a complex network. Based on hourly simulations of the produced energy and using a simulated annealing process as the foundation for an optimization procedure, the methodology was tested in a sub-grid of the WSN of Lausanne, Switzerland.

The case study showed rapid convergence for the cases of installing up to three turbines. The model was applied to a real network with 335 branches, 312 nodes and 76 intersections of more than two branches. The simulations proved that it is possible to locate the optimal positions for one, two and three turbines if the neighborhood function is well adapted to the problem. The sensitivity of the algorithm was tested by changing certain restrictions in selected branches of the grid such that the initial point for the optimization procedure was changed. The model still showed a good convergence.

The optimal solutions tended to choose positions for the turbines in the link between the upstream water tank and the connection with the sub-grid downstream. This corresponds to the path with the higher flows in the network, but the generalization of this result is still under study since not all networks have clear main paths of supply.

One result from the model is that although the results tended to be placed in branches with high energetic potential, the best solutions were not the combinations of the branches with highest energetic potential. This indicates the need for a detailed analysis in terms of daily variation of flow and turbine efficiency.

5.4 Feasibility of a micro-hydropower plant in water supply networks

5.4.1 Methodology

In this sub-chapter 5.4, the feasibility of installing micro turbines in WSN within urban areas is analyzed. This assessment is carried out through the conception of an installation arrangement and

the optimization of its location within a network. In the previous sub-chapter, an optimization routine was developed to identify the locations of N_t turbines in a given network that maximize the energy production. However, these locations may not be the optimal from an economical point of view.

Hence, a micro-hydropower arrangement, its position within WSN and its optimization are analyzed both in terms of energy production and economic feasibility. Specific and realistic configurations are defined (section 5.4.2), which are the basis of an economical study, and the concept is applied to a real case study to be validated. For this purpose, the turbine tested in Chapter 4 is considered for the simulation. The process of simulation of energy generation and location optimization employs an upgraded version of the previously developed algorithm based on the Simulated Annealing strategy from section 5.3, summarized in section 5.4.3. Also in this section the recent developments made to the algorithm considering the new multiple turbine configurations and objective functions are described. Section 5.4.4 and section 5.4.5 present and discuss the results in terms of the energy production and economic analysis for two case studies. Finally, in section 5.4.6 the main conclusions are drawn.

5.4.2 The micro-hydropower arrangement

Based on the 5BTP, constructive solutions are proposed to install it within a network. These configurations need to be enough detailed to allow a consistent estimation of costs for the economic analysis. The base of the proposed arrangement is the construction of a buried concrete chamber, as schematically represented in Figure 5.13, connected to an existing pipe.

As for other typical axial turbines, the runner is nested in a contracted section with the purpose of accelerating gradually the flow, aligning the streamlines and reducing secondary flows (i.e. vorticity and turbulence). Therefore, the runner diameter (D_t) is usually inferior to the diameter of the existing pipe (D_p), and the installation includes a contraction taper on the high pressure (HP) upstream side and an enlargement taper on the low pressure (LP) downstream side. Measurements of the flow, as well as a generator and a converter and connections with the network are required. The converter controls the rotational speed of the runner according to the flow measurements and converts the frequency of the generated energy to match the local network. No step-up transformers to local electrical grids are included in this study. All this equipment must be accessible for operations and maintenance. Given that the circuit needs two curves to allow the axis to connect with the generator, there is in fact space to include more than one turbine. Up to four turbines can be installed within the same buried chamber, as sketched lighter in Figure 5.13. This allows producing more energy and having a more versatile system in terms of operation range per chamber and operation redundancy without increasing the costs in the same proportion.

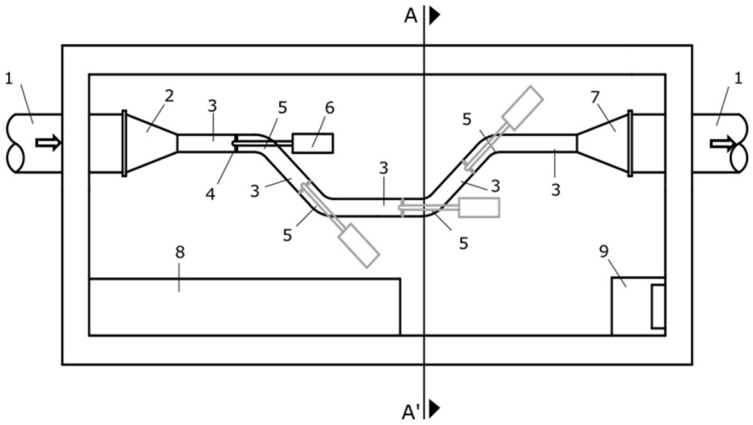

Legend:

1 – Existing parent pipe (D_p);

2 – HP contraction taper;

3 – Straight pipe (D_t);

4 – Turbine runner module (D_t);

5 – 45° bend (D_t);

6 – Generator;

7 – LP enlargement taper;

8 – Electric cubicle;

9 – Access manhole;

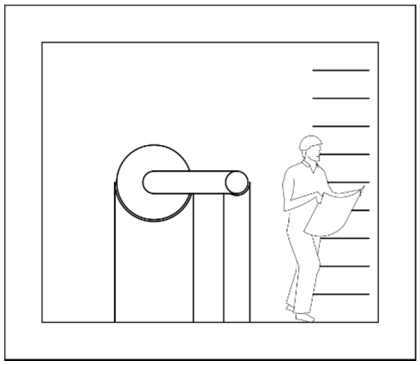

Figure 5.13 Schematic lay-out of a chamber equipped with one to four turbines. Top: plan view. Below: cross-section A-A'.

Another important factor is the possibility to isolate the chamber for maintenance. This is an important aspect to take into account also during construction. Nevertheless, since most WSN are meshed, there is often redundancy in the supply to a particular node. Thus, two possible arrangements are defined (Figure 5.14 shows examples for one turbine installation): arrangement A, where there is redundancy and it is assumed that valves exist to isolate the branch; arrangement B, where there is no redundancy and a bypass must be built.

However, the installation of more than two turbines inline in an arrangement B requires a longer bypass and additional curves, as presented in Figure 5.15. Both arrangements will be considered in this study of the feasibility to install one, two, three and four turbines.

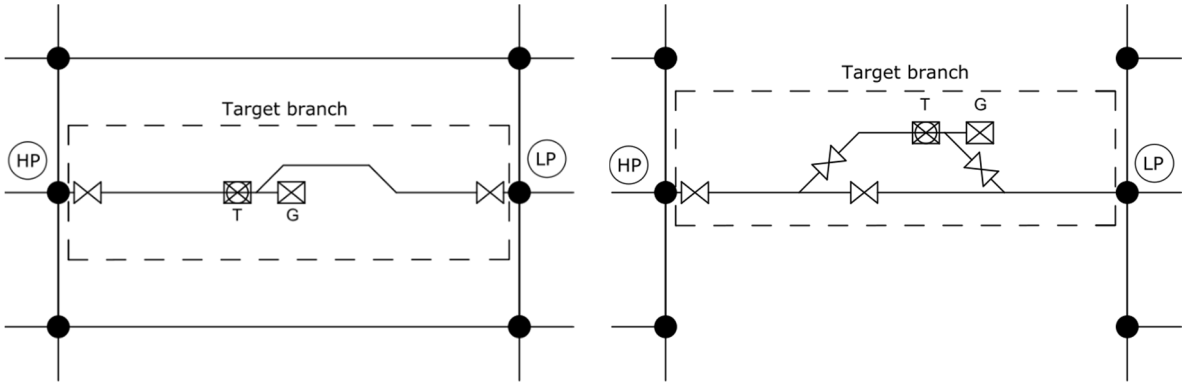

a) Arrangement A b) Arrangement B

Figure 5.14 Possible micro-hydropower chamber arrangements in a network, with one turbine (T) and generator (G). a) Type A: with supply redundancy; b) Type B: without supply redundancy.

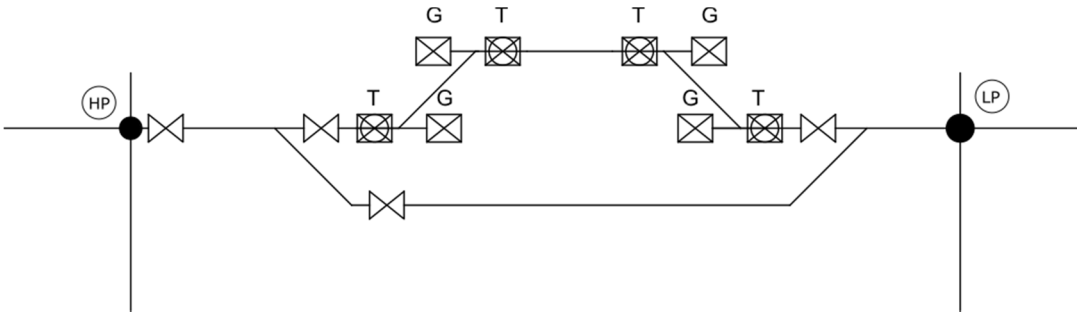

Figure 5.15 Arrangement B with four turbines.

5.4.3 Model

The optimal location of the energy converter within the urban network is the first step to evaluate the feasibility of the arrangement. The search algorithm presented in sub-chapter 5.3 (Figure 5.8) was further developed to optimize both the energy production and the economic value of the hydropower arrangement. These new developments of the model allow the installation of more than one turbine in each branch as well as estimating the energy production and investment costs associated to each solution.

Objective function for energy optimization

For energy production optimization, the objective (or cost) function to minimize is defined by Equation (5.3). The following new features were implemented to the algorithm, improving the computation of the produced energy:

1. The characteristic curves of the 5BTP obtained from experimental tests of Chapter 4 are used. It is considered that the converter will regulate the rotational speed of the turbine to ensure the maximum power generation at each time step. Since each diameter has a single characteristic curve, the extrapolation to other diameters is done using the similarity laws of turbo-machine equations. The design flow rate and, consequently, the turbine diameter for

each branch is selected according to the experimental curves. In this phase, the highest recorded flow in each branch, according to the hourly available data, is assumed as the design flow rate.

2. The runner diameter for each branch is initially obtained through the similarity laws matching the design flow rate with the experimental operating point of the turbine which, with the highest experimentally tested flow, reached the maximum energy. The minimum turbine diameter herein considered was 85 mm. Afterwards, having a first simulation of a full year, the diameter is updated by: either increasing de diameter to rend the solution valid, in case the initial values induced pressures below the limit or interfered with particular restrictions concerning the discharge rates; either decreasing, to match the highest discharge flow for the situation with the turbine installed, optimizing the installed power.
3. A specific minimum pressure restriction was assumed, according to the Swiss Directive for Water Supply (SVGW, 2013). In fact, the minimum service pressure in Switzerland is a function of the average number of building stories. A service pressure of 10 m should be available at the highest floor, and most buildings should be equipped with pressure dissipation valves. Hence, considering the typical height of buildings in Lausanne, the minimum pressure on the network was adjusted to 30 m, considering that a 6 story building would not require a pump to have 10 m of water pressure in the upper floor.
4. The maximum velocity was defined as 2 m/s.
5. Local head losses in contractions and expansions inside the turbine chambers were added to the hydraulic calculations.
6. A stopping criterion was defined: if there are no more possible solutions in the neighborhood of the current solution, the run is stopped. This criterion represents the depletion of possible solutions within the neighborhood.
7. The range was amplified to 10% of the branches in the network, increasing considerably the solution space.
8. Finally, the algorithm was modified to allow installing more than one turbine in the same branch. The number of possible solutions is hence increased.

Objective function for economic optimization

For the optimization of the economic value of the micro turbine arrangement, a second objective function was defined considering the NPV (Equation (2.15)) of the project discounted cash-flows over a period of 20 years:

$$f(X) = {}^{1}/_{NPV_{20\ years}} \tag{5.10}$$

Two different types of remuneration can be considered depending on the economic model assumed: selling to the grid or self-consumption. When selling to the grid, the revenues are given by the produced energy and the considered sell-tariff. However, for a self-consumption scheme, it

is assumed that the generated energy is consumed in operations within the network. In this case, the gain is in the savings in the electricity bill of the network.

To estimate the stream of revenues, the electricity selling price was fixed at 0.33 $/kWh. The latter is aligned with the current Swiss feed-in-tariff mechanism for renewable energy production (SFC, 1998; SFOE, 2015). A discount rate of 4% was adopted. The electricity production was computed considering Equation (5.4).

To estimate the investment costs, the main quantities of the arrangement were evaluated and unit prices (Table 5.11) were selected based on available databases (EPFL, 2015; Gabathuler, et al., 2015). The stainless steel pipes include flanges and tapers. All straight pipes are at least as long as three times the diameter to minimize turbulence influence and flow separation zones. The walls of the chamber were assumed in reinforced concrete with an average thickness of 40 cm. The excavation was defined assuming that the chamber is fully buried with the top slab at surface level and excavation side slopes at 1:1 (H:V). The volume of earth fill was assumed to be 10% of the excavated volume. The electromechanical equipment includes the generators, the frequency converter, the turbines, the electrical cubicles and the connection to the local electricity network. Both the flowmeters and the maintenance valves are installed in pipes with the same diameter as the turbines. For feasibility purposes a linear cost function was adopted for the single bill of quantities item related with equipment. For most technological elements within this item there are proven mature solutions, except for the 5BTP turbine for which average prices of other turbine types were considered assuming it will reach a similar development level. After screening of possible solutions of location and installed capacity, the detailed design for a specific site will require specific cost functions or market quotations for each equipment item allowing refinement. The costs for connections to the grid and site access were considered negligible, since the arrangements are installed in urban areas (Gallagher, et al., 2015).

Table 5.11 Unit prices considered in the present study.

Element	Unit price
Stainless steel	7 $/kg
Reinforced concrete	250 $/m^3
Excavation	30 $/m^3
Earth fill	20 $/m^3
Electromechanical equipment	1 $/W
Maintenance valve w/ wheel drive	190 000 $/m^2
Flowmeter	550 $/unit

For the NPV analysis, all investment costs were allocated to the year prior to commissioning. A surplus of 25% regarding the “equipment and civil works” sub-total was assumed for engineering and construction supervision and 15% for miscellaneous items not quantified at such initial phase, which would include the access manhole to the chamber, plus ventilation, drainage, power and thermal insulation. These percentages were applied independently of the number of turbines in the chamber. Also, 2% of cost savings were considered when more than one chamber was retained to take into account group ordering prices.

Finally, each new chamber means there will be one to four more objects requiring operation and maintenance (O&M) follow-up in networks with already several nodes, valves and other machinery installed. Nevertheless, given the characteristics of the micro-hydropower chamber and equipment, the corresponding O&M costs can be easily diluted in the overall O&M of the network and were considered not relevant for the cost estimation.

5.4.4 Application to the case study of Lausanne

System description

The upgraded optimization algorithm was once again applied to the case study of Lausanne WSN 1, with the same distribution of hourly flows as described in 5.3.3. However, a supplementary restriction concerning the downstream boundary condition was added. As before, it was assumed that the "reservoir" node has a fixed constant pressure to ensure the continuity of the model downstream. This node has no redundancy in its supply, hence the outflows of the sub-system will decrease when a turbine is placed in any of the links that lead to this particular node due to the re-equilibrium of the system. However, for the validity of the model, such decrease should not hinder adequate supply to the downstream consumers and must remain within acceptable limits. The maximum relative flow differences obtained between an "initial condition", without turbines, and a "modified condition" with four turbines, considering the same level imposed in the "reservoir" was limited to 25%. This difference is small and was thus considered acceptable in this case study. In reality, a downstream reservoir and other sources in the network would absorb this difference. Also, should the downstream node be defined as a regular node instead of a reservoir, the water pressure level would be adjustable and submitted to the same restrictions as the remainder sub-grid.

Annual energy production

To obtain optimal results for the annual energy production in the network case study, the search algorithm was used with the firstly defined cost function given by Equation (5.3) for one to four turbines. The generator efficiency was set to 100% to have results that do not depend on the choice of the generator type. Also, the run was repeated three times with the restriction of not allowing the previous best locations, to have also estimations of second, third and fourth best solutions to optimize the energy production. In Table 5.12 the results of these simulations are presented, as well as the diameters of the pipes and turbines. The location of the selected pipes in the network can be seen in Figure 5.16.

The best solutions tend to use the best individual locations. The highest production is achieved by distributing the turbines in different pipes. This can be explained by the fact that the equilibrium of the energy lines will result in different flow rates for distinct solutions and by the restriction of maximum 25% of difference in flow rate exiting from the system, which affects the diameter choice.

Table 5.12 Lausanne case study: Results from the optimization of energy production with one to four turbines.

N° of turbines	Restrictions	X	E (MWh/year)
1	-	127	54.9
	Without 127	142	54.8
	Without 127 and 142	206	54.8
	Without 127, 142 and 206	139	54.8
2	-	(127, 294)	57.5
	Without 127	(142,294)	57.5
	Without 127 and 142	(206,294)	57.5
	Without 127, 142 and 139	(206, 294)	57.5
3	-	(15, 37, 57)	80.3
	Without 57	(15, 37, 128)	80.3
	Without 57 and 128	(15, 37, 163)	80.3
	Without 57, 128 and 163	(15, 37, 156)	79.6
4	-	(15, 17, 107, 142)	95.8
	Without 142	(15, 17, 107, 156)	94.7
	Without 142 and 156	(15, 17, 57, 107)	94.5
	Without 142, 156 and 57	(15, 17, 107, 163)	94.5

Another visible trend is the installation of turbine units in the main link between the upstream water tank and the main outlet of the network. This is due to the morphology of the network, resulting in most of the network being linked to a main path where the flow is higher. However, the placement of more than one turbine in this path, in order to respect the outflow discharge constrain, implies the installation of bigger turbine runner diameters, which is overall a less efficient solution for the present discharge rates. Hence, it compensates to distribute the turbines in the network. As an example, Figure 5.17 presents a comparison between the initial node pressures and those achieved with the best solution with four turbines, for the instant when the pressure is minimum.

Economic value

The search algorithm was run once again, this time to maximize the NPV with one to four turbines. The generator efficiency was considered to be 85%, to have a more reliable balance between costs and revenues. As before, the run was repeated three times with the restriction of not allowing the previous best solutions, to have also estimations of second, third and fourth best places. In Table 5.13 the results of these simulations are presented, as well as the diameters of the pipes and turbines, as well as the generated energy. The location of the pipes in the network can be visualized in Figure 5.16.

The optimal solutions obtained with the two different objective functions are not always identical (Table 5.12 and Table 5.13). In fact, they are the same for three and four turbines but not for one and two.

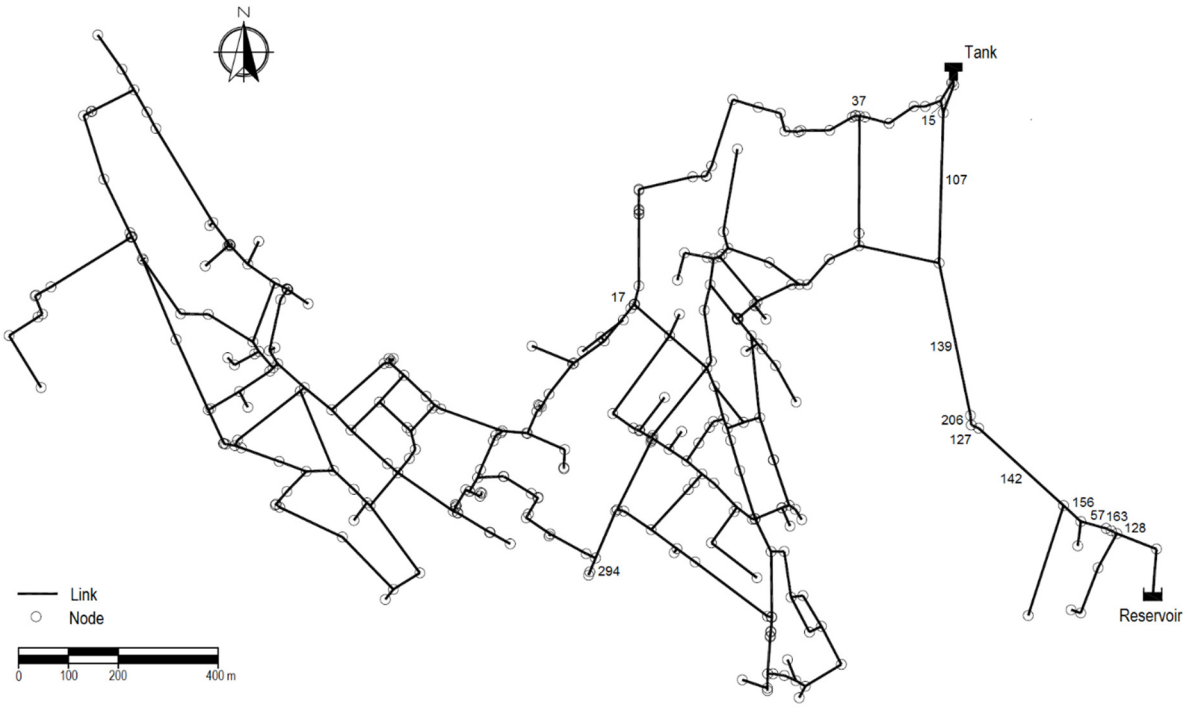

Figure 5.16 Lausanne case study: Location of selected pipes considering optimization of energy production optimization.

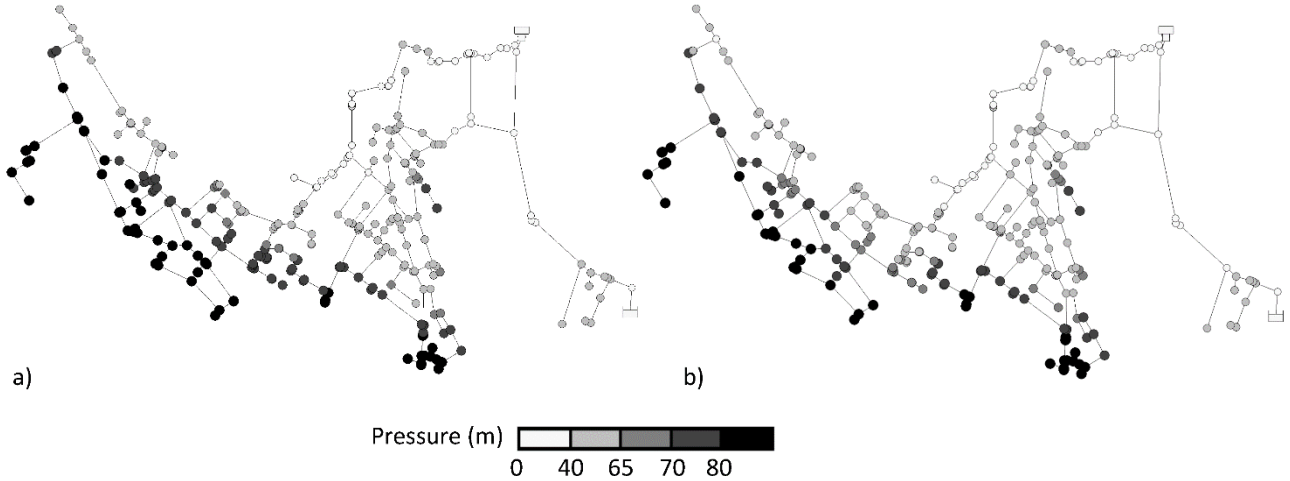

Figure 5.17 Pressure in the nodes of the network for the instant when the pressure is minimum. a) Initial conditions; b) 4 turbines (15,17,107,142).

Once again, the results show that the best solutions tend to use the best individual locations. For two turbines, all the proposed solution place both turbines in the same pipe. Although the energy production is smaller, there is an economic advantage in not constructing two separate chambers. However, for the placement of three and four turbines the solutions are the same as for energy optimization. The effect of changing the energy equilibrium in the system is still evident, since producing more energy may compensate building a second, third or even fourth chamber due to a better distribution of flow rates and pressures.

Table 5.13 Lausanne case study: Results from the optimization of $NPV_{20years}$ with one, two, three and four turbines.

N° of turbines	Restrictions	X	$NPV_{20years}$ ($)			E (MWh/year)
			Discount rate: 4%	Discount rate: 6%	Discount rate: 8%	
1	-	142	191 656	159 036	133 625	46.6
	Without 142	156	191 000	158 484	133 154	46.5
	Without 142 and 156	128	190 209	157 818	132 586	46.3
	Without 142, 156 and 128	57	190 209	157 818	132 586	46.3
2	-	(142, 142)	200 099	166 235	139 856	48.4
	Without 142	(156, 156)	199 249	165 520	139 245	48.2
	Without 142 and 156	(57, 57)	198 226	164 658	138 509	48.0
	Without 142, 156 and 57	(163, 163)	198 226	164 658	138 509	48.0
3	-	(15, 37, 57)	241 700	193 954	156 761	68.2
	Without 57	(15, 37, 128)	241 700	193 954	156 761	68.2
	Without 57 and 128	(15, 37, 163)	241 700	193 954	156 761	68.2
	Without 57, 128 and 163	(15, 37, 156)	238 889	191 572	154 713	67.6
4	-	(15, 17, 107, 142)	290 142	233 505	184 386	80.9
	Without 142	(15, 17, 107, 156)	289 592	233 046	188 997	80.8
	Without 142 and 156	(15, 17, 57, 107)	288 409	232 030	188 111	80.6
	Without 335, 127 and 142	(156, 156, 156, 163)	288 273	231 939	188 054	80.5

Discussion

From the two considered objective functions, optimization of energy production and optimization of $NPV_{20\ years}$, distinct best solutions were obtained. A greater energy production does not imply a better economic value, as it can be seen in Figure 5.18. The $NPV_{20\ years}$ for all visited and approved solutions, i.e which not rejected for violating restrictions or for not fulfilling the acceptance criterion, during all runs of the algorithm for the optimization of economic value, are presented with their respective energy production. For the same amount of annual energy production, different $NPV_{20\ years}$ can be obtained. This can be explained by the different costs of the solutions, as they depend on the diameters of both turbine and existing pipe, on the maximum power output and also on the presence of valves. It also shows that while there are solutions where there is an increment of maximum $NPV_{20\ years}$ with the number of turbines, for most of the obtained solutions it happens the inverse. This is due to the respect of constraints and, consequently, due to the diameters used in each solution.

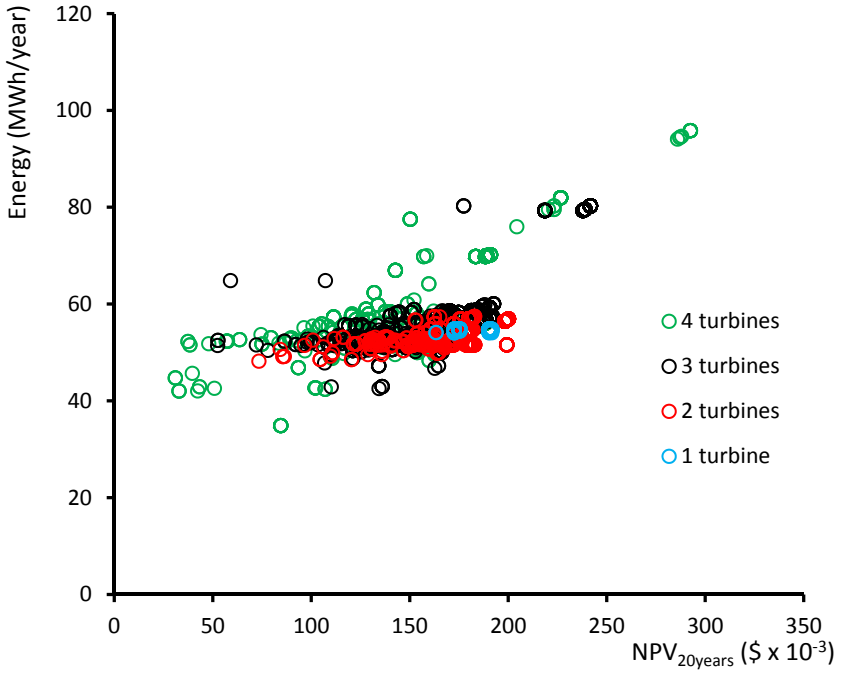

Figure 5.18 Lausanne case study: Visited approved solutions for the optimization of $NPV_{20years}$.

All the solutions obtained for both objective functions and the corresponding restrictions are presented in

The annual energy produced by these solutions is presented in Figure 5.19, with the $NPV_{20\ years}$ for 4%, 6% and 8% discount rates to analyze the sensitivity to its variation. Although all solutions with three and four turbines are similar, there are small differences of $NPV_{20\ years}$ between the solutions with one and two. These small differences can be justified by the differences in costs for identical revenues, as it can be seen in Figure 5.20. This figure shows the breakdown of costs of each of the analyzed solutions between the main types of investment. The average cost price per kWh, obtained dividing the investment costs by the total annual energy produced, is also shown, demonstrating that some more costly solutions have smaller average cost price per kWh due to their higher energy production.

Table 5.14, as well as the maximum installed power P_{max}, the average turbine flow $Q_{T\_average}$, head $H_{T\_average}$ and turbine efficiency $\eta_{Tu\_average}$, as well as the existing pipe and turbine respective diameters, D_p and D_t.

The average runner efficiency does not vary significantly when considering all solutions. The flow and head are more variable and depend on how many turbines are installed and where. The turbine diameters for this network were between 105 and 175 mm, chosen according to the maximum flow criterion and constraints as described before. The installed power per turbine is, therefore, between 1 and 11 kW. , except for pipe 15. In fact, pipe 15 does not produce any energy, as its discharge rates are not enough to generate torque. However, they do induce a head loss, which has an impact on the pressures in the surrounding nodes and flow distribution. This change allows, for example in the

case of three turbines, the installation of smaller and more efficient diameters in pipes 37 and 156 that, without the head loss, would disrespect the pressure constrain. With four turbines, it happens the same. In fact, the best solution when analyzing these results would be to place a PRV in pipe 15 and place only two turbines or three turbines.

The annual energy produced by these solutions is presented in Figure 5.19, with the $NPV_{20\ years}$ for 4%, 6% and 8% discount rates to analyze the sensitivity to its variation. Although all solutions with three and four turbines are similar, there are small differences of $NPV_{20\ years}$ between the solutions with one and two. These small differences can be justified by the differences in costs for identical revenues, as it can be seen in Figure 5.20. This figure shows the breakdown of costs of each of the analyzed solutions between the main types of investment. The average cost price per kWh, obtained dividing the investment costs by the total annual energy produced, is also shown, demonstrating that some more costly solutions have smaller average cost price per kWh due to their higher energy production.

Table 5.14 Lausanne case study: Details of the analyzed optimal solutions.

N° of turbines	X	E (MWh)	P_{max} (kW)	$Q_{T\_average}$ (l/s)	$H_{T\_average}$ (m)	$\eta_{Tu\_average}$	D_p (mm)	D_t (mm)
1	127	46.6	7	85	14.3	0.52	300	160
	142	46.6	7	85	14.3	0.52	300	160
	206	46.6	6	85	14.3	0.52	250	160
	139	46.6	6	85	14.3	0.52	250	160
	156	46.5	6	85	14.3	0.52	250	160
	128	46.3	6	85	14.3	0.52	250	160
	57	46.3	6	85	14.3	0.52	250	160
2	(127, 294)	48.9	7+ 1	85 + 15	14.3 + 3.0	[0.52, 0.47]	[250, 300]	[160, 105]
	(142, 294)	48.9	7 + 1	85 + 15	14.3 + 3.0	[0.52, 0.47]	[250, 250]	[160, 105]
	(139, 294)	48.9	7 + 1	85 + 15	14.3 + 3.0	[0.52, 0.47]	[250, 250]	[160, 105]
	(206, 294)	48.9	7 + 1	85 + 15	14.3 + 3.0	[0.52, 0.47]	[250, 250]	[160, 105]
	(142, 142)	48.4	3 + 3	87 + 87	6.9+ 6.9	[0.56, 0.56]	[250, 250]	[195, 195]
	(156, 156)	48.2	3 + 3	86 + 86	6.8+ 6.8	[0.56, 0.56]	[250, 250]	[195, 195]
	(57, 57)	48.0	3 + 3	86 + 86	6.8+ 6.8	[0.56, 0.56]	[250, 250]	[195, 195]
	(163, 163)	48.0	3 + 3	86 + 86	6.8+ 6.8	[0.56, 0.56]	[250, 250]	[195, 195]
3	(15, 37, 57)	68.2	0 + 3 + 10	10 + 35 + 100	0 + 5.9 + 15.1	[0, 0.50, 0.52]	[200, 300, 250]	[130, 135, 175]
	(15, 37, 128)	68.2	0 + 3 + 10	10 + 35 + 100	0 + 5.9 + 15.1	[0, 0.50, 0.52]	[200, 300, 250]	[130, 135, 175]
	(15, 37, 163)	68.2	0 + 3 + 10	10 + 35 + 100	0 + 5.9 + 15.1	[0, 0.50, 0.52]	[200, 300, 250]	[130, 135, 175]
	(15, 37, 156)	67.6	0 + 3 + 10	10 + 35 + 100	0 + 5.8 + 15.0	[0, 0.50, 0.52]	[200, 300, 250]	130, 135, 175]
4	(15, 17, 107, 142)	80.9	0 + 1 + 2 + 11	6 + 15 + 57 + 107	0 + 3.0 + 4.2 + 17.3	[0, 0.47, 0.49, 0.51]	[200, 200, 200, 250]	[105, 105, 180, 175]
	(15, 17, 107, 156)	80.8	0 + 1 + 2 + 11	6 + 15 + 57 + 107	0 + 3.0 + 4.2 + 17.3	[0, 0.47, 0.49, 0.51]	[200, 200, 200, 250]	[105, 105, 180, 175]
	(15, 17, 57, 107)	80.6	0 + 1 + 11 + 2	6 + 15 + 106 + 57	0 + 3.0 + 17.2 + 4.2	[0, 0.47, 0.51, 0.49]	[200, 200, 250, 200]	[105, 105, 175, 180]
	(156, 156, 156, 163)	80.5	0 + 1 + 2 + 11	6 + 15 + 57 + 106	0 + 3.0 + 4.2 + 17.2	[0, 0.47, 0.49, 0.51]	[200, 200, 200, 250]	[105, 105, 180, 175]

For the case of installing one single turbine, a difference of effort between installing in positions 127, 206 and 139 or in the remaining others can be appreciated in Figure 5.21. This is mainly due to redundancy in these positions (arrangement Type A from Figure 5.14), without isolating valves.

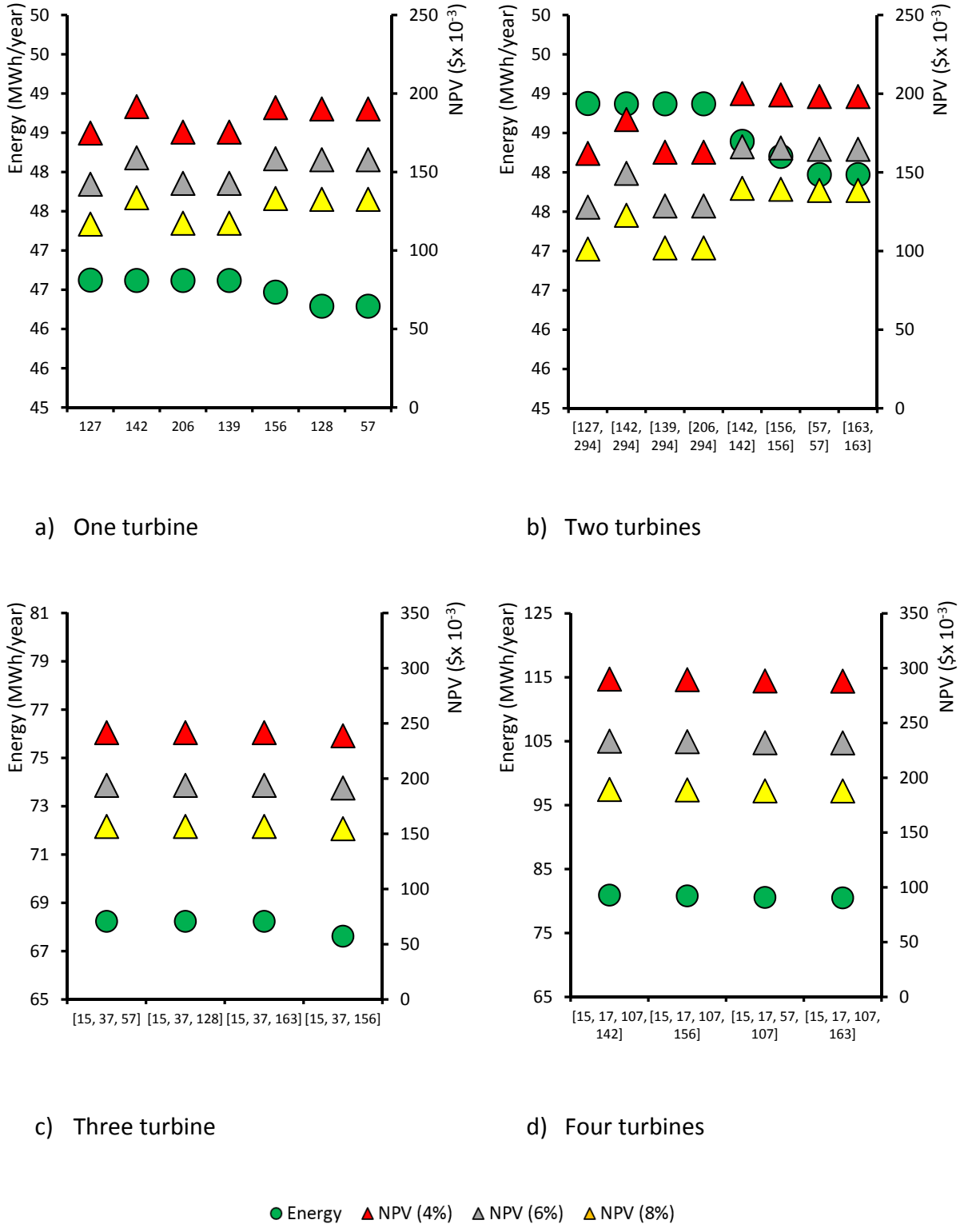

Figure 5.19 Lausanne case study: Sensitivity analyses to the discount rate, in terms of energy produced and $NPV_{20years}$.

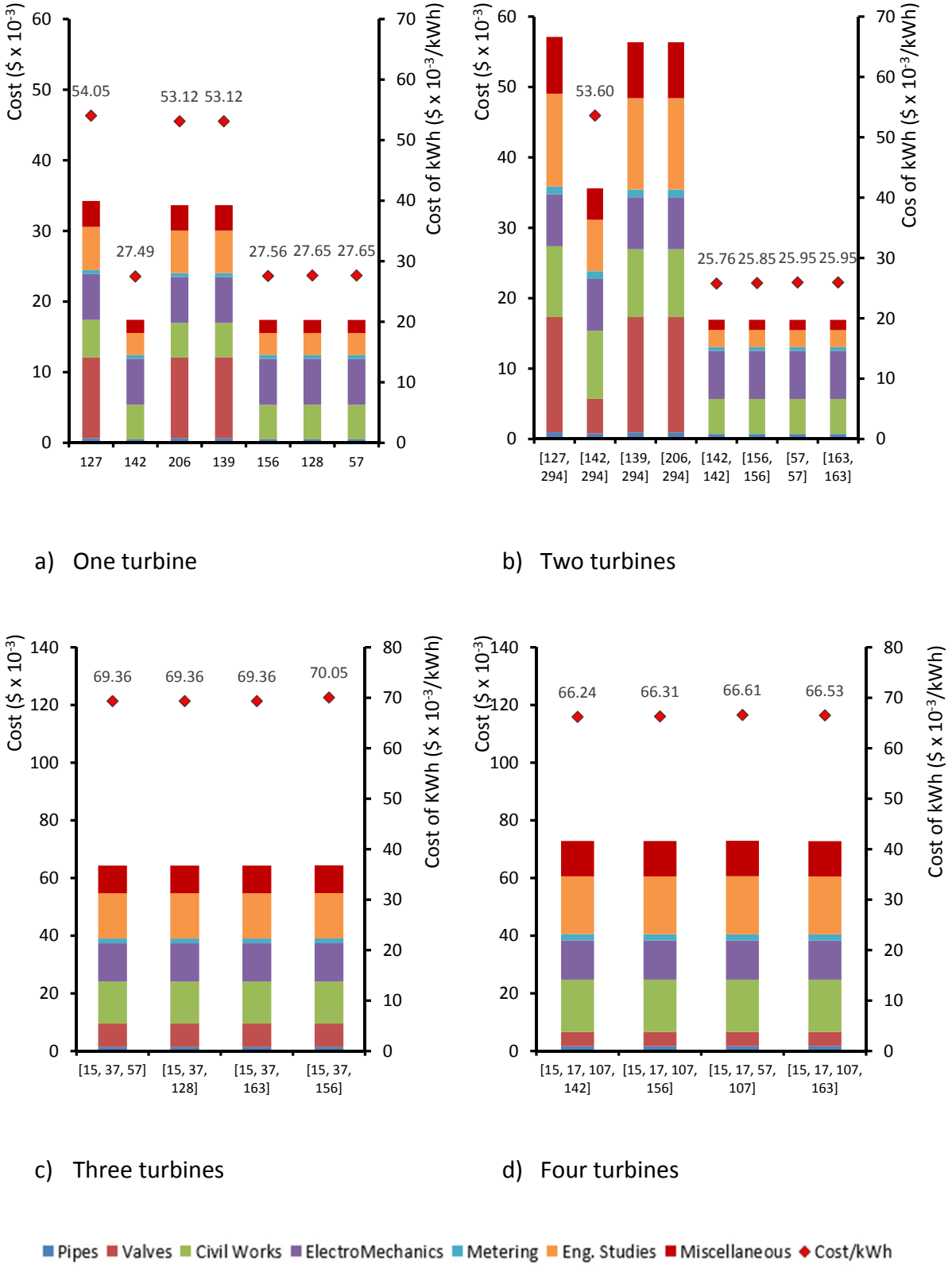

Figure 5.20 Lausanne case study: Breakdown of investment costs and average cost price per kWh.

The cost items “pipes” and “metering” have the smallest influence on the total investment costs. On the other hand, the importance of the electro-mechanical equipment grows with the increasing number of turbines.

Figure 5.21 shows the benefit-cost ratio (B/C) for the analyzed solutions, considering that the benefits correspond to the revenues obtained from selling all the electricity generated at the feed-in-tariff rate:

$$B/C = {0.33CHF \times \sum_{t=1}^{T} E_t(X)} \Big/ {\sum Costs} \tag{5.11}$$

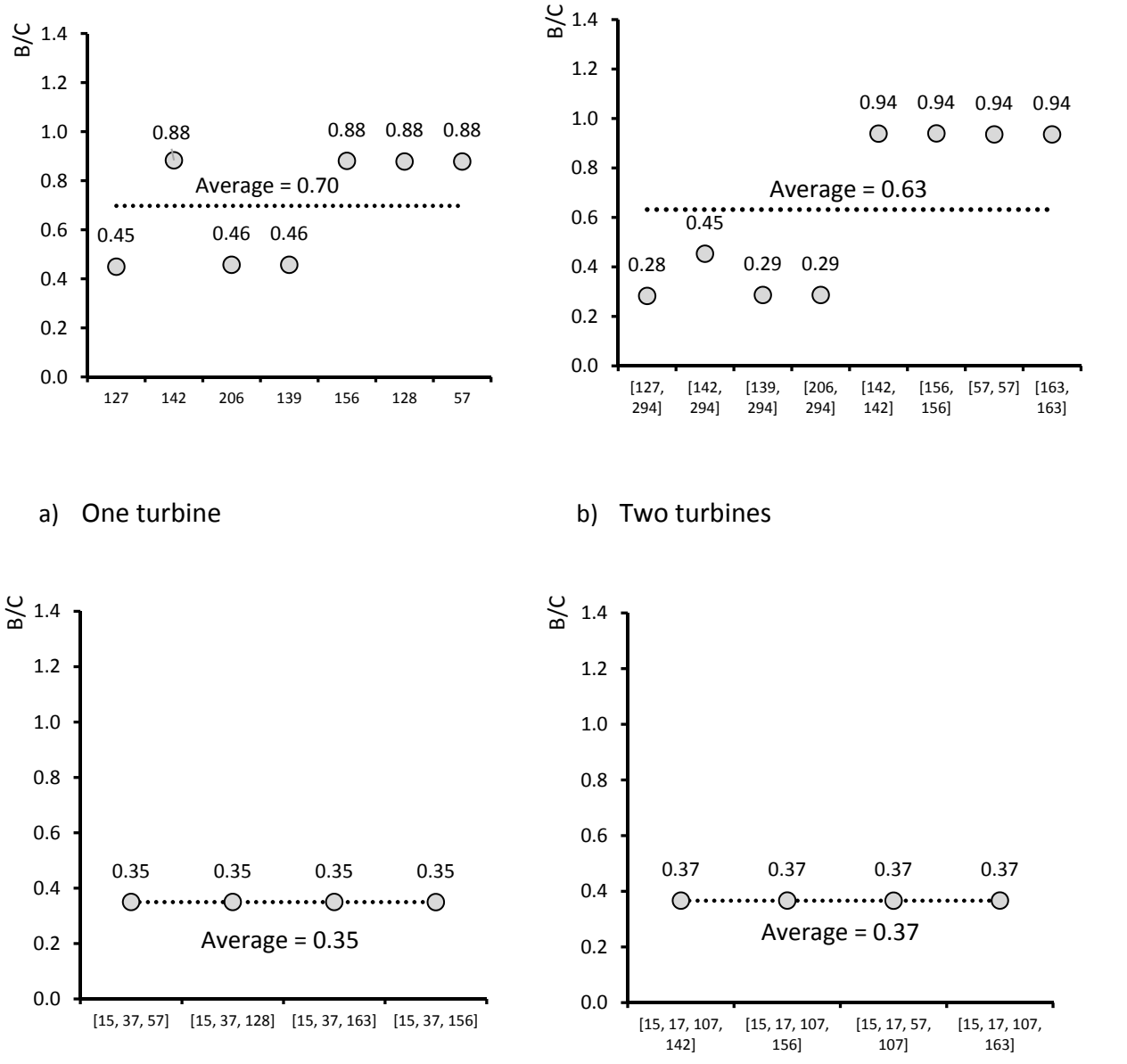

a) One turbine

b) Two turbines

c) Three turbines

d) Four turbines

Figure 5.21 Lausanne case study: Benefit-cost ratio (B/C).

According to Figure 5.21, in general the solutions with the highest (B/C) are solutions for which there is redundancy in the supply of the downstream network (type A) and therefore do not require provision of a valve-isolated bypass. This underlines the importance of the arrangement type on the overall cost. It can be concluded also from Figure 5.21 that the average B/C diminishes with the number of installed turbines. The best B/C ratio is obtained, however, for solutions with two turbines. This shows that, even though the costs are higher with two turbines, they are better in general compensated by the energy production.

The fact that it does not seem to compensate to install three and four turbines is highly dependent on the characteristics of the case study, in particular on the imposed restriction on the outlet discharge. For a case where the full network is known, it could pay off to place all four turbines in the same chamber. The interest remains in showing how complex can be the exploitation of hydropower in a system whose main use is to supply water to the consumers.

Finally, the effect of the tariff was analyzed for the case of two turbines, considering electricity feed-in-tariffs of 0.2 and 0.1 $/kWh (Figure 5.22). The best solution is not very sensitive to the tariff, as the order of higher $NPV_{20\ years}$ among the solutions remains the same for the three considered tariffs. With lower tariffs, the payback time is naturally longer, as the NPV takes more time to become positive. Nevertheless, all analyzed solutions have a positive $NPV_{20\ years}$, proving the good economic feasibility of the micro-hydropower arrangement under the given conditions.

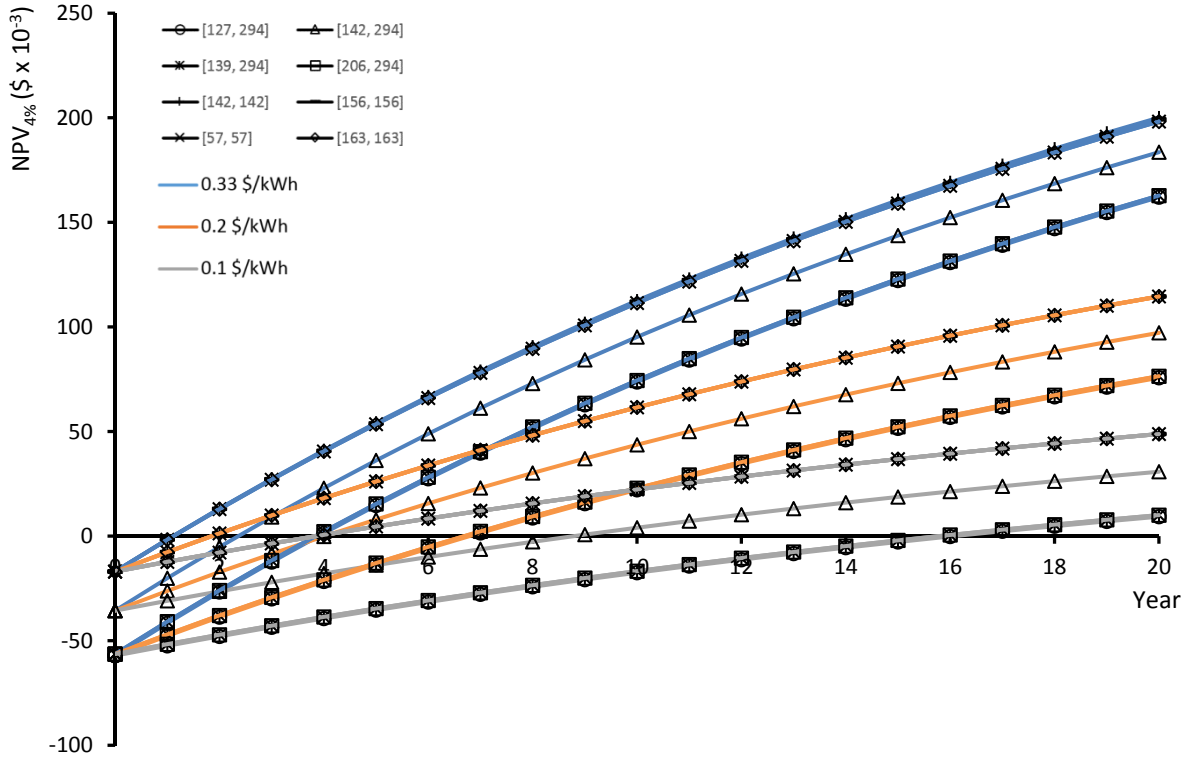

Figure 5.22 Lausanne case study: NPV for 4% of discount rate for the presented solutions with two turbines for three different electricity tariffs.

5.4.5 Application to the case study of Fribourg

System description

Another case study was used to test the upgraded version of the algorithm, the WSN of the city Fribourg (sub-chapter 3.5). Since this network is more complex and includes other elements such as PRVs, pumps and water tanks, extra restrictions and considerations were added.

Whenever the solution includes a location where a PRV concrete chamber already exists, the turbine is assumed to be installed either in line with the valve, either replacing it in the same chamber. Hence, the construction costs (concrete, excavation and earth fill) are omitted. Since these solutions tend to be cheaper than installing in new locations, they were given priority within the search algorithm. In these cases, it was assumed that the valve ensures a constant downstream pressure unless the pressure immediately upstream from it is already lower. Since there is a defined minimum pressure in all the network, it was considered that this constraint was enough to ensure adequate pressure levels in the network. However, in the case of a mandatory constant downstream pressure value, the hydraulic regulation strategy developed by Carravetta, et al. (2012) could be adopted. According to this strategy, when the pressure drop needs to be smaller than the head taken by the turbine, a by-pass is opened to divide the flow discharge.

In the economic model considered for this case study, the capital costs include all investment costs for the construction of the micro-hydropower plants. The maintenance costs of the micro-hydropower plants are considered negligible when compared with the maintenance costs of the entire network. The operational costs of a network are given by the electricity bought for pumping operations and the personnel costs for managing the WSS. In this case, since the focus is given only to the construction and operation of the turbines, and not of the entire network, only the costs for pumping that are superior to the original operational costs are considered. The operational costs are thus given by the electricity buying tariff and the difference between the electrical energy needed for pumping in a situation with the turbines installed and the energy needed for pumping in the initial situation (without turbines). The considered buy-price depends on the period as indicated in Figure 3.14.

Finally, six of the water tanks are considered as water sources, with fixed constant levels. The seventh water tank however has a known geometry and its level varies along the simulation. In each iteration, the initial level in the seventh water tank was defined in order to have in the end of a cycle of 24 h the same initial level. The capacity and elevation of this tank represent also a restriction to the algorithm.

Results

The search algorithm was applied to the city of Fribourg network model to obtain the optimal locations for the installation of 1, 2, 3 and 4 turbines. A discount rate of 4% was considered in the calculation of the net present value. A few interesting results were identified. The results for the

selling to the grid scheme are presented in Table 5.15, showing the also the 2nd and the 3rd best results in terms of $NPV_{20\ years}$ for each case. These latter results were defined restricting one of the pipes belonging to the previous best solution.

In an initial phase, whenever the solution includes a location where a PRV concrete chamber already exists, the turbine is assumed to be installed either in line with the valve, or replacing it in the same chamber. Hence, the construction costs (concrete, excavation and earth fill) are omitted. Since these solutions tend to be cheaper than installing in new locations, they were given priority within the search algorithm.

Table 5.15 Fribourg case study: Results from the search algorithm applied to the Fribourg network model.

Best solution	N_t	X	E (MWh)	P_{max} (kW)	D_t (mm)	$H_{T\_average}$ (m)	$Q_{T\_average}$ (l/s)	$NPV_{20years}$ (k$)	Cost price (cts$/kWh)	Payback period (years)
Best solution	1	2986	60.5	8.1	165	17.6	95.7	258	2	1
	2	(2986, 2986)	120.9	16.2	165	35.2	191.3	521	1	1
	3	(2986, 2986, 2986)	131.7	17.8	155	44.4	239.9	569	1	1
	4	(2986, 2986, 2986,2987)	136.2	18.5	165, 135	43.4	275.4	586	1	1
2nd best solution	1	2730	60.5	8.1	165	17.6	95.7	250	3	2
	2	(2730, 2730)	120.9	16.2	165	35.2	191.3	513	2	1
	3	(2730, 2730, 2730)	131.8	17.8	155	44.4	240.0	561	2	1
	4	(2730, 2730, 2730, 2987)	136.2	18.5	165, 135	43.4	275.4	575	2	1
3rd best solution	1	2987	1.5	0.2	85	3.4	11.3	5	7	3
	2	(2987, 2987)	1.3	0.2	85	3.7	17.1	5	7	4
	3	(2987,2987, 2987)	1.1	0.2	85	3.9	21.5	4	8	4
	4	(2982,2982, 2987, 2987)	1.6	0.3	85, 95	4.5	29.3	5	12	6

The location in the network of the retained solutions is shown in Figure 5.23. In Table 5.15 the annual energy production, turbine runner diameters, average head, average turbinated flow, installed power, net present value after 20 years of operation and respective cost price of the best solutions are shown. No increase in pumping energy was necessary. All the energy generated was representative of excess pressure in the network.

Figure 5.23 shows that the replacement of PRVs is often the best solution. In these locations excess pressure is already recognized. Furthermore, the considered exemption of construction costs for existing chambers made these solutions more economically interesting.

According to these results, it can also be concluded that the installation of three turbines in one pipe represents a smaller increase of energy production from two turbines than the increase of energy production of installing two turbines when compared to one turbine. This is due to the effect of obstruction of flow discharge, in particular when the extracted head is bigger than the original head dissipated in the PRV. This effect can be appreciated in Figure 5.24, where the annual energy production is presented with the $NPV_{20\ years}$ for 4%, 6% and 8% discount rates to analyze the

sensitivity to its variation. Figure 5.25 presents the breakdown of costs of each of the analyzed solutions between the main types of investment and the average cost price per kWh.

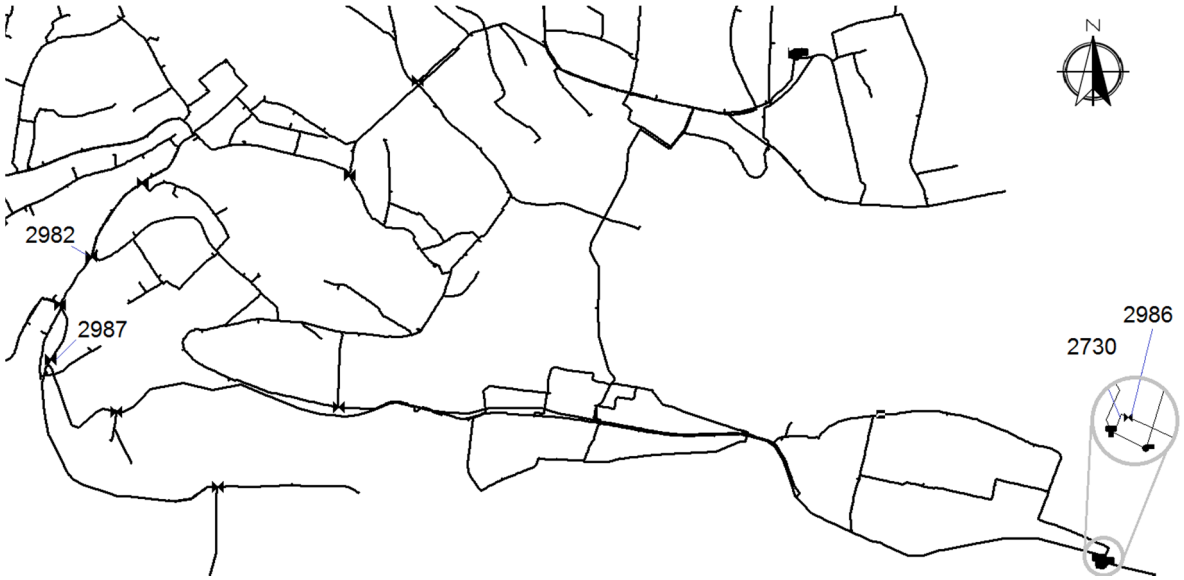

Figure 5.23 Fribourg case study: Localization of selected pipes (Zoom A from Figure 3.12).

The best and second best solutions, for all the number of turbines, are identical is terms of energy production and in terms of $NPV_{20\ years}$. Pipes 2896 and 2730 (Figure 5.23) are presented in the best and second best solutions respectively. Since they are share one node and are inline, the expected production is similar. The differences between both $NPV_{20\ years}$ are mainly due to the construction costs.

The third best solution has a very small energy production when compared with others, since the discharges and heads are lower. It can be concluded that the pipes where the best and second best solutions are located, upstream from one of the main water tanks, is the most interesting area for hydropower production.

Other solutions for the installation of micro-hydropower in water supply systems can be found in the literature. For example, the installation of PATs in replacement for a PRV in the an urban water distribution system of Pompei, with discharges between 20 and 50 l/s and heads between 35 and 90 m, would produce between 20 and 94 MWh/year (Carravetta, et al., 2012). In Portland, OR, a PRV was replaced by a 10'' (approx. 250 mm) micro turbine that generates 150 MWh/year with 30 kW of installed power (Lisk, et al., 2012). In Hong Kong, an eight blade spherical turbine inline turbine is expected to produce 700 kWh/year in the city's water main pipes (PolyU, 2012). Finally, the installation of a turbine replacing a break pressure tank in Kildare in Ireland could generate approximately 237 MWh/year from 200 kPa and 17 910 m3/day (McNabola, et al., 2014b). The obtained production in the city of Fribourg is within the order of magnitude.

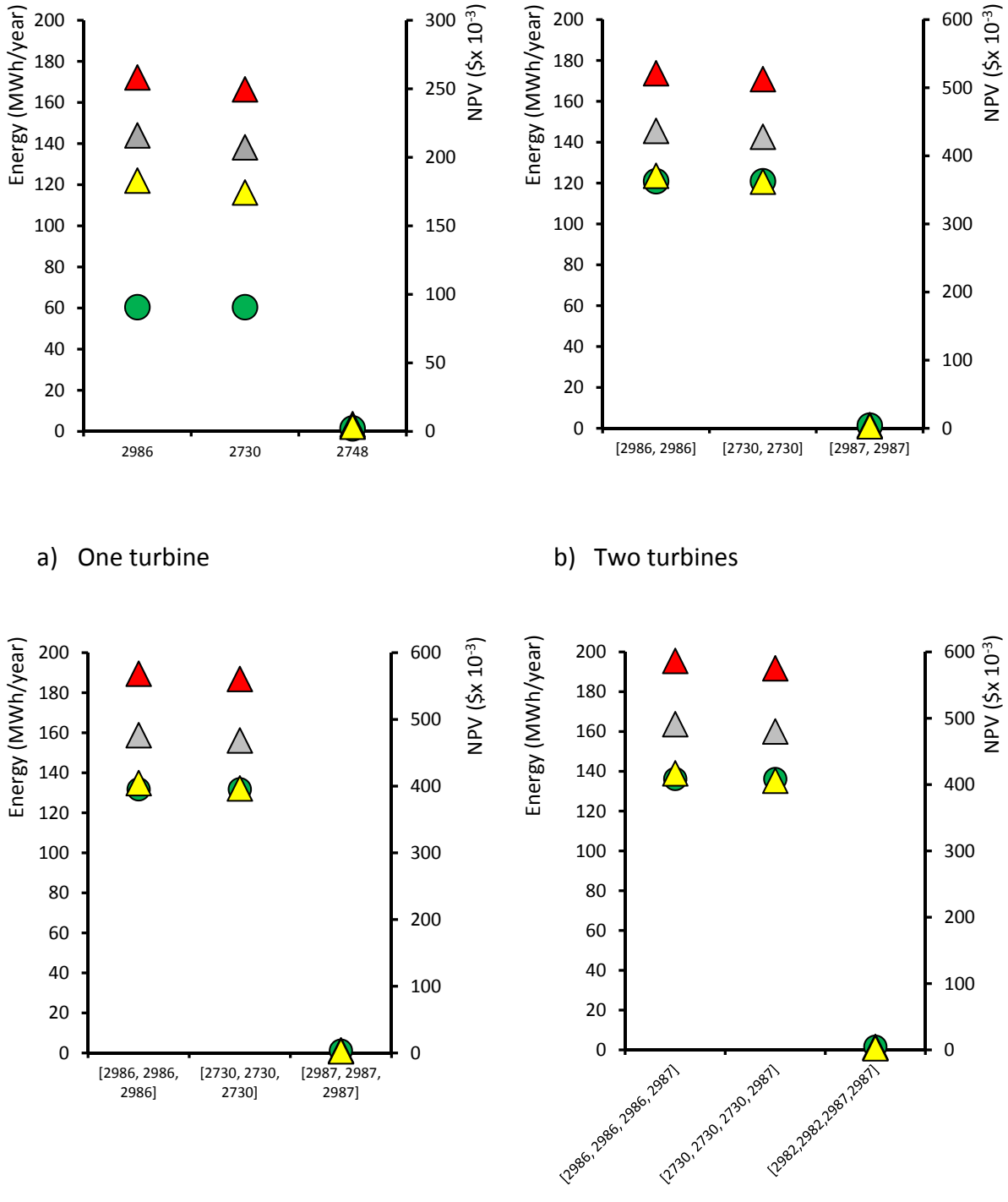

a) One turbine

b) Two turbines

c) Three turbine

d) Four turbines

Figure 5.24 Fribourg case study: Sensitivity analyses to the discount rate, in terms of energy produced and $NPV_{20years}$.

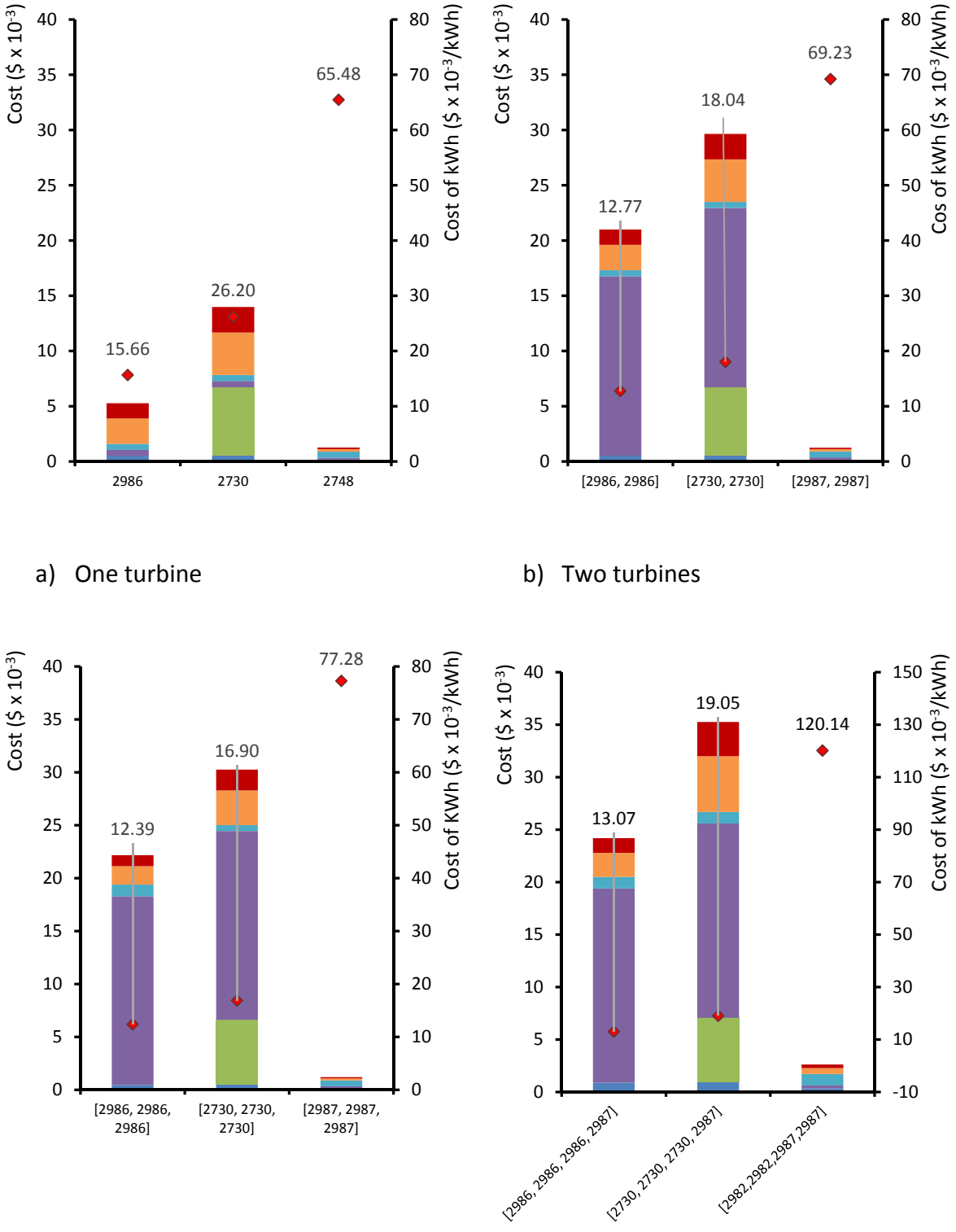

a) One turbine

b) Two turbines

c) Three turbines

d) Four turbines

Figure 5.25 Fribourg case study: Breakdown of investment costs and average cost price per kWh.

Considering the PAT used in the Beliche hydropower station presented in sub-chapter 3.6, in the location 2986 it would produce an annual energy similar to two 5BTP (Table 5.16).

Table 5.16 Energy production in the optimal location of Fribourg with a PAT.

X	E (MWh)	P_{max} (kW)	D_t (mm)	$H_{T\_average}$ (m)	$Q_{T\_average}$ (l/s)
2986	121.7	13.9	270	19.1	95.7

Not considering construction costs for the sites where PRVs are located may reveal to be optimistic. Hence, a second batch of simulations were carried out considering that additional construction works will be necessary to enlarge and adapt the existing chamber. Site conditions being very varied and coupling old and new chambers being sometimes cumbersome it was assumed that the construction costs would be equivalent to that of a new chamber. Under these conditions, the best solutions from Table 6 became equivalent in terms of $NPV_{20\ years}$ to the 2nd best solution. For a 3rd best solution, no locations were found were it would be feasible to install turbines. The construction costs have hence a considerable weight in the feasibility of these chambers.

Effects of a reduction in the water consumption

Based on the three best solutions previously identified, a 20%decrease of the water consumption was imposed on the network. A new energetic equilibrium was computed for these conditions, leading to a new energy production estimate for the network. Considering the same costs as in the previous solutions, the $NPV_{20\ years}$ was recalculated. The results of this sensitivity analysis are presented in Table 5.17, which can be directly compared with Table 5.15.

Table 5.17 Fribourg case study: Previous solutions with 80% of the consumption.

Best solution	E (MWh)	$NPV_{20years}$ (k$)	Payback period (years)
Best solution	60.5	258	1
	120.9	521	1
	130.3	563	1
	124.9	451	1
2nd best solution	60.5	250	2
	120.9	513	1
	130.4	555	1
	124.9	440	1
3rd best solution	2.0	7	3
	1.6	6	3
	1.5	6	3
	2.1	7	5

Considering that the consumption was decreased and that the energy production is highly dependent on the flow discharge, it was to be expected a decrease in the energy production. However the best and 2nd best solutions present negligible changes and in the 3rd best solution there was an increase of energy production. For the best and 2nd best solutions, the chambers are installed immediately upstream from a regulation water tank. The 20% reduction in the consumption did not strongly influence the flow discharges in this area, which are highly dependent on the levels of the water tank and water source. For the 3rd best solution the flow discharge increased due to the new

network equilibrium. The majority of pipes in the network suffered a decrease of flow discharge with the smaller consumption. However, the pipe 2987 was one of the exceptions.

These results illustrate the complexity of installing micro-hydropower arrangements in urban networks and evoke the need of careful sensibility analysis to the consumption. Considering the small differences in the results with a 20% decrease in water consumption, there is no interest to present the analysis with a 10% decrease. Tests with higher consumptions (% increase) were tried but lead, even for less than 10% increase, to instabilities in the network model, locally reaching negative pressure values. However, a complete sensibility analysis should always be performed. Also, carrying out long period simulations is recommended in order to achieve a robust estimation of the produced energy and economic value of the installation (Sitzenfrei & Leon, 2014).

5.4.6 Conclusions

This sub-chapter presents an arrangement of micro-hydropower in urban WSNs, corresponding to the inline installation of one to four micro-turbines. The best location for such a micro-hydropower arrangement within a network is assessed through the developed optimization algorithm considering energy production, supply service quality and economic present value. The optimization was based on two different objectives: the maximization of the annual energy production and of the NPV after 20 years.

The methodology was applied to a sub-grid of the WSN of the city Lausanne and to the complete network of the city Fribourg, both in Switzerland. It was concluded that the arrangement is economically feasible for both the analyzed case studies.

For the case of Lausanne, the identified locations belong mostly to the main path of the network, and it comes with no surprise that the most favorable locations correspond to the highest flow discharges, depending on the available head. With the performed simulations, it was concluded that a larger energy production does not imply better economic value. This is justified by the different investment costs of the solutions. Also, with the presented arrangement, the most profitable configuration is the installation of two turbines in the same chamber. The energy production is higher, but the investment costs do not increase in the same proportion. Also, the case study underlined the relevance of the redundancy to the nodes of the target branch. A branch without redundancy requires the installation of a higher number of valves, which may have an important weight on the investment costs. Finally, it was concluded that the number of turbines to install is highly dependent on the constraints of the network, since the quality of the supply to the population should always be ensured.

For the case of Fribourg, the identified locations where preferentially where PRVs exist. It can also be concluded that the installation of three turbines in one pipe represents a smaller increase of energy production from two turbines than the increase of energy production of installing two turbines when compared to one turbine. This is due to the effect of obstruction of flow discharge, in particular when the extracted head is bigger than the original head dissipated in the PRV.

Locations where PRVs are already in place are attractive especially if civil infrastructure which can be adapted is already in place. The costs for civil construction were seen to have an important weight on the feasibility results. Sensibility analysis to the demand should be considered to verify its impact in the energy production and in the behavior of the network.

The conclusions of the performed study can be generalized, although attention must be paid to local service requirements, of legal or operational nature, as well as to the considered construction unit rates and equipment costs and local market conditions.

5.5 Method for expedite assessment of micro-hydropower plant feasibility assessment

The obtained results in sub-chapters 5.3 and 5.4 were achieved through an optimization process, using the simulated annealing algorithm and hourly simulations, where a considerable amount of data and also of time are needed. Based on the experience gained in the course of this work, an expedited method to preliminarily evaluate the interest of placing one turbine in a given location of network is here provided. The topography of the network, the maximum discharge in the pipes and the temporal variation of the consumption are assumed to be known.

Two auxiliary figures are provided. Since the choice of diameter of the turbine is dependent on the maximum discharge in the pipe, the corresponding head is given by the characteristic curve of the turbine according to the similarity equation (Equation (2.10)). Figure 5.26 presents the variation of head with the maximum pipe discharge, which is obtained considering different runner diameters of the 5BTP. Figure 5.27 plots the investment costs and the installed power as a function of the maximum pipe discharge and, consequently, the diameter of the runner. Figure 5.27 was obtained considering the unit prices from Table 5.11 and the existing pipe has a diameter which allows a design velocity of 1 m/s.

The expedite method follows the following steps:

1. Identify all PRV and obtain the respective maximum discharge.
2. Order all pipes by maximum discharge and select a feasible number to analyze (20 for example) of the highest discharges.
3. Verify if the difference between the lowest pressure in the downstream node of each selected pipe and the limit minimum pressure is bigger than the maximum head according to Figure 5.26.
4. Estimate for each PRV site and selected pipe the cost of the arrangement and generation potential according to Figure 5.27.

5. Estimate an energy production based on the installed power and the temporal variation of the consumption.

These steps allow for preliminary identification of potential locations in a network for the installation of a micro-hydropower plant with one turbine in the network. However, a more detailed simulation, as proposed in the methodology, is required to ensure that the minimum pressure in all nodes is maintained and account for possible discharge variation due to the redundancy of the network, estimating with higher precision both energy production and costs. Combinations with more than one turbine also require detailed simulations.

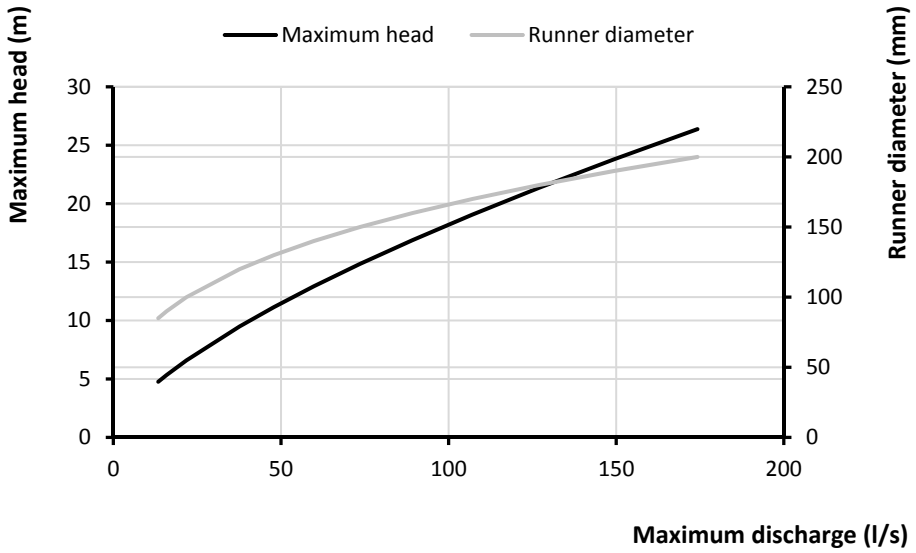

Figure 5.26 Characteristic curve of maximum discharges, considering different diameters, of the 5BTP.

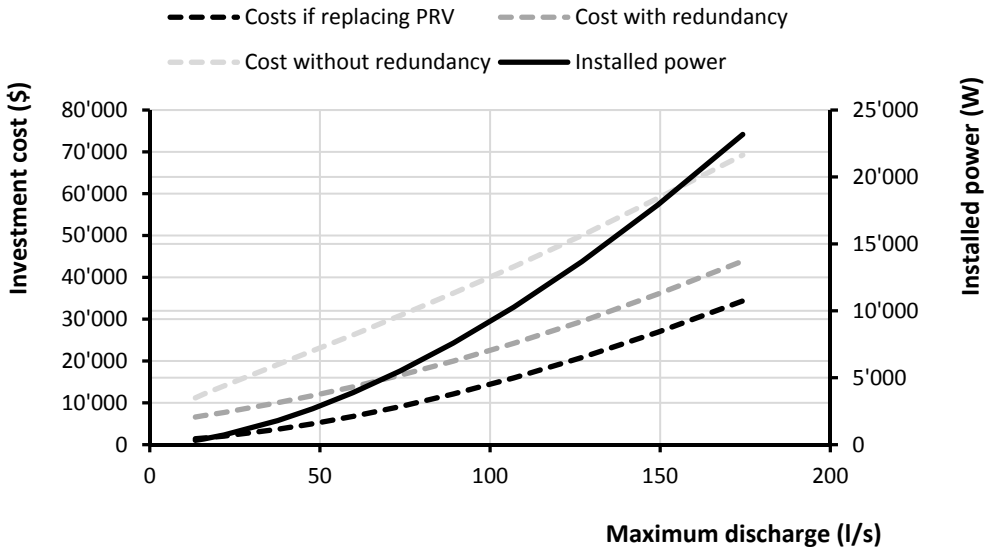

Figure 5.27 Variation of average investment cost and installed power of the 5BTP with pipe maximum discharge (assuming design head from Figure 5.26).

5.6 Conclusions

In this Chapter, the placement of turbines in WSN was analyzed in the search for optimal configurations and operations. The main concern lied with ensuring that the quality of service of the WSN, since supplying water to the consumers is the fundamental function of the system, would not be affected by the micro-hydropower plants. This evaluation allowed concluding that the best placements for turbines in WSN are:

- Upstream from water tanks, due to the typically high discharges and low fluctuations, although attention must be given to the variation inside the water tank to ensure quality standards;
- Replacement of PRVs, due to the recognized existing pressure excess and possible already constructed infrastructure;
- Main pipes of the WSN, due to the high discharges.

These conclusions were obtained with the use of optimization algorithms that considered both energy production and economic value. The application of the developed search algorithm for identifying ideal locations could be interesting in two situations: the evaluation of harvesting energy potential in existing WSN; and during the design of new WSN. In an existing WSN, the presence of PRVs will likely lead to the conclusion that replacing them with turbines is the most interesting solution due to the use of existing infrastructure. However, for cases with no PRVs, the algorithm can give useful insight on turbine placement. Moreover, the optimization allows to infer on the number of turbines do install. In the design of a new WSN, the placement of turbines can be optimized and the optimal solution for turbines can be different from the traditional analysis of PRVs installation. Also, the analysis of energy production and number of turbines to install could have an influence on the choice of diameters of the pipes.

Chapter 6

Evaluation of the energy potential in urban water supply networks

Sub-chapter 6.2 is based on the scientific article "Energy recovery with micro-hydropower plants in the water supply networks: the case study of the city of Fribourg" by I. Samora, P. Manso, M. J. Franca, A. J. Schleiss and H. M. Ramos published in Water. The simulations and algorithms hereafter are original and were developed and performed by the author.

6.1 Introduction

The potential for energy production within urban WSNs has been verified to exist but it is difficult to quantify. The distribution networks are complex systems, usually composed by multiple loops and asymmetric consumption. However, before enduring a deep analysis and simulations of turbine operations, a measure of the excess energy available within the city's network, indicating the potential of that network to be used for hydropower, is useful for WSS managers.

The hydraulic energy (Wh) is a function of the fluid density (kg/m^3), the flow rate (m^3/s), the hydraulic head (m), meaning the total flow energy subtracted by the topographic elevation of the point, and the considered time interval (h). The fluid density can be considered constant and equal to 1000 kg/m^3 and a time interval can be defined as representative for the potential assessment. However, the other two elements depend on a variety of factors: H depends on the topographic elevations, on the existence of tanks and valves, on the pipes materials and diameters and, ultimately, on the flow discharge. Q depends on the population and its consumption patterns, seasonality and density, but also on the redundancy of the network.

In this Chapter, a methodology is proposed to quantify the available energy in a network. Also, an exploratory analysis of the shape of networks and its influence in energy production is presented. In sub-chapter 6.2, the first methodology is presented, along with the results of its application to the case study networks. The second methodology and corresponding results are shown in sub-chapter 6.3.

6.2 Potential for hydropower

6.2.1 Excess energy and available energy

In any pipe of a network at a certain instant with a steady flow regime, the total energy line (Figure 6.1) can be defined as a straight line, if there are no local head losses, between the head in each boundary nodes. The head in each node will be higher or equal to a minimum pressure p_{min}, usually imposed by regulations to guarantee a quality service to the population. In each point of the pipe, whenever the head is higher than this minimum pressure, there is energy in excess. This excess of energy will vary in time, as the demand in the network is not constant, affecting both the pipe flow and the pressure in the nodes.

To estimate the excess energy in the upstream and downstream nodes of Figure 6.1, the minimum pressure is subtracted to the hydraulic charges:

$$E_{up} = \rho g Q_t (H_{up} - p_{min}) \Delta t$$
$$E_{dn} = \rho g Q_t (H_{dn} - p_{min}) \Delta t \quad (6.1)$$

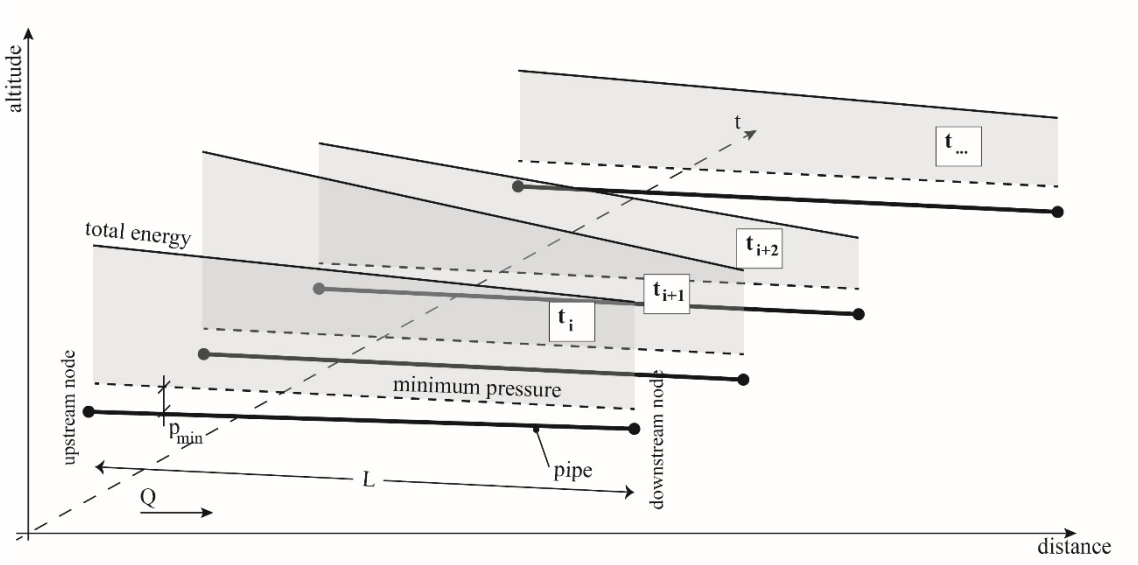

Figure 6.1 Energy excess in each point of a pipe, defined as the hydraulic charge above minimum pressure, for several instants.

It can be argued, however, the application of this definition of the excess energy in an entire network cannot be done without taking into account the topography. The excess energy in a given point is often needed to ensure the minimum pressure in another and hence is not available.

Considering the reach, defined as a sequence of pipes, sketched in Figure 6.2a), excess energy exist in every point of its water path, but none of this excess is available, since the most downstream point is at the minimum pressure and extra head losses would cause this pressure to decrease. Instead, if we consider the reach sketched in Figure 6.2b), the minimum pressure is not limited at

the downstream extremity but at a high point along the path. The excess downstream from this point is partly available and is represented in the figure. During the networks design, there is usually an effort to minimize this difference by using smaller diameters, as a means to control the pressure. Alternatively, the installation of turbines could be used to dissipate this excess energy.

The available energy at a point in a WSN can hence be defined as the excess energy that can be extracted from the flow without causing pressure below the minimum in any other point. To quantify how much of the excess energy is available for hydropower production, critical points must then be identified. The critical point corresponds to the position in a network where the difference between the total energy and the minimum pressure is minimum but higher than zero. This difference is the head that can be taken from the total energy line. This head and the downstream total energy line are represented by a dotted line in Figure 6.2b).

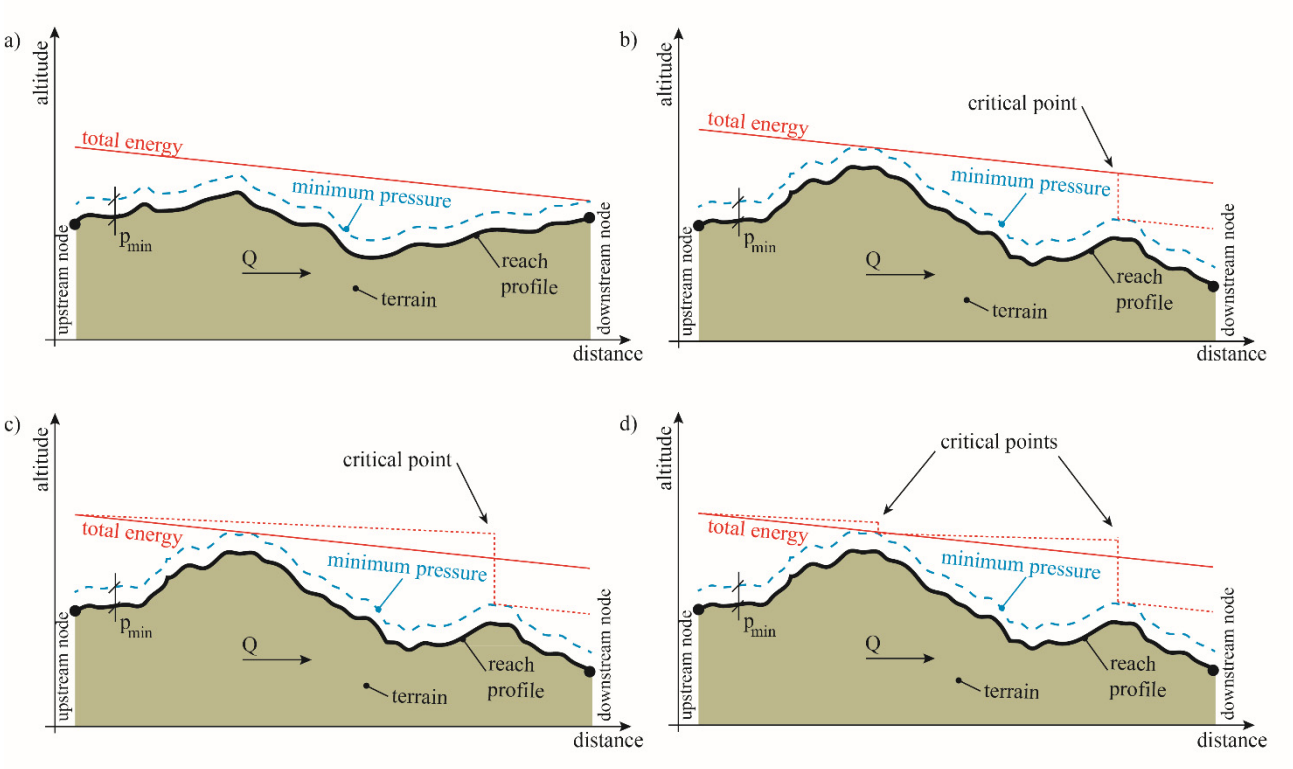

Figure 6.2 Examples of reaches. a) Reach without available energy: the downstream node of the reach has an imposed minimum pressure and does not allow for any energy extraction. b) Reach with available energy. The minimum pressure conditions the upstream energy extraction. However, a critical point downstream has available energy that can be extracted. c) Reach belonging to a closed network with available energy: effect of the extraction in one critical point. d) Reach belonging to a closed network with available energy: effect of the extraction in two critical points.

The former examples always considered a single reach with no other connecting path between the upstream and the downstream sections either than the presented reach. The positioning of a valve or a turbine in Figure 6.2b) would not have an impact in the discharge along the reach. However, if the reach is was in a closed network, which is common in urban WSNs, the introduction of an energy converter and consequent adjustment of the energy distribution would have an impact in the

discharge, as represented in Figure 6.2c). Moreover, the following critical point in the reach is now the point that was at minimum pressure before. If the new critical point is considered for the extraction of energy, a new readjustment occurs and the resulting total energy distribution is presented in Figure 6.2d).

The available energy in a network is given by the sum of the available energy in every critical point and hence its assessment requires a dynamic process. Also, as mentioned, the available head varies with the demand, which in a WSN is variable throughout the day. Nevertheless, a simpler and more immediate way for estimating available energy is to solemn consider the steady state conditions with maximum flows, and hence the minimum heads.

6.2.2 Available energy assessment

An algorithm was developed to assess the potential for hydropower in WSN taking into account the previous considerations for available energy in a network (Figure 6.3). Input data is composed of the network geometry, available consumption data (discharges distributed along the WSN) and minimum pressures to be assured at every node.

The consumption that leads to the average lowest pressure in the network is identified in the analysis. The nodes that do not fulfill the criteria of minimal pressure under these conditions are considered to be non-consumptive nodes, where the pressure is only required to be positive to avoid cavitation.

Since energy depends on both head and flow rate, the available energy cannot be evaluated solely based on available head in the critical points. For all the nodes in the network, a value A is defined, if the node is valid, as:

$$A_n = \Delta H_n * \max(Q_l) \tag{6.2}$$

where the index l refers to the ID of all pipes connecting to the node n,

$$\Delta H_n = H_n - p_{min}, \tag{6.3}$$

and H_n is the hydraulic charge over the node n in the current hydraulic state. If the node is not valid, A is zero. The nodes are then re-ordered in decreasing order of A.

For the node with the highest A, the head from Equation (6.3) is extracted by applying a local head loss in the pipe connecting to the node with the highest discharge. This extraction implies a new energetic equilibrium in the network that needs to be calculated. If the minimum pressure is satisfied in all the consumptive nodes after the network recalculation, the extracted head is given by the imposed head loss, and the available power in that node is given by the head and $\max(Q_l)$. The power P of the new state is given by the sum of the available power in the new node, the available power in the all the nodes where a head loss was previously imposed and the power that is dissipated in each PRV, if they exist, multiplied by the water volumetric weight. The new node is

accepted only if there is an increment in the calculation of the power, to ensure that it does not negatively affect the nodes previously gathered. If it is not accepted, the following highest A is tested and so forth until there is an acceptance or the valid nodes are exhausted.

The procedure of ordering the potential is repeated with each new accepted equilibrium in the network. Moreover, when extracting the head in a new node, the flow discharge in the previous ones will be affected, and so the potential of both has to be calculated.

When all valid nodes have been evaluated, an estimation of the annual available energy can be given by the power P times the considered time window Δt.

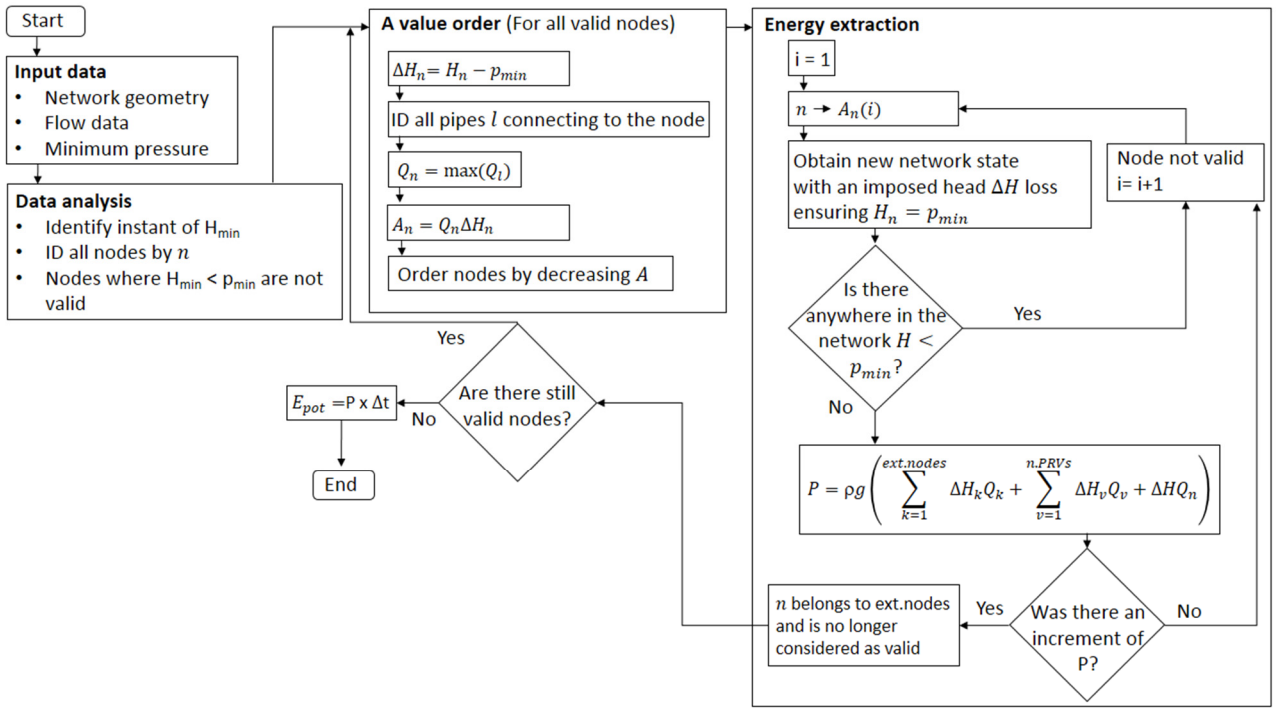

Figure 6.3 Algorithm to estimate the available energy in a network.

6.2.3 Results

The algorithm developed for the evaluation of the available energy in an urban water network (Figure 6.3) was applied to the case studies of Lausanne WSN 1 (sub-chapter 3.3), Lausanne WSN 2 (sub-chapter 3.4) and Fribourg (sub-chapter 3.5).

Lausanne WSN 1

The Lausanne WSN 1 was initially a sub-grid model with a reservoir representing the connection to downstream with a fixed level. Since the application of the developed algorithm to such situation would not make sense, the downstream reservoir was replaced by a regular node. The node was placed 82 m lower than the original reservoir level to ensure the existence of available pressure. Also, two cases were considered, the case of no consumption in this new node and the case of

consumption equivalent to the inflow to the downstream reservoir in the initial situation. The results are presented in Table 6.1.

Table 6.1 Results from the evaluation of potential for hydropower in Lausanne sub-grid 1 with downstream node.

	E_{pot} (MWh/year)
No consumption in downstream node	46
Equivalent consumption in downstream node	199

It is not possible to use the results of the optimization of energy production (Table 5.12) for comparison with Table 6.1 because the boundary conditions of the network were different (the downstream reservoir was replaced by a regular node). Thus, the search algorithm from Chapter 5 was used again, this time considering the two cases with a downstream node. The results for the optimization with one to four turbines are presented in Table 6.2.

For the case of the boundary condition with equivalent consumption, one turbine extracts a considerable amount of the potential, 46%. With two turbines the amount practically doubles to 91% and it almost does not increase with more of turbines, since fewer nodes have available head to be extracted.

However, for the case of the boundary condition without consumption, the energy production is much lower and one turbine can only attain 6% of the potential in the network. The flow discharge in the pipe where the turbine is installed is much smaller than in the case with equivalent consumption.

Table 6.2 Energy production with the 5BTP in Lausanne sub-grid 1 with downstream node.

Nt	Condition in downstream node	E_{prod} (MWh/year)	E_{prod}/ E_{pot}
1	No consumption	2.65	6%
	Equivalent consumption	90.68	46%
2	No consumption	6.53	14%
	Equivalent consumption	181.36	91%
3	No consumption	8.78	19%
	Equivalent consumption	183.91	93%
4	No consumption	8.78	19%
	Equivalent consumption	186.60	94%

Lausanne WSN 2

The application of the algorithm for the evaluation of the available energy to the sub-grid 2 of Lausanne network resulted in 12.02 MWh/year. However, the installation of turbines in this network is not particularly attractive, as it can be seen in Table 6.3. One turbine can extract only 1% of the available energy in this case.

Table 6.3 Energy production with the 5BTP in Lausanne sub-grid 2.

Nt	E_{prod} (MWh/year)	E_{prod}/ E_{pot}
1	0.14	1%
2	0.28	2%
3	0.42	3%
4	0.56	5%

Fribourg

The algorithm for the evaluation of the available energy in an urban water network (Figure 6.3) was applied to the case study of Fribourg. The results, presented in Table 6.4, show that there is approximately
170 MWh/year in the network not being used. If accounting for the 430MWh/year extracted from the systems by PRVs, a total of approximately 600 MWh/year of available energy exists. The PRVs' energy contribution represent 72% of the total.

Table 6.4 Results from the evaluation of potential for hydropower in Fribourg.

	E_{pot} (MWh/year)
Network	168
Existing PRV	430
Total	598

Table 6.5 shows the pipes of the network where the energy is extracted and Table 6.6 shows the energy extracted by the PRVs. Taking into account these results, pipe 2986 is the best location to install a turbine in the network and it can be confirmed in Table 5.15 since this was the result found in the previous chapter. One, two, three and four 5BTP turbines would recover approximately 10%, 20%, 22% and 23% of the available energy, respectively, according to the results of Table 5.15.

Some locations in Table 6.5 show high available heads although the corresponding available energy is relatively low. This indicates that these locations are served with low discharges, thus hardly good position for the installation of a turbine.

Table 6.5 Pipes where energy has been extracted in Fribourg.

Pipe ID	H (m)	P (W)
2986	12.3	11 514
2824	59.2	501
2914	11.1	1 018
1928	1.5	136
2973	39.4	3 333
786	40.8	2 351
2427	5.9	319
2415	0.6	29

Table 6.6 Power extracted in RPVs in Fribourg.

Valve ID	H (m)	P (W)
2978	49.2	2 694
2979	43.2	1 973
2981	49.2	1 822
2982	49.6	2 782
2983	49.5	1 065
2984	50.0	508
2985	50.0	254
2986	40.3	37 812
2987	0.3	121

In pipe 2986, although the existence of a PRV (Tables 6.5 and 6.6), 12.3 m of head are still available which corresponds to an available energy of 102 MWh/year.

6.3 Empirical equations for network assessment

6.3.1 Synthetic networks

When considering a turbine such as the 5BTP, the power that it can generate at each instant depends exclusively on the discharge rate and on the rotational speed, as long as the pressure is available. Considering only a characteristic curve with variable speed such as Figure 4.17, the generated power depends only on the discharge, since the rotational speed is programmed as function of the flow rate. However, even if the pressure is largely available, the presence of closed loops and asymmetrical consumptions makes it complicated to estimate the energy produced in a network just from the population and capitation.

To give an insight on the influence of the network geometry in its potential for energy production, an exploratory analysis was initiated based on the successive construction of synthetic networks. To ensure the availability of pressure, the topographic difference of 100 m was considered constant, as presented in Figure 6.4. The connection between the source and the network is not considered as part of the network and all pipes have 100 m except when indicated. In the intersection of pipes there is always a consumption node. The diameters of the pipes are designed to have flow velocities close to 1 m/s, with a maximum of 2 m/s and a minimum of 0.6 m/s, except if the pipe belongs to a dendritic dead-end path (i.e. without loops) where velocities are allowed to be lower. A minimum diameter of 80 mm was considered and only commercial diameters were used (80, 90, 100, 200, 300, …, 800).

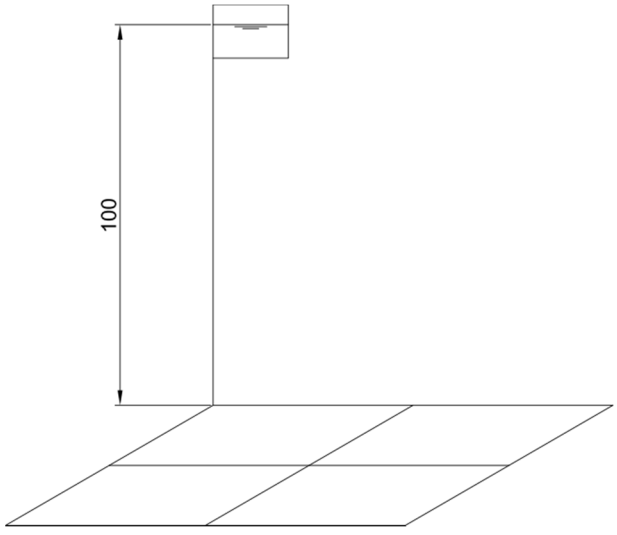

Figure 6.4 Sketch of synthetic networks where a constant topographic difference was considered.

According to these principles, 28 different networks were generated, according to Figure 6.5. The arrows in Figure 6.5 represent the connection to the water source.

To ensure viable discharge rates and a daily pattern, the consumption per node of the synthetic networks was based on the case study of the Lausanne WSN 1 (sub-chapter 3.3) and it was

considered that the average discharge per link in the synthetic network Q_{syn} should be the same as the sum of the average discharges in each link of the Lausanne sub-grid Q_i divided by the number of links of the sub-grid ($links\_L$):

$$\frac{Q_{syn}}{links\_r} = \frac{\sum_{i=1}^{links\_L} Q_i}{links\_L} \tag{6.4}$$

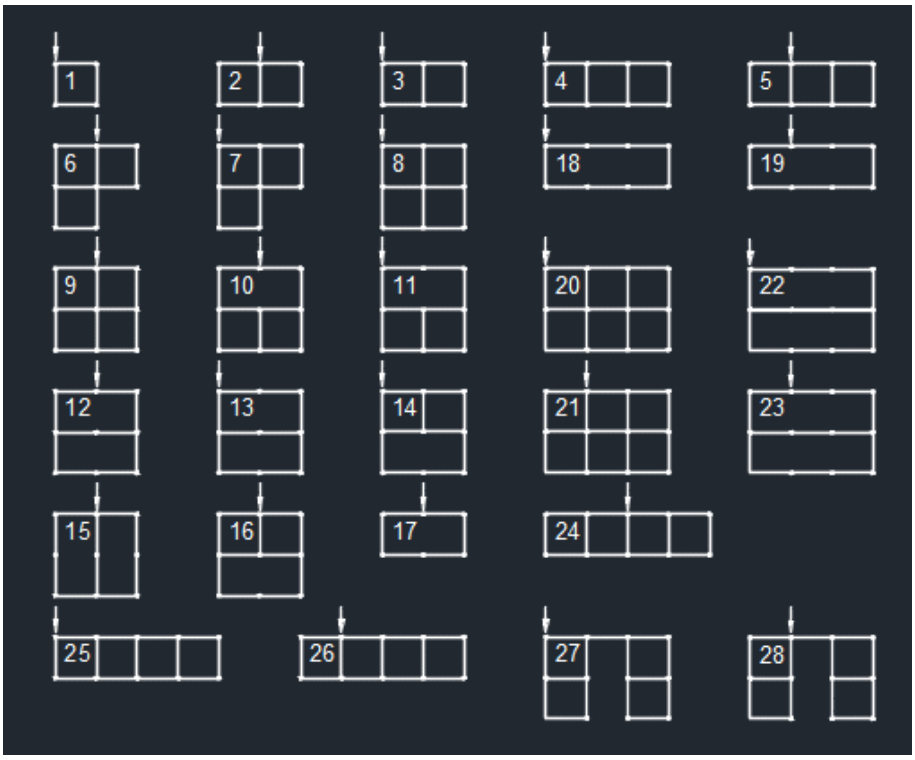

Figure 6.5 Sketches of synthetic networks.

This average discharge per link was then associated to the nodes considering the hourly data of the upper tank outflows in the sub-grid, using a process similar to the one described in section 5.3.3. Hence, a daily distribution with hourly step $q(h)$ was defined for each month, with no distinction between weekday and weekend/holiday.

The consumption in the network can influence the distribution of the flow discharges. To include cases with asymmetrical consumptions, the five consumption types represented in Figure 6.6 were considered, where the notations affect the base consumption as follows:

$$\begin{aligned} q_1(h) &= 0.5q(h) \\ q_2(h) &= 1.5q(h) \end{aligned} \tag{6.5}$$

Bigger networks were generated as well to infer the effect of the scale. These are presented in Figures 6.7 to 6.10. A consumption type A was considered for these networks.

Finally, a random process was used in a 10x10 mesh to create the four networks presented in Figures 6.12 to 6.15. Network R5 (Figure 6.15) was obtained by eliminating a few nodes from network R1

and network R6 (Figure 6.16) resulted from the combination of networks R2 and R3. The consumption in the nodes of these networks was defined randomly between 0 and $2q(h)$.

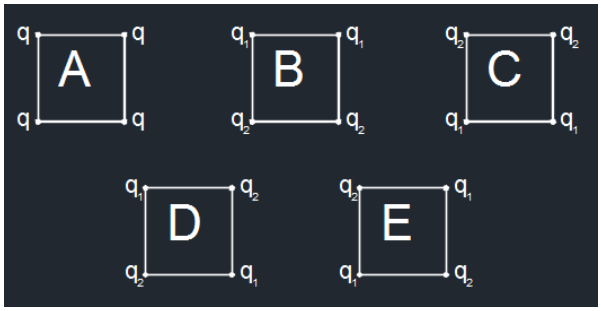

Figure 6.6 Types of consumption distribution.

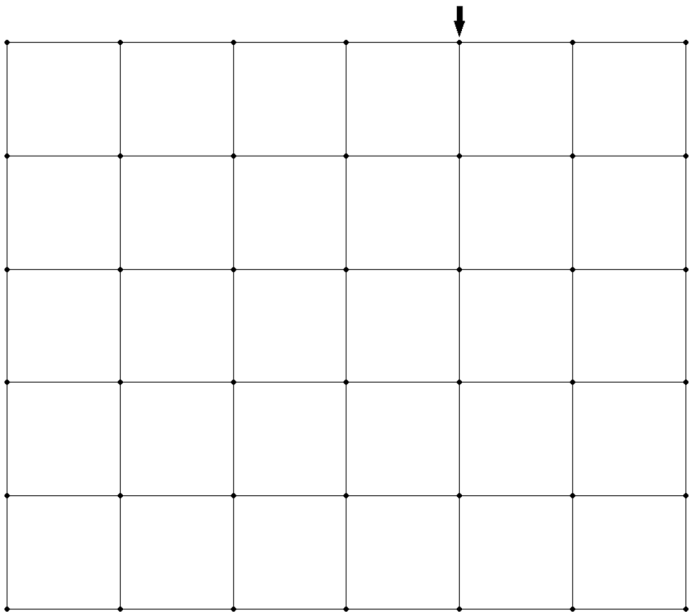

Figure 6.7 Sketch of Network 29.

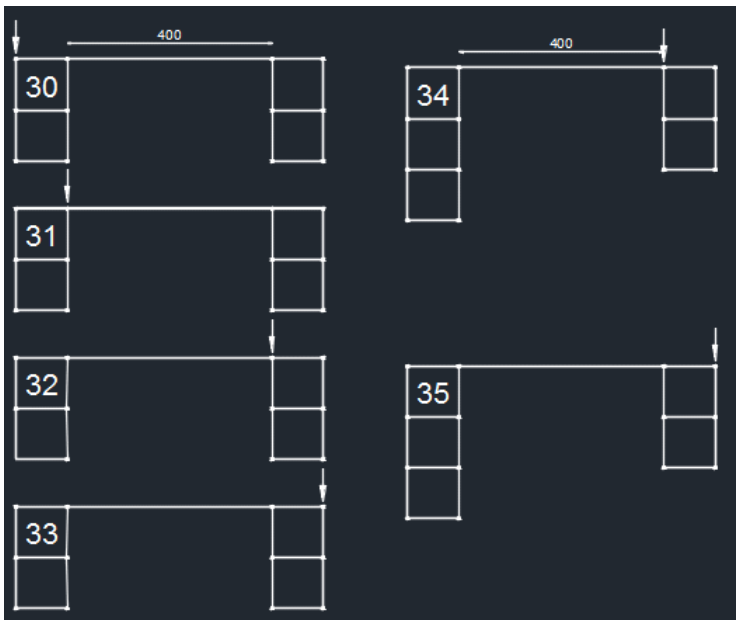

Figure 6.8 Sketch of Networks 30 to 35.

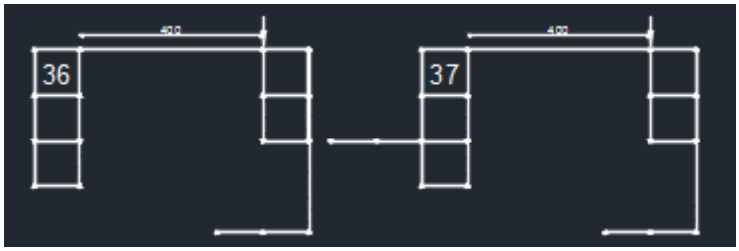

Figure 6.9 Sketch of Networks 36 and 37.

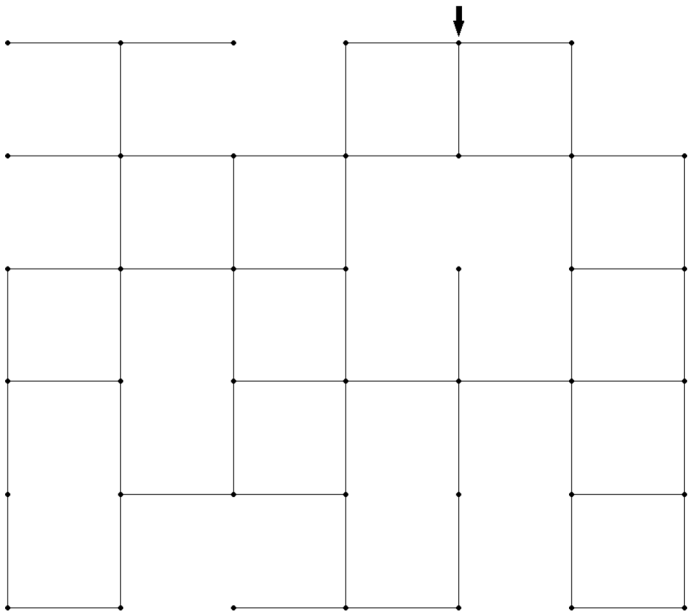

Figure 6.10 Sketch of Network 38.

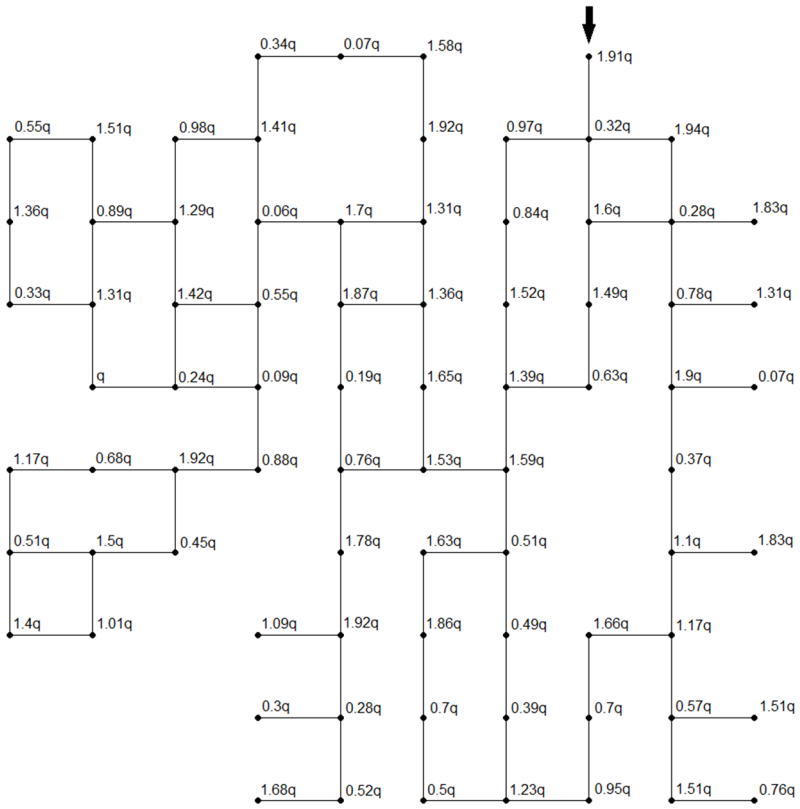

Figure 6.11 Sketch of Network R1.

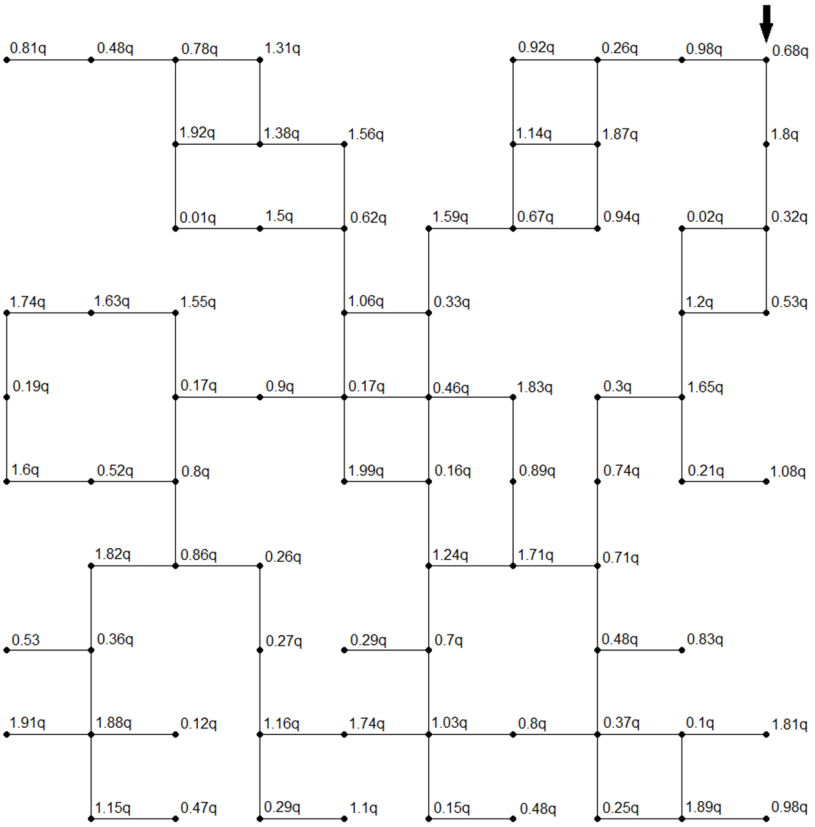

Figure 6.12 Sketch of Network R2.

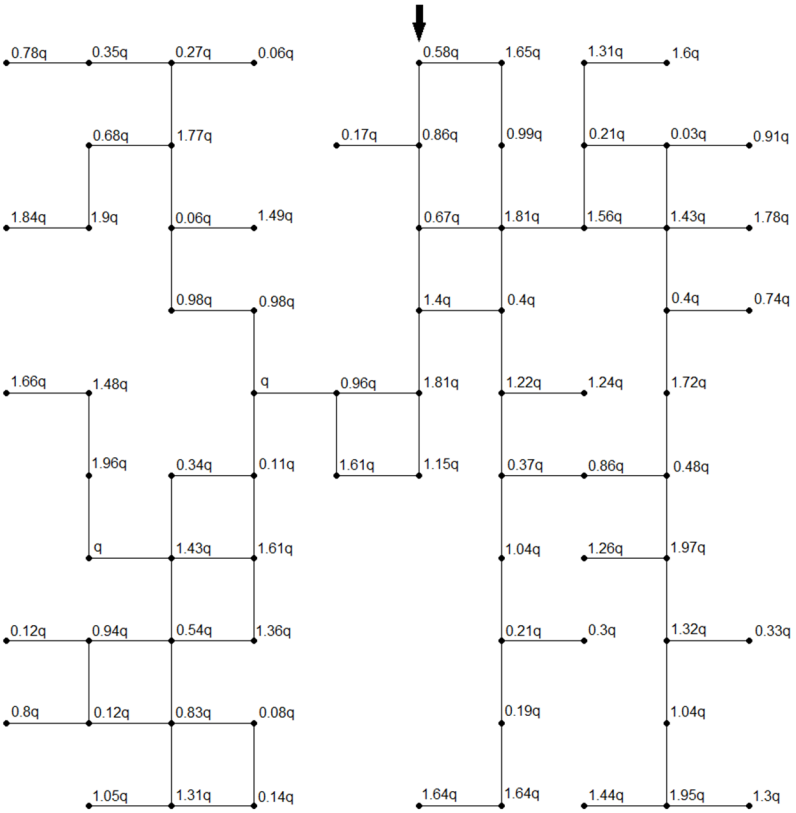

Figure 6.13 Sketch of Network R3.

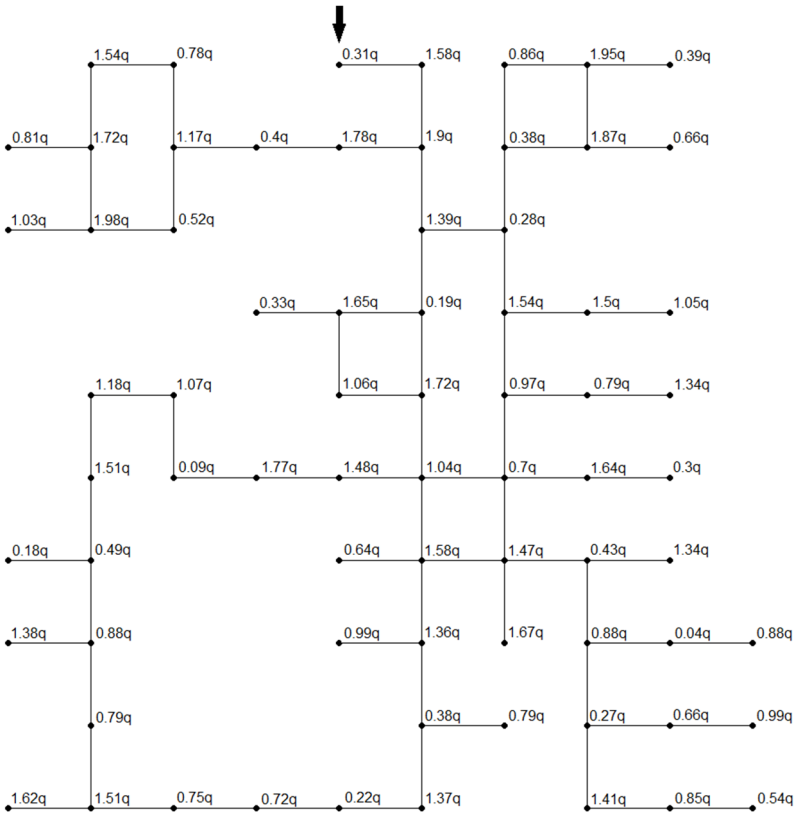

Figure 6.14 Sketch of Network R4.

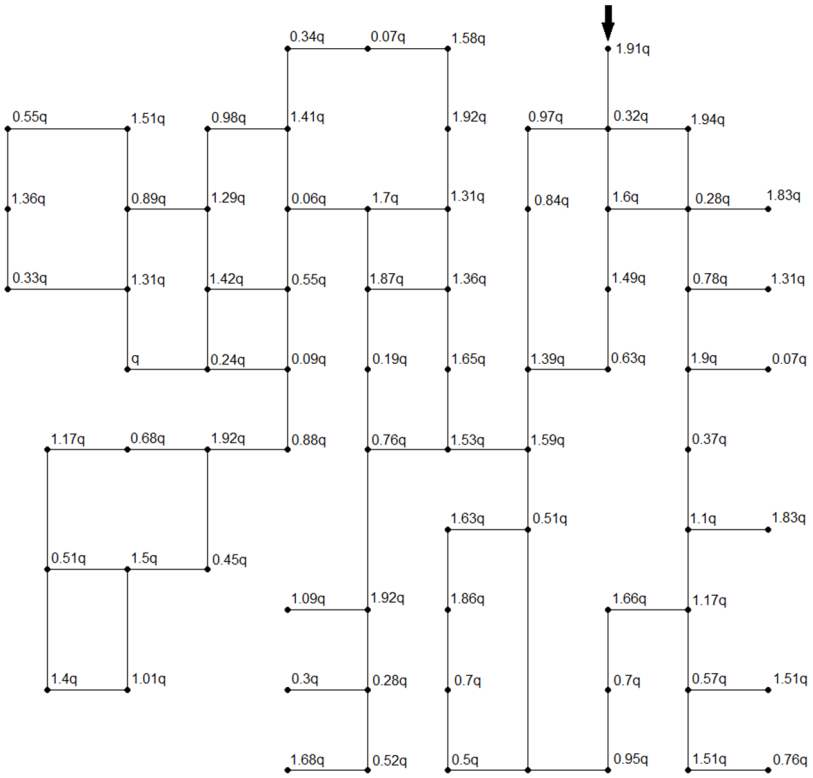

Figure 6.15 Sketch of Network R5.

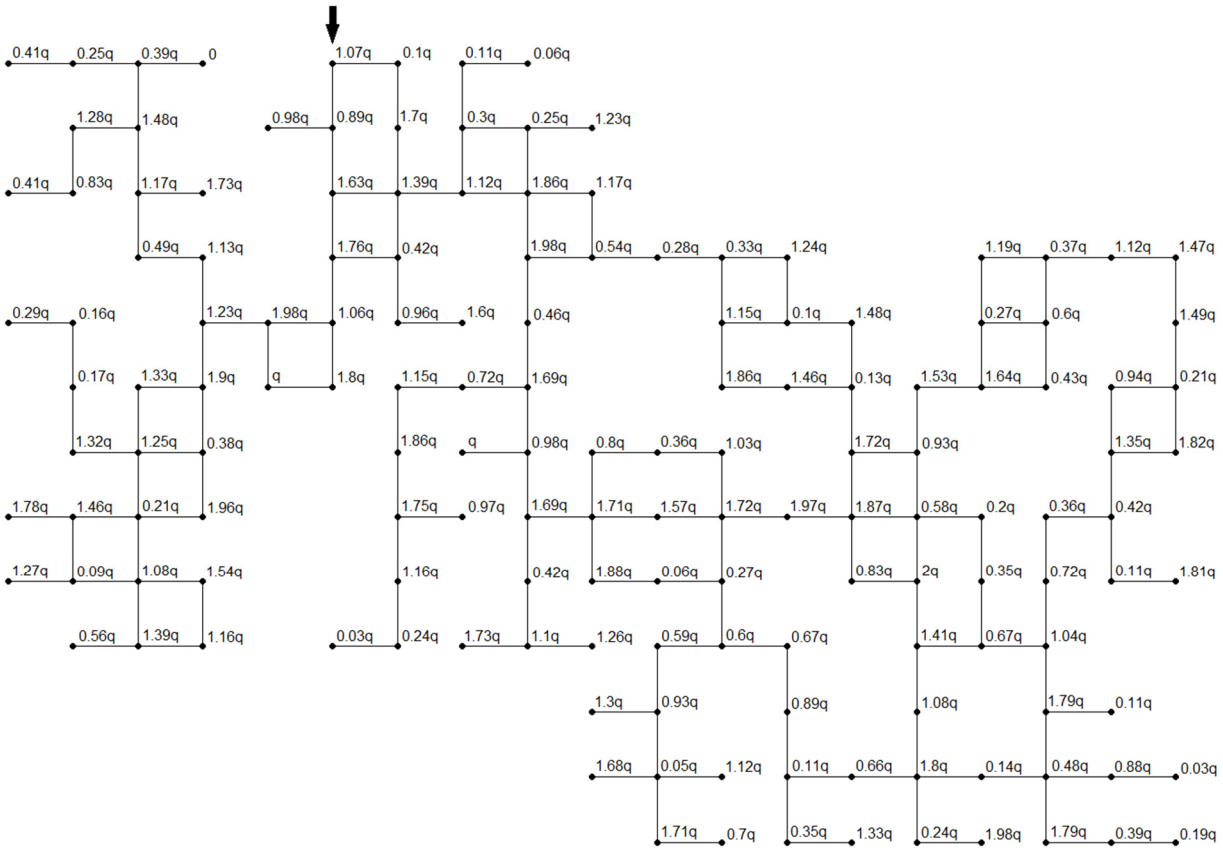

Figure 6.16 Sketch of Network R6.

6.3.2 Dimensional analysis of network geometry

To characterize the energy extracted from a water supply network, the following variables may be considered:

- $\rho = 1000$ kg/m^3 : water density;
- $g = 9.8$ m/s^2 : acceleration due to gravity;
- Q_{inflow} (m^3/s): average inflow (in time) discharge that enters the network;
- n : number of nodes;
- t : number of links;
- $q' = 2\frac{t}{n(n-1)}$: link density, which is the number of links divided by the maximum possible links (Yazdani & Jeffrey, 2011);
- $e = t/n$: link per node ratio (Yazdani & Jeffrey, 2011);
- $f = t - n + 1$: number of independent loops for single source networks (Yazdani & Jeffrey, 2011);
- $r = \frac{f}{2n-5}$: meshedness coefficient, quantifying the density of any kind of loop (Yazdani & Jeffrey, 2011);
- L_c (m): length of the main path, defined by the shortest path without loops that connects the source to the furthest node with the highest discharge.
- L_t (m): total length of the network;
- Q_{aver} (m^3/s) : average (in time and in the network) discharge;
- Q_{max} (m^3/s) : maximum average link discharge;
- D_{aver} (mm) : average diameter in the network;
- v_{aver} (m/s) : average velocity in the network;
- S (m^2) : total surface occupied by the network. For a dendritic network, the surface is zero;
- L_S (m) : equivalent length, given by the length of all external pipes that define the boundary of the network;
- $K_C = \frac{L_S}{S}$: Gravelius coefficient, usually defined for watersheds but here applied to a network;

- L_q (m) : distance corresponding to the average ordinate of the curve relating distance to the source and accumulated consumption (Figure 6.17);
- L_n (m) : distance corresponding to the average ordinate of the curve relating distance to the source and accumulated number of nodes (Figure 6.17).

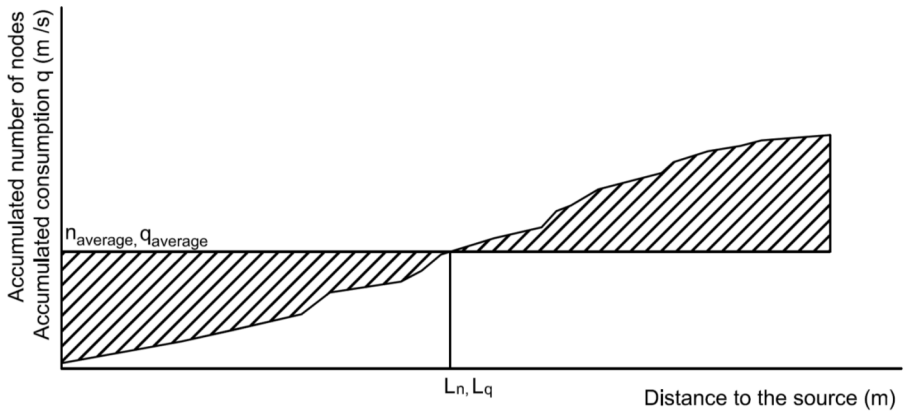

Figure 6.17 Cumulated curves in relation to distance to source.

All these variables are related to either the consumption, either the size of the network, either the interconnections between pipes, either a combination of these characteristics. The surface defined by the mesh and the Gravelius coefficient cannot be applied to characterize purely dendritic networks. These, however, are not considered in the present analysis.

Taking into account the defined variables, dimensional analysis was performed to aid in the search for the estimation of energy production. The energy produced by a turbine E_{1T} may be generically related to these variables as follows:

$$E_{1T} = \mathrm{f}(\rho, g, Q_{inflow}, n, t, q', f, r, L_c, L_t, , Q_{aver_r}, Q_{max}, D_{aver}, v_{aver}, L_S, K_c, L_q, L_n,) \quad (6.6)$$

For normalization purposes, the gravitational acceleration, g, was used as kinematic parameter, the water density, ρ, was used as dynamic parameter and, after several iterations to assess the best option, the equivalent length, L_S, was used as geometric parameter. g, ρ and L_S are dimensionally independent, hence, using the theorem of Vaschy-Buckingam, the dimensionless expression of (6.6) comes:

$$\Pi_{E_{1T}} = \Phi\left(\Pi_{Q_{inflow}}, \Pi_n, \Pi_t, \Pi_{q\prime}, \Pi_f, \Pi_r, \Pi_{L_c}, \Pi_{L_t}, \Pi_{Q_{aver_r}}, \Pi_{Qmax}, \Pi_{D_{aver_r}}, \Pi_{v_{aver_r}}, \Pi_{K_c}, \Pi_{L_q}, \Pi_{L_n}\right) \quad (6.7)$$

where each $\Pi_i$is dimensionless and obtained by

$$\Pi_i = \frac{parameter}{g^{\alpha_i}\rho^{\beta_i}{L_S}^{\gamma_i}} \quad (6.8)$$

where α_i, β_i and γ_i are determined by dimentional analysis.

In the following, equation (6.7) and the corresponding dimensionless numbers will be the basis of the tests aiming at a good expression describing E_{1T}.

6.3.3 Results

The installation of a single 5BTP was tested for several combinations of the synthetic network types and consumption types. The simulated energy production with one turbine in each case, as well as the analyzed variables, are presented in Table.A 3 of Appendix C. The energy production with one turbine was also tested for a few synthetic network types with the consumption in the nodes affected by a factor lower than one to obtain smaller average velocities in the pipes.

An exponential type function was chosen, where each exponent and the constant β were curve-fitted to match the simulation results.

$$\Pi_{E_{1T}} = \beta \Pi_{Q_{inflow}}^{aQ_{inflow}} \Pi_{n}^{an} \Pi_{t}^{at} \Pi_{q'}^{aq'} \Pi_{f}^{af} \Pi_{r}^{ar} \Pi_{L_c}^{aL_c} \Pi_{L_t}^{aL_t} \Pi_{Q_{aver_r}}^{aQ_{aver_r}} \Pi_{Qmax}^{aQmax} \Pi_{D_{aver_r}}^{aD_{aver_r}} \Pi_{v_{aver_r}}^{av_{aver_r}} \Pi_{K_c}^{aK_c} \Pi_{L_q}^{aL_q} \Pi_{L_n}^{aL_n} \quad (6.9)$$

Several expressions involving the defined variables were tried, as presented in Table 6.7, using a least squared method to curve-fit the exponents of equation (6.9). For each expression, the coefficient of determination (R^2) was obtained comparing the simulated value of E_{1T} with the modeled $\Pi_{E_{1T}}$. All estimations of R^2 between simulated energy and calculated with the proposed expressions are presented in Figures A.33 to A.58 of Appendix C. In these graphics it is also presented the estimation of energy production with each expression in the case study sub-grids Lausanne WSN 1 and Lausanne WSN 2.

From Table 6.7 it appears that most combinations give good estimations, since the R^2 is often superior to 0.9. The best expression according to this criterion is number 2. However, other indicators can be analyzed. In Table 6.8 the mean squared error (MSE) between the simulated energy and calculated with all expressions is presented and, according to this criterion, the best expression is number 6.

The application of the expressions to the real cases of the sub-grids Lausanne and Lausanne 2 is presented in Table.A 4 of Appendix C. Taking into account the MSE presented in Table 6.9 relative to the case studies, the best expression is number 21.

Most combinations do not give good estimations for the cases studies, which can be explained by the different nature of the synthetic networks. Several elements were ignored in the construction of the synthetic networks that should be addressed such as dendritic structures, the topographic differences and more diverse pipe lengths and velocities. As it has been seen before, in the method developed in sub-chapter 6.2, the topography has a limitative role in hydropower production in a network in the sense that the installation of a turbine in a pipe may cause pressures under the minimum in other areas. This effect is very hard to predict without simulating the network.

Table 6.7 Exponents for several dimensionless expressions determined empirically.

Expression	β	a_n	a_t	$a_{q'}$	a_f	a_r	a_{Ln}	a_{Lt}	a_{Lc}	a_{Qaver_r}	a_{Lq}	a_{Qmax}	a_{Kc}	a_{Qinf}	a_{vaver}	a_{Daver}	R^2
1	6.61	-6.86	3.04	-3.64	0.01	0.05	-0.35	-0.06	0.11	-0.19	0.39	1.78	0.18	-0.01	-0.08	-0.43	0.9913
2	5.87	-4.26	1.86	-2.35			-0.37	-0.08	0.12	-0.16	0.43	1.77	0.14	0.00	-0.10	-0.49	0.9932
3	7.02	-5.36	2.47	-2.96			-0.36	-0.09	0.09	-0.39	0.40	1.81	0.33	0.01	0.08		0.992
4	5.05			-0.29			-0.31	-0.18	0.16	-0.42	0.38	1.77	0.30	-0.05	0.24		0.9924
5	5.21			-0.30			-0.28	-0.14		-0.35	0.46	1.79	0.25	-0.10	0.24		0.9928
6	3.72						-0.37	0.18		-0.31	0.52	1.80	0.22	-0.35	0.37		0.993
7	3.89						-0.35	0.29			0.39	1.75	0.00	-0.52	0.26		0.9921
8	3.39						-0.64				0.72	1.78	-0.03	-0.59	0.19		0.9881
9	3.96										0.14	1.78	0.00	-0.53	0.20		0.9843
10	3.96						-0.55				0.65	1.79		-0.53	0.10		0.9835
11	4.23						-0.10					1.92	-0.01	-0.63	0.19		0.987
12	4.18											1.87	0.00	-0.58	0.19		0.9855
13	0.87						-0.46				1.42			0.86	0.10		0.8859
14	3.96						-0.55				0.65	1.79		-0.53	0.10		0.9835
15	4.00										0.14	1.78		-0.53	0.19		0.9838
16	4.24											1.87		-0.58	0.18		0.9848
17	4.29										0.12	1.77		-0.45			0.9898
18	4.00						-0.64				0.72	1.79	-0.01	-0.49			0.9853
19	4.09						-0.61				0.69	1.79		-0.49			0.9847
20	4.29										0.12	1.77		-0.45			0.9898
21	3.27						-0.54				0.84	1.20					0.9772
22	5.43			-0.36			-0.28				0.36	1.49					0.9808
23	6.31			-0.54			-0.22	-0.28			0.31	1.59					0.9916
24	6.67			-0.59				-0.31			0.08	1.63					0.9922
25	6.31			-0.54			-0.22	-0.28			0.31	1.59					0.9916

Table 6.8 Mean squared error of all test expressions.

Expression	MSE
1	265.50
2	159.98
3	161.80
4	143.84
5	143.33
6	115.80
7	165.88
8	321.97
9	674.96
10	373.24
11	509.09
12	612.43
13	2050.33
14	373.24
15	674.80
16	611.24
17	841.78
18	388.94
19	388.07
20	841.78
21	866.05
22	335.62
23	139.65
24	140.87
25	139.65

Table 6.9 Estimation and mean squared error for every expression applied to case study networks.

Expression	E_{1T} Lausanne WSN 1 (MWh/year)	E_{1T} Lausanne WSN 2(MWh/year)	MSE
Real value	90.68	0.01	-
1	4.01	0.33	3756.02
2	7.55	0.35	3455.02
3	1.52	0.34	3975.20
4	2.41	0.48	3896.12
5	4.18	0.56	3741.58
6	4.71	1.98	3697.01
7	32.98	3.27	1669.98
8	45.64	5.79	1030.95
9	34.23	3.77	1600.46
10	35.53	4.67	1531.86
11	28.14	3.43	1961.19
12	29.57	3.41	1872.72
13	226.43	0.69	9214.57
14	35.53	4.67	1531.86
15	33.71	3.73	1629.53
16	28.82	3.35	1919.02
17	33.96	3.04	1613.35
18	37.81	4.47	1407.45
19	35.86	4.34	1512.20
20	33.96	3.04	1613.35
21	58.17	1.67	529.85
22	49.96	0.44	829.33
23	51.07	0.31	784.46
24	49.03	0.25	867.28
25	51.07	0.31	784.47

Moreover, the study case of Lausanne WSN 2 does not have the same pattern of consumption as the synthetic grids. The temporal variation of the consumption was not throughout studied.

The previously identified expressions, numbers 6 and 21, would result in the following formulations:

$$E_{1T} = 3.72\left(\frac{Q_{max}}{g^{1/2}L_S{}^{5/2}}\right)^{1.8}\left(\frac{L_n}{L_S}\right)^{-0.37}\left(\frac{L_q}{L_S}\right)^{-0.52}\left(\frac{L_t}{L_S}\right)^{0.18}\left(\frac{Q_{aver\_r}}{g^{1/2}L_S{}^{5/2}}\right)^{-0.31}\left(\frac{Q_{inf}}{g^{1/2}L_S{}^{5/2}}\right)^{-0.35}\left(\frac{K_c}{L_S}\right)^{0.22}\left(\frac{v_{aver}}{g^{1/2}L_S{}^{1/2}}\right)^{-0.35} \quad (6.10)$$

$$E_{1T} = 3.27\left(\frac{Q_{max}}{g^{1/2}L_S{}^{5/2}}\right)^{1.2}\left(\frac{L_n}{L_S}\right)^{-0.54}\left(\frac{L_q}{L_S}\right)^{0.84} \quad (6.11)$$

The two equations obtained, Equation (6.10) and Equation (6.11), are both dependent of the equivalent length L_S, on the maximum flow in the network Q_{max}, and on L_n and L_q, distances corresponding to the average ordinates of the curves relating distance to the source and accumulated number of nodes and consumption, respectively. The latter variables represent the distribution of the consumption and the shape of the network. However, Equation (6.11) is much simpler than Equation (6.10), which also depends on the average network flow discharge, the total inflow, the Gravelius coefficient and the average velocity.

The second best MSE, according to Table 6.8, is from expression 25, which is the following:

$$E_{1T} = 6.31\left(\frac{Q_{max}}{g^{1/2}L_S^{5/2}}\right)^{1.59}\left(\frac{L_n}{L_S}\right)^{-0.22}\left(\frac{L_q}{L_S}\right)^{0.31}\left(\frac{L_t}{L_S}\right)^{-0.28} q'^{-0.54} \quad (6.12)$$

This expression is similar to Equation (6.11), with the addition of the variables q', the link density, and L_t, total length of the network. Also, the MSE for the estimation with this expression of the production of energy in the case studies is one of the lowest (Table 6.9). In Figure 6.18 it is presented expression 25 in logarithmic scale. No similar formula was found in literature for comparison.

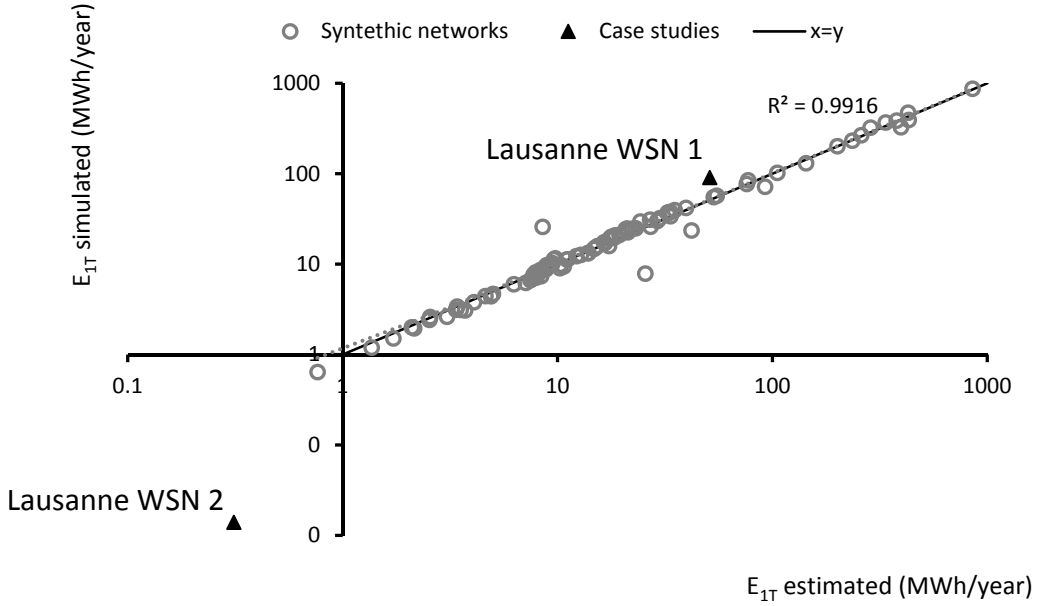

Figure 6.18 Representation of estimation of energy produced with one 5BTP with expression 25 against the simulated energy in logarithmic scale.

6.4 Conclusions

The aim of this Chapter was to analyze the possibility of evaluating the potential of a WSN for hydropower without resorting to long and/or detailed simulations.

The first methodology proposed estimates the potential for hydropower in urban water supply networks based on an available energy concept. It is applied to several case study networks in Switzerland (two sub-grids of Lausanne and the complete network of Fribourg) and, for comparison, the optimization algorithm, model 2 from Chapter 5, was used to estimate the actual energy production in the best locations of the network with the 5BTP.

Figure 6.19 presents the potential energy, based on the available energy assessment method, and the energy produced with one turbine, obtained from simulation, for the four presented case studies. As it can be seen in this figure, there is not a clear relationship between the two. The potential energy results from the assembling of all the excess energy that is available considering

critical nodes while the energy produced depends on the particular pipe where the turbine is installed, which is conditioned by the local flow discharge and pressure availability.

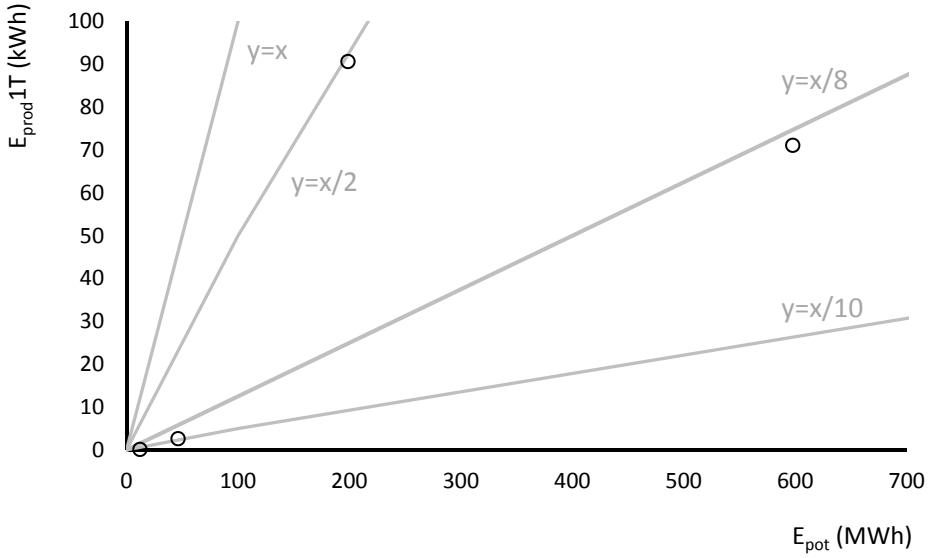

Figure 6.19 Potential energy and produced energy with one 5BTP in case study networks.

Hence, the estimation of the available energy in a network can give an insight on how much energy is not being used, possibly useful for network management and pressure control, and that could theoretically be exploited with hydropower. However, in practice, the hydropower production is dependent on the conditions (discharge flow and turbine) in the particular location of the network where it is installed.

The second methodology intends to estimate the energy production with one 5BTP turbine in a given network without resorting to long simulations as a measurement of the potential. In fact, in this research, two methods have been proposed. The first, the expedite method presented in sub-chapter 5.5 is based on the experience gained in the performed simulations and intends to infer the economic interest. However, the second method, developed in this sub-chapter 6.3, intends not only to estimate the energy production but also highlight the characteristics of the network geometry that influence the most its potential for hydropower.

The prediction of the energy produced in the real case studies of Lausanne WSN 1 and WSN 2 with this method was not satisfying. However, the direct application of the method to real case studies is not yet fully evident. A few variables can only be applied to networks with closed loops and the topographic differences are not taken into account. It is possible that the method has a better application in cities where the urban networks are symmetric and straight (for example, typical USA cities). Also, the case study of Lausanne WSN 2 may have a potential for hydropower that is too low for the method to be applied. Another explanation could be the different load curves in each case study and the lack of a parameter that takes this variance into account.

Although it is not clear which equation is more suitable, the maximum flow seems to be one of the most relevant variables. Taking into account that this parameter is also used in the method for expedite assessment presented in sub-chapter 5.5, this conclusion appears to be logic. It is interesting to notice that the maximum flow is not enough, however, to infer the energy production and that the size of the network and the demand distribution influence the estimation. This influence could be due to the demand driven condition of these networks and to the re-distribution of the flow rates and pressures that occur when a turbine is installed.

Equation (6.12) seems to be the expression that gives a better combined result of predicting the energy production in the synthetic networks and in the case studies.

Despite the reserves considering the application of the method to real networks, the curve-fitting process gave very good approximations of the simulated energy production with one turbine. It can thus be concluded that the chosen variables duly represent the governing processes allowing to estimate the energy production potential in WSN.

Chapter 7
Conclusions and future developments

7.1 Conclusion of main findings

The use of micro-hydropower in WSS has many advantages, since it can be considered a green technology that profits from the existence of infrastructure and electric connections. However, needs for assessment were identified related to: the technologies that should be used within the WSN; the maximum energy and economic value that can be explored in WSN; and the energetic potential of WSN. To cover these issues, both experimental work and computational simulations and optimization routines were performed.

The performance of a novel micro-turbine, the 5BTP, was characterized experimentally in Chapter 4. This procedure intended to answer to the first research question initially raised in the introduction on the appropriateness to apply the 5BTP in urban water supply networks. The experiments of the 85 mm model of the 5BTP turbine provided promising results when referring to micro/pico machines. A best efficiency point of about 64 % was obtained, which is good for such small machines. The maximum power obtained was of 328 W, with 51% of efficiency. Hill diagrams were obtained, which can be extrapolated to other diameters through the turbomachine affinity law. The 5BTP is simple, without flow regulation. Given these characteristics and the fact that it can be installed directly in a pipe in line with the flow, it can be concluded that this is an attractive solution to be used in water supply networks.

A study of the placement of turbines was carried in Chapter 5, with the intention of answering the second research question on the best locations within the networks for the installation of micro-hydropower devices. Initially, the installation of a turbine upstream from a storage tank was analyzed taking into account energy production and water quality. A genetic algorithm was applied to obtain an operating schedule and maximize the energy production within a certain period, while forcing the level inside the reservoir to vary, preventing stagnation of the water inside the reservoir. The developed algorithm was based on predictions of consumption obtained from historical data. An operational methodology was also conceived, so that the system reacts to the actual consumption and follows the operating schedule given by the optimization algorithm. On a second

step, the installation of turbines considering whole urban networks was studied. Using the 5BTP, a hydropower arrangement was defined consisting of buried chambers built around existing pipes, suitable for urban networks, where up to four turbines can be installed inline. The location of such arrangements within networks was optimized regarding energy production and economic value. The optimization algorithm was developed based on the simulated annealing strategy and an analysis of conversion was carried, considering different restrictions. The search algorithm was then applied to two case studies, a sub-grid of the Lausanne WSN and the entire WSN of Fribourg. Both case studies resulted in positive results, concluding that the installation is feasible. The obtained results from the simulations and optimizations allowed concluding that the most favorable locations in networks are the replacement of PRVs, if they exist, and the paths of highest discharge flow. Dissipation upstream from water tanks is often needed and typically the discharges are high. Within the network however, a larger energy production does not necessarily imply better economic value since the costs related to the construction of several chambers and to the equipment can justify a lower production of energy. Finally, the installation of turbines in a network should be analyzed with small time steps and subjected to sensibility analysis. The introduction of pressure reductions in the network has a direct influence on the distribution of the discharge flows, flow direction and pressures. The risk of inducing fragility in the network should be analyzed resorting to different consumption scenarios.

Finally, methods are proposed to estimate the energy potential for any network for micro-hydropower with the intention of answering the third research question: how much potential is there in water supply networks for micro-hydropower? The potential in water supply networks depends on a variety of factors. Among them, the most important are the demand (population and industry), the density of the network, the network redundancy and the topography. An algorithm was developed to estimate the maximum amount of energy that could be taken from a network while respecting demand conditions and pressure limits. This methodology is based on the identification of critical points where the energy line is closest to the limit pressure. The head in these critical points is sequentially removed and the effect of these imposed head losses taken into account in the network's equilibrium. However, such methodology cannot be directly related to the energy produced with one turbine in the network as the latter depends heavily on the local flow discharge and pressure availability. For an estimation of the energy produced with one turbine, two methods were developed. The first is an expedite method based on the experience gathered during the performed simulations with the 5BTP. Taking into account that the best placements are PRVs sites and paths with high flow discharge, the identification of these locations is the first step. The installed power and economic benefit can be roughly estimated based on the maximum discharges and the redundancy of the targeted pipe. The second method is conceptual and it intends to predict the energy produced with one 5BTP based on geometrical characteristics of the network and consumption information. To reach this prediction, a dimensional analysis was performed on synthetic networks constructed with constant topography and in accordance with a few rules concerning diameters. Although this method displayed difficulties in being applied to real networks, the obtained predictions for the synthetic networks were promising. It was concluded that the

highest discharge flow is an important element to predict the energy production, but not enough. The size and the demand distribution also play important roles in this prediction.

In conclusion, the main original contributions of this work are: the experimental characterization of the 5BTP turbine; an optimization algorithm that identifies the optimal locations in networks to install turbines; a methodology for the estimation of the available energy in a network; and a methodology to estimate the production with one 5BTP based on network characteristics.

7.2 Future developments

In the course of the work presented in this research, several lines of research were identified that could be pursued in future developments.

The simulations performed in the developed algorithms were based on the affinity law equation applied to the data collected with an 85 mm model. Experimental validation of the turbine behavior for larger diameters would be reassuring for the further development of the technology.

Further testing of the optimization algorithm in other WSN, in networks with different utilities and with other turbine technologies, will contribute to better characterize the potential for this type of energy recovery. This would contribute to the creation of a database and to the identification of the types of network that are better suited for exploiting micro-hydropower.

Furthermore, there has been only one in-situ experiment of the 5BTP. Different in-situ implementations of the 5BTP, or of other turbines, in WSN would allow for a proof-of-concept validation of the methodology. These pilot installations would as well allow for troubleshooting of eventual practical issues.

To fully develop the initiated conceptual model on the influence of the shape of the network, more synthetic networks need to be constructed, considering other rules for network design, topography elements and other structures. The accumulation of data from more case study WSNs with different characteristics would complete and validate this method. The developed equations can only be applied to single source networks, and hence the Fribourg network model was not used. The effect of multiple sources should hence be addressed. Finally, this conceptual method was based on the 5BTP. The extrapolation to other turbines should be envisaged.

References

Abbasi, T. & A., A. S., 2011. Small hydro and the environmental implications of its extensive utilization. *Renewable and Sustainable Energy Reviews,* Volume 15, p. 2134–2143.

Adhau, S., Moharil, R. & Adhau, P., 2010. *Reassessment of Irrigation Potential for Micro Hydro Power Generation.* Kandy, IEEE.

Andolfatto, L. et al., 2016. *Simulation of energy recovery on water utility networks by a micro-turbine with counter-rotating runners.* Grenoble, 28th IAHR symposium on Hydraulic Machinery and Systems, pp. 1701-1710.

Andreev, I. et al., 2012. *Installation of large scale model of a hydrostatic pressure machine on Iskar River.* Sofia, 5th Bulgarian-Austrian Seminar, Small dams and HPP.

Araújo, L. S., Ramos, H. M. & Coelho, S. T., 2006. Pressure Control for Leakage Minimisation in Water. *Water Resources Management,* Volume 20, p. 133–149.

Arriaga, M., 2010. Pump as turbine – A pico-hydro alternative in Lao People's Democratic Republic. *Energy Strategy Reviews,* Volume 35(5), pp. 1109-1115.

Azizi, N. & Zolfaghari, S., 2004. Adaptive temperature control for simulated annealing: a comparative study. *Computers & Operations Research,* Volume 31, pp. 2439-2451.

Balachandran, P., 2011. *Engineering fluid mechanics.* New Delhi: PHI Private Learning Limited.

Batten, W. M. J. & Müller, G. U., 2011. *Potential for using the floating body structure to develop head difference to increase the efficiency of a free stream energy converter.* Brisbane, 34th IAHR Biennial Congress, pp. 2364-2371.

Bertsimas, D. & Tsitsikis, J., 1993. Simulated Annealing. *Statistical Science,* Volume 8(1), pp. 10-15.

Biner, D., Hasmatuchi, V., Avellan, F. & Münch-Alligné, C., 2015. *Design & performance of a hydraulic micro-turbine with counter-rotating runners.* Pisa, 5th International Youth Conference on Energy, IYCE.

Bousquet, C. et al., submitted in 2016. Assessment of hydropower potential in wastewater systems and application to Switzerland. *Renewable Energy.*

Bousquet, C. et al., 2015. Hydropower in wastewater. Which potential in Switzerland? (in French). *Aqua & Gas,* Volume 10, pp. 54-61.

Bresse, M., 1987. Water-Wheels. In: *Hydraulic Motors.* Paris: Translation by Mahan, F. from the "Cours de Mécanique Appliquée". École des Ponts et Chausées.

Bryner, A., 2011. *Water and Energy, Information sheet for Switzerland – in French,* Dübendorf: Eawag Aquatic Research.

Burdis, A. R., 2009. Using Pumps As Power Recovery Turbines. *WaterWorld,* Volume 25(8), pp. 12-15.

Carravetta, A., Giudice, G. D. & Ramos, O. F. H., 2013. PAT design strategy for energy recovery in water distribution networks by electrical regulation. *Energies,* Volume 6(1), pp. 411-424.

Carravetta, A. & Giugni, M., 2006. *Functionality factors in the management and rehabilitation of water networks.* Ferrara, Efficient management of water networks, FrancoAngeli, pp. 40-54.

Carravetta, A., Giuseppe, G., Fecarotta, O. & Ramos, H. M., 2012. Energy production in water distribution networks: A PAT design strategy. *Water Resources Management,* Volume 26(13), pp. 3947-3959.

Caxaria, G., Mesquita e Sousa, D. & Ramos, H., 2011. *Small scale hydropower: generator analysis and optimization for water supply systems.* Sweden, World Renewable Energy Congress, European council for an energy efficient economy, pp. 1386-1393.

Cenor, 2011. *Beiriz Small Hydropower Plant. Base Study - in Portuguese.* Lisbon: Cenor-Projectos de Engenharia.

Chapallaz, J. M., Eichenberger, P. & Fischer, G., 1992. *Manual on Pumps Used as Turbines. MHPG Series, Harnessing Water Power on a Small Scale, V. 11..* Eschborn, Germany: GATE – GTZ.

Chen, S. & Chen, B., 2013. Net energy production and emissions mitigation of domestic wastewater treatment system: A comparison of different biogas–sludge use alternatives. *Bioresource Technology,* Volume 144, p. 296–303.

Corcoran, L., McNabola, A. & Coughlan, P., 2015. Optimization of Water Distribution Networks for Combined hydropower Energy Recovery and Leakage Reduction. *Journal of Water Resources Planning and Management,* Volume 142(2).

Cunha, M. C. & Sousa, J., 2001. Hydraulic infrastructures design using simulated annealing. *Journal of Infrastructure Systems,* Volume 7(1), p. 32–39.

David, L., Almeida, M. & David, C., 2010. *Rehabilitation of the Alcântara Sewage Treatment Plant – Effect of the design capacity on CSO discharges.* Lyon, NOVATECH.

Deng, Y., Blok, K. & van der Leur, K., 2012. Transition to a fully sustainable global energy system. *Energy Strategy Reviews,* Volume 1(2), pp. 109-121.

Desphande, M. V., 2010. *Elements of Electrical Power Sation Design..* New Delhi: PHI Learing Private Limited.

DGEG, 2013. *Renowables, Rapid statistics, June 2013 (in Portuguese),* Lisbon: Direcção Geral de Energia e Geologia.

Dias, C., 2016. Roxo small-hydropower plant, inaugurated by Sócrates in 2010, will produce energy in 2016 - in Portuguese. *Público*, 8 June.

Donovan, C. & Nuñez, L., 2012. Figuring what's fair: The cost of equity capital for renewable energy in emerging markets.. *Energy Policy,* Volume 40, pp. 49-58.

EEA, 2006. *Urban sprawl in Europe,* Copenhagen: European Environment Agency.

EEA, 2011. *About the urban environment' – in Portuguese.* [Online] Available at: http://www.eea.europa.eu/pt/themes/urban/about-the-urban-environment [Accessed 12 2013].

EIA, 2013. *International Energy Statistics.* [Online] Available at: http://www.eia.gov/cfapps/ipdbproject/iedindex3.cfm?tid=2&pid=33&aid=12&cid=regions&syi [Accessed 14 June 2016].

Elbatran, A., Yaakob, O. B., Ahmed, Y. M. & Shabara, H. M., 2015. Operation, performance and economic analysis of low head micro-hydropower turbines for rural and remote areas: A review. *Renewable and Sustainable Energy Reviews,* Volume 43, pp. 40-50.

EPA, U., 2013. *Energy Efficiency in Water and Wastewater Facilities. A Guide to Developing and Implementing Greenhouse Gas Reduction Programs.* s.l.:Environmental Protection Agency.

EPFL, 2015. *Database of the Laboratory of Hydraulic Constructions,* Lausanne: École Polytechnique Fédérale de Lausanne.

ESHA, 2005. *Technical guide for project design (in French). Belgium,* Belgium: European Small Hydropower Association.

ESHA, 2012. *Statistical releases from the stream map project,* Brussels: EU-27 Statistical Relase.

EU, 2011. *Energy Roadmap 2050. Communication from the Commission to the European Parliament, the Council, the European Economic and Social Committee and the Committee of the Regions.,* Brussels: European Union.

Ezilion Maps, 2015. *Political Maps.* [Online] Available at: http://www.ezilon.com/maps/europe/portugal-maps.html [Accessed 4 May 2016].

Fairbairn, W., 1874. *Treatise on Mills and Mill-Works Part 1.* London: Longmans, Green & Co..

Fantozzi, M., Calza, F. & Kingdom, A., 2009. *Introducing advanced pressure management at Enia utility (Italy): Experience and results achieved.* Hague, the Netherlands, IWA International Specialized Conference on Water Loss.

Farmani, R., Savic, D. A. & Walters, G. A., 2005. Evolutionary multi-objective optimization in water distribution network design. *Engineering Optimization,* Volume 37(2), p. 167–183.

Fayzul, M., Pasha, K. & Lansey, K., 2014. Strategies to develop warm solutions for real-time pump scheduling for water distribution systems. *Water Resources Management,* Volume 28, p. 3975–3987.

Fecarotta, O. et al., 2014. Hydropower potential in water distribution networks: Pressure control by PATs. *Water Resources Planning and Management,* Volume 29(3), pp. 699-714.

Fecarotta, O. et al., 2015. Hydropower potential in water distribution networks: Pressure control by PATs. *Water Resources Management,* Volume 29(3), pp. 699-714.

Fontana, N., Giugni, M. & Portolano, D., 2012. Losses reduction and energy production in water-distribution networks.. *Journal of Water Resources Planning and Management,* Volume 138(3), pp. 237-244.

Gabathuler, S., Pavanello, D. & Münch, C., 2015. Pump-storage at small-scale for energy storage – in French. *VSE Bulletin,* Volume 2, pp. 49-55.

Gaius-obaseki, T., 2010. Hydropower opportunities in the water industry. *International Journal of Environmental Sciences,* Volume 1(3), pp. 392-402.

Gallagher, J. et al., 2015. A strategic assessment of micro-hydropower in the UK and Irish water industry: Identifying technical and economic constraints. *Renewable Energy,* Volume 81, pp. 808-815.

Gan, L., Eskeland, G. & Kolshus, H., 2007. Green electricity market development: Lessons from Europe and the US. *Energy Policy,* Volume 35, p. 144–155.

Gan, L., Eskeland, G. S. & Kolshus, H. H., 2007. Green electricity market development: Lessons from Europe and the US. *Energy Policy,* Volume 35, pp. 144-155.

Haimerl, L., 1960. The Cross-Flow turbine. *Water Power,* Volume 12(1), pp. 5-13.

Hasmatuchi, V., Botero, F., Gabathuler, S. & Munch, C., 2015a. Design and control of a new hydraulic test rig for small hydro turbines. *Hydropower & Dams,* Volume 22(4), pp. 54-60.

Hasmatuchi, V., Botero, F., Gabathuler, S. & Munch, C., 2015b. *New hydraulic test rig for small-power turbomachines.* Hague, IAHR World Congress.

Henderson, H., Jacobson, S. H. & Johnson, A. W., 2003. The Theory and Practice of Simulated Annealing. International Series in Operations Research & Management Science. *Handbook in Metaheuristics,* Volume 57, pp. 287-319.

Hickey, H., 2008. *Water Supply Systems and Evaluation Methods Vol II.* s.l.:U.S. Fire Administration.

HYLOW, 2010. *Periodic Report Summary,* United Kingdom: European Commission.

HYLOW, 2012. *Periodic Report Summary 2,* United Kingdom: European Commission.

IEA, 2004. *Energy security and climate change policy interactions, anassessment framework. IEA information paper,* s.l.: International Energy Agency.

IEA, 2014. *Key World Statistics,* s.l.: International Energy Agency.

IEA, 2015. *Global renewable energy policies and measures database..* [Online] Available at: http://www.iea.org/policiesandmeasures/renewableenergy/ [Accessed 2 September 2015].

IEC, 1999. *Hydraulic Turbines, Storage Pumps and Pump-Turbines – Model Acceptance Tests..* Geneva: International Electrotechnical Commission.

IRENA, 2012. *Hydropower. Renewable energy technologies analysis: cost analysis series,* Abu Dhabi: International Renewable Energy Agency.

Jain, S. & Patel, N., 2014. Investigations on pump running in turbine mode: A review of the state-of-the-art. *Renewable & Sustainable Energy Reviews.,* pp. 841-868.

Joshi, S., Holloway, A., Chang, L. & Kojabadi, H., 2005. *Development of a Stand Alone Micro-Hydro System using Pump as Turbine Technology for Low Head Sites in Remote Areas.* Tehran, 20th International Power System Conference.

Keeling, M. & Sullivan, M., 2012. *Fixing the future. Why we need smarter water management for the world's most essential resource,* New York: IBM Global Business Services, Executive Report.

Khan & H., B., 2009. *Non-conventional energy resources.* New Delhi: Tata McGraw-Hill.

Kirkpatrick, S., Gelatt, C. D. & Vecchi, M. P., 1983. Optimization by Simulated Annealing. *Science, New Series,* Volume 220(4598), pp. 671-680.

Kougias, I., Patsialis, T., Zafirakou, A. & Theodossiou, N., 2014. Exploring the potential of energy recovery using micro hydropower systems in water supply systems. *Water Utility Journal,* Volume 7, pp. 25-33.

Laarhoven, P. J. M. V., Aarts, E. H. L. & Lenstra, J. K., 1992. Job Shop Scheduling by Simulated Annealing. *Operations Research,* Volume 40(1), pp. 113-125.

Lee, J. et al., 2012. A watershed-scale design optimization model for stormwater best management practices. *Environmental Modelling & Software,* Volume 37, pp. 6-17.

License to Plumb, 2009. *License to Plumb. Groundwork - Water detention systems.* [Online] Available at: https://www.dlsweb.rmit.edu.au/toolbox/plumbing/toolbox12_01/units/cpcpdr4002a_stormwater/00_groundwork/page_005.htm
[Accessed 28 February 2014].

Liébard, A., Nahon, C. & Auzet, M., 2013. Electricity production in the world: general forecasts. In: *Worldwide electricity production from renewable energy sources.* Paris: Observ'ER.

Lior, N., 2012. Sustainable energy development with some game-changers. *Energy,* Volume 40(1), pp. 3-18.

Lisk, B., Greenberg, E. & F., B., 2012. *Implementing Renewable Energy at Water Utilities. Case Studies,* Denver: Water Research Foundation.

Livramento, J. M., 2013. *Central micro-hídrica incorporada em adutora, M.Sc. Thesis for Renewable Energies and Energy Management,* Faro: Faculdade de Ciências e Tecnologia, Universidade do Algarve.

Lyons, M. W. K., 2014. *Lab Testing and Modeling of Archimedes Screw Turbines,* Canada: MSc Thesis, University of Guelph.

Martins, T. C., Sato, A. K. & Tsuzuki, M. S. G., 2012. Adaptive Neighborhood Heuristics for Simulated Annealing over Continuous Variables. In: *Simulated Annealing - Advances, Applications and Hybridizations.* s.l.:Marcos Sales Guerra Tsuzuki.

McNabola, A., A.P., W. & Coughlan, P., 2011. *The technical & economic feasibility of energy recovery in water supply networks.* Las Palmas de Gran Canaria, European Association for the Development of Renewable Energy, Environment and Power Quality, pp. 1123-1127.

McNabola, A. et al., 2014a. Energy recovery in the water industry using micro-hydropower: an opportunity to improve sustainability.. *Water Policy,* Volume 16, pp. 168-183.

McNabola, A., Coughlan, P. & Williams, A. P., 2014b. Energy Recovery in the Water Industry: An Assessment of the Potential of Micro Hydropower. *Water and Environment Journal,* Volume 28, pp. 294-304.

Melly, D. et al., 2014. *Development of a PM-Generator for a Counter-Rotating Micro-Hydro Turbine.* Berlin, Association for Electrical, Electronic & Information Technologies.

Mora, D. M., 2012. *Ph.D Thesis: Design of water supply networks applying evolutionary algorithms. Eficiency analysis (in Spanish).* Valencia: Universitat Politécnica de València.

Müller, G., 2004. *Water wheels as a power source.* [Online] Available at: http://hmf.enseeiht.fr/travaux/CD0708/beiere/3/html/bi/3/fichiers/Muller_histo.pdf

Müller, G. & Senior, J., 2009. Simplified theory of Archimedean screws. *Journal of Hydraulic Research,* Volume 47(5), pp. 666-669.

Müller, W., 1899. *The iron water wheels, Part 1: the cell wheels & Part 2: the paddle.* Leipzig: Veit & Comp.

Münch-Alligné, C. et al., 2014. Numerical simulations of a counter rotating micro turbine. *Advances in Hydroinformatics,* Volume Springer Hydrogeology, pp. 363-373.

Neves, M., 2005. *Some suggestions for water management in the Oporto region,* Oporto: FEUP.

NYSERDA, 2008. *Statewide Assessment of Energy Use by the Municipal Water and Wastewater Sector,* New York: New York State Energy Research and Development Authority.

NYSERDA, 2010. *Water & Wastewater Energy Management, Best Practices Handbook.* New York: New York State Energy Research and Development Authority.

Olsson, G., 2012. Water energy: conflicts and connections. *International Water Association, Water 21,* Volume October, pp. 12-16.

Omer, A. M., 2008. Energy, environment and sustainable development. *Renewable and Sustainable Energy Reviews,* Volume 12, p. 2265–2300.

OSSBERGER, 2016. *The original OSSBERGER® Crossflow Turbine,* Weißenburg: OSSBERGER.

Paish, O., 2002. Small hydro power: technology and current status. *Renewable and Sustainable Energy Reviews,* Volume 6(6), pp. 537-556.

Pakenas, L., 1995. *Energy Efficiency in Municipal Wastewater Treatment Plants. Technology Assessment.* New York: New York State Energy Research and Development Authority.

Pardalos, P. M., Romeijn, H. E. & Tuy, H., 2000. Recent developments and trends in global optimization. *Numerical Analysis, Vol. IV: Optimization and Nonlinear Equations,* Volume 124(1), pp. 209-228.

Pérez-Sánchez, M. et al., 2016. Modeling Irrigation Networks for the Quantification of Potential Energy Recovering: A Case Study. *Water,* Volume 8(6), p. 234.

PLUREL, 2011. *Peri-urban land use relationships,* Copenhagen: PLUREL project – Strategies and sustainability assessment tools for urban-rural linkages.

PolyU, 2012. *Novel inline hydropower system for power generation from water pipelines.* [Online] Available at: http://phys.org/news/2012-12-inline-hydropower-powerpipelines.html [Accessed 24 May 2016].

Portela, M. M., 2000. Chapter 10 - Economic analysis. In: *Guidelines for the design of small hydropower plants.* Belfast, North Ireland: CEHIDRO/WREAN/DED, pp. 167-190.

Quintela, A. C., 1981. *Hydraulics - in Portuguese.* Lisbon: Fundanção Calouste Gulbenkian.

Ramos, H., 2000. *Guidelines for design of small hydropower plants.* Belfast: CEHIDRO, WREAN (Western Regional Energy Agency & Network) and DED (Department of Economic Development).

Ramos, H. & Almeida, B., 2002. Dynamic orifice model on waterhammer analysis of high or medium heads of small hydropower schemes. *Journal of Hydraulic Research,* Volume 39(4), pp. 429-436.

Ramos, H. B. A., 2000. Pumps yielding power. *Dam Engineering, Water Power & Dam Construction,* Volume 10(4), pp. 197-217.

Ramos, H. & Borga, A., 1999. Pumps as turbines: an unconventional solution to energy production. *Urban Water,* Volume 1, pp. 261-263.

Ramos, H. M., Borga, A. & Simão, M., 2009a. New design for low-power energy production in water pipe systems. *Water Science and Engineering,* Volume 2(4), pp. 69-84.

Ramos, H. M., Borga, A. & Simão, M., 2009b. *Cost-effective energy production in water pipe systems: theoretical analysis for new design solutions.* British Columbia, 33rd IAHR Congress.

Ramos, H. M., Kenov, K. N. & Pillet, B., 2012. Stormwater Storage Pond Configuration for Hydropower Solutions: Adaptation and Optimization. *Journal of Sustainable Development,* Volume 5(8), pp. 27-42.

Ramos, H. M., Kenov, K. & Vieira, F., 2011a. Environmentally friendly hybrid solutions to improve the energy and hydraulic efficiency in water supply systems. *Energy for Sustainable Development,* Volume 15(4), pp. 436-442.

Ramos, H. M., Mello, M. & De, P., 2010a. Clean power in water supply systems as a sustainable solution: from planning to practical implementation. *Water science and technology: water supply,* Volume 79(10), pp. 24-26.

Ramos, H. M., Theyssier, C., Samora, I. & Schleiss, A. J., 2013a. Energy recovery in SUDS towards smart water grids: a case study. *Energy Policy,* Volume 62, pp. 463-472.

Ramos, H. M., Vieira, F. & Covas, D. I. C., 2010b. Energy efficiency in a water supply system: Energy consumption and CO2 emission. *Water Science and Engineering,* Volume 3(3), pp. 331-340.

Ramos, H. et al., 2014. Micro-hydro generation in the algarve multi-municipal water supply system. In: *Intervention concepts for energy saving, recovery and generation from the urban water system.* Lisbon: EU, pp. 182-2009.

Ramos, H., Simão, M. & Borga, A., 2013b. Experiments and CFD Analyses for a New Reaction Microhydro Propeller with Five Blades. *Journal of Energy Engineering,* Volume 139, pp. 109-117.

Ramos, H., Simão, M. & Kenov, K., 2011b. Low-Head Energy Conversion: A Conceptual Design and Laboratory Investigation of a Microtubular Hydro Propeller. *International Scholarly Network of Mechanical Engineering.*

Ramos, J. & Ramos, H., 2009. Sustainable application of renewable sources in water pumping systems: Optimized energy system configuration. *Energy Policy,* Volume 37(2), pp. 633-643.

Romero, S. R., Santos, A. C. & C., G. M. A., 2012. EU plans for renewable energy. An application to the Spanish case. *Renewable Energy,* Volume 43, pp. 322-330.

Rossman, L. A., 2000. *Rossman LA (2000) EPANET 2 Users Manual.* Cincinnati, United States Environmental Protection Agency: National Risk Management Research Laboratory.

Rutenbar, R. A., 1989. Simulated Annealing Algorithms: An Overview.. *Circuits and Devices Magazine,* Volume 5(1), pp. 19-26.

Saket, 2008. *Design, development and reliability evaluation of micro hydro power generation system based on municipal waste water.* Vancouver, Electrical power and energy conference, IEEE Canada.

Samora, I., Franca, M. J., Schleiss, A. J. & M., R. H., 2015. *Optimal location of micro-turbines in a water supply network.* The Hague, 36th IAHR World Congress.

Samora, I., Franca, M. J., Schleiss, A. J. & M., R. H., 2016. Simulated annealing in optimization of energy production in a water supply network. *Water Resources Management,* Volume 30(4), pp. 1533-1547.

Samora, I. et al., 2016. *Energy production with a tubular propeller turbine.* Grenoble, 28th IAHR symposium on Hydraulic Machinery and Systems.

Samora, I. et al., 2016. Experimental characterization of a five blade tubular propeller turbine for pipe inline installation. *Renewable Energy,* Volume 95, pp. 356-366.

Samora, I. et al., 2016. Energy recovery with micro-hydropower plants in the water supply networks: the case study of the city of Fribourg. *Water,* Volume 8(8), p. 344.

Samora, I. et al., 2016. *Feasibility assessment of micro-hydropower for energy recovery in the water supply network of the city of Fribourg.* Liège, 4th IAHR Europe Congress.

Samora, I. et al., 2016. Opportunity and economic feasibility of inline micro-hydropower units in water supply networks. *Journal of Water Resources Planning and Management.*

Samora, I., Ramos, H. M., Covas, D. & Schleiss, A. J., 2013. *Micro-generation in the multi-municipal water supply system of Algarve. Beliche hydropower station (in Portuguese).* Buenos Aires, SEREA - XII Simposio Iberoamericano sobre planificación de sistemas de abastecimiento y denaje.

Samora, I., Ramos, H. M. & Schleiss, A. J., 2014. *Energy recovery for sustainable Urban drainage systems (SUDS).* Oporto, 3rd IAHR Europe Congress: Water–Engineering and Research.

Santos, R., 2011. *Urban flooding and construction measures for its mitigation – in Portuguese.* Lisbon: M.Sc. Thesis in Civil Engineering, IST.

Schleicher, W. et al., 2014. Characteristics of a micro-hydro turbine. *Journal of Renewable and Sustainable Energy,* Volume 6(1).

Senior, J., O., W. & G., M., 2008. *The Rotary Hydraulic Pressure Machine for very low head hydropower sites,* University of Southampton: HYLOW Project.

SFC, 1996. *Ordonnance sur l'énergie (Energy law).* Bern: Swiss Federal Council.

SFC, 1998. *Directive for energy – in French,* Bern: Swiss Federal Council.

SFC, 2014. *Revision of the energy law.* Bern: Swiss Federal Council.

SFOE, 2013. *Global statistics of energy in Switzerland – in French,* Bern: Swiss Federal Office of Energy.

SFOE, 2015. *Directive for feed-in-tariff of injected current – in French. Art. 7a LEne. Version 1.8 of the 1st of April,* Bern: Swiss Federal Office of Energy.

Shrestha, E., Ahmadn, S., Johnson, W. & Batista, J. R., 2012. The carbon footprint of water management policy options. *Energy Policy,* Volume 42, pp. 201-212.

Simão, M., 2009. *Hydrodynamics and performance of low power turbines: conception, modeling and essays. – in Portuguese.,* Lisbon: MSc Thesis. Instituto Superior Técnico.

Simão, M. & Ramos, H., 2010. Hydrodynamic and performance of low power turbines: conception, modelling and experimental tests. *International Journal of Energy and Environment,* Volume 1(3), pp. 431-444..

Simpson, A. & Marchi, A., 2013. Evaluating the approximation of the affinity laws and improving the efficiency estimate for variable speed pumps. *Journal of Hydraulic Engineering,* Volume 139(12), pp. 1314-1317.

Sing, P. & Nestmann, F., 2009. Experimental optimization of a free vortex propeller runner for micro hydro application. *Experimental Therlam and Fluid Science,* Volume 33, pp. 99-1002.

Sitzenfrei, R. & Leon, J. v., 2014. Long-time simulation of water distribution systems for the design of small hydro power systems. *Renewable Energy,* Volume 72, pp. 182-187.

Sousa, J., Muranho, J., Sá Marques, A. & Gomes, R., 2015. Optimal Management of Water Distribution Networks with Simulated Annealing: The C-Town Problem. *Journal of Water Resources Planning and Management,* Volume 124.

Su, P. & Karney, B., 2015. Micro hydroelectric energy recovery in municipal water systems: A case study for Vancouver. *Urban Water Journal,* Volume 12(8), pp. 678-690.

Suwa, A., 2009. *How Things Work: Micro Hydroelectricity in Japan.* [Online] Available at: http://ourworld.unu.edu/en/rice-water-power-micro-hydroelectricity-in-japan [Accessed 20 June 2016].

SVGW, 2013. *W4 – Directive for Water Supply (in French).* Zurich: Swiss Gas and Water Industry Association.

Taulan, J. P., 1983. *Pressure Surges in Hydroelectric Installations: Peculiar Effects of Low Specific Speed Turbine Characteristics.* Bath, BHR Group.

Thode, H. & Azbill, D., 1984. Typical applications of induction generators and control system considerations. *IEEE Transactions on Industry Applications,* Volume A-20(6), pp. 1418-1423.

Tingsanchali, T., 2011. Urban flood disaster management. *Procedia Engineering,* Volume 32, pp. 25-37.

Ulanicki, B., Bounds, P. L. M., Rance, J. P. & Reynolds, L., 2000. Open and closed loop pressure control for leakage reduction. *Urban water,* Volume 2, pp. 105-114.

Vairavamoorthy, K. & Lumbers, J., 1998. Leakage reduction in water distribution systems: Optimal valve control. *Journal of Hydraulic Engineering,* Volume 124(11), p. 1146–1154.

Valadas, M., 2002. *An unconventional solution in the renewable energy context for excess energy recover in irrigation systems – in Portuguese,* Lisbon: M.Sc dissertation. Instituto Superior Técnico.

Valadas, M. & Ramos, H., 2003. Use of pumps as turbines for energy recover in irrigation systems – in Portuguese. *APRH, Revista Recursos Hídricos,* Volume 24(3), pp. 63-76.

Varanelli, J. & Cohoon, J., 1999. A fast method for generalized starting temperature determination in homogeneous two-stage simulated annealing systems. *Computers & Operations Research,* Volume 26, pp. 481-503.

Viana, A., 2012. *Pumps as turbines – in Portuguese.* Brazil: Acta editora.

Vicente, D. J., Garrote, L., Sánchez, R. & Santillán, D., 2016. Pressure Management in Water Distribution Systems: Current Status, Proposals, and Future Trends. *Journal of Water Resources Planning and Management,* Volume 142(2).

Vieira, F. & Ramos, H. M., 2008. Hybrid solution and pump-storage optimization in water supply system efficiency: A case study. *Energy Policy,* Volume 36(11), pp. 4142-4148.

Vilanova, M. R. N. & Balestieri, J. A. P., 2014. Energy and hydraulic efficiency in conventional water supply systems. *Renewable and Sustainable Energy Reviews,* Volume 30, pp. 701-714.

Walid, B., 2004. Computing the initial temperature of simulated annealing. *Computational Optimization and Applications,* Volume 29, pp. 369-385.

Walseth, E. C., 2009. *Investigation of the Flow through the Runner of a Cross-Flow Turbine.* Trondheim: NTNU.

Wang, L. et al., 2008. *Economic Analysis of Installing Micro Hydro Power Plants in Chia-Nan Irrigation Association of Taiwan Using Water of Irrigation Canals.* Pittsburgh, IEE.

Weijermars, R. et al., 2012. Review of models and actors in energy mix optimization – can leader visions and decisions align with optimum model strategies for our future energy systems?. *Energy Strategy Reviews,* Volume 1(1), pp. 5-18.

Wiemann, P., Müller, G. & Senior, J., 2008. *Risk management and resolution strategies for established and novel technologies in the low head small hydropower market,* Karlsruhe: HYLOW Project, European Commission.

Williams, A., 1996. *Pumps as turbines for low cost micro hydro power.* Denver, World Renewable Energy Congress, pp. 1227-1234.

Williams, A., Smith, N. P. A., Bird, C. & Howard, M., 1998. Pumps as turbines and the inductions motors as generators for energy recovery in water supply systems. *Water and Environmental Journal,* Volume 12(3), pp. 175-178.

Wüstenhagen, R. & Menichetti, E., 2012. Strategic choices for renewable energy investment: Conceptual framework and opportunities for further research.. *Energy Policy,* Volume 40, p. 1–10.

Xu, Q. et al., 2014. Water saving and energy reduction through pressure management in urban water distribution networks. *Water Resources Management,* Volume 28, p. 3715–3726.

Yao, X., 1993. *Comparison of different neighborhood sizes in simulated annealing.* Melbourne, Fourth Australian Conference on Neural Networks (A CNN'9 3), Sydney University Electrical Engineering.

Yazdani, A. & Jeffrey, P., 2011. Complex network analysis of water distribution systems. *Chaos,* Volume 21, pp. 1-10.

Youssef, H., Sait, S. & Adiche, H., 2001. Evolutionary algorithms, simulated annealing and tabu search: a comparative study. *Engineering Applications of Artificial Intelligence,* Volume 14, pp. 167-181.

Zakkour, P. et al., 2002. Developing a sustainable energy strategy for a water utility. Part II: a review of potential technologies and approaches. *Journal of Environmental Management,* Volume 66(2), pp. 115-125.

Zeiner-Gundersen, D. H., 2015. A novel flexible foil vertical axis turbine for river, ocean, and tidal applications. *Applied Energy,* Volume 151, pp. 60-66.

Appendices

A. Data of the experimental campaign on the 5BTP

Table.A 1 – Hydraulic performance measurements.

Q (m^3/h)	H (bar)	Ht (bar)	M1 (bar)	M2 (bar)	M3 (bar)	T (°C)	Tmec (Nm)	N (rpm)
5.808215	0.00897	0.011121	1.808672	1.81162	1.81126	20.21381	0.064592	48.1
6.538288	0.013083	0.014807	1.819145	1.844444	1.841757	20.23285	0.088216	50.6
5.131912	0.007225	0.010037	1.826756	1.832693	1.842988	20.04928	0.051975	48.8
7.476216	0.016095	0.016511	1.853497	1.857229	1.851954	20.22297	0.102827	51
8.40894	0.021147	0.020336	1.84408	1.851378	1.850997	20.15191	0.131231	50.8
9.68347	0.028351	0.025943	1.87216	1.86118	1.872081	20.12548	0.172972	50.1
10.98263	0.035543	0.031612	1.907388	1.911603	1.881568	20.27413	0.213305	50.4
12.34528	0.048154	0.03989	1.942685	1.922397	1.887793	20.21385	0.278315	51.3
13.95248	0.062359	0.04985	1.953491	1.956469	1.911992	20.15613	0.356261	52
15.67082	0.07835	0.061794	1.985146	1.969552	1.915106	20.19191	0.446099	52.2
17.71852	0.101671	0.078492	2.020884	1.991152	1.931443	20.10789	0.570148	49.2
19.72221	0.127863	0.097037	2.037488	2.02826	1.95714	20.16496	0.712645	52
22.10405	0.157706	0.119448	2.111056	2.08437	1.968136	20.16918	0.87908	53.1
24.42834	0.197348	0.146699	2.148442	2.137056	2.009704	20.15252	1.097092	51.5
26.66152	0.23552	0.17338	2.188243	2.181524	2.03333	20.07396	1.300419	52.4
28.46878	0.26909	0.197928	2.239136	2.235604	2.060353	20.05571	1.49025	53.3
30.44363	0.306327	0.224094	2.306468	2.302567	2.092853	20.01277	1.693147	52
32.44844	0.346835	0.25359	2.381243	2.359157	2.102757	19.97103	1.918162	52.4
34.4629	0.393341	0.286201	2.433123	2.407231	2.141783	19.91117	2.172729	53.1
36.67598	0.44313	0.321324	2.495628	2.469505	2.168682	19.84963	2.445717	51.7
39.45669	0.512484	0.37063	2.608472	2.550044	2.187395	19.81212	2.822724	53.8
42.01089	0.581957	0.420886	2.660615	2.643803	2.23614	19.69557	3.203571	50.4
44.31996	0.646391	0.466293	2.739625	2.717782	2.265683	19.55585	3.551596	47.1
46.61333	0.713837	0.514037	2.82119	2.79092	2.294763	19.4754	3.915991	47.8
9.326416	0.017963	0.019396	1.752671	1.749451	1.750515	19.01031	0.103335	249
9.902941	0.021774	0.021148	1.78793	1.787205	1.780593	19.0202	0.119321	247.4
10.41156	0.024893	0.023601	1.800509	1.802478	1.788737	19.05268	0.133348	249.9
11.26286	0.029773	0.027951	1.820202	1.810465	1.792263	19.0081	0.161746	247.2
11.92415	0.035458	0.031684	1.840809	1.797443	1.795773	19.01012	0.193116	247.2
12.71831	0.041249	0.035861	1.840772	1.828757	1.816071	19.02664	0.223967	248.1
13.61977	0.047988	0.041486	1.881778	1.863717	1.826824	19.05501	0.257095	251.1
15.00438	0.059948	0.050011	1.903456	1.888865	1.859408	18.94961	0.318348	250.4
16.31949	0.072093	0.058971	1.897702	1.952273	1.88496	18.97852	0.3856	251.5
18.15758	0.092698	0.074453	1.971791	1.969301	1.906223	18.98359	0.497789	254.5
19.79128	0.109973	0.086904	2.007608	1.996009	1.924266	18.91209	0.589451	250.6
21.45397	0.131735	0.102683	2.036334	2.032985	1.939178	18.88871	0.705562	252.2
23.54705	0.16092	0.122351	2.086831	2.098378	1.967308	18.92235	0.8657	250.2
25.13735	0.185775	0.141626	2.110438	2.103277	1.985422	18.84465	1.007305	252
27.05417	0.215728	0.162725	2.175014	2.146504	2.011381	18.84781	1.169622	248.6
28.8799	0.249642	0.187122	2.220268	2.232734	2.047267	18.70714	1.353998	253.6
31.16961	0.291862	0.216274	2.243546	2.211815	1.998468	18.6995	1.579349	249.9
33.29163	0.33445	0.246372	2.280582	2.271634	2.031504	18.62329	1.806947	252.5
35.4723	0.382743	0.280351	2.346276	2.33191	2.071886	18.60297	2.066003	249.5
37.21985	0.420984	0.308564	2.400232	2.35591	2.076794	18.50437	2.277047	249.3
38.94264	0.46207	0.337361	2.460007	2.444538	2.1149	18.44905	2.498979	251.8
41.27656	0.521947	0.380001	2.539226	2.535635	2.153749	18.33573	2.816546	254.1

Q (m^3/h)	H (bar)	Ht (bar)	M1 (bar)	M2 (bar)	M3 (bar)	T (°C)	Tmec (Nm)	N (rpm)
43.12164	0.576851	0.41979	2.604892	2.58889	2.183734	18.13272	3.115944	249.5
45.45467	0.637001	0.463176	2.71592	2.670552	2.224527	17.84147	3.449911	249
47.73482	0.706949	0.511007	2.811666	2.789561	2.292801	17.25961	3.817429	248.1
13.20365	0.029199	0.029566	1.95881	1.956701	1.937581	21.53266	0.126688	501.7
13.8881	0.033984	0.033302	1.985585	1.977782	1.955324	21.53371	0.150678	499.9
14.634	0.040257	0.038123	2.005872	1.993387	1.970341	21.55685	0.180077	501.5
15.2027	0.045438	0.041907	1.981027	1.973864	1.951155	21.38868	0.202169	500.8
16.25061	0.05351	0.047719	2.014977	2.013508	1.974906	21.38908	0.24978	498.5
17.06574	0.061018	0.053126	1.859234	1.863957	1.817406	21.38725	0.283668	498.7
18.38298	0.074369	0.062939	1.911968	1.905613	1.859734	21.26582	0.356612	500.6
20.13264	0.092307	0.075721	1.975733	1.970543	1.908213	21.28827	0.453011	499.4
21.8353	0.112952	0.090568	2.02751	2.02945	1.942859	21.25957	0.560641	501.7
23.77749	0.138878	0.109978	2.075309	2.063128	1.970779	21.18739	0.689329	499.2
25.44749	0.165363	0.129995	2.107319	2.100929	1.983104	21.18382	0.830415	499.6
27.42353	0.195427	0.152767	2.14474	2.143427	2.004143	21.18053	0.969878	500.8
29.31215	0.226443	0.175925	2.207161	2.196811	2.025954	21.15797	1.127042	500.6
31.1476	0.26156	0.20224	2.191982	2.18261	1.990055	21.10948	1.321086	502.4
33.22888	0.298443	0.230221	2.227901	2.22984	2.007234	20.97781	1.509153	499.4
35.38738	0.344461	0.264431	2.29511	2.280603	2.027529	21.03353	1.759499	498.5
37.375	0.391741	0.299671	2.340142	2.323493	2.044016	20.94258	2.000602	500.8
39.67173	0.442746	0.337445	2.421748	2.39263	2.074669	20.81727	2.298388	501
42.28563	0.508021	0.38525	2.484147	2.480459	2.105847	20.73295	2.631988	499.2
44.96244	0.580051	0.437809	2.572847	2.552468	2.131651	20.60743	3.006063	501.7
47.7827	0.65883	0.494941	2.686498	2.651753	2.173807	20.46919	3.445622	499.2
13.84025	0.018171	0.021372	1.891589	1.899626	1.886814	19.89455	0.052662	750.3
14.27498	0.021657	0.024347	1.914311	1.90878	1.893335	19.91412	0.067815	749.8
15.00311	0.026585	0.028626	1.911588	1.908122	1.8996	19.88723	0.0891	750.3
15.94648	0.03403	0.034296	1.945554	1.933072	1.915608	19.87318	0.122251	750.7
16.68843	0.040747	0.040315	1.89266	1.870337	1.848826	19.9949	0.152821	749.8
17.51606	0.046244	0.044832	1.902959	1.890942	1.853337	19.97443	0.180217	749.6
18.05302	0.050779	0.048441	1.979866	1.978693	1.925313	19.76303	0.202585	751.2
18.64489	0.057518	0.053403	1.994905	1.973509	1.937322	19.72881	0.232234	750.7
19.2518	0.06183	0.057073	2.010827	2.006472	1.967062	19.68836	0.25338	749.1
19.7858	0.068229	0.061908	2.061798	2.049838	1.987456	19.68331	0.284768	750.3
20.79021	0.078394	0.069762	2.070985	2.064208	2.010994	19.58656	0.337915	749.4
21.68966	0.087881	0.076801	2.050046	2.039768	1.974885	19.51494	0.389935	749.4
22.43477	0.097667	0.084437	2.072319	2.055097	1.990029	19.49681	0.43827	750.7
23.37546	0.107874	0.09199	2.092716	2.072354	1.994648	19.41606	0.492735	749.1
24.2473	0.118729	0.099785	2.129852	2.12629	2.032169	19.43714	0.542369	749.1
25.80317	0.140214	0.115427	1.978651	1.97394	1.867543	19.23198	0.647833	749.8
27.31123	0.162875	0.131526	2.020488	1.995764	1.882434	19.15531	0.7627	750.5
28.60514	0.183573	0.146409	2.067107	2.046659	1.906854	19.12528	0.868104	750.7
29.96081	0.205663	0.162783	2.078812	2.07118	1.926476	19.06753	0.97798	750.7
31.44564	0.230197	0.180384	2.118987	2.112963	1.940311	19.03665	1.108713	749.8
32.80814	0.25734	0.199759	2.160432	2.138809	1.956578	18.99358	1.238348	750.7
34.12285	0.284251	0.219651	2.201649	2.171544	1.969365	18.92744	1.368566	749.6
35.80089	0.319055	0.246007	2.233764	2.217053	1.990359	18.86838	1.555123	749.4
37.62534	0.358563	0.275911	2.283963	2.276527	2.014765	18.71963	1.745697	749.6
39.75175	0.408152	0.31282	2.373876	2.351713	2.051898	18.55808	1.993395	749.6
42.33295	0.472209	0.360784	2.465141	2.435659	2.085421	18.54428	2.331948	751.4
45.08903	0.543151	0.413779	2.552704	2.512947	2.116599	18.30759	2.686963	750
47.76066	0.620689	0.472822	2.644441	2.612047	2.150987	18.16486	3.08078	750.5
21.98841	0.04228	0.042738	1.893025	1.89546	1.86063	22.45359	0.08399	1249.9
22.89432	0.050377	0.04996	1.908881	1.905558	1.867473	22.46037	0.116846	1249.7
23.52178	0.058994	0.057493	1.933094	1.916876	1.871017	22.40549	0.148873	1249.9
24.26036	0.067084	0.064002	1.925616	1.916145	1.875206	22.43039	0.181434	1250.2
25.09106	0.076977	0.072354	1.960938	1.952709	1.891843	22.43395	0.227054	1249.7
25.85463	0.086263	0.080128	1.976213	1.962852	1.901455	22.33567	0.268877	1250.2
26.41546	0.093177	0.086146	2.010998	2.001749	1.918324	22.37694	0.304793	1250.6
27.30945	0.103764	0.095264	2.017382	2.013209	1.926727	22.38198	0.356822	1249.9

Q (m^3/h)	H (bar)	Ht (bar)	M1 (bar)	M2 (bar)	M3 (bar)	T (°C)	Tmec (Nm)	N (rpm)
28.02832	0.114963	0.104067	2.036425	2.019699	1.930297	22.32193	0.409261	1250.4
28.90952	0.126559	0.113624	2.069128	2.058654	1.949725	22.32287	0.465039	1250.4
29.64706	0.1381	0.122705	2.018775	2.004828	1.890177	22.21134	0.520021	1249.9
30.7341	0.154276	0.13561	2.037705	2.020752	1.899117	22.158	0.598517	1249.7
31.80059	0.17035	0.148492	2.072563	2.051129	1.917452	22.14725	0.675601	1249.7
33.02485	0.189118	0.163078	2.09665	2.079803	1.931726	22.03211	0.766277	1250.6
33.93552	0.207097	0.177108	2.120676	2.091108	1.935393	21.9817	0.853898	1250.2
35.22362	0.226536	0.191901	2.096859	2.072211	1.8955	21.87113	0.946427	1250.8
36.45785	0.250453	0.210009	2.135175	2.107744	1.909989	21.77952	1.063419	1250.4
37.42037	0.272196	0.225903	2.14552	2.131218	1.92585	21.66833	1.166947	1249.7
39.18178	0.306056	0.251186	2.240829	2.210542	1.973456	21.32104	1.336836	1251.1
40.4649	0.334807	0.271512	2.271696	2.255889	1.999344	21.17601	1.478835	1249.2
42.21584	0.374365	0.300627	2.331916	2.298559	2.017169	21.05566	1.676125	1250.8
43.7602	0.411998	0.327047	2.369054	2.347501	2.038774	20.86543	1.863416	1249.9
45.60555	0.457572	0.360155	2.447473	2.425628	2.080052	20.59879	2.09293	1249.5
47.91027	0.517868	0.404231	2.513216	2.495976	2.107848	20.46826	2.401057	1250.2
26.32142	0.061483	0.059495	1.959657	1.938587	1.897386	20.03319	0.102708	1500.3
27.05131	0.070258	0.06703	1.977504	1.989541	1.91725	19.96987	0.140198	1500.3
27.60699	0.077762	0.073318	2.005872	1.999717	1.9166	19.98771	0.170305	1499.9
28.16636	0.083944	0.079227	2.017884	1.999603	1.928853	19.94136	0.201995	1500.3
29.08151	0.097938	0.090799	2.025912	2.033812	1.934234	19.93508	0.262445	1500.1
29.89651	0.110133	0.101341	2.057456	2.043635	1.9545	19.88844	0.318591	1499.9
30.97239	0.126143	0.114907	2.080359	2.04587	1.954004	19.83015	0.392002	1500.5
32.30481	0.144401	0.130091	2.115773	2.095706	1.978373	19.80712	0.481613	1499.9
33.49854	0.163437	0.146066	1.990592	1.964952	1.832167	19.54987	0.573024	1499.4
35.02772	0.189463	0.167186	2.014232	2.007761	1.851986	19.4859	0.696956	1499.6
36.73345	0.218712	0.190098	2.077896	2.044657	1.866619	19.41615	0.834775	1499.4
38.24533	0.246992	0.212793	2.106145	2.075314	1.877693	19.35966	0.970559	1499.6
39.99768	0.283318	0.241034	2.138832	2.101393	1.884525	19.26348	1.142269	1499.6
41.67724	0.319089	0.268353	2.173272	2.162409	1.909738	19.16312	1.322533	1500.3
43.86601	0.366676	0.304536	2.248705	2.217923	1.928289	19.0297	1.554415	1499.9
46.03048	0.419574	0.343818	2.31121	2.28204	1.953799	18.87184	1.817287	1500.3
48.15193	0.476432	0.384696	2.388121	2.354634	1.988588	18.58461	2.087276	1500.1
30.42306	0.077111	0.072898	1.998827	1.990405	1.922452	25.46279	0.124	1750.3
31.30607	0.090924	0.085239	2.001111	1.99214	1.921697	25.3511	0.169084	1750.3
32.18224	0.103692	0.09626	2.033993	2.027537	1.938767	25.32947	0.21781	1749.6
33.22442	0.118634	0.109253	2.055433	2.039764	1.946853	25.29984	0.286728	1749.1
34.5341	0.139389	0.126684	2.090601	2.079534	1.960558	25.29124	0.376359	1750.3
35.73351	0.161185	0.144646	2.15319	2.114191	1.975812	25.13437	0.47382	1750.5
37.24026	0.186641	0.166537	2.072062	2.06272	1.906184	25.06034	0.5908	1750.3
39.01797	0.218823	0.193395	2.110485	2.105736	1.921571	24.99767	0.746948	1750
40.84731	0.256258	0.223686	2.173167	2.149927	1.938532	24.80184	0.917702	1749.6
42.99417	0.29828	0.25717	2.227107	2.189403	1.953742	24.65194	1.118905	1750.3
44.77556	0.339072	0.28939	2.248161	2.229937	1.960866	24.56751	1.315864	1750
46.48728	0.378059	0.319796	2.314356	2.290599	1.988854	24.34344	1.508264	1749.1
48.034	0.412864	0.34673	2.365114	2.342832	2.010159	24.13404	1.673736	1749.1
34.48047	0.099238	0.092148	2.007735	1.999931	1.916827	23.63945	0.125947	2000.2
35.16465	0.10797	0.100318	2.023782	2.017324	1.922296	23.61449	0.169531	1999.7
35.81646	0.119099	0.1103	2.044785	2.032673	1.933666	23.5775	0.214703	1999.5
36.33702	0.128174	0.118171	2.047686	2.036378	1.933687	23.51674	0.253127	2000
37.13115	0.141827	0.13008	2.078779	2.054756	1.940374	23.44181	0.312023	1999.7
38.19315	0.159465	0.145164	2.099217	2.106742	1.953991	23.39956	0.389137	1999.5
39.30766	0.181238	0.163603	2.126862	2.104468	1.965421	23.24058	0.481736	2000.7
40.50745	0.202477	0.181609	2.169976	2.146339	1.978583	23.18088	0.575167	1999.3
42.00571	0.232357	0.206938	2.194086	2.172478	1.983049	23.08485	0.715342	2000.2
43.66351	0.26855	0.236809	2.277936	2.255768	2.022798	22.61367	0.881286	1999.3
45.66427	0.31205	0.273065	2.337288	2.312434	2.049164	22.44226	1.089593	1999.3
48.04802	0.365747	0.315913	2.219943	2.200916	1.896011	22.20802	1.344956	2000.4
46.33396	0.168897	0.153143	2.040151	1.980473	1.863912	21.86895	0.156432	2750.7
46.8456	0.17843	0.161907	2.049929	2.018697	1.87489	21.55145	0.194374	2749.8

Q (m^3/h)	H (bar)	Ht (bar)	M1 (bar)	M2 (bar)	M3 (bar)	T (°C)	Tmec (Nm)	N (rpm)
47.61869	0.192703	0.175352	2.079044	2.056281	1.890377	21.38912	0.248514	2748.9
48.36838	0.209069	0.18993	2.099308	2.072896	1.900376	21.26037	0.314129	2750.2
38.26097	0.118386	0.109153	2.013269	2.005793	1.911395	20.88131	0.122434	2249.2
38.91855	0.129225	0.118961	2.048468	2.025789	1.917297	20.80226	0.172398	2250.1
39.39115	0.139107	0.127919	2.047103	2.038514	1.925577	20.73554	0.212587	2249.7
40.10737	0.150474	0.138152	2.074742	2.056106	1.92946	20.70056	0.26882	2250.1
40.9919	0.16523	0.150685	2.104883	2.10204	1.951911	20.58384	0.328716	2248.8
41.72609	0.180684	0.16453	2.127484	2.093791	1.944957	20.46603	0.395474	2250.4
42.57327	0.195144	0.177277	1.969955	1.935393	1.777032	20.24204	0.459969	2249.5
43.96623	0.227267	0.203718	2.018758	1.988447	1.798009	20.12911	0.59742	2249.7
46.18696	0.273949	0.24439	2.060856	2.033155	1.805395	19.90088	0.809346	2249.5
48.28337	0.322296	0.284327	2.127187	2.100002	1.825827	19.53688	1.039003	2249.7
41.55297	0.128951	0.117847	1.940922	1.936485	1.813334	19.2425	0.082716	2499.8
42.18999	0.140648	0.128421	1.978075	1.948831	1.824908	19.10989	0.13997	2500.1
42.92421	0.155352	0.141861	2.00022	1.960549	1.830339	19.00946	0.193535	2500.5
44.32859	0.180952	0.16509	2.03119	1.99543	1.843869	18.82978	0.306355	2499.6
45.66882	0.210389	0.190341	2.037664	2.022084	1.844485	18.86448	0.434875	2500.3
47.04623	0.239799	0.216787	2.08955	2.065035	1.854801	18.74599	0.568246	2499.6
48.47917	0.270807	0.243296	2.112829	2.089448	1.85729	18.69223	0.697648	2499.6
17.35702	0.026137	0.028046	1.940674	1.938357	1.929429	17.60655	0.053411	999.8
17.74445	0.030073	0.031218	1.951917	1.953086	1.941718	17.58589	0.066169	1000.2
18.25567	0.033652	0.034146	1.982501	1.97036	1.949543	17.56134	0.083798	1000
19.21095	0.041825	0.040992	1.986396	2.008147	1.964	17.57141	0.120991	999.8
20.32954	0.052459	0.049728	2.034549	2.009015	1.976383	17.57625	0.166502	999.8
21.43763	0.062679	0.058676	1.953807	1.956329	1.911379	17.50479	0.215414	1000
22.63223	0.076273	0.069943	1.992201	1.990773	1.926778	17.48576	0.281195	1000
23.52788	0.08633	0.077895	2.008718	1.992819	1.934585	17.45122	0.331181	1000.2
24.64324	0.0978	0.087556	1.974693	1.95628	1.884056	18.16146	0.388351	999.5
25.75439	0.11525	0.100363	2.058931	2.018159	1.929544	17.39923	0.468699	1000.2
26.66502	0.1268	0.109718	2.000023	2.000415	1.900322	18.01208	0.525058	999.8
27.70175	0.13927	0.119319	2.101278	2.10158	1.982724	17.16628	0.593617	1000.2
29.40324	0.162323	0.13768	2.069567	2.034017	1.909479	18.01185	0.70529	1000.2
31.552	0.201177	0.165605	2.171513	2.159794	2.011828	17.10622	0.893012	999.3
35.83609	0.277643	0.220718	2.284448	2.258709	2.046552	17.05646	1.280458	999.8
39.87019	0.362947	0.282518	2.352479	2.331518	2.083269	17.01089	1.718856	1000.9
44.04111	0.466201	0.35554	2.49261	2.478341	2.122163	16.95441	2.219426	998.8
47.89033	0.578182	0.440034	2.60073	2.585343	2.159076	16.77612	2.778608	1000.9

Table.A 2 – Runaway speed conditions.

Q (m^3/h)	H (bar)	Ht (bar)	M1 (bar)	M2 (bar)	M3 (bar)	T (°C)	Tmec (Nm)	N (rpm)
3.532763	0.000844	0.005718	1.941856	1.942343	1.945169	21.11488	0	129
7.087146	0.003856	0.008417	1.944755	1.935798	1.948393	21.12354	0	386
10.82479	0.008559	0.012737	1.961145	1.972361	1.969065	21.15467	0	632
12.29173	0.011121	0.014888	1.982367	1.992905	1.982211	21.12048	0	725
13.60513	0.013431	0.016766	1.999375	1.993753	1.984492	21.13471	0	806
14.92497	0.016338	0.019533	1.993695	1.981179	1.981657	21.10387	0	899
16.28104	0.019551	0.021943	2.018332	2.012519	1.997635	21.13185	0	981
17.68064	0.022476	0.024592	2.022196	2.012964	2.000249	21.13306	0	1064
18.92385	0.026324	0.027774	2.046798	2.039623	2.012999	21.15487	0	1151
20.38139	0.029817	0.030938	2.055254	2.062291	2.028104	21.1656	0	1233
21.71021	0.033873	0.034396	2.056028	2.059226	2.031121	21.13124	0	1319
22.92357	0.037651	0.037801	2.058287	2.046258	2.029919	21.13834	0	1402
24.65931	0.04354	0.042476	2.093868	2.088343	2.054342	21.01206	0	1500
25.95913	0.047596	0.046467	1.968015	1.956034	1.915055	21.03377	0.004276	1582
27.18262	0.051571	0.050661	1.970385	1.970469	1.923889	21.05856	0	1664
28.55392	0.057807	0.055085	1.991702	1.972226	1.927973	20.82989	0.012331	1745
29.92856	0.062519	0.059702	1.990937	1.971795	1.93208	20.76144	0.025135	1826
31.24744	0.069087	0.064969	2.014209	2.000216	1.946983	20.70885	0.037069	1911
32.46552	0.07535	0.070467	2.015467	1.988788	1.942362	20.66239	0.043657	1995
33.88337	0.081408	0.07554	2.056424	2.017609	1.96948	20.52421	0.044781	2079
35.23482	0.087959	0.081101	2.051665	2.065852	1.988088	20.42587	0.03804	2158
37.11821	0.09727	0.089442	2.085153	2.065415	1.990054	20.30285	0.042444	2272
38.70479	0.105634	0.096744	2.087993	2.071392	1.992336	20.13564	0.042748	2369
39.96677	0.113385	0.10344	2.111657	2.104644	2.012789	20.00611	0.04331	2456
41.66152	0.121745	0.111055	2.145805	2.117378	2.025092	19.85595	0.043588	2549
43.04939	0.130496	0.118378	2.184716	2.149632	2.039909	19.69795	0.04365	2635
44.29153	0.139256	0.125628	2.027884	2.001296	1.893417	19.34799	0.042918	2723
45.61385	0.148226	0.133567	2.044897	2.017059	1.90214	19.23711	0.04334	2810
47.24079	0.157889	0.141932	2.071209	2.042681	1.916105	19.0565	0.045296	2900
48.56194	0.16699	0.149992	2.103834	2.06991	1.930973	18.86498	0.057126	2987

B. Simulations for neighborhood definition

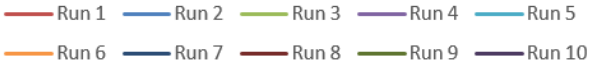

Figure.A 1 – Legend for figures of Appendix B.

First stage of neighborhood definition

Simulations results with one turbine for neighborhood function definition

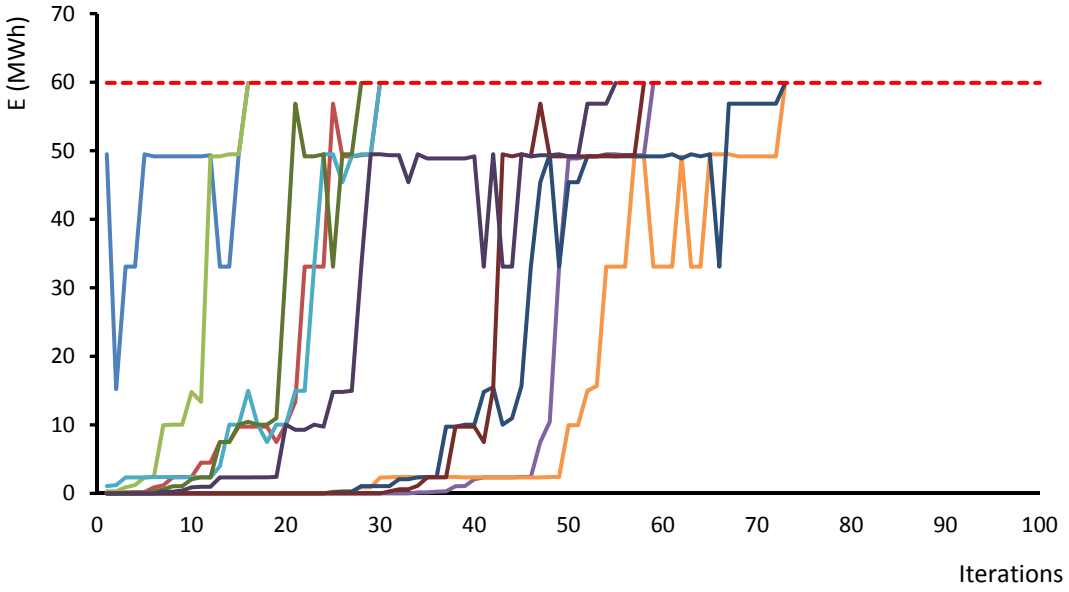

Figure.A 2 – Installation of one turbine, neighborhood number function n°1.

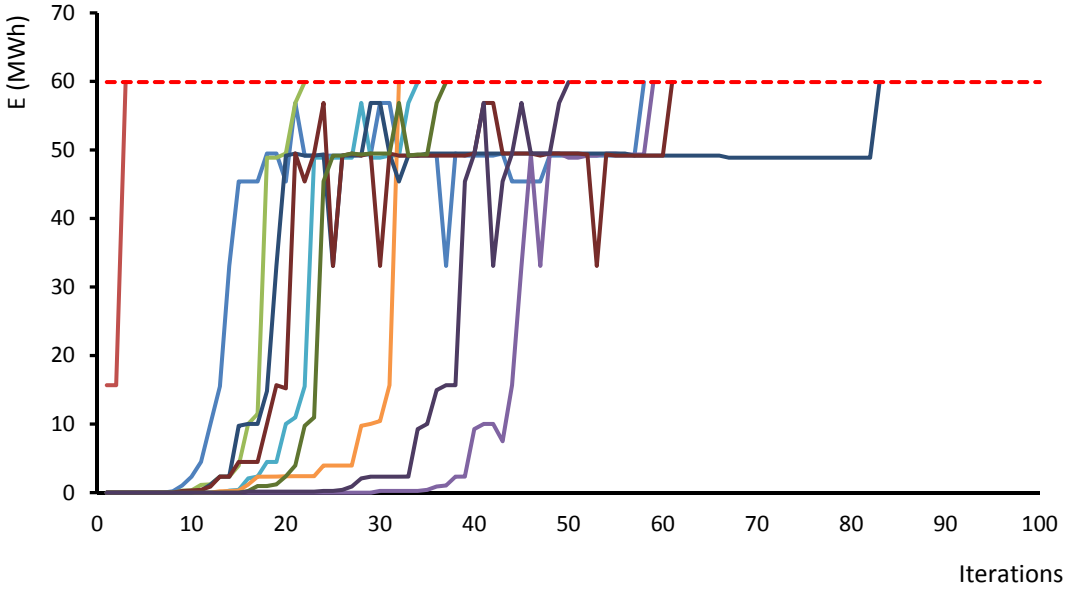

Figure.A 3 – Installation of one turbine, neighborhood number function n°2.

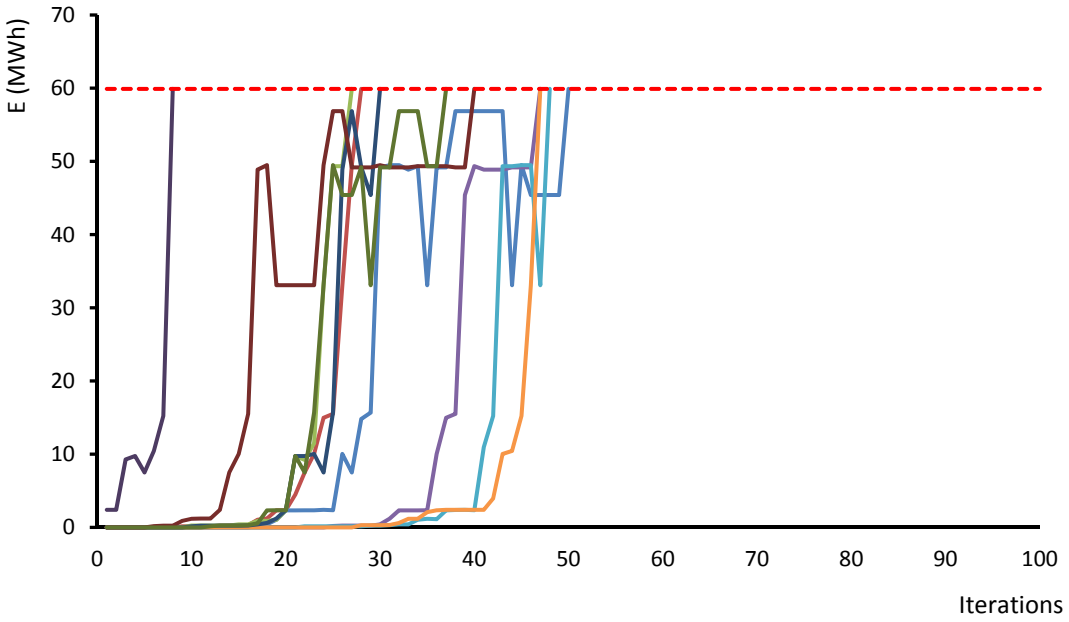

Figure.A 4 – Installation of one turbine, neighborhood number function n°3.

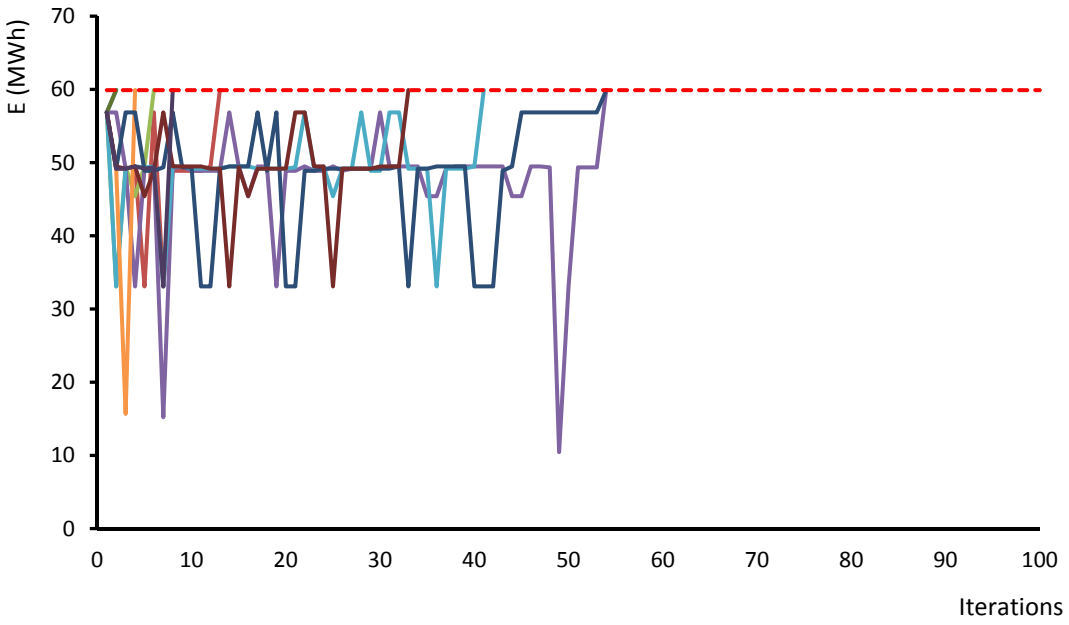

Figure.A 5 – Installation of one turbine, neighborhood number function n°4.

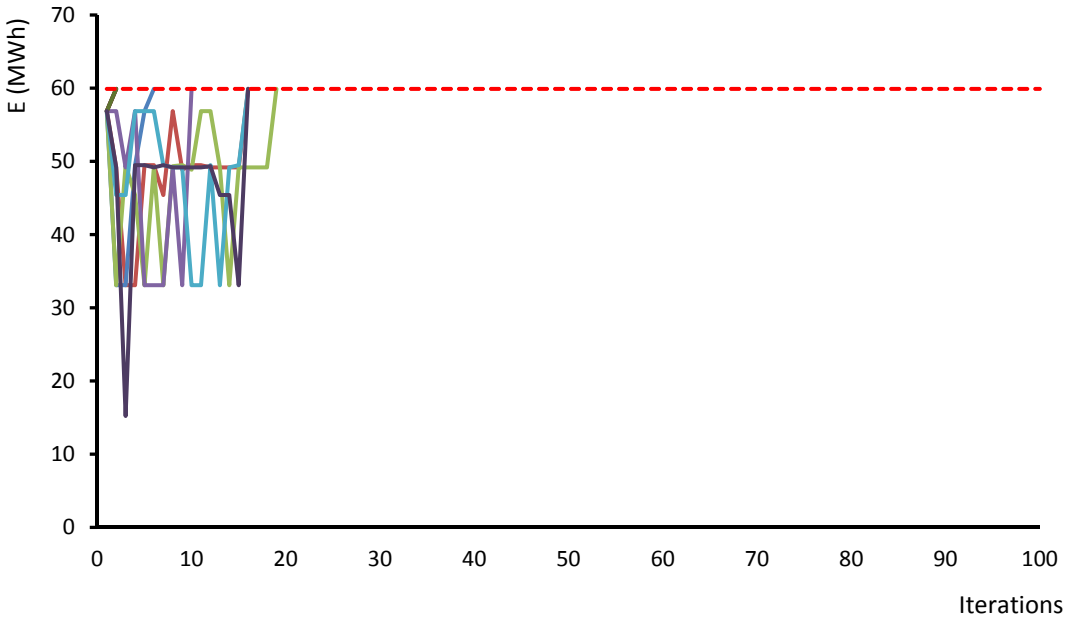

Figure.A 6 – Figure.A 7 – Installation of one turbine, neighborhood number function n°5.

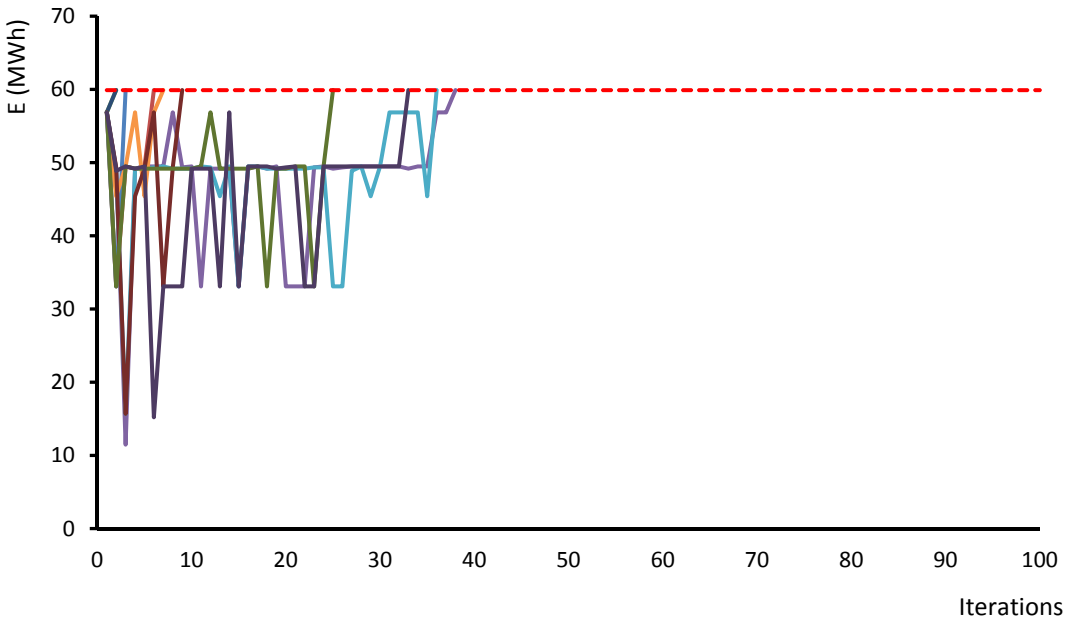

Figure.A 8 – Figure.A 9 – Figure.A 10 – Installation of one turbine, neighborhood number function n°6.

Simulations results with two turbines for neighborhood function definition

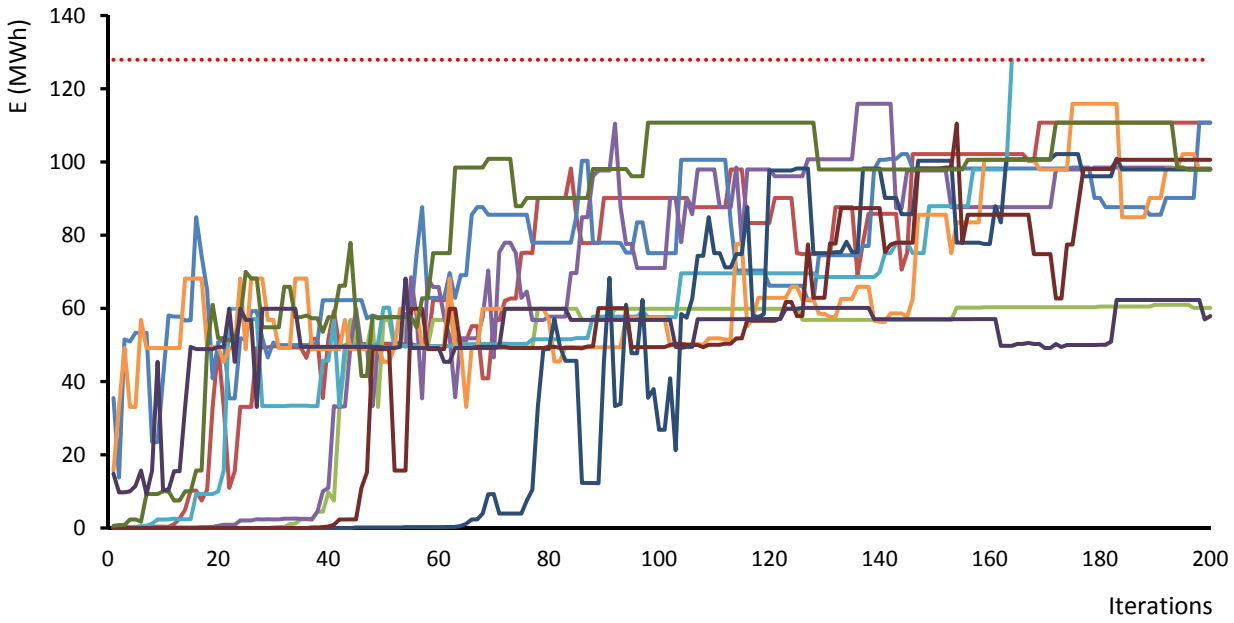

Figure.A 11 – Installation of two turbines, neighborhood number function n°1.

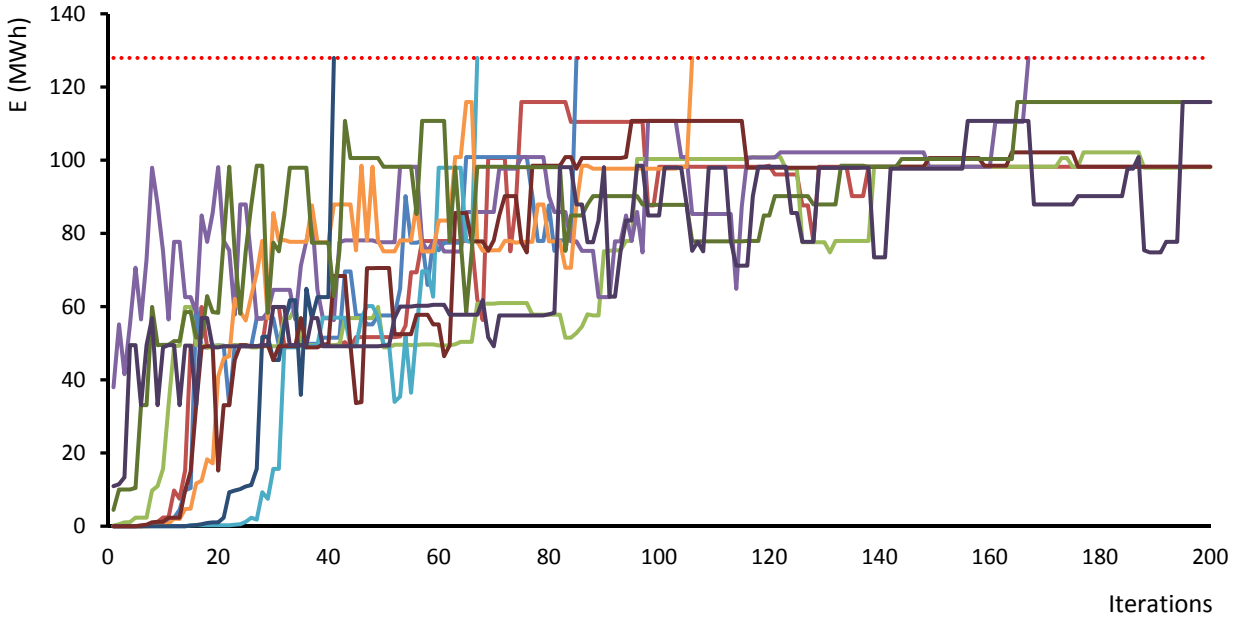

Figure.A 12 – Installation of two turbines, neighborhood number function n°2.

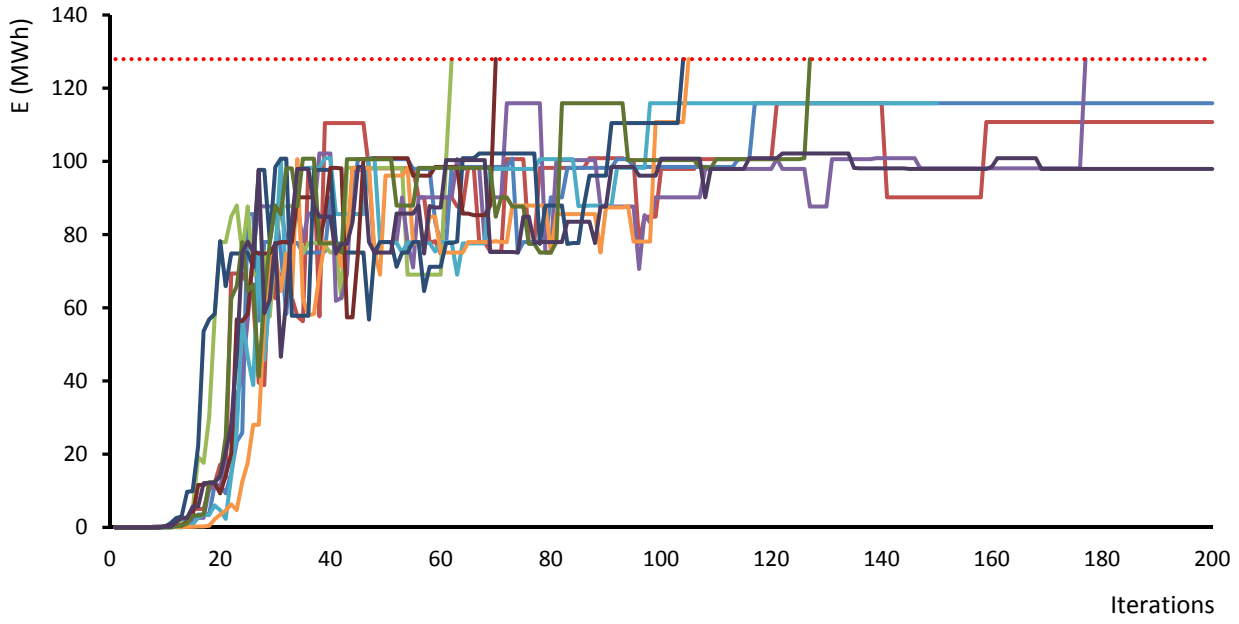

Figure.A 13 – Installation of two turbines, neighborhood number function n°3.

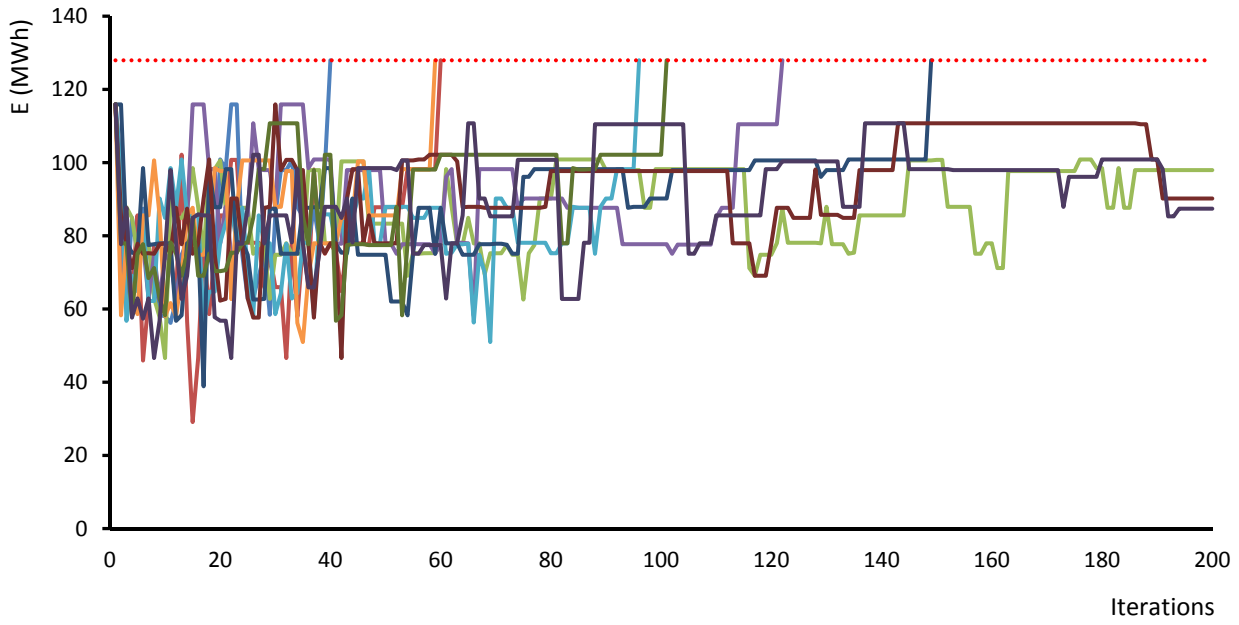

Figure.A 14 – Installation of two turbines, neighborhood number function n°4.

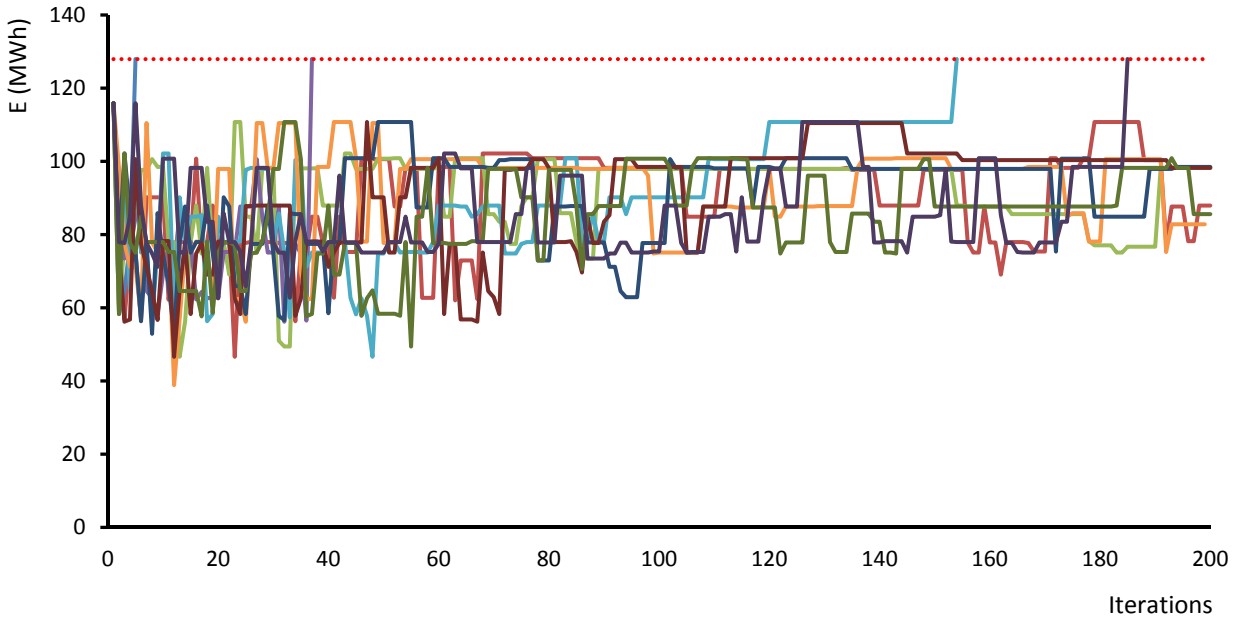

Figure.A 15 – Installation of two turbines, neighborhood number function n°5.

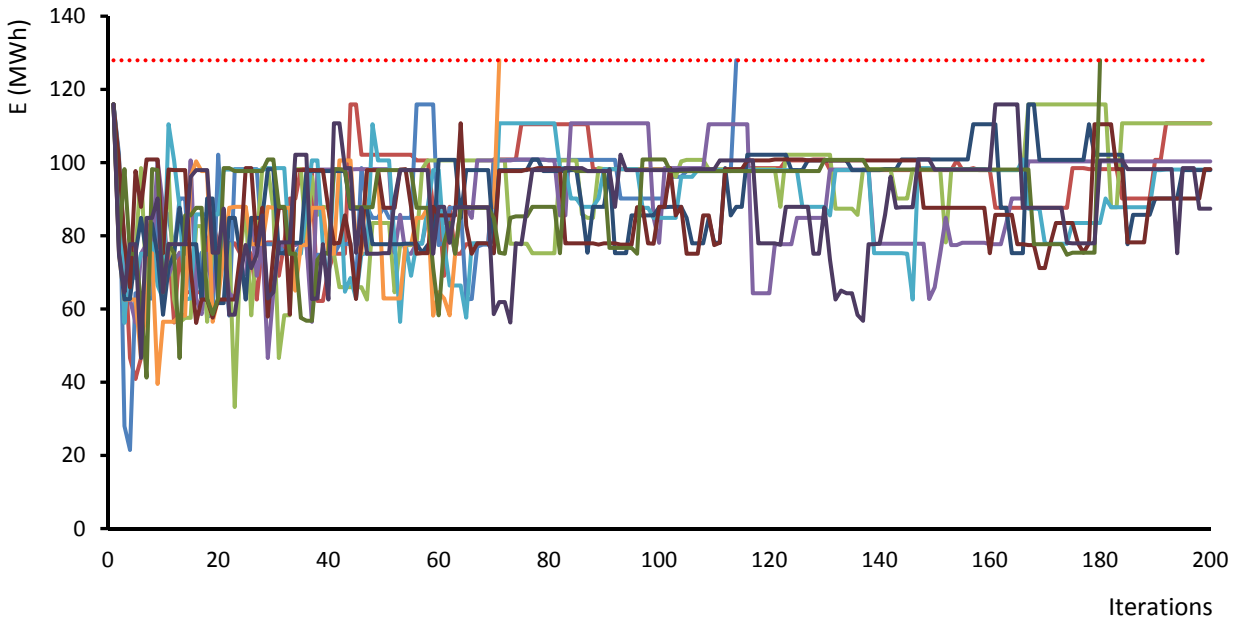

Figure.A 16 – Installation of two turbines, neighborhood number function n°6.

Simulations results with one and two turbines with neighborhood function n°4

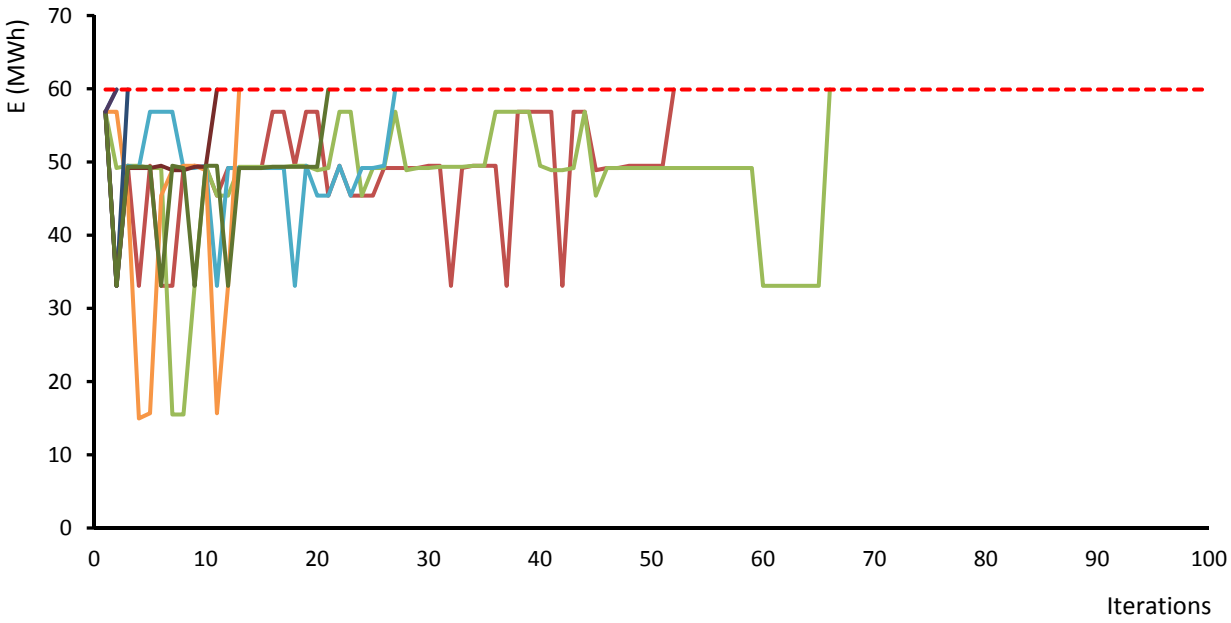

Figure.A 17 – Installation of one turbine, neighborhood number function n°4, case type 2.

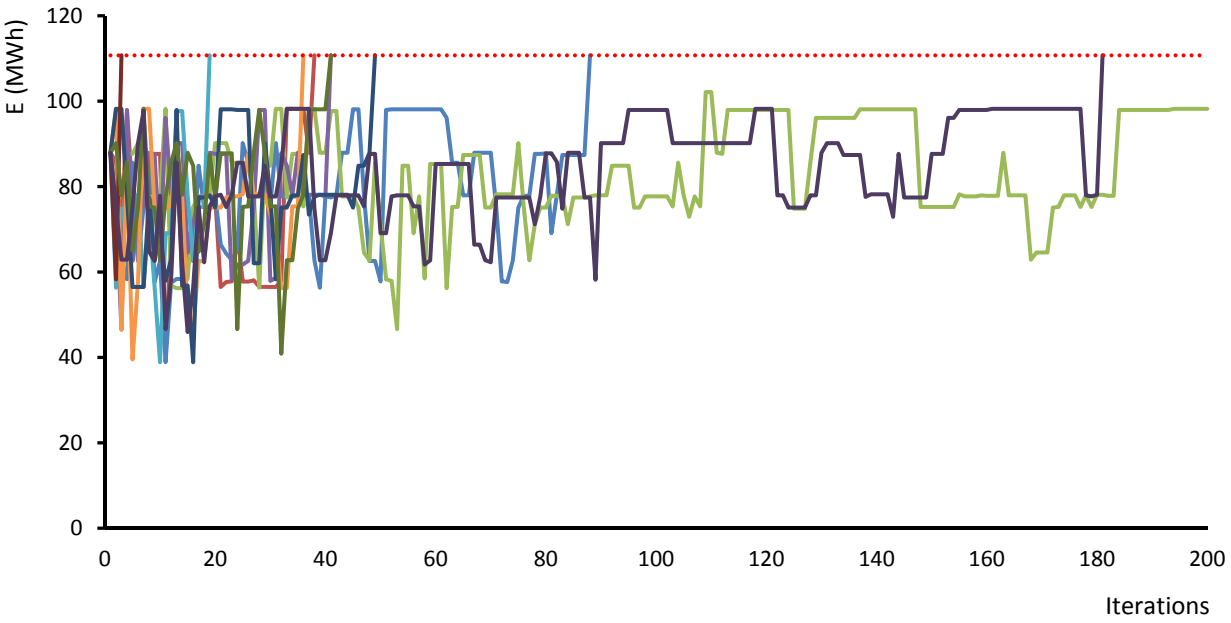

Figure.A 18 – Installation of two turbines, neighborhood number function n°4, case type 2.

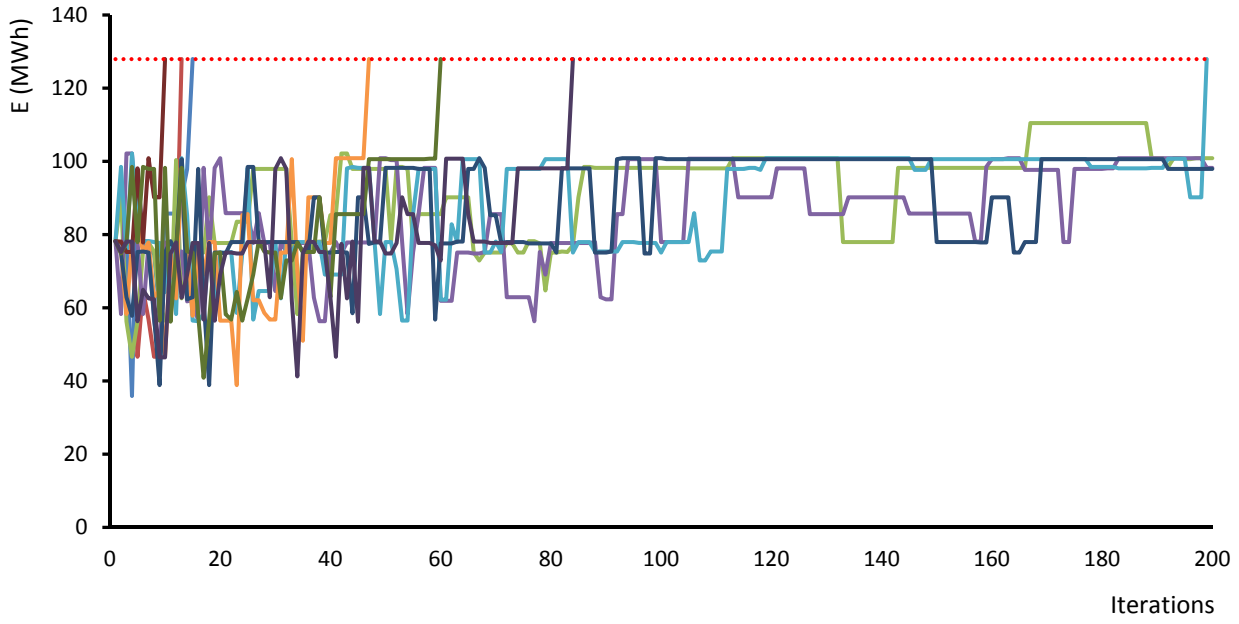

Figure.A 19 – Installation of two turbines, neighborhood number function n°4, case type 3.

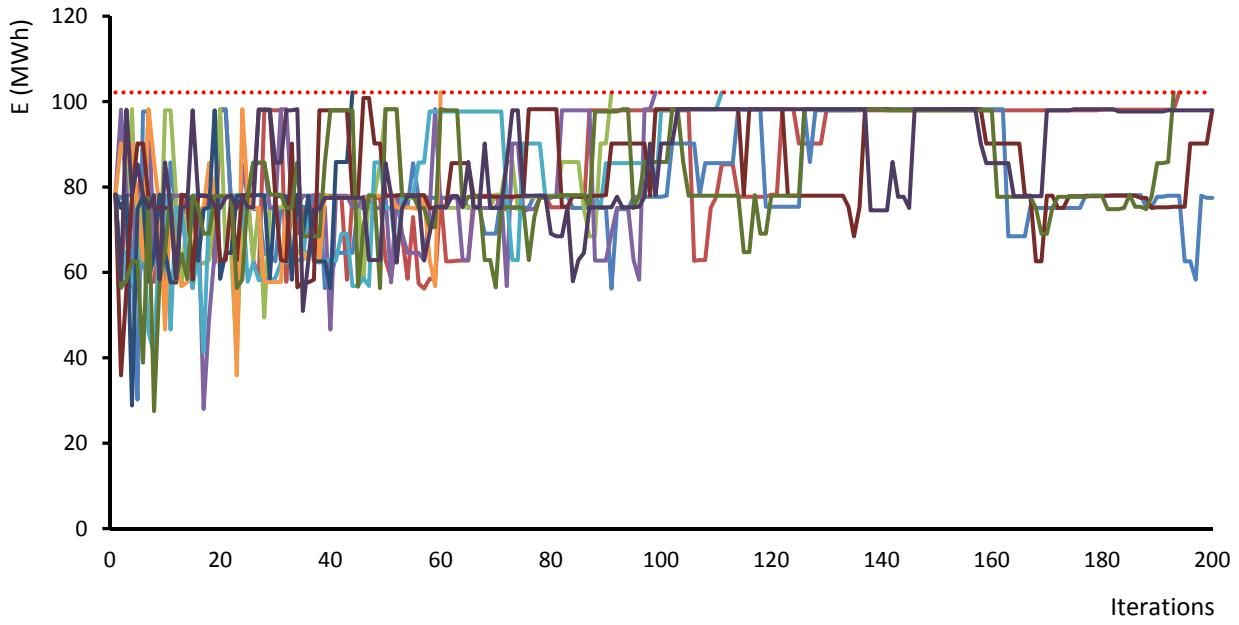

Figure.A 20 – Installation of two turbines, neighborhood number function n°4, case type 4.

Second stage of neighborhood definition

Simulations results with three turbines for neighborhood function definition

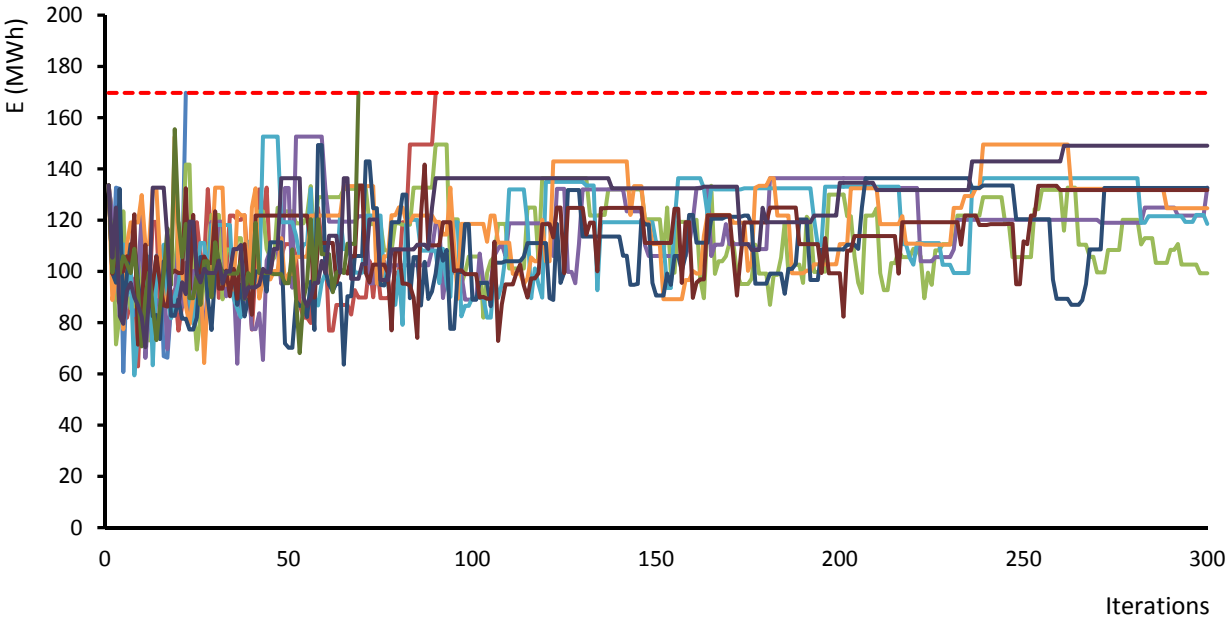

Figure.A 21 – Installation of three turbines, neighborhood number function n°4.

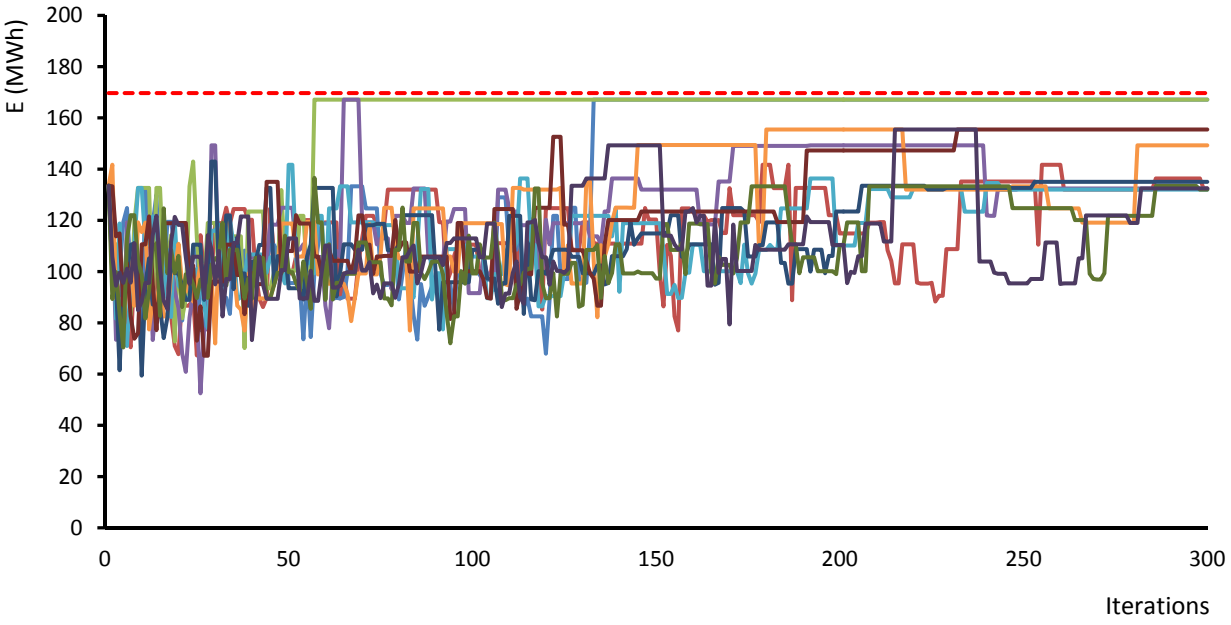

Figure.A 22 – Installation of three turbines, neighborhood number function n°7.

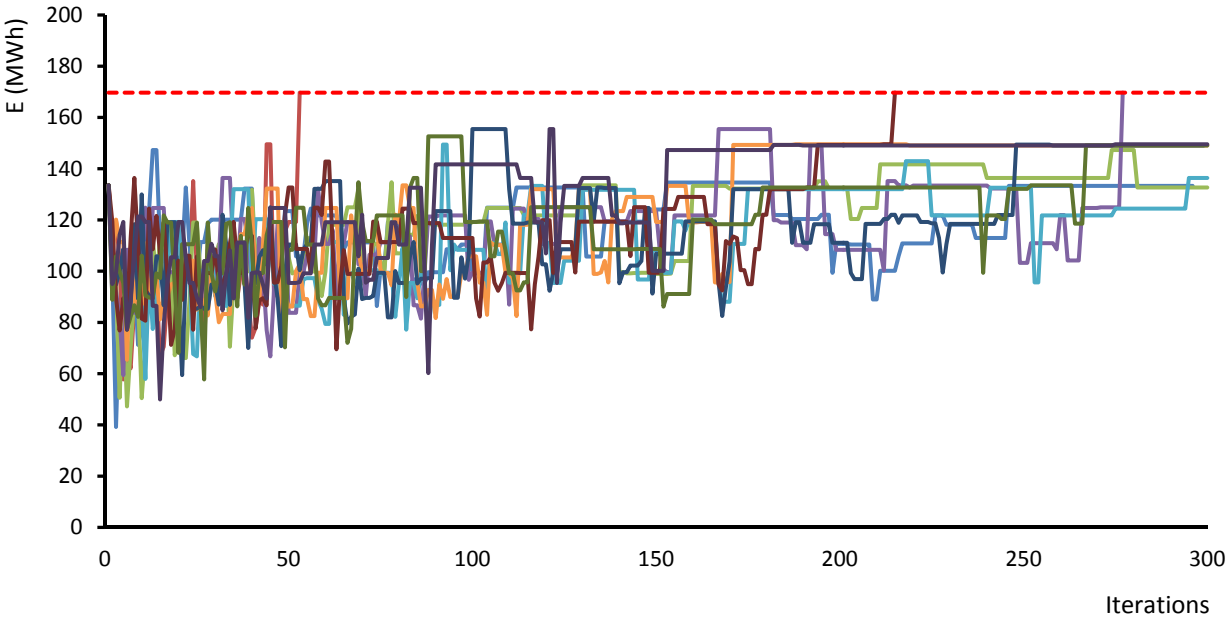

Figure.A 23 – Installation of three turbines, neighborhood number function n°8.

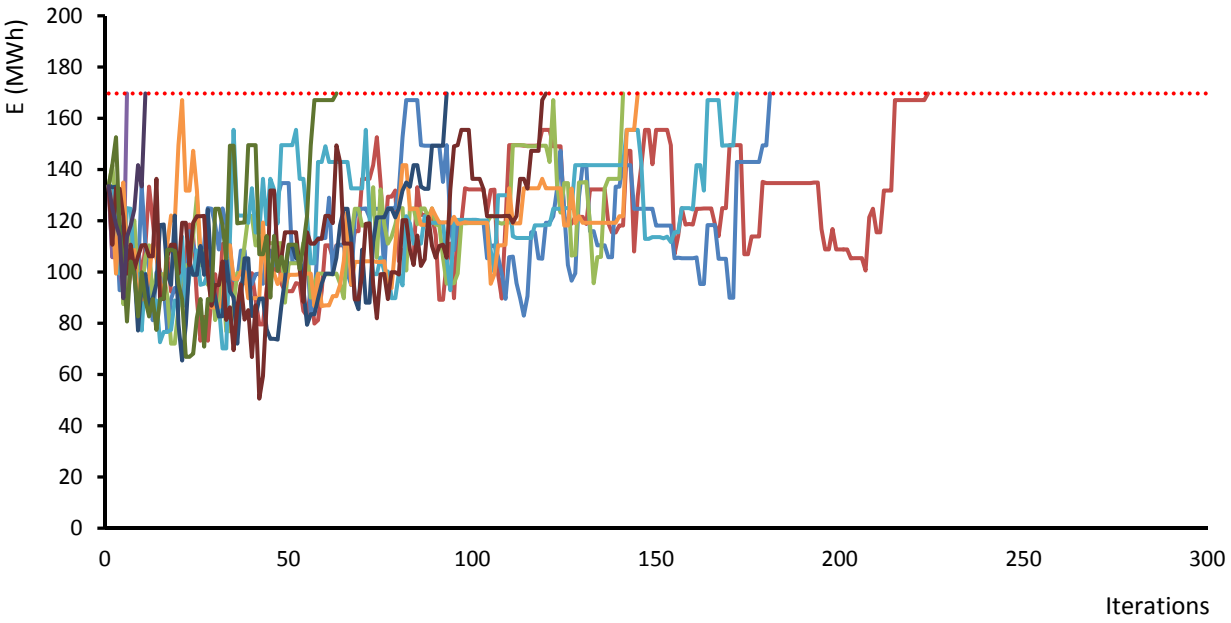

Figure.A 24 – Installation of three turbines, neighborhood number function n°9.

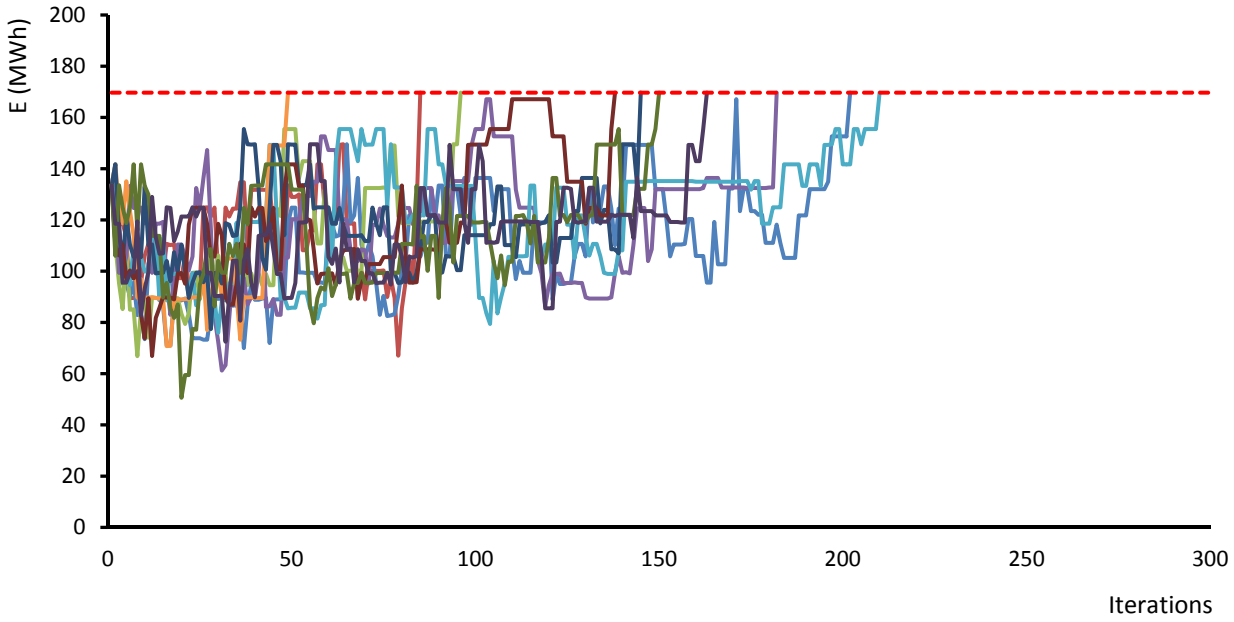

Figure.A 25 – Installation of three turbines, neighborhood number function n°10.

Simulations results with two and three turbines with neighborhood function n°9

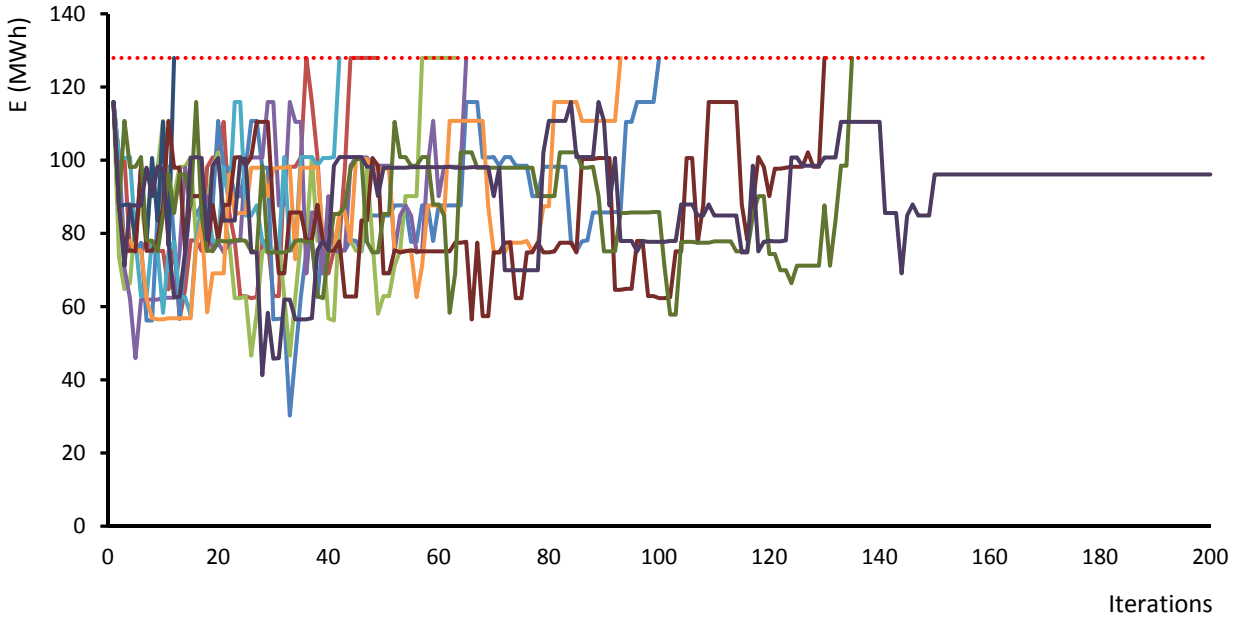

Figure.A 26 – Installation of two turbines, neighborhood number function n°9, case type 1.

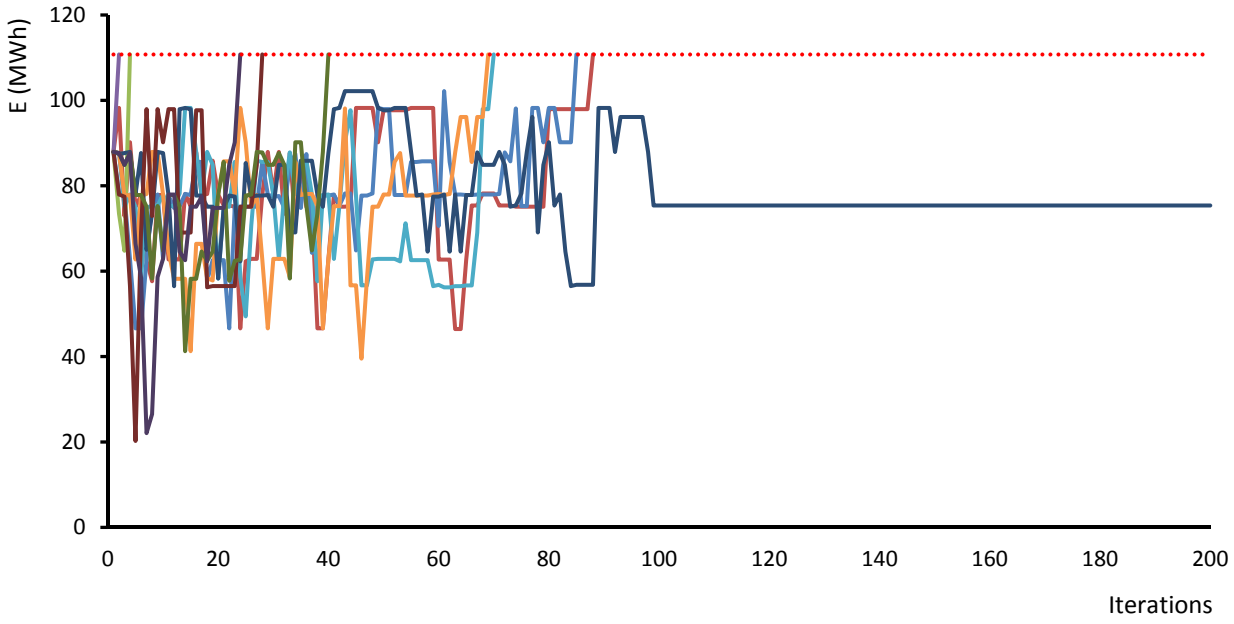

Figure.A 27 – Installation of two turbines, neighborhood number function n°9, case type 2.

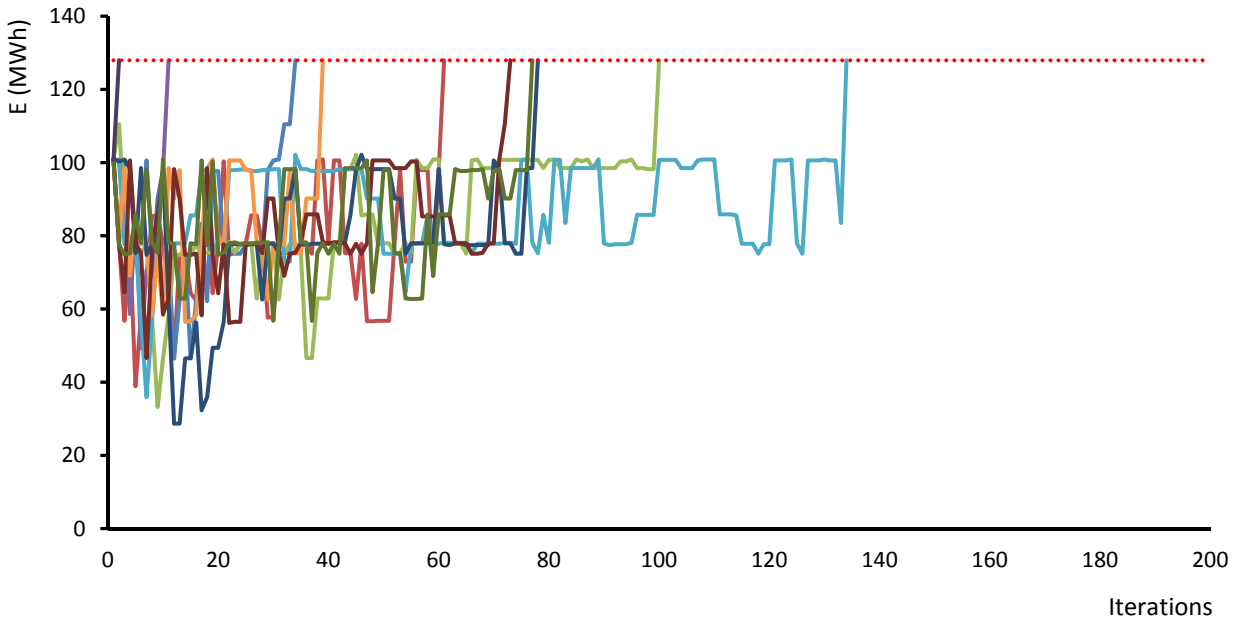

Figure.A 28 – Installation of two turbines, neighborhood number function n°9, case type 3.

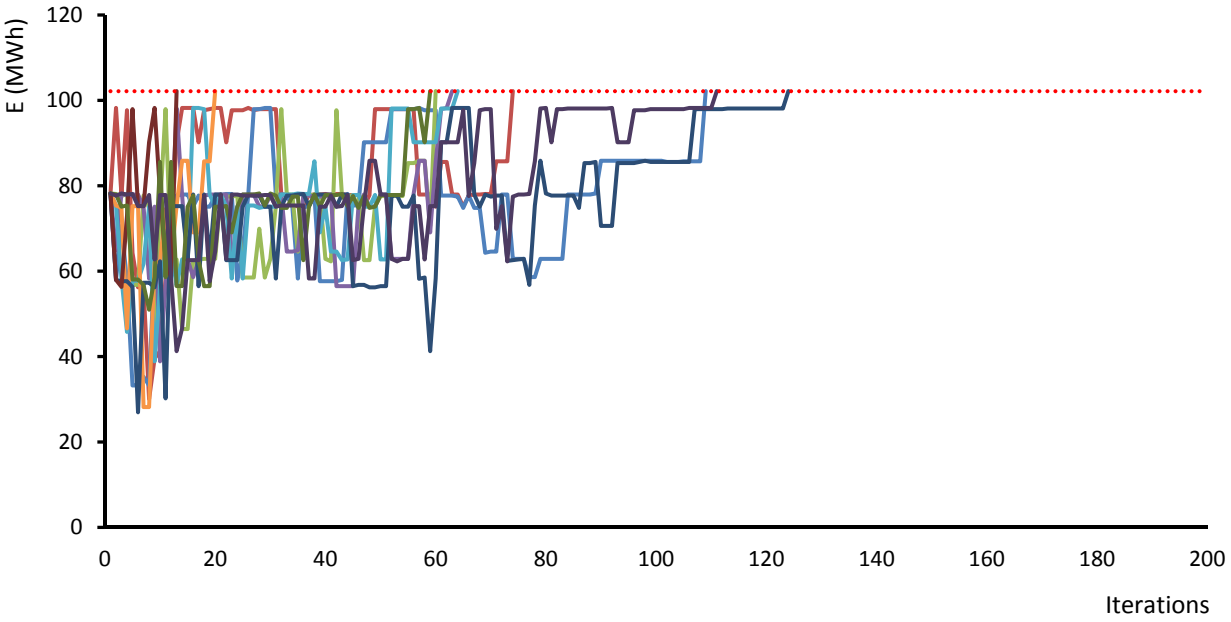

Figure.A 29 – Installation of two turbines, neighborhood number function n°9, case type 4.

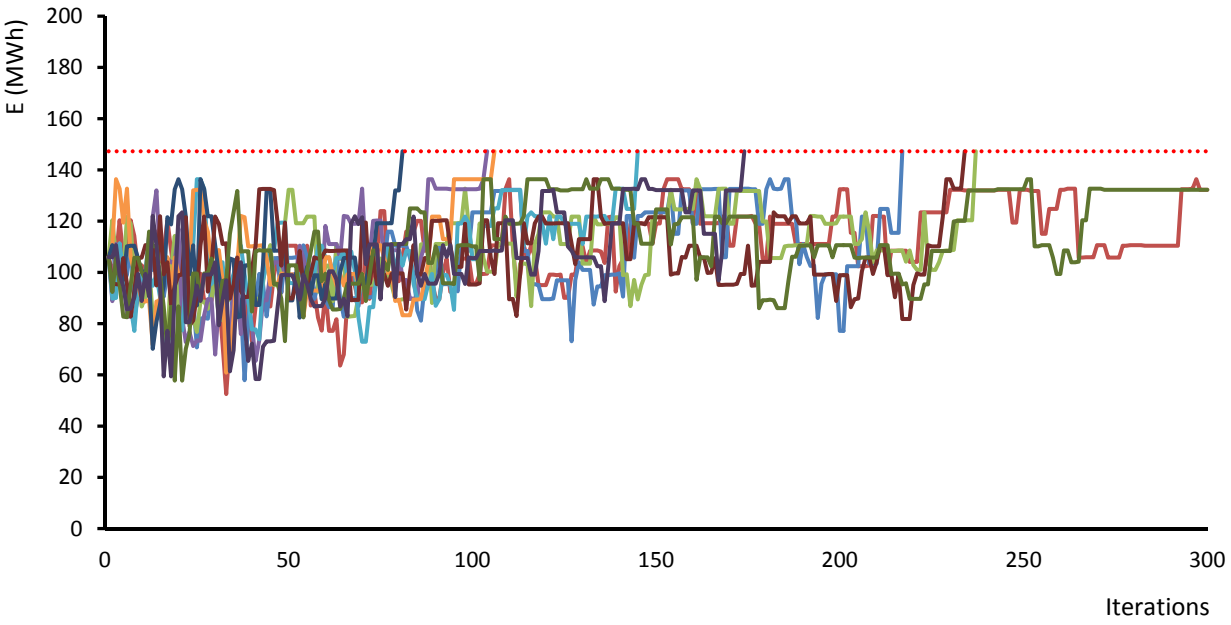

Figure.A 30 – Installation of three turbines, neighborhood number function n°9, case type 2.

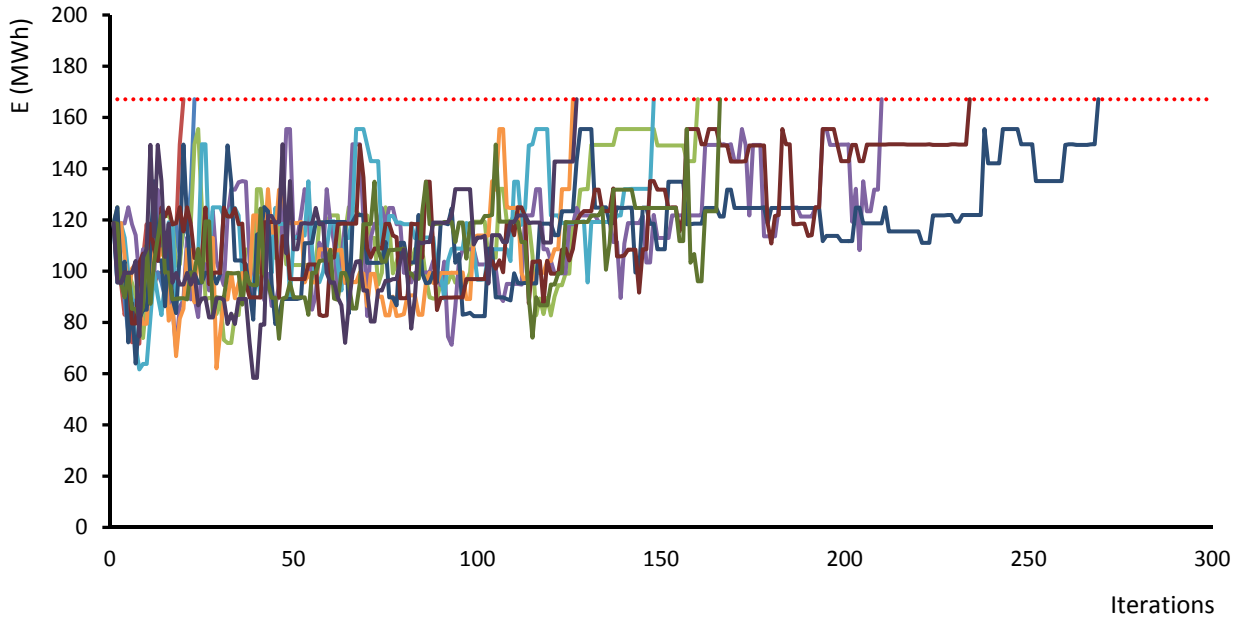

Figure.A 31 – Installation of three turbines, neighborhood number function n°9, case type 3.

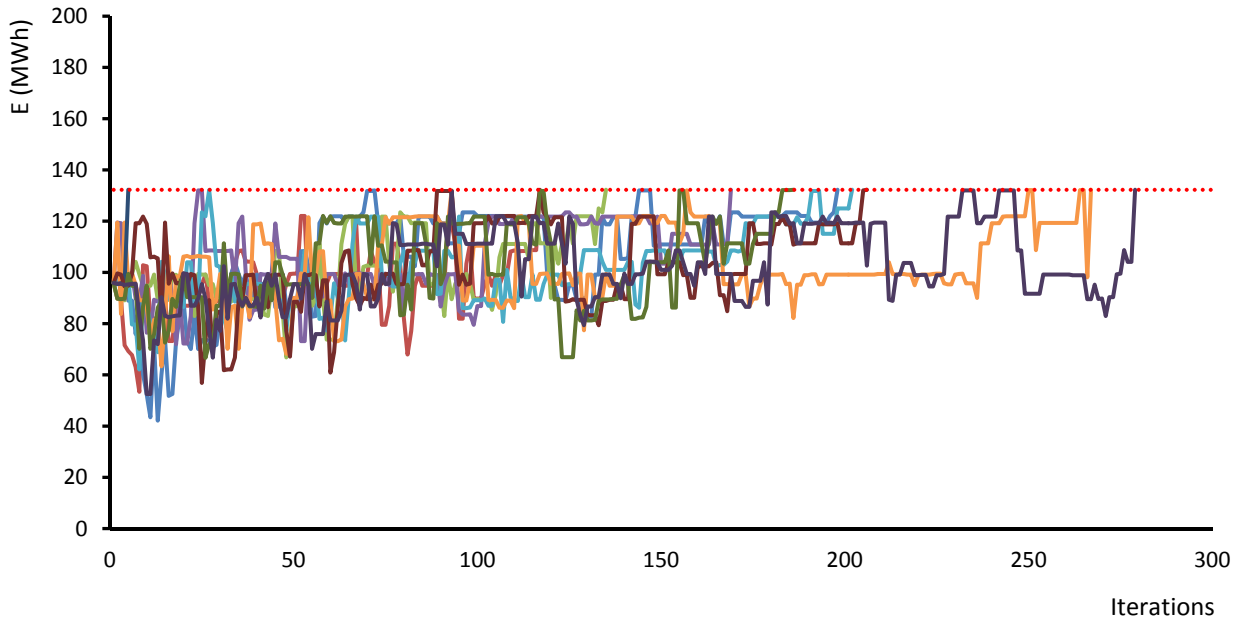

Figure.A 32 – Installation of three turbines, neighborhood number function n°9, case type 4.

C. Synthetic networks analysis

Table.A 3 – Characterization of synthetic networks and production with one 5BTP.

Type of network	Type of consumption	Q_{inflow} (l/s)	n	t	q'	e	f	r	Lc (m)	Lt (m)	Q_{aver_r} (l/s)	D_{aver} (mm)	A (m^2)	Kc	Lq (m)	Ln (m)	L_S (m)	V_{aver} (m/s)	E_{1T} (kWh)
1	A	43.64	4	4	0.67	1.00	1	0.33	200	400	10.91	135.00	10000	1.128	71.97	71.97	400	0.704	1.51
1	B	43.64	4	4	0.67	1.00	1	0.33	100	400	8.18	97.50	10000	1.128	68.31	71.97	400	0.896	2.01
1	C	43.64	4	4	0.67	1.00	1	0.33	200	400	13.64	127.50	10000	1.128	75.63	71.97	400	1.002	2.62
1	D	43.64	4	4	0.67	1.00	1	0.33	200	400	10.91	105.00	10000	1.128	86.61	71.97	400	1.246	1.20
1	E	43.64	4	4	0.67	1.00	1	0.33	200	400	10.91	110.00	10000	1.128	67.09	71.97	400	0.891	1.95
2	A	76.37	6	7	0.47	0.86	2	0.29	200	700	12.73	135.71	20000	1.196425	74.41	74.41	600	0.804	2.42
2	B	76.37	6	7	0.47	0.86	2	0.29	100	700	10.00	105.71	20000	1.196425	68.83	74.41	600	0.882	2.61
2	C	76.37	6	7	0.47	0.86	2	0.29	200	700	15.46	135.71	20000	1.196425	82.22	74.41	600	0.977	4.69
2	D	76.37	6	7	0.47	0.86	2	0.29	200	700	11.82	117.14	20000	1.196425	67.90	74.41	600	0.822	3.40
2	E	76.37	6	7	0.47	0.86	2	0.29	200	700	13.64	117.14	20000	1.196425	93.93	74.41	600	1.217	3.12
3	A	76.37	6	7	0.47	0.86	2	0.29	300	700	16.37	148.57	20000	1.196425	112.52	112.52	600	0.835	6.66
3	B	76.37	6	7	0.47	0.86	2	0.29	300	700	13.64	122.86	20000	1.196425	113.59	112.52	600	0.842	8.32
3	C	76.37	6	7	0.47	0.86	2	0.29	300	700	19.09	141.43	20000	1.196425	112.16	112.52	600	1.108	6.01
3	D	76.37	6	7	0.47	0.86	2	0.29	300	700	15.46	138.57	20000	1.196425	98.02	112.52	600	0.725	9.71
3	E	76.37	6	7	0.47	0.86	2	0.29	300	700	17.27	137.14	20000	1.196425	118.34	112.52	600	1.082	8.13
4	A	109.10	8	10	0.36	0.80	3	0.27	400	1000	21.82	163.00	30000	1.302502	158.42	158.42	800	0.876	15.29
4	B	109.10	8	10	0.36	0.80	3	0.27	400	1000	19.09	141.00	30000	1.302502	165.60	158.42	800	0.829	21.12
4	C	109.10	8	10	0.36	0.80	3	0.27	400	1000	24.55	152.00	30000	1.302502	140.35	158.42	800	1.119	20.12
4	D	109.10	8	10	0.36	0.80	3	0.27	400	1000	21.82	149.00	30000	1.302502	151.15	158.42	800	0.991	20.87
4	E	109.10	8	10	0.36	0.80	3	0.27	500	1000	22.24	149.00	30000	1.302502	180.22	158.42	800	0.883	22.54
5	A	109.10	8	10	0.36	0.80	3	0.27	300	1000	16.37	147.00	30000	1.302502	111.16	111.16	800	0.837	6.22
5	B	109.10	8	10	0.36	0.80	3	0.27	300	1000	13.64	118.00	30000	1.302502	102.43	111.16	800	0.907	9.78
5	C	109.10	8	10	0.36	0.80	3	0.27	300	1000	19.09	139.00	30000	1.302502	114.07	111.16	800	1.128	8.18
5	D	109.10	8	10	0.36	0.80	3	0.27	300	1000	16.37	133.00	30000	1.302502	92.25	111.16	800	0.921	11.32
5	E	109.10	8	10	0.36	0.80	3	0.27	300	1000	16.37	129.00	30000	1.302502	119.69	111.16	800	1.043	9.77
6	A	109.10	8	10	0.36	0.80	3	0.27	300	1000	16.37	143.00	30000	1.302502	111.16	112.25	800	0.853	11.32
7	A	109.10	8	10	0.36	0.80	3	0.27	300	1000	19.09	144.00	30000	1.302502	124.51	124.51	800	0.964	8.81
8	A	130.92	9	12	0.33	0.75	4	0.31	400	1200	21.82	160.00	40000	1.128	159.57	159.57	800	0.939	12.28
9	A	130.92	9	12	0.33	0.75	4	0.31	300	1200	18.18	145.83	40000	1.128	112.25	112.25	800	0.897	17.51
10	A	120.01	9	11	0.31	0.82	3	0.23	400	1100	23.03	143.64	40000	1.128	112.25	112.25	800	1.124	11.30
11	A	120.01	9	11	0.31	0.82	3	0.23	400	1100	21.82	147.27	40000	1.128	159.57	159.57	800	1.033	15.89
12	A	109.10	9	10	0.28	0.90	2	0.15	400	1000	23.03	142.00	40000	1.128	112.25	112.25	800	1.230	9.87
13	A	109.10	9	10	0.28	0.90	2	0.15	400	1000	21.82	151.00	40000	1.128	159.57	159.57	800	1.032	13.23
14	A	120.01	9	11	0.31	0.82	3	0.23	400	1100	22.37	147.27	40000	1.128	159.57	159.57	800	1.110	14.76
15	A	109.10	9	10	0.28	0.90	2	0.15	300	1000	18.18	135.00	40000	1.128	112.25	112.25	800	1.086	7.02
16	A	120.01	9	11	0.31	0.82	3	0.23	400	1100	20.61	141.82	40000	1.128	112.25	112.25	800	1.167	12.68

Type of network	Type of consumption	Q_{inflow} (l/s)	n	t	q'	e	f	r	Lc (m)	Lt (m)	Q_{aver_r} (l/s)	D_{aver} (mm)	A (m^2)	Kc	Lq (m)	Ln (m)	L_S (m)	V_{aver} (m/s)	E_{1T} (kWh)
17	A	65.46	6	6	0.40	1.00	1	0.14	300	600	16.37	126.67	20000	1.196425	74.41	74.41	600	1.173	3.81
17	B	65.46	6	6	0.40	1.00	1	0.14	300	600	11.82	113.33	20000	1.196425	68.83	74.41	600	0.935	3.15
17	C	65.46	6	6	0.40	1.00	1	0.14	300	600	20.91	140.00	20000	1.196425	82.22	74.41	600	1.276	4.43
17	D	65.46	6	6	0.40	1.00	1	0.14	300	600	17.27	130.00	20000	1.196425	67.90	74.41	600	1.212	4.44
17	E	65.46	6	6	0.40	1.00	1	0.14	300	600	15.46	126.67	20000	1.196425	93.93	74.41	600	1.001	3.08
18	A	87.28	8	8	0.29	1.00	1	0.09	400	800	21.82	147.50	30000	1.302502	158.42	158.42	800	1.156	6.88
18	B	87.28	8	8	0.29	1.00	1	0.09	300	800	19.66	147.50	30000	1.302502	165.60	158.42	800	0.992	9.44
18	C	87.28	8	8	0.29	1.00	1	0.09	400	800	24.55	160.00	30000	1.302502	140.35	158.42	800	1.100	13.35
18	D	87.28	8	8	0.29	1.00	1	0.09	400	800	21.82	156.25	30000	1.302502	156.87	158.42	800	1.033	7.12
18	E	87.28	8	8	0.29	1.00	1	0.09	400	800	22.35	155.00	30000	1.302502	163.07	158.42	800	1.008	9.05
20	A	175.63	12	17	0.26	0.71	6	0.32	500	1700	24.67	149.41	60000	1.15126	189.09	189.09	1000	1.121	24.94
21	A	175.63	12	17	0.26	0.71	6	0.32	400	1700	19.79	145.29	60000	1.15126	144.07	144.07	1000	0.926	19.85
22	A	134.31	12	13	0.20	0.92	2	0.11	500	1300	24.67	148.46	60000	1.15126	189.09	189.09	1000	1.153	29.66
23	A	134.31	12	13	0.20	0.92	2	0.11	500	1300	27.07	155.38	60000	1.15126	144.07	150.14	1000	1.150	15.91
24	A	141.83	10	13	0.29	0.77	4	0.27	300	1300	18.55	153.85	40000	1.41	117.15	117.15	1000	0.856	7.64
24	B	141.83	10	13	0.29	0.77	4	0.27	300	1300	15.82	126.15	40000	1.41	110.61	117.15	1000	0.899	10.23
24	C	141.81	10	13	0.29	0.77	4	0.27	300	1300	21.27	143.85	40000	1.41	119.33	117.15	1000	1.175	8.62
24	D	141.83	10	13	0.29	0.77	4	0.27	300	1300	18.00	135.38	40000	1.41	124.96	117.15	1000	0.981	10.26
24	E	141.83	10	13	0.29	0.77	4	0.27	300	1300	19.09	140.77	40000	1.41	96.64	117.15	1000	1.002	11.62
25	A	141.83	10	13	0.29	0.77	4	0.27	500	1300	27.28	183.85	40000	1.41	217.64	207.11	1000	0.871	26.00
25	B	141.83	10	13	0.29	0.77	4	0.27	500	1300	24.55	150.00	40000	1.41	199.81	207.11	1000	0.854	37.95
25	C	141.83	10	13	0.29	0.77	4	0.27	500	1300	30.00	166.92	40000	1.41	209.55	207.11	1000	1.124	36.42
25	D	141.83	10	13	0.29	0.77	4	0.27	500	1300	26.73	153.85	40000	1.41	193.28	207.11	1000	0.961	37.36
25	E	141.83	10	13	0.29	0.77	4	0.27	500	1300	27.82	163.85	40000	1.41	212.19	207.11	1000	0.934	39.66
26	A	141.83	10	13	0.29	0.77	4	0.27	400	1300	20.73	161.54	40000	1.41	136.25	136.25	1000	0.844	17.05
26	B	141.83	10	13	0.29	0.77	4	0.27	400	1300	18.00	130.00	40000	1.41	143.17	136.25	1000	0.889	24.25
26	C	141.83	10	13	0.29	0.77	4	0.27	400	1300	23.46	149.23	40000	1.41	133.91	136.25	1000	1.166	19.09
26	D	141.83	10	13	0.29	0.77	4	0.27	500	1300	20.53	146.92	40000	1.41	137.41	136.25	1000	0.828	24.64
26	E	141.83	10	13	0.29	0.77	4	0.27	400	1300	21.27	141.54	40000	1.41	135.86	136.25	1000	1.051	24.39
27	A	157.45	12	15	0.23	0.80	4	0.21	500	1500	27.27	148.00	40000	1.833	162.62	198.90	1300	1.203	31.12
28	A	157.45	12	15	0.23	0.80	4	0.21	400	1500	24.89	148.00	40000	1.833	149.25	149.25	1300	1.185	24.78
29	A	774.62	42	71	0.08	0.59	30	0.38	900	7100	47.54	203.80	300000	1.13269	323.97	323.97	2200	1.071	473.82
30	A	163.63	12	15	0.23	0.80	4	0.21	800	1800	27.27	154.67	40000	1.41	222.62	222.62	1000	1.077	32.30
31	A	163.65	12	15	0.23	0.80	4	0.21	700	1800	24.91	154.67	40000	1.41	222.62	222.62	1000	1.058	24.78
32	A	196.35	14	18	0.20	0.78	5	0.22	800	2100	28.83	155.56	50000	1.261142	300.59	300.59	1000	1.105	33.98
33	A	196.35	14	18	0.20	0.78	5	0.22	700	2100	28.29	155.56	50000	1.261142	285.77	285.77	1000	1.109	30.09
34	A	196.35	14	18	0.20	0.78	5	0.22	1000	2100	29.85	157.78	50000	1.261142	337.54	337.54	1000	1.111	41.95
35	A	196.35	14	18	0.20	0.78	5	0.22	1100	2100	37.63	175.56	50000	1.261142	365.29	365.29	1000	1.081	77.18
36	A	229.08	17	21	0.15	0.81	5	0.17	1200	2500	37.22	179.52	50000	1.765599	367.97	367.97	1400	1.037	57.14

Type of network	Type of consumption	Q_{inflow} (l/s)	n	t	q'	e	f	r	Lc (m)	Lt (m)	Q_{aver_r} (l/s)	D_{aver} (mm)	A (m^2)	Kc	Lq (m)	Ln (m)	L_S (m)	V_{aver} (m/s)	E_{1T} (kWh)
37	A	250.89	19	23	0.13	0.83	5	0.15	1200	2700	37.32	180.43	50000	2.017828	309.67	309.67	1600	1.030	55.22
38	A	599.96	41	57	0.07	0.72	17	0.22	900	5700	53.53	226.36	210000	2.030736	329.06	345.14	3300	1.042	387.58
1	0.6A	26.18	4	4	0.67	1.00	1	0.33	200	400	6.55	135.00	10000	1.128	71.97	71.97	400	0.423	0.64
68	0.6A	464.77	42	71	0.08	0.59	30	0.38	900	7100	28.52	203.80	300000	1.13269	323.97	323.97	2200	0.642	201.75
78	0.6A	150.54	41	57	0.07	0.72	17	0.22	900	5700	23.81	226.36	210000	2.030736	329.06	345.14	3300	0.457	23.64
68	0.4A	309.85	42	71	0.08	0.59	30	0.38	900	7100	19.01	203.80	300000	1.13269	323.97	323.97	2200	0.428	102.51
78	0.4A	239.98	41	57	0.07	0.72	17	0.22	900	5700	21.41	226.36	210000	2.030736	329.06	345.14	3300	0.417	84.74
78	0.2A	60.00	41	57	0.07	0.72	17	0.22	900	5700	5.35	226.36	210000	2.030736	329.06	345.14	3300	0.104	25.86
64	0.6A	85.10	12	13	0.20	0.92	2	0.11	500	1300	17.46	155.38	60000	1.15126	144.07	150.14	1000	0.749	7.38
78	0.1A	119.99	41	57	0.07	0.72	17	0.22	900	5700	10.70	226.36	210000	2.030736	329.06	345.14	3300	0.208	7.88
R1	random	423.22	79	91	0.03	0.87	13	0.08	2200	9100	47.88	215.82	250000	4.5684	526.69	527.17	8100	0.820	369
R2	random	353.96	78	90	0.03	0.87	13	0.09	1700	9000	41.75	203.22	390000	2.980305	672.52	660.18	6600	0.814	130.67
R3	random	360.10	75	83	0.03	0.90	9	0.06	1500	8300	40.41	190.00	150000	5.679343	470.83	472.63	7800	0.856	232.37
R4	random	342.03	72	77	0.03	0.94	6	0.04	1500	7700	36.71	179.09	250000	4.0608	517.36	569.84	7200	0.828	266.95
R5	random	392.22	73	85	0.03	0.86	13	0.09	2200	8800	44.82	212.47	221000	5.03886	579.83	572.24	8400	0.807	324.06
R6	random	738.27	151	173	0.02	0.87	23	0.08	2500	17300	57.55	216.42	680000	4.343085	859.09	878.70	12700	0.844	870.85

Table.A 4 – Characterization of case study networks and production with one 5BTP.

Network	Q_{inflow} (l/s)	n	t	q'	e	f	r	Lc (m)	Lt (m)	Q_{aver_r} (l/s)	D_{aver} (mm)	A (m^2)	Kc	Lq (m)	Ln (m)	L_S (m)	V_{aver} (m/s)	E_{1T} (kWh)
Lausanne WSN 1	147.40	310	312	0.01	0.99	3	0.00	1225	16962	10.91	193.64	642455	3.475336	1108.27	1187.90	9878	0.287	90.68
Lausanne WSN 2	0.20	119	126	0.02	0.94	8	0.03	2423	10493	0.81	143.81	385588.	3.505531	1065.16	1078.41	7719	0.060	0.01

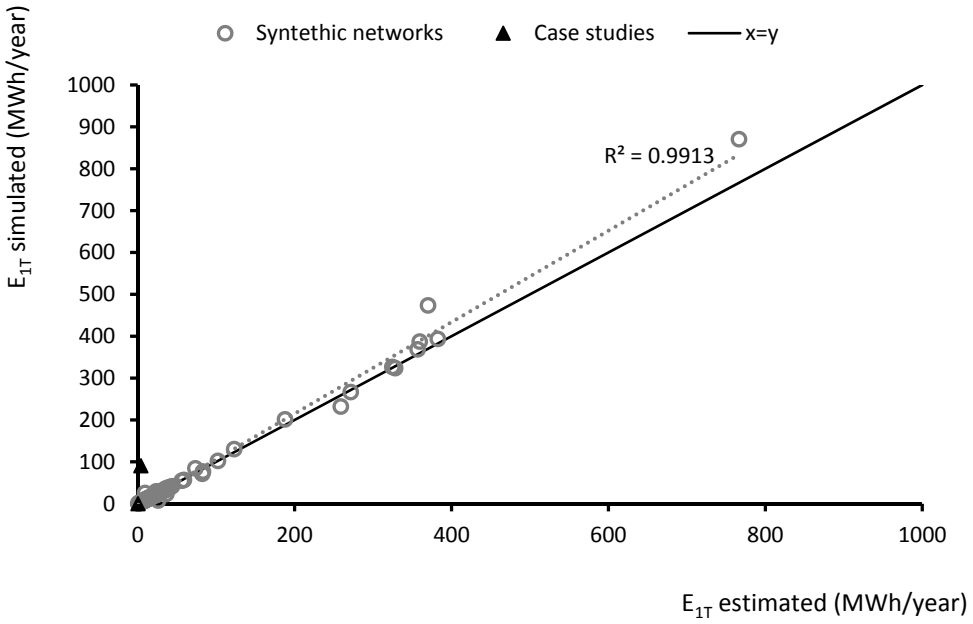

Figure.A 33 – Representation of estimation of energy produced with one 5BTP with expression 1 against the simulated energy.

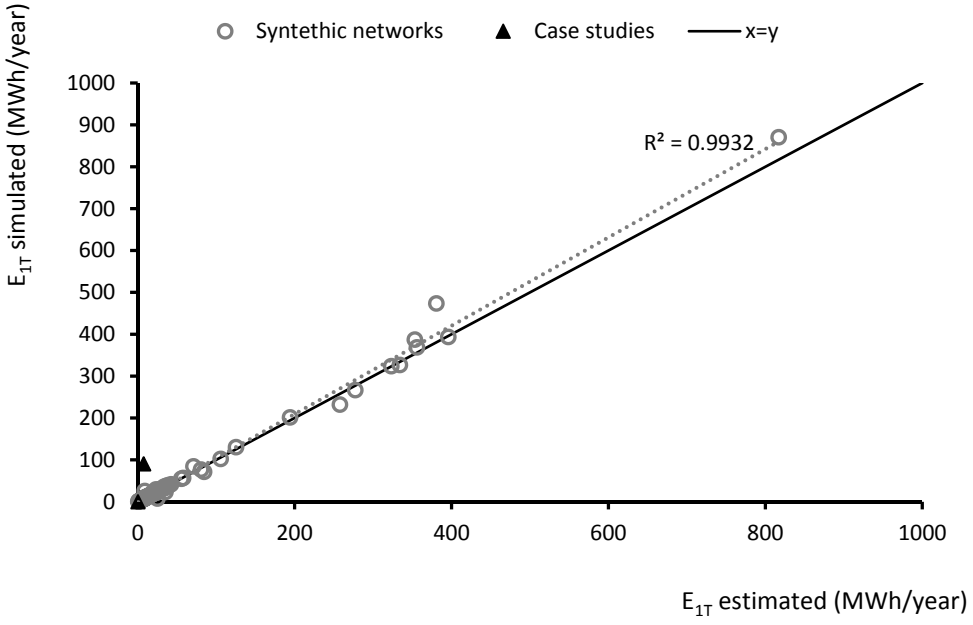

Figure.A 34 – Representation of estimation of energy produced with one 5BTP with expression 2 against the simulated energy.

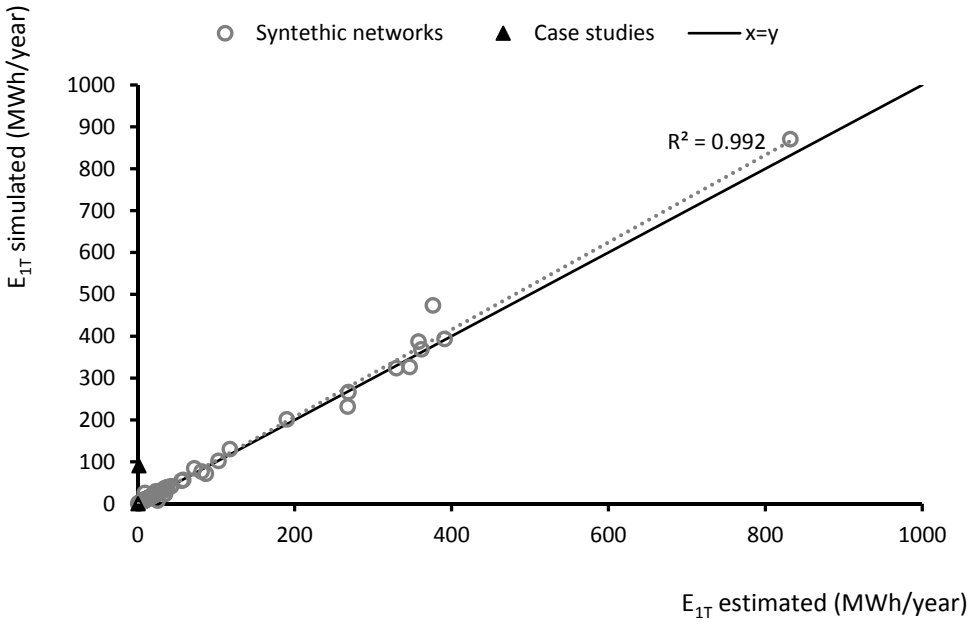

Figure.A 35 – Representation of estimation of energy produced with one 5BTP with expression 3 against the simulated energy.

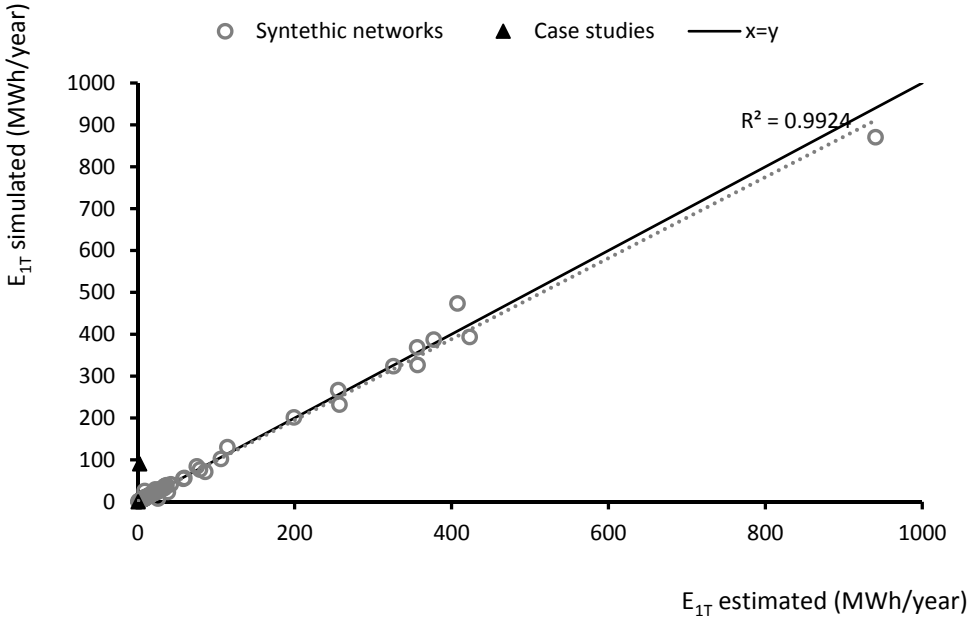

Figure.A 36 – Representation of estimation of energy produced with one 5BTP with expression 4 against the simulated energy.

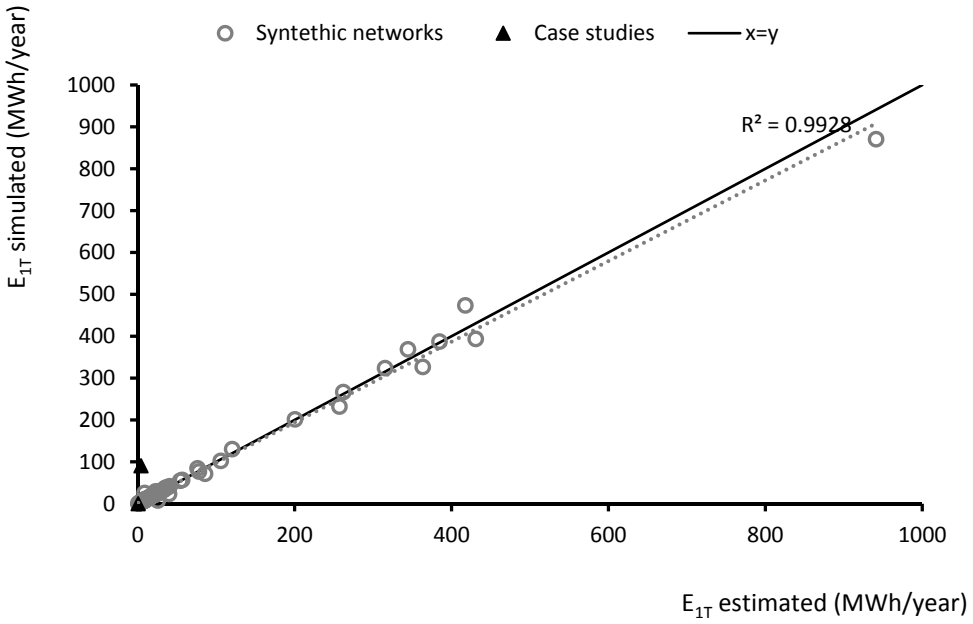

Figure.A 37 – Representation of estimation of energy produced with one 5BTP with expression 5 against the simulated energy.

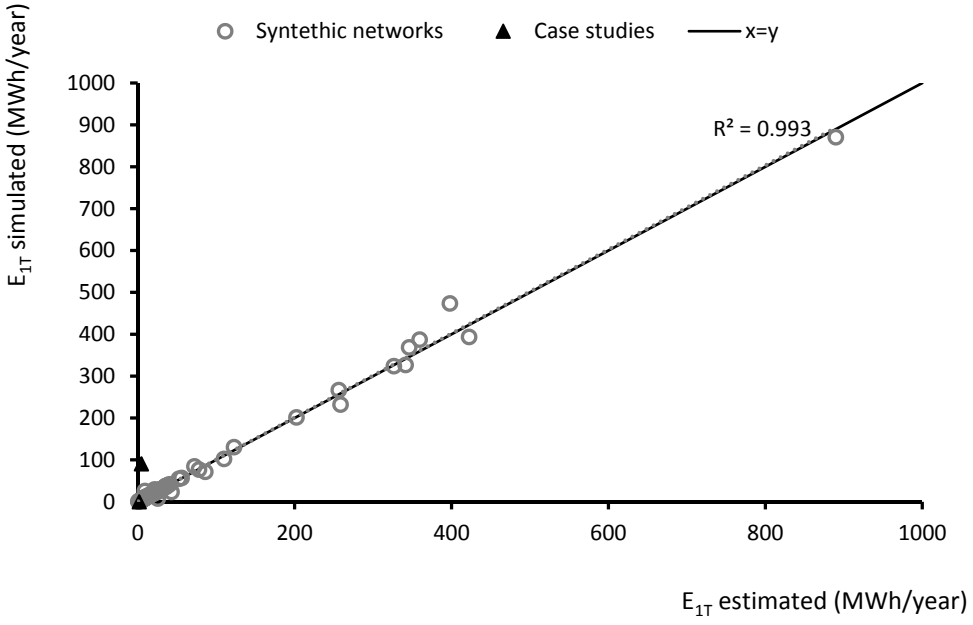

Figure.A 38 – Representation of estimation of energy produced with one 5BTP with expression 6 against the simulated energy.

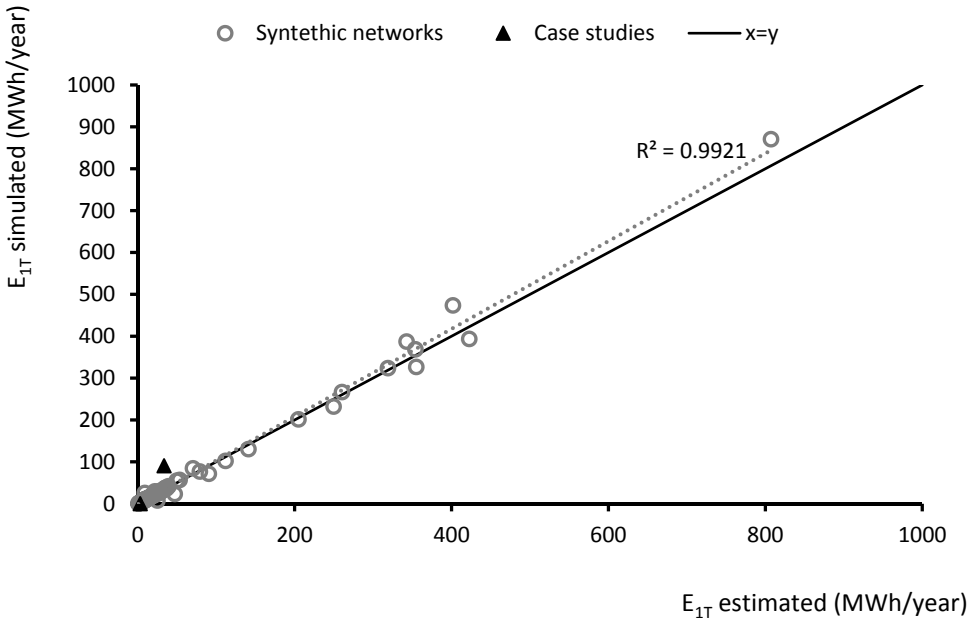

Figure.A 39 – Representation of estimation of energy produced with one 5BTP with expression 7 against the simulated energy.

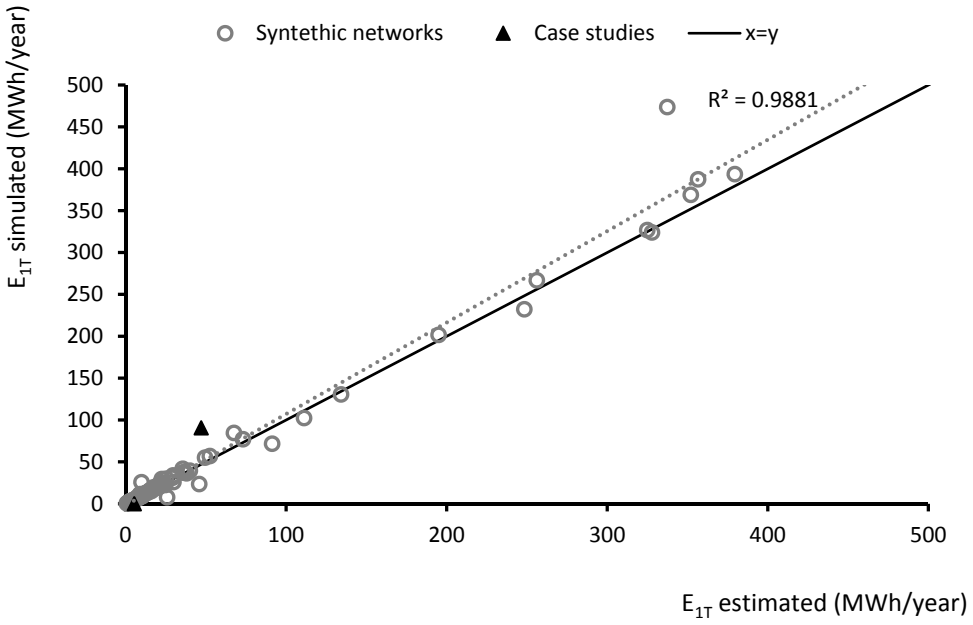

Figure.A 40 – Representation of estimation of energy produced with one 5BTP with expression 8 against the simulated energy.

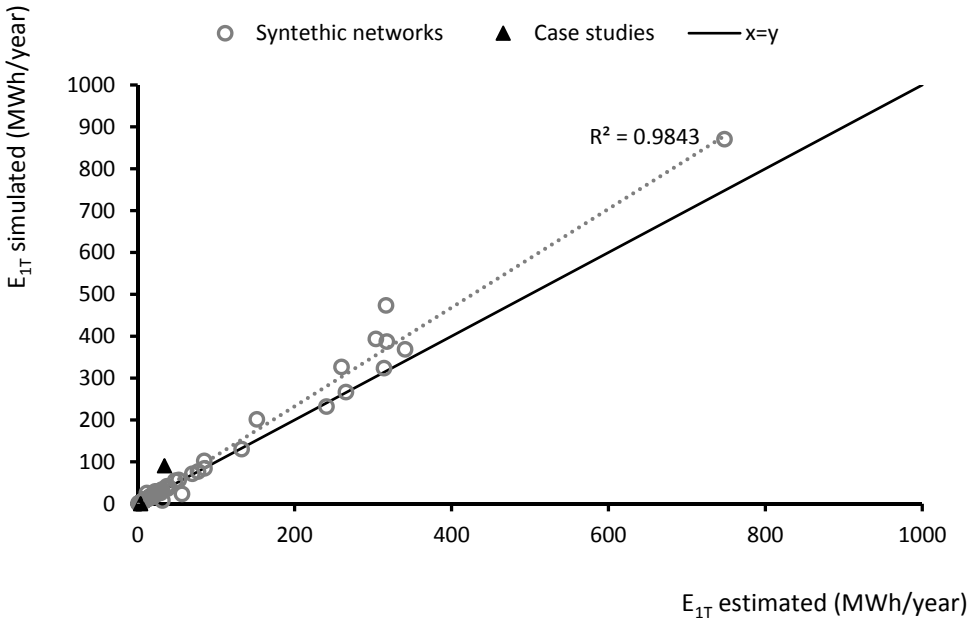

Figure.A 41 – Representation of estimation of energy produced with one 5BTP with expression 9 against the simulated energy.

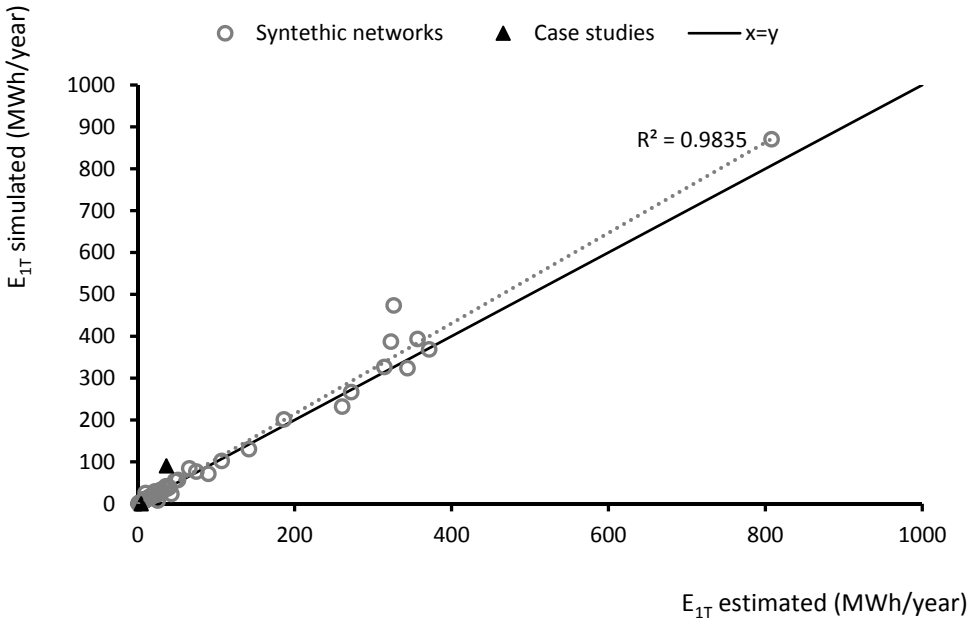

Figure.A 42 – Representation of estimation of energy produced with one 5BTP with expression 10 against the simulated energy.

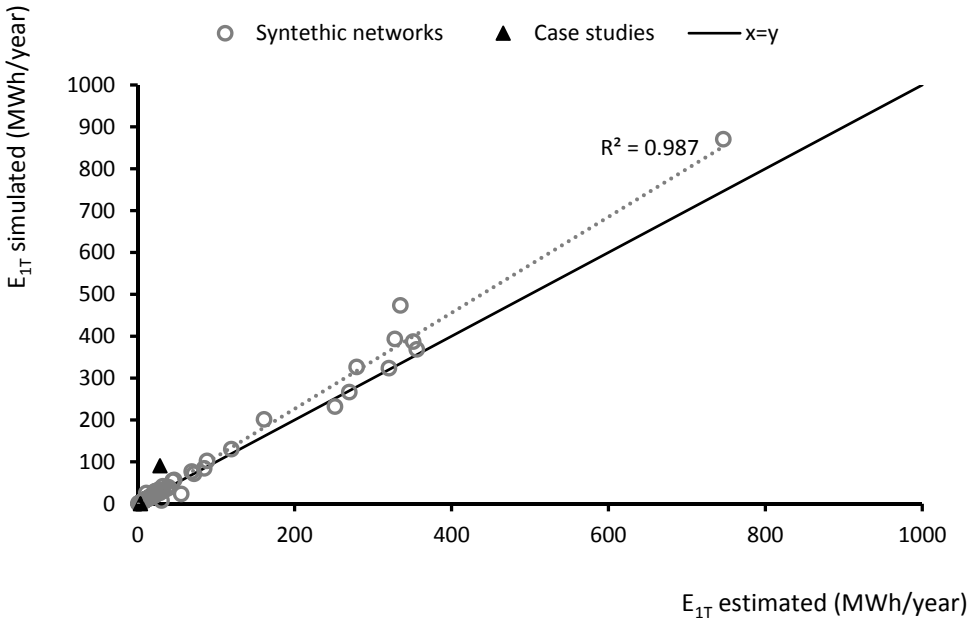

Figure.A 43 – Representation of estimation of energy produced with one 5BTP with expression 11 against the simulated energy.

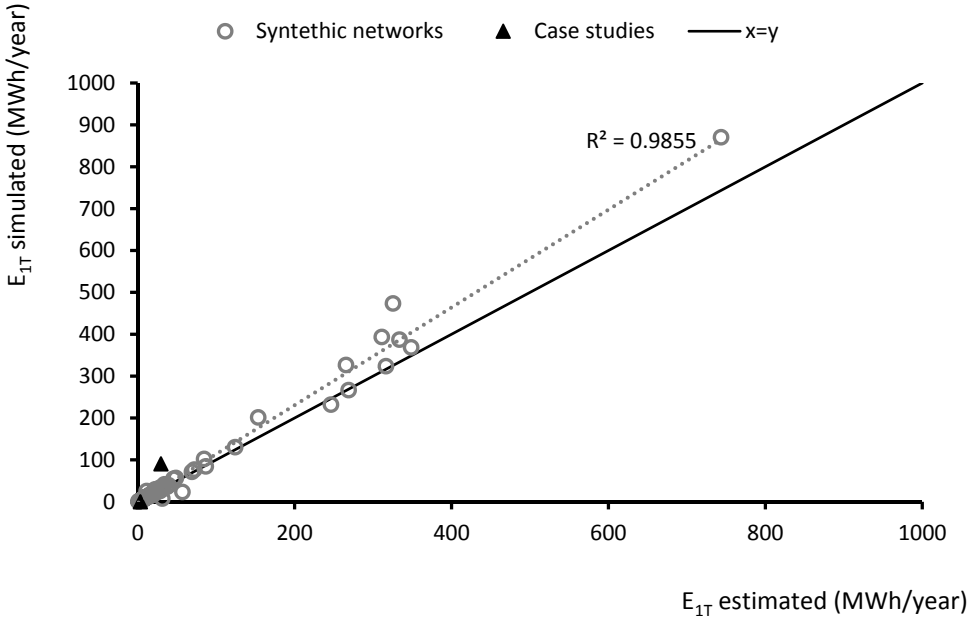

Figure.A 44 – Representation of estimation of energy produced with one 5BTP with expression 12 against the simulated energy.

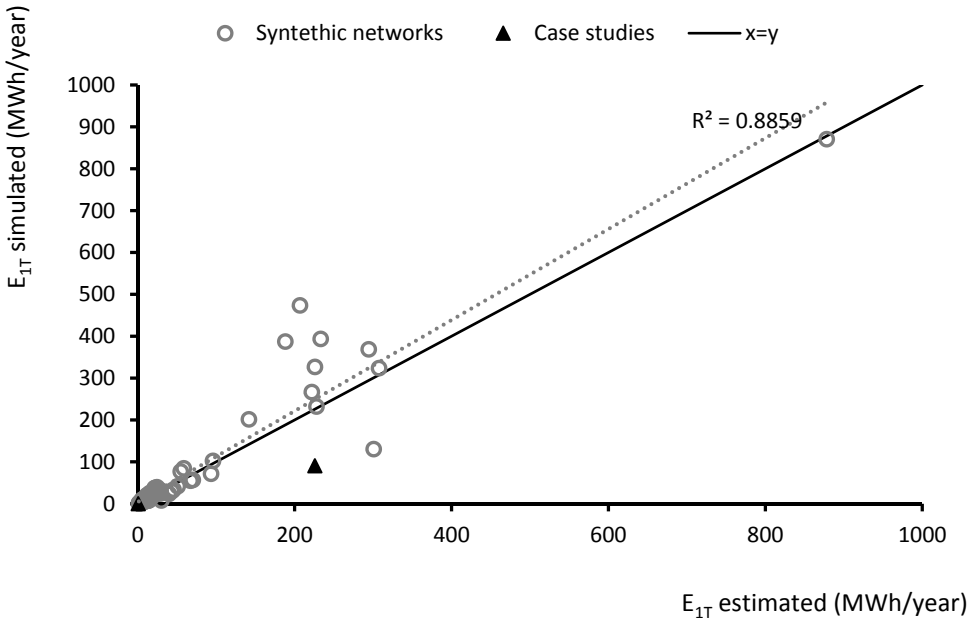

Figure.A 45 – Representation of estimation of energy produced with one 5BTP with expression 13 against the simulated energy.

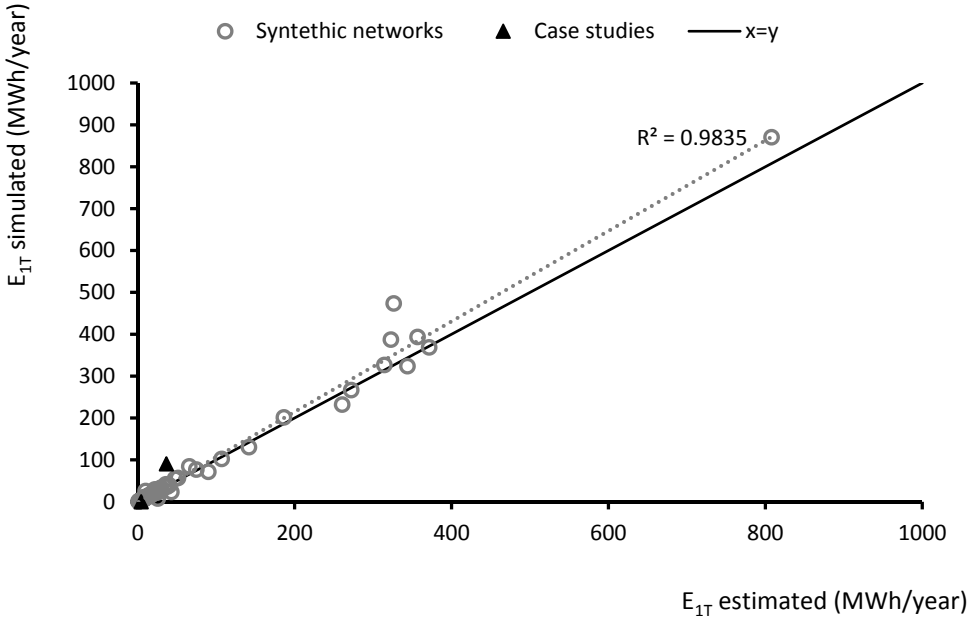

Figure.A 46 – Representation of estimation of energy produced with one 5BTP with expression 14 against the simulated energy.

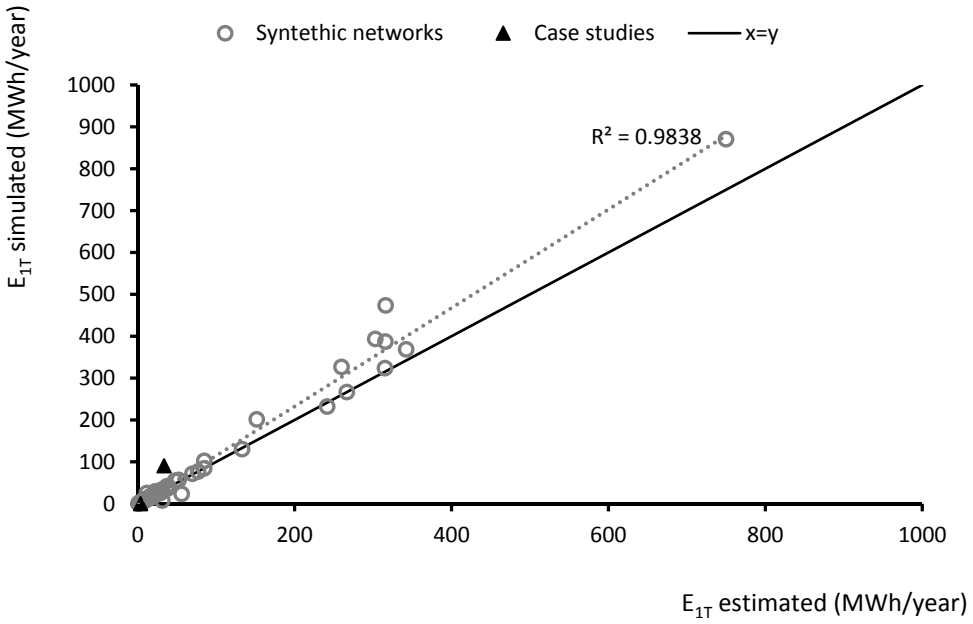

Figure.A 47 – Representation of estimation of energy produced with one 5BTP with expression 15 against the simulated energy.

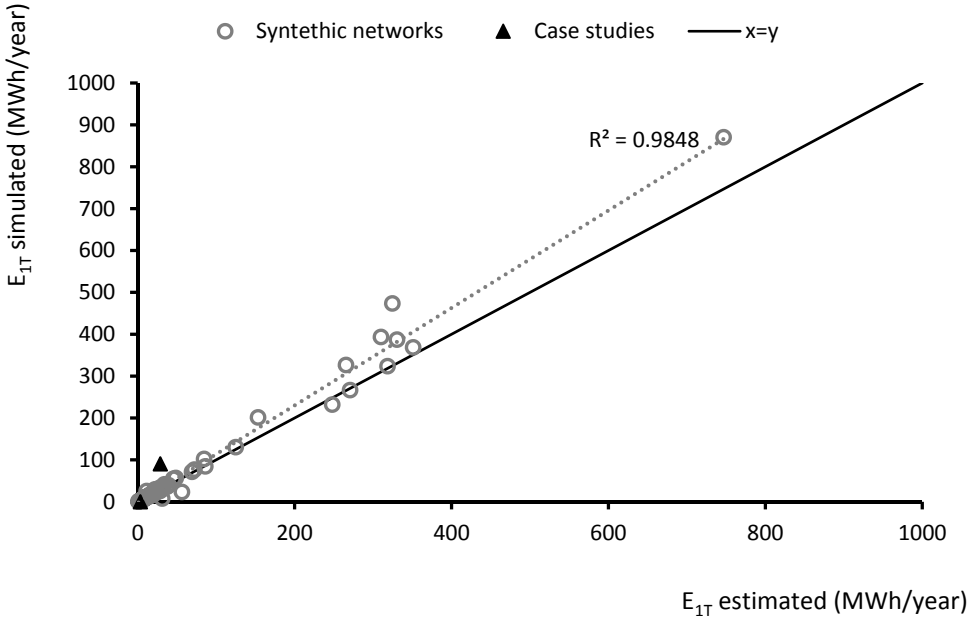

Figure.A 48 – Representation of estimation of energy produced with one 5BTP with expression 16 against the simulated energy.

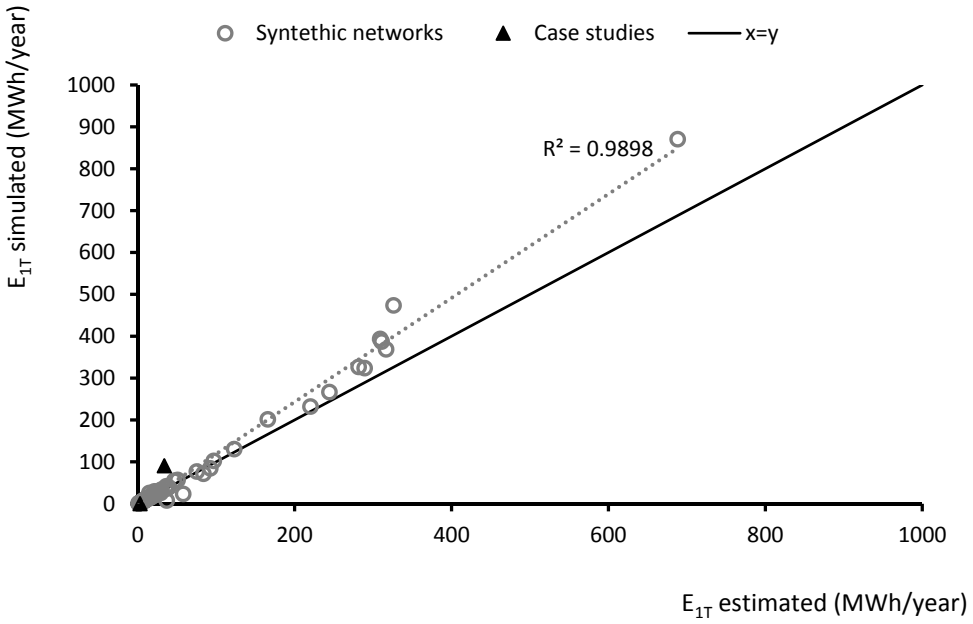

Figure.A 49 – Representation of estimation of energy produced with one 5BTP with expression 17 against the simulated energy.

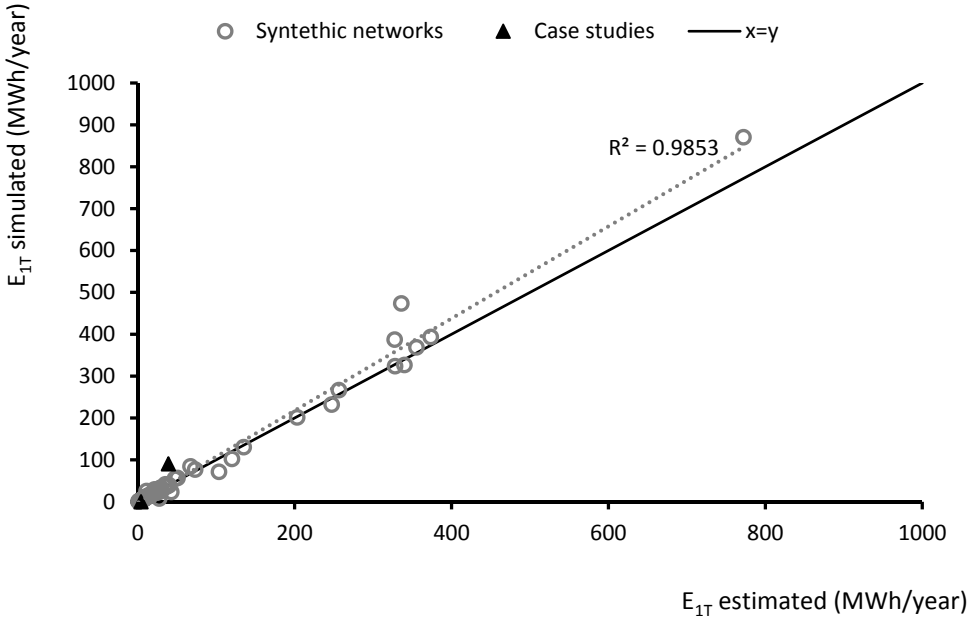

Figure.A 50 – Representation of estimation of energy produced with one 5BTP with expression 18 against the simulated energy.

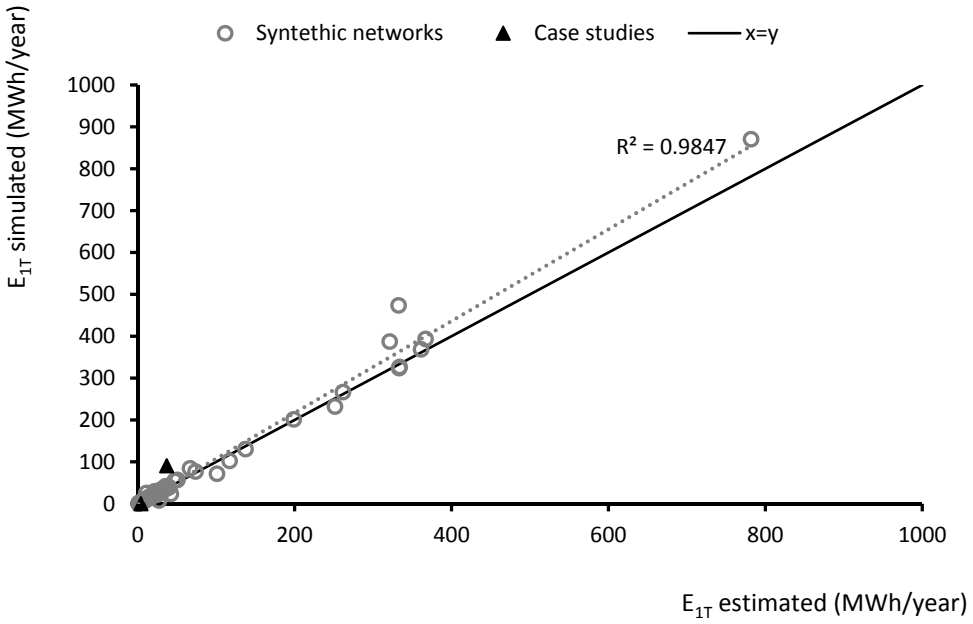

Figure.A 51 – Representation of estimation of energy produced with one 5BTP with expression 19 against the simulated energy.

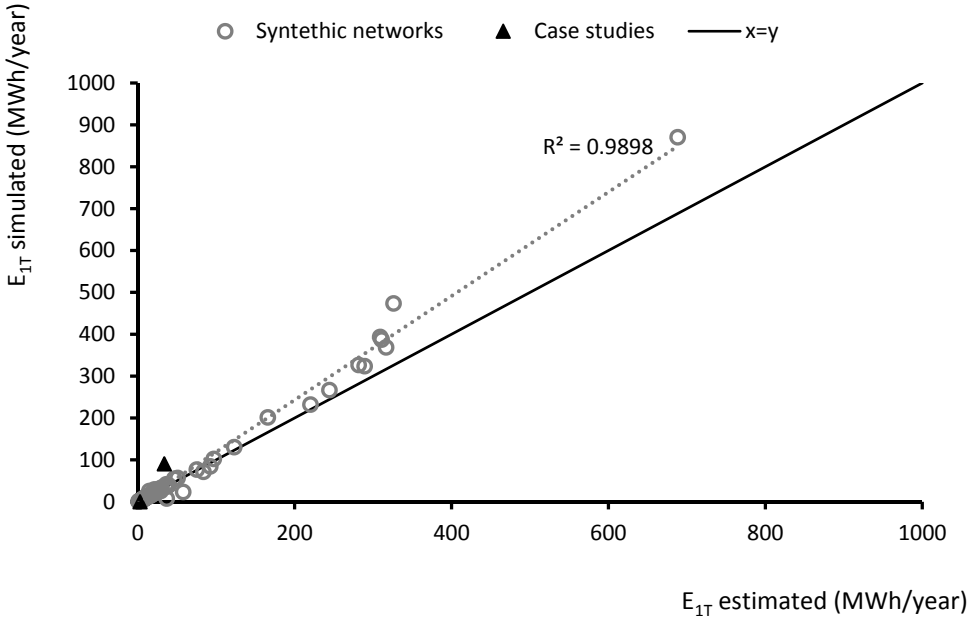

Figure.A 52 – Representation of estimation of energy produced with one 5BTP with expression 20 against the simulated energy.

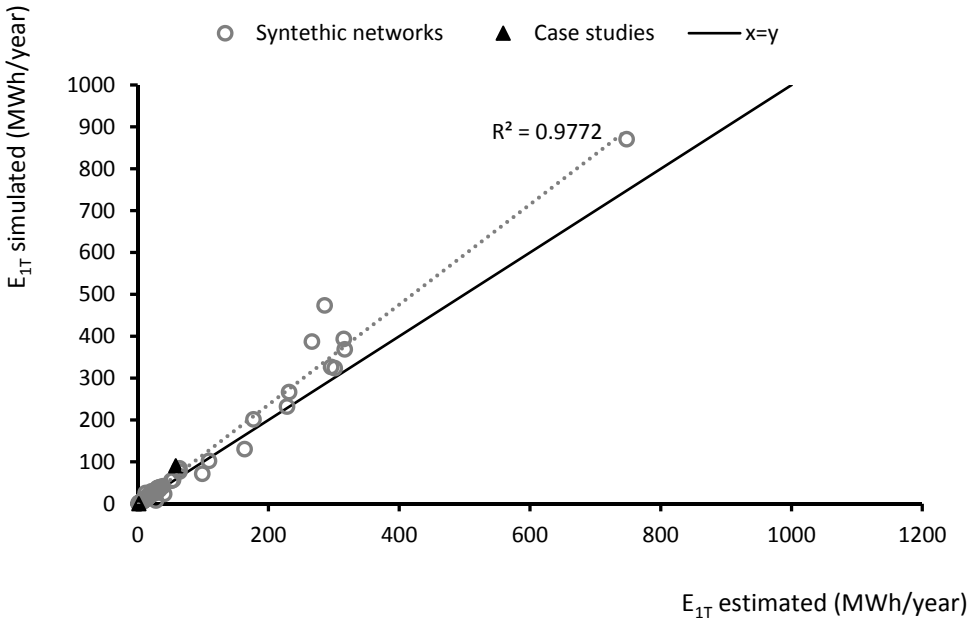

Figure.A 53 – Representation of estimation of energy produced with one 5BTP with expression 21 against the simulated energy.

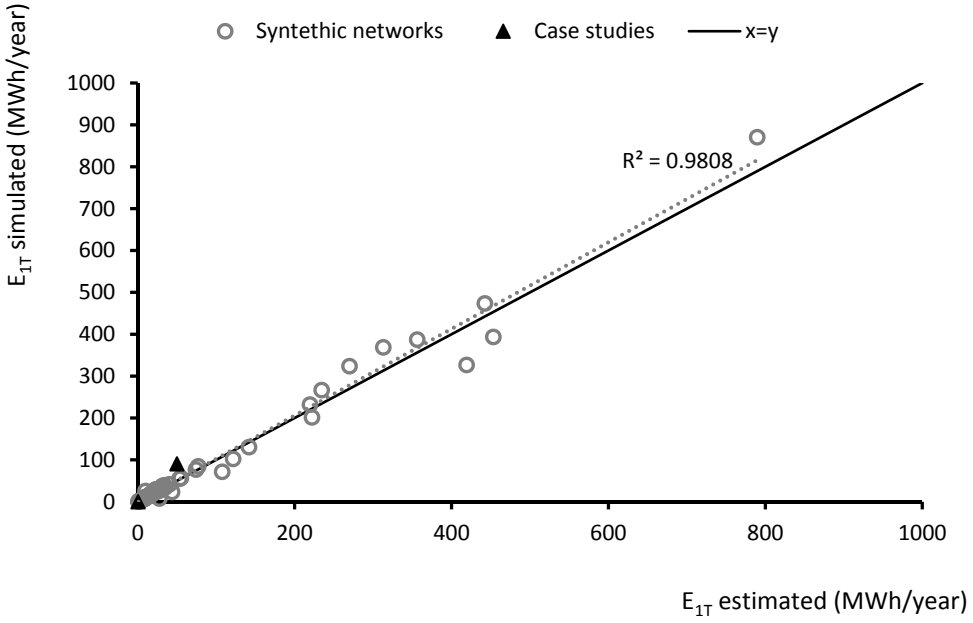

Figure.A 54 – Representation of estimation of energy produced with one 5BTP with expression 22 against the simulated energy.

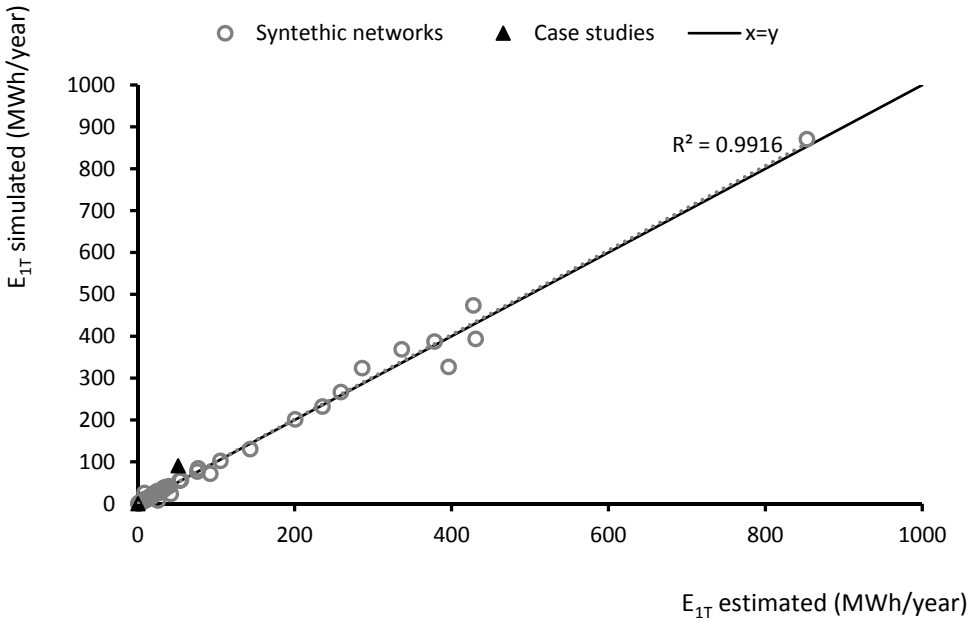

Figure.A 55 – Representation of estimation of energy produced with one 5BTP with expression 23 against the simulated energy.

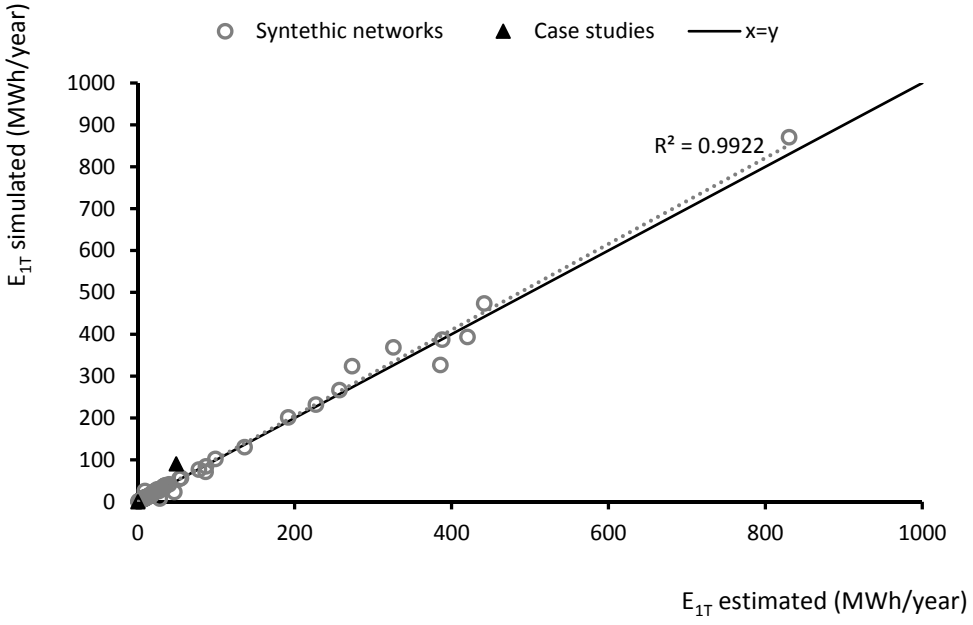

Figure.A 56 – Representation of estimation of energy produced with one 5BTP with expression 24 against the simulated energy.

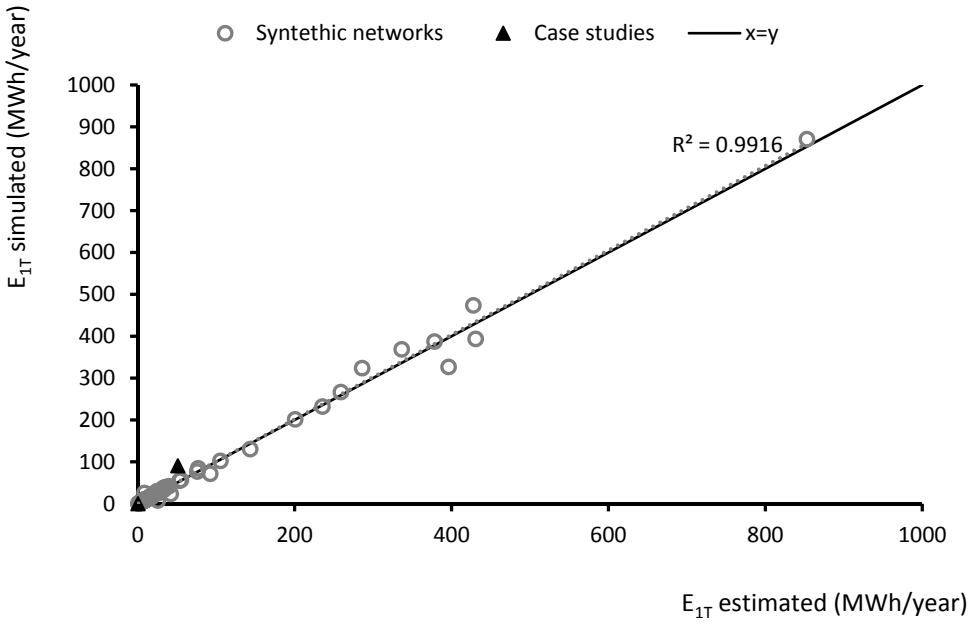

Figure.A 57 – Representation of estimation of energy produced with one 5BTP with expression 25 against the simulated energy.

Communications du Laboratoire de Constructions Hydrauliques ISSN 1661-1179
Ecole Polytechnique Fédérale de Lausanne
Editeur: Prof. Dr A. Schleiss

N° 53 2012 M. Müller
Influence of in- and outflow sequences on flow patterns and suspended sediment behavior in reservoirs

N° 54 2013 V. Dugué
Influencing river morphodynamics by means of a bubble screen: application to open-channel bends

N° 55 2013 E. Person
Impact of hydropeaking on fish and their habitat

N° 56 2013 T. Cohen Liechti
Influence of dam operation on water resources management under different scenarios in the Zambezi River Basin considering environmental objectives and hydropower

N° 57 2014 A. M. da Costa Ricardo
Hydrodynamics of turbulent flows within arrays of circular cylinders

N° 58 2014 T. Ghilardi
Sediment transport and flow conditions in steep rivers with large immobile boulders

N° 59 2014 R. Duarte
Influence of air entrainment on rock scour development and block stability in plunge pools

N° 60 2014 J. P. Matos
Hydraulic-hydrologic model for the Zambezi River using satellite data and artificial intelligence techniques

N° 61 2015 S. Guillén Ludeña
Hydro-morphodynamics of open-channel confluences with low discharge ratio and dominant tributary sediment supply

N° 62 2016 M. Jafarnejad Chaghooshi
Time-dependent failure analysis of large block size riprap as bank protection in mountain rivers

N° 63 2016 S. Terrier
Hydraulic performance of stepped spillway aerators and related downstream flow features

N° 64 2016 M. Ostad Mirza
Experimental study on the influence of abrupt slope changes on flow characteristics over stepped spillways

N° 65 2016 I. Almeida Samora
Optimization of low-head hydropower recovery in water supply networks

ISSN 1661-1179

DOI: 10.5075/epfl-lchcomm-65

Prof. Dr A. Schleiss
Laboratoire de constructions hydrauliques - LCH
EPFL, Bât. GC, Station 18, CH-1015 Lausanne
http://lch.epfl.ch
e-mail: secretariat.lch@epfl.ch